CHAPTER 4

RESULTS

A total number of 61 new Palaeolithic sites have been reported during the explorations (Map. 4.1). Based on the extent of sites, the freshness of the artefacts, and the presence of debitage (< 2 cm) and hammerstones, most of the sites are of primary context. It is observed that a maximum of the sites located in badland areas were exposed due to rill and sheet erosion. Among 61 sites, 33 are from the upper Paleru basin, 27 are from the upper Gundlakamma basin, and two are from the upper Manneru basin. A few microlithic sites are also reported from the Upper Paleru basin, which was unknown previously. Microliths were found in association with the inland dune deposits. Site distribution patterns and the composite stratigraphy were discussed separately for each river basin in Chapter 4.1.

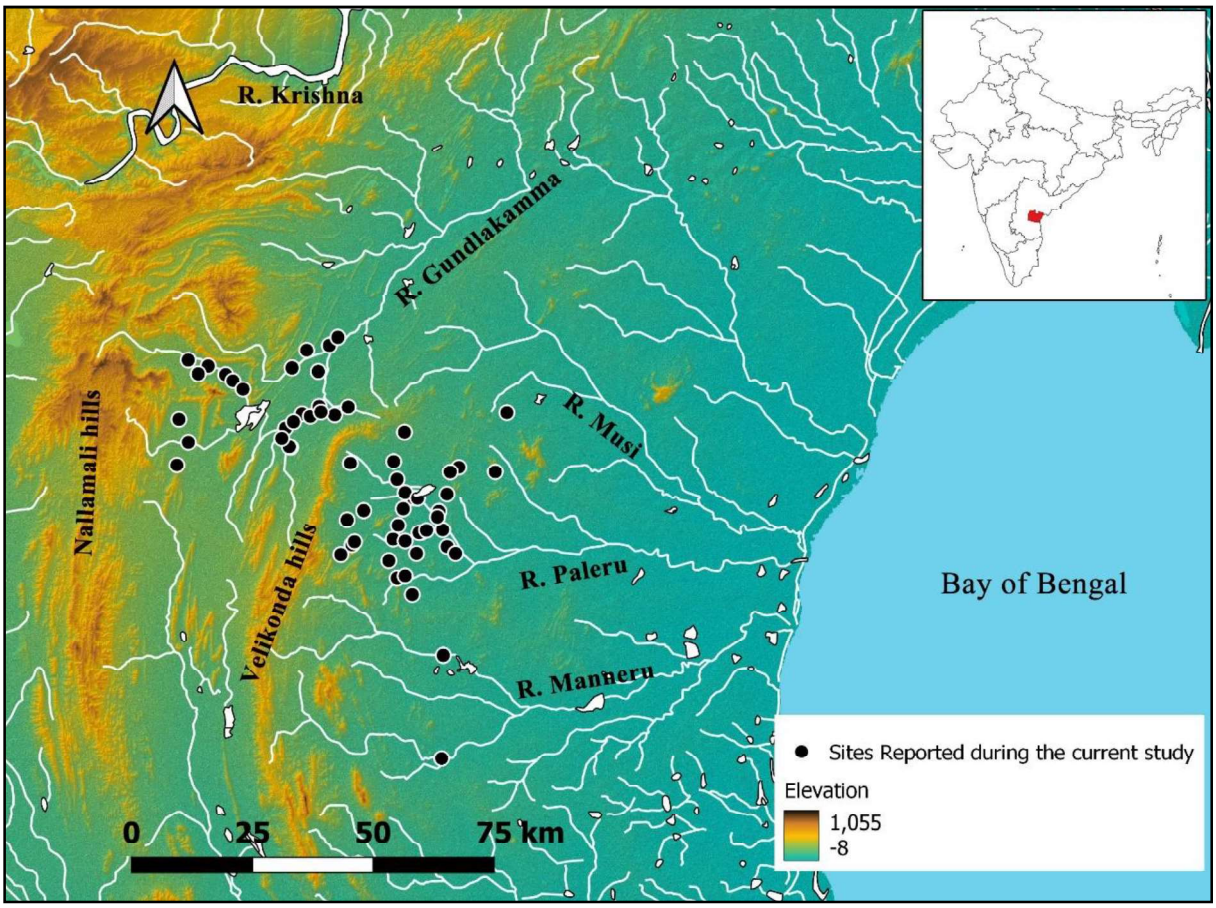

Map. 4.1: Map showing the distribution of sites reported during the current research.

4.1 Composite Stratigraphy and Site Distribution

4.1.1 Upper Gundlakamma River Basin

Field surveys were conducted in an area of ~ 350 sq. km in the upper reaches of the Gundlakamma river basin, which resulted in locating 26 new sites (Map. 4.1.1 and Table 4.1.1). Among the 26 newly reported sites, in six sites – Retlapalle, Vemulapeta, JP Cheruvu, Kalagotla, Kagitalagudem, and Telladinne – natural erosional activities have resulted in the exposure of ash (Youngest Toba Tuff) bearing sediments. Based on the observations from the above 26 archaeological sites and neighbouring areas, a composite stratigraphy comprising six sedimentary units was reconstructed (Fig. 4.1.1). These observations were supported by a step trench laid out at Retlapalle. A pebble conglomerate directly overlying the bedrock forms the base of composite stratigraphy in the upper reaches of the Gundlakamma river basin (Unit F, Fig. 4.1.1 & Fig. 4.1.2a). The pebble conglomerate includes rounded to amorphous quartzite pebbles, rock clasts, and Acheulian artefacts (Fig. 4.1.2b&c). These sediments are well exposed at Chintakunta and Vemulapeta towards the northeastern part of Cumbum lake and the Southwestern part. A calcrete-rich sandy silt Unit with a maximum thickness of 1 m (Unit E in Fig. 4.1.1) overlies this conglomerate Unit. The exposure of this Unit was observed only at the Retlapalle step trench, and no natural surface exposures were identified in the region.

Unit E is overlain by the reddish-brown silts well represented at the site of Retlapalle with a thickness of 110 cm (Unit D in Fig. 4.1.1). The reddish-brown silt is overlain by YTT deposits having a maximum thickness of 50 cm (Unit C in Fig. 4.1.1). YTT deposits are overlain by a brown coloured organic-rich silt (Unit B in Fig. 4.1.1) having a maximum thickness of 230 cm; it is well represented at Vemulapeta. The topmost sediments are reddish sandy silts (Unit A in Fig. 4.1.1), which has a maximum thickness of 160 cm and are well represented at the site of Kalagotla III (Fig. 4.1.3).

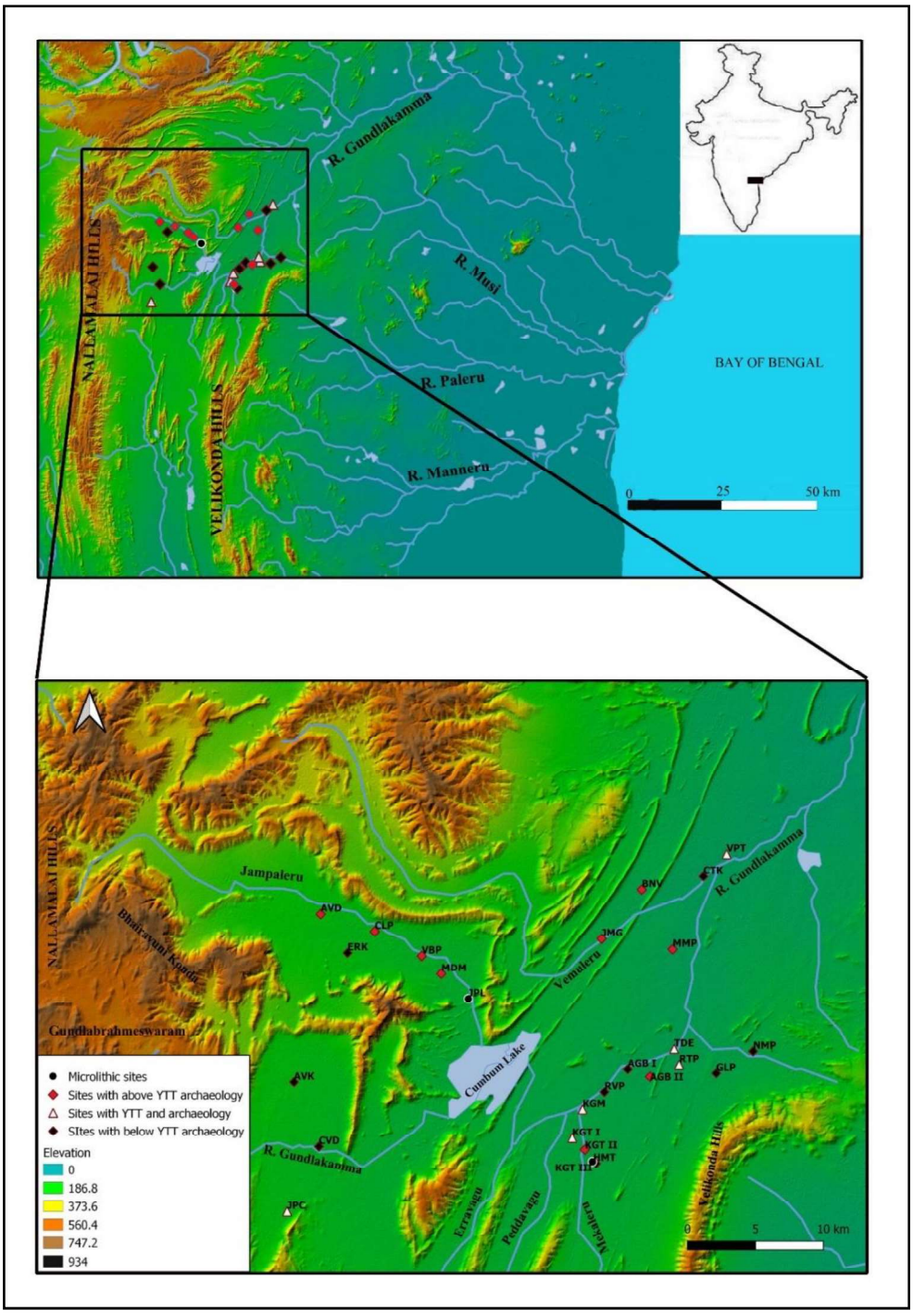

Map. 4.1.1: Map showing study region and sites mentioned in the text. Sites key; AVK: Araveetikota; AVD: Ardhaveedu; AGB I: Aurangabad I; AGB II: Aurangabad II; BNV :Birudalanarava; CLP: Chimaletipalle; CTK: Chintakunta; CVD: Cholaveedu; ERK: Erronka; GLP: Gollapalle; HMT: Hanuman Temple; JPC: J P Cheruvu; JPL: Jampaleru; JMG: Jangamguntla; KGM: Kagitalagudem; KGT I: Kalagotla I; KGT II: Kalagotla II; KGT III: Kalagotla III; MDM: Maddalamadaka; MMP: Mittamidapalle; NMP: Nagellamudupu; RVP: Ravipadu; RTP: Retlapalle; TDE: Telladinne; VBP: Veerbhadrapuram; VPT: Vemulapeta (Source: Anil et al., 2022).

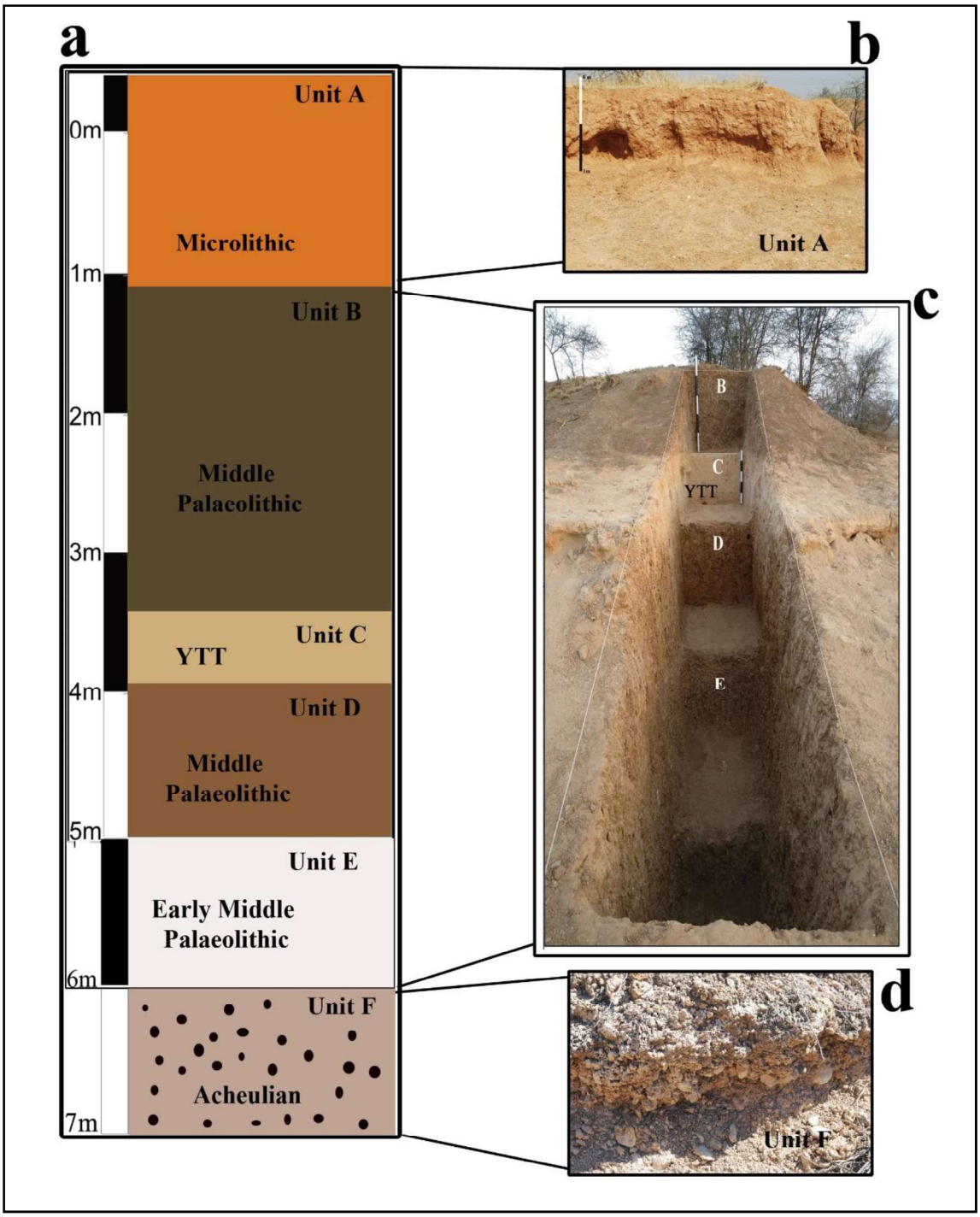

Figure. 4.1.1: a: Composite stratigraphy of the upper Gundlakamma river basin. b: Unit A exposed at Kalagotla III; c: step trench from Retlapalle; d: Unit F exposed at Chintakunta.

Figure. 4.1.2: a: Unit F exposures at Chintakunta; b: Conglomerate with artefacts; c: Handaxe eroded from Unit F.

Figure. 4.1.3: The site of Kalagotla III shows well-represented Unit A sediments and associated microlithic artefacts (Source: Anil et al., 2022).

YTT deposits are exposed at six sites due to natural erosional activities (Map. 4.1.1 and Table 4.1.1). The YTT beds have a maximum thickness of 50 cm and are laterally observed as discontinuous beds spread up to a maximum distance of 1.5 to 2 Km. This observation contrasts the adjacent Jurreru river valley, Kurnool, where the YTT beds have a maximum of 5 m thickness. Notably, all these six sites are geomorphologically associated with shallow and large topographic depressions now filled with sediments. These areas are currently undergoing rill and sheet erosion during the monsoon resulting in the exposure of the buried ash and the Palaeolithic artefacts. At all these six sites, the ash beds are associated with carbonate concretions (Fig. 4.1.4).

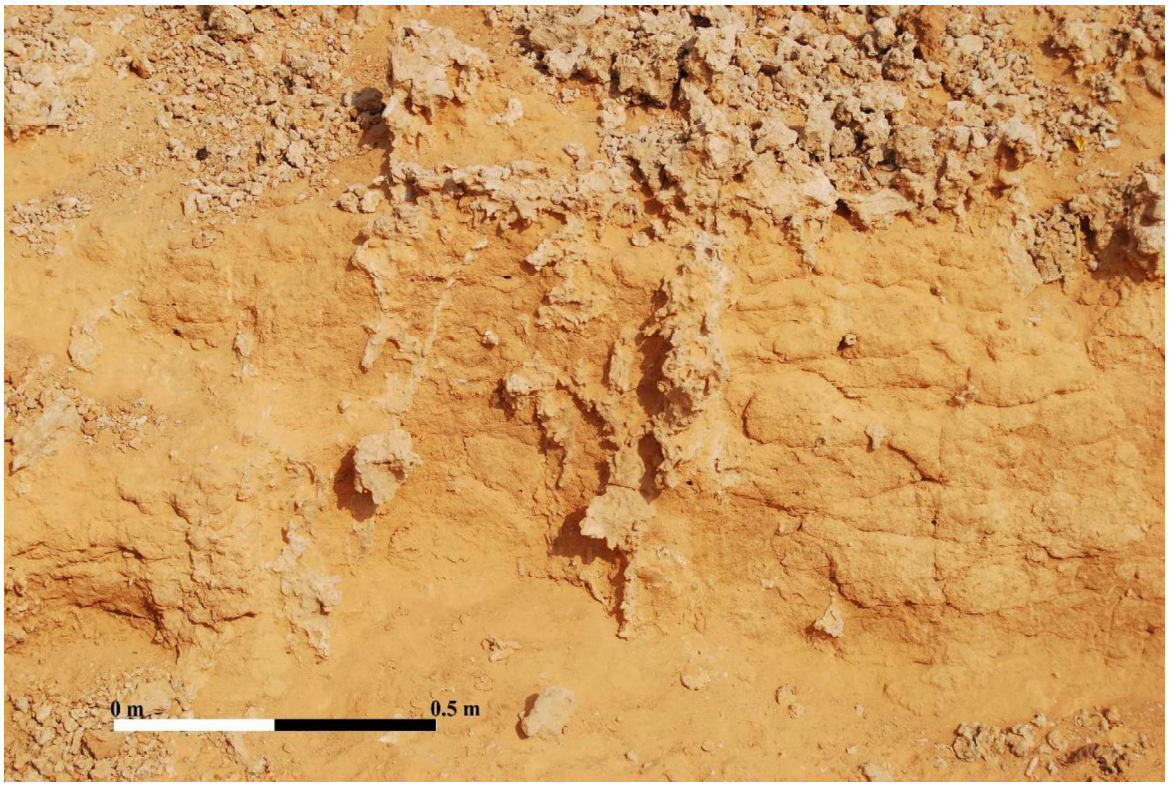

Figure. 4.1.4: Carbonate concretions above and within the ash beds observed at Kagitalagudem (Source: Anil et al., 2022).

Except for Retlapalle, the remaining five sites show rich Palaeolithic artefact assemblages within the sediments underlying and overlying the ash deposit. At Kalagotla, Kagitalagudem, and Telladinne, the sediments underlying YTT are well preserved and are exposed due to erosional and anthropogenic activities. In situ artefacts, mostly belonging to the Middle Palaeolithic, were observed eroding out from these sediments underlying the YTT beds (Fig. 4.1.5). JP Cheruvu and Vemulapeta preserve sediments that contain rich Palaeolithic material overlying the ash beds (Fig. 4.1.6).

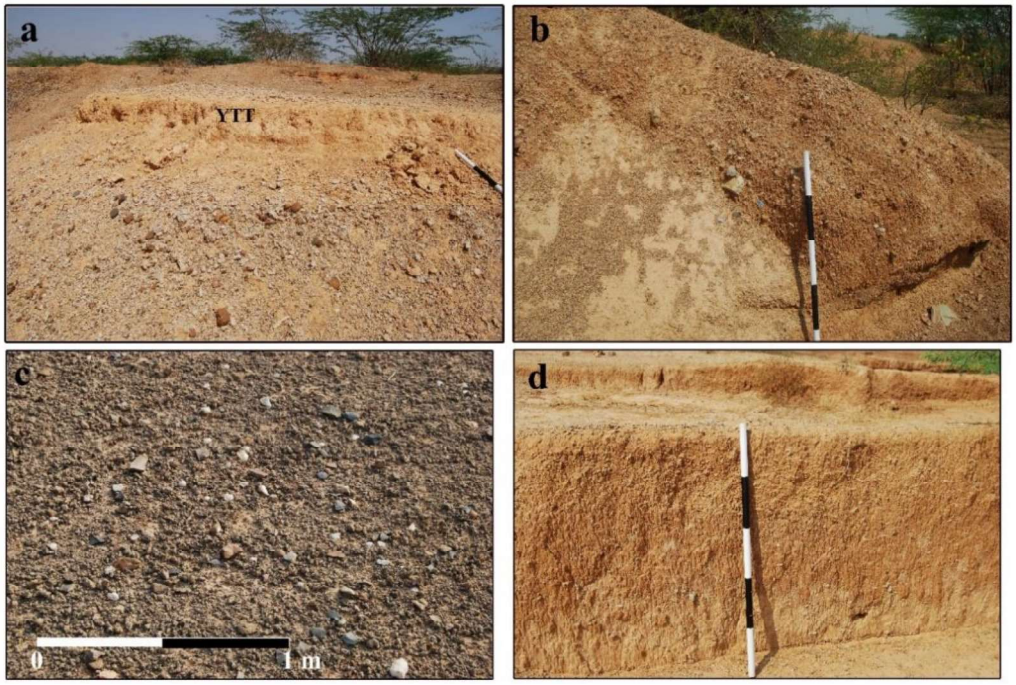

Figure. 4.1.5: Images showing the sites with sediments (Unit D) underlying the YTT deposits. a: below YTT sediments with artefacts exposed at Telladinne, b: Unit D sediments exposed at Kalagotla-I due to anthropogenic activities; c and d: below YTT sediments exposed at Kagitalagudem (Source: Anil et al., 2022).

Figure. 4.1.6: Sediments with artefacts overlying the ash beds exposed at JP Cheruvu (Source: Anil et al., 2022)

At two sites (Kalagotla III and Jampaleru), microlithic artefacts were found associated with the reddish sandy silts. Apart from these, at two sites (Aurangabad 3 and Vemulapeta 2), microlithic artefacts were observed within this sediment, but these were poorly represented and possibly got mixed with the sediment by disturbance. Overall, across the upper reaches of the Gundlakamma basin, at 12 sites, lithics were found to be associated with sediments underlying the YTT and 11 were found in the overlying sediments (Table. 4.1.1).

Table. 4.1.1: Sites mentioned in this chapter and their geological and cultural association (Source: Anil et al., 2022).

S.NO.	Site Code	Site Name	Sedimentary Contexts	Cultural Affiliation
1	TDE	Telladinne	Unit D, C	Middle Palaeolithic (Unit D)
2	NMP	Nagellamudupu	Unit D	Middle Palaeolithic
3	KGT I	Kalagotla I	Unit D, C	Middle Palaeolithic (Unit D)
4	HMT	Hanuman Temple	Unit D	Middle Palaeolithic
5	KGM	Kagitalagudem	Unit D, C	Middle Palaeolithic (Unit D)
6	RVP	Ravipadu	Unit D	Middle Palaeolithic
7	CTK	Chintakunta	Unit D	Middle Palaeolithic
8	AVK	Araveetikota	Unit D	Middle Palaeolithic
9	AGB	Aurangabad	Unit D	Middle Palaeolithic
10	CVD	Cholaveedu	Unit D	Middle Palaeolithic

11	ERK	Erronka	Unit D	Middle Palaeolithic
12	GLP	Gollapalee	Unit D	Middle Palaeolithic
13	RTP	Retlapalle	Unit A to D	Early Middle Palaeolithic
14	BNV	Birudalanarava	Unit B	Middle Palaeolithic
15	AGB II	Aurangabad	Unit B	Middle Palaeolithic
16	VPT	Vemulapeta	Unit B, C	Middle Palaeolithic (Unit B)
17	JMG	Jangamguntla	Unit B	Middle Palaeolithic
18	CLP	Chimaletipalle	Unit B	Middle Palaeolithic
19	AVD	Ardhaveedu	Unit B	Middle Palaeolithic
20	VBP	Veerabhadrapuram	Unit B	Middle Palaeolithic
21	MDM	Maddalamadak	Unit B	Middle Palaeolithic
22	MMP	Mittamidapalle	Unit B	Middle Palaeolithic
23	JPC	JP Cheruvu	Unit B, C	Middle Palaeolithic (Unit B)
24	KGT II	Kalagotla II	Unit B	Middle Palaeolithic
25	JPL	Jampaleru	Unit A	Microlithic
26	KGT III	Kalagotla III	Unit A	Microlithic

Unit A= Top Soil; Unit B = Above the YTT; Unit C = YTT; Unit D = Below YTT

Notably, the artefacts are not associated with high-energy materials such as gravels; instead, they are found in situ within the fine silty sand (Fig. 4.1.7). All these 26 sites have well-preserved prehistoric materials associated with the YTT beds, which are unique to the region.

Figure. 4.1.7: In situ artefacts eroding from the sediments (Unit B) stratigraphically overlying the YTT deposits. Artefact clusters from, a: Chimaletipalle; b: JP Cheruvu; c: Ardhaveedu; d: Veerabhadrapuram (Source: Anil et al., 2022).

4.1.2 Upper Paleru River Basin

Surveys yielded 33 sites along the upper reaches of the Paleru river basin (Map. 4.1.2). The sites were found to be distributed on different geomorphic landforms, namely foothills and colluvial fans, sand dunes, riverbanks and channel bars (Anil et al., 2018).

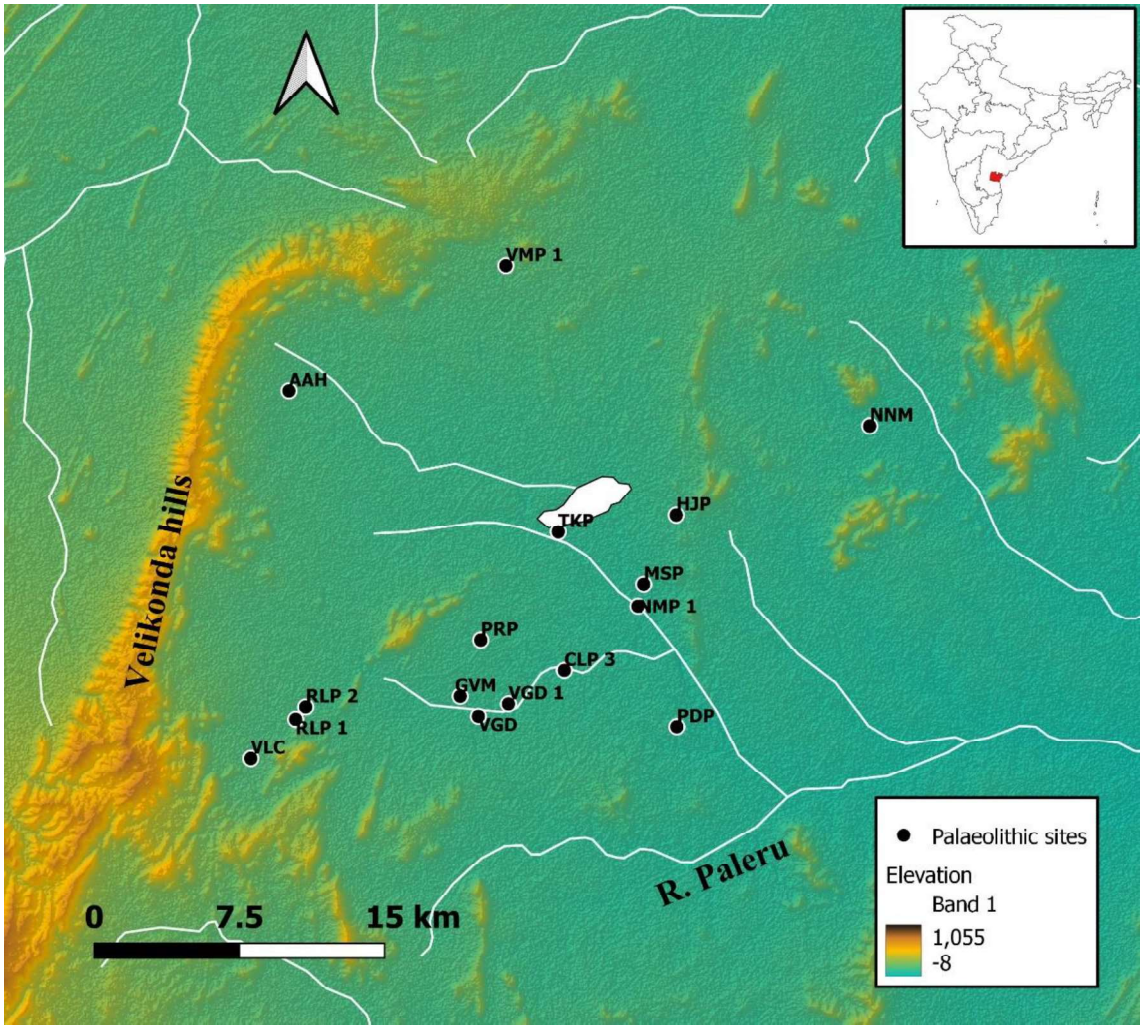

Map. 4.1.2: Map showing the distribution of the sites in the upper Paleru river basin.

Most sites revealed both Late Acheulian and Early Middle Palaeolithic artefacts in a mixed context due to natural erosion (Table. 4.1.2). However, the co-existence of two technologically distinct traditions can also possibly not be ruled out. Topographically most of the sites are located in low-lying areas near water bodies such as ponds, shallow lakes and small streams. A significant feature observed is that the lateral extension of the artefacts at the sites ranged between an average area of 1.5 Km x 1 Km and 3 Km x 3 Km. The sites near the foothills of the Velikondas and local ridges have a maximum area of extension, suggesting that the

Palaeolithic populations preferred these areas due to the availability of extensive resources along the foothill.

The study area falls into the semi-arid zone and is characterised by water scarcity. To conserve rainwater, the Government of Andhra Pradesh initiated several measures to restore and renovate small streams and existing ponds. These undertakings exposed sections at several localities in the region with palaeoliths embedded in them (Fig. 4.1.8).

Figure. 4.1.8: Embedded artefacts exposed at Rangannapalle (Source: Anil et al. 2018).

The colluvial/alluvial fans consist of Cuddapah conglomerates, and other sedimentary rocks emanating from the adjoining Velikonda hills occur on top of the bedrock form the bottom of the Paleru basin. The thickness of the fan was earlier observed to be 1.5 m in its maximum extent (Rao, 1979). However, during our surveys, we observed the fan thickness as a thin veneer resting on the bedrock/calcrete (Fig. 4.1.9). At a few localities, the pebble conglomerate was observed to lie on top of the bedrock (Fig. 4.1.10). In contrast, at most localities a thick calcrete bed or Tufa (1 to 1.5 m) was observed below this gravel horizon (Fig. 4.1.11). At the foothill and close to the foothill regions of Velikondas, this gravel horizon/conglomerate/colluvial fans were topped by reddened sandy silts of fluvial origin. The lower part of this reddened sandy silt Unit was calcretized (Fig. 4.1.12).

Figure. 4.1.9: Colluvial fan exposed at Rangannapalle (Source: Anil et al., 2018).

Figure. 4.1.10: Pebble conglomerate observed at Kutagundla (Source: Anil et al., 2018).

Figure. 4.1.11: Calcrete bed (Tufa) exposed on the surface at Vemulapadu 2 (Source: Anil et al., 2018).

Figure. 4.1.12: Calcretized sandy silt at Hanumanthunipadu (Source: Anil et al., 2018).

At places, this calcretized sandy silt Unit was topped by modern soil, and at others, it was overlain by red-coloured (dark brown) stabilised sand dunes (Fig. 4.1.13). These sand dunes, in turn, were overlain by a pale yellow/yellow-coloured loose sand dune. Geological studies undertaken by the Geological Survey of India characterised these dunes as A-1 and A-2 units: A-1 being the pale yellow/yellow coloured sand dunes and A-2 being the red coloured/dark brown dunes (Mishra & Singaraju, 2009; Reddy et al., 2013). These dunes were called inland sand dunes and spread over an area of ~ 500 Km^2 ~ 75 Km inland from the east coast. OSL dating of these dune samples ranged from the present to ~ 50 ka suggesting a long duration of sand dune aggradation and reworking history (Reddy et al., 2013).

Figure. 4.1.13: Calcretized sandy silt overlain by A-2 sand dunes at Vemulapadu (Source: Anil et al., 2018).

Intensive surveys in the upper part of the Paleru basin brought to light 33 Palaeolithic sites distributed in different geomorphic settings (Table. 4.1.2). Based on geomorphic and stratigraphic contexts of these 33 sites, a composite stratigraphy and associated cultural material was prepared (Fig. 4.1.14). The colluvial/alluvial fans on the bedrock form the bottom of the Paleru basin, which contains Late Acheulian and early Middle Palaeolithic artefacts. At a few localities, a calcrete bed/tufa has been observed at the bottom or below the gravel horizon, whereas at others, a pebble conglomerate was observed resting on the bedrock. This calcrete

bed/tufa formation indicates a dry period after the formation of colluvial/alluvial fans. These fans were overlain by red sandy clay deposits, where the bottom of this Unit was calcretized. This calcretized sandy clay horizon contains Palaeolithic artefacts. Dark brown coloured aeolian sand dunes, which overlie the calcretized sandy clay, contain the microlithic artefacts. Loose pale-yellow coloured sand dunes overlay these stabilised dunes. Thus, the Paleru basin has stratified rich archaeological records ranging from Acheulian to microlithic within stratified horizons. These stratified archaeological deposits have enormous potential for addressing issues regarding hominin behaviour in South Asia.

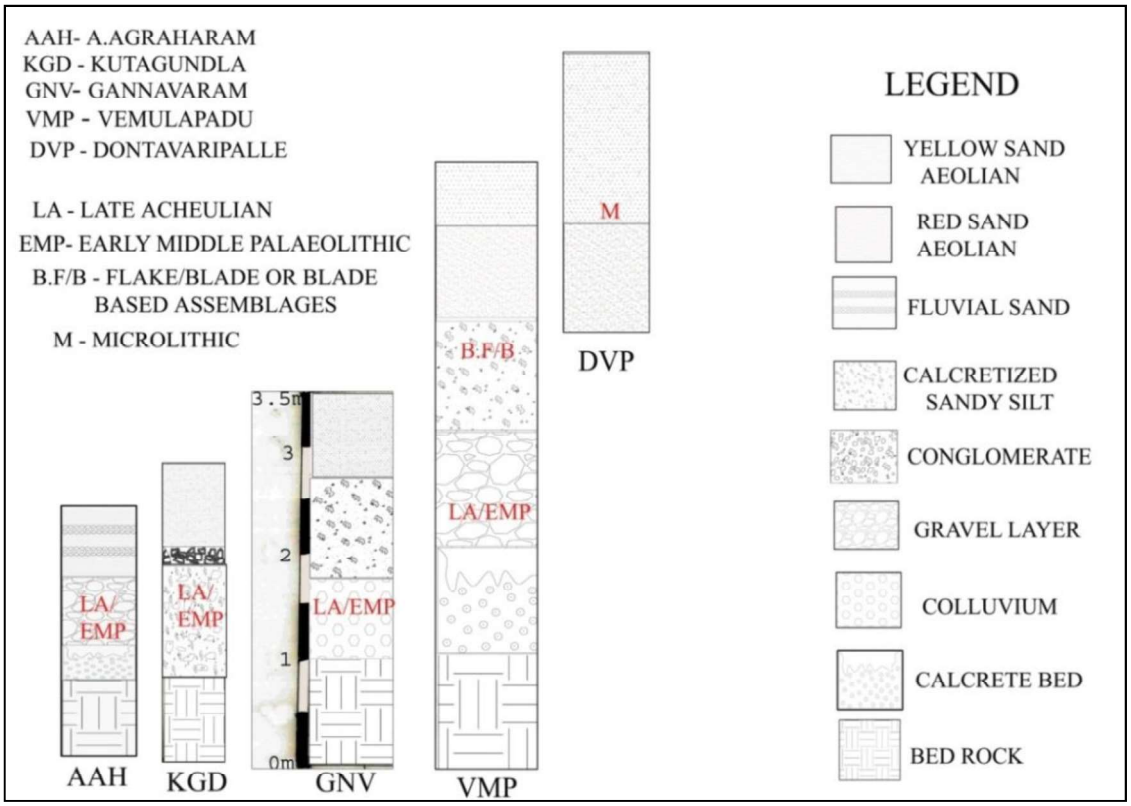

Figure. 4.1.14: Composite Stratigraphy of the upper Paleru basin (Source: Anil et al., 2018).

Table. 4.1.2: List of the sites reported during the surveys and mentioned in this chapter (Source: Anil et al., 2018).

SITE NAME	GEO-COORDINATES		CULTURAL MATERIAL	GEOLOGICAL CONTEXT
	Longitude	Latitude		
Kutagundla	79.36632 E	15.42958 N	LA	Stratified
Chanduluripadu 1	79.38112 E	15.36504 N	LA	Stratified
Chanduluripadu 2	79.37694 E	15.36446 N	MP	Stratified
Chanduluripadu 3	79.39071 E	15.36908 N	M	Stratified
Chinnagollpalle	79.33601 E	15.46403 N	LA, MP	Stratified
Chodavaram	79.36432 E	15.24936 N	LA	Stratified
Dontavaripalle	79.34753 E	15.40940 N	M	Stratified
Ganugapenta	79.45095 E	15.48669 N	LA, MP	Stratified
Gayamvaripalle	79.32863 E	15.35254 N	LA, MP	Stratified
Gokulam	79.37226 E	15.32578 N	LA, MP	Stratified
Hajipuram	79.42889 E	15.43664 N	LP	Stratified
Jallapalem	79.24324 E	15.38884 N	LA, MP	Surface
K. Agraharam	79.24914 E	15.49449 N	LA, MP	Stratified
Kottalapalle	79.33628 E	15.28005 N	LA	Surface
Krishanpuram	79.43492 E	15.47777 N	LA	Stratified
Kudumulakunta	79.32972 E	15.49774 N	LA, MP	Surface
Marapaguntla	79.35108 E	15.28400 N	LA, MP	Surface
Masaipeta	79.413793 E	15.40452 N	LP	Stratified
Nandanamarella	79.51863 E	15.47810 N	LA	Stratified
Narasamabapuram 1	79.42083 E	15.37001 N	LA, MP	Stratified
Narasamabapuram 2	79.41113 E	15.39436 N	LP	Stratified
Narvagopalpuram	79.35098 E	15.43941 N	LP, M	Stratified
Padmavaripalle 1	79.42916 E	15.33843 N	M	Surface
Padmavaripalle 2	79.44476 E	15.32574 N	LA	Surface
Papireddypalle	79.33818 E	15.37862 N	LP	Surface
Rallapalle 1	79.25226 E	15.34183 N	LP	Stratified
Rallpalle 2	79.25692 E	15.34759 N	MP	Surface

Ramayyapalle	79.27397 E	15.40601 N	LA,MP	Stratified
Rangannapalle	79.32076 E	15.31220 N	LA, MP	Stratified
Tenkayalapalle	79.37413 E	15.42892 N	MP	Surface
Vedullacheruvu	79.23141 E	15.32367 N	MP	Surface
Veligandla	79.35102 E	15.34903 N	LP	Surface
Vemulapadu	79.34983 E	15.55260 N	LA, MP, M	Stratified

Key: LA – Late Acheulian, MP – Middle Palaeolithic, LP – Late Palaeolithic, M - microlithic

4.1.3 Upper Manneru River Basin

Surveys along the upper reaches of the Manneru river basin were limited to revisiting the previously reported sites. As the region was explored recently by Srinivasulu (2012), no new surveys were conducted. However, two new sites were identified during the current research: Jadadevi and Motravulapadu (Map. 4.1.3). At Motravulapadu, small-scale excavations were conducted to understand the site stratigraphy and associated cultural material, details of which are presented in Chapter 4.7.

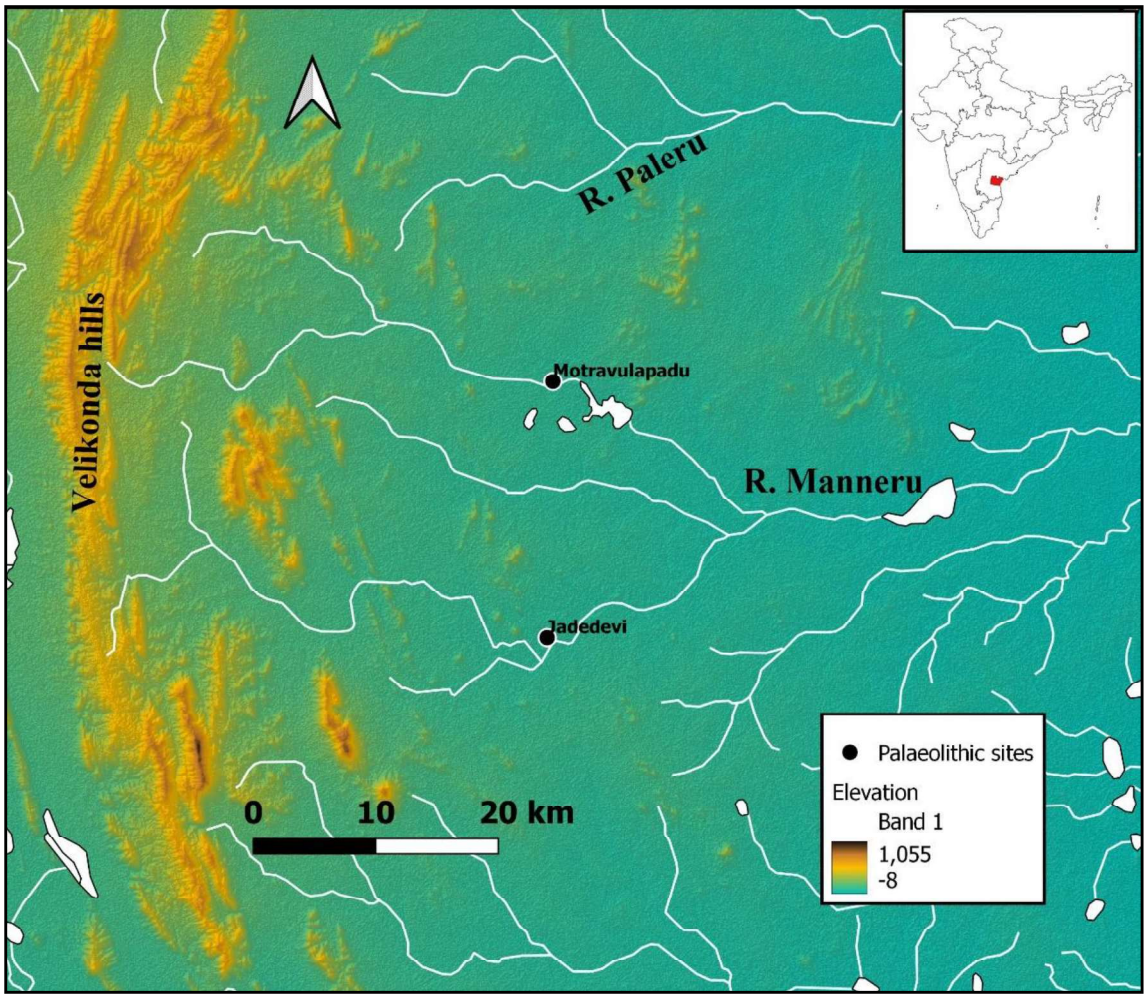

Map. 4.1.3: Map showing the location of two sites newly reported in current research in the upper Manneru river basin.

To reconstruct the Prehistoric cultural sequence of the Gundlkamma and adjoining river basins, seven newly reported sites were investigated in detail (Map. 4.1.4). The sites were selected based on the criteria of having rich cultural material from in situ contexts and assuming they can provide material from oldest to youngest time ranges. These sites are Vemulapadu (VMP), A. Agraharam (AAH), Nandanavanam (NNV), Hanumanthunipadu (HMP), Retlapalle (RTP),

Motravulapadu and Ardhaveedu (AVD). Excavations, section scrapings and step trenches were conducted at these sites to recover sediment samples for Luminescence dating and cultural material.

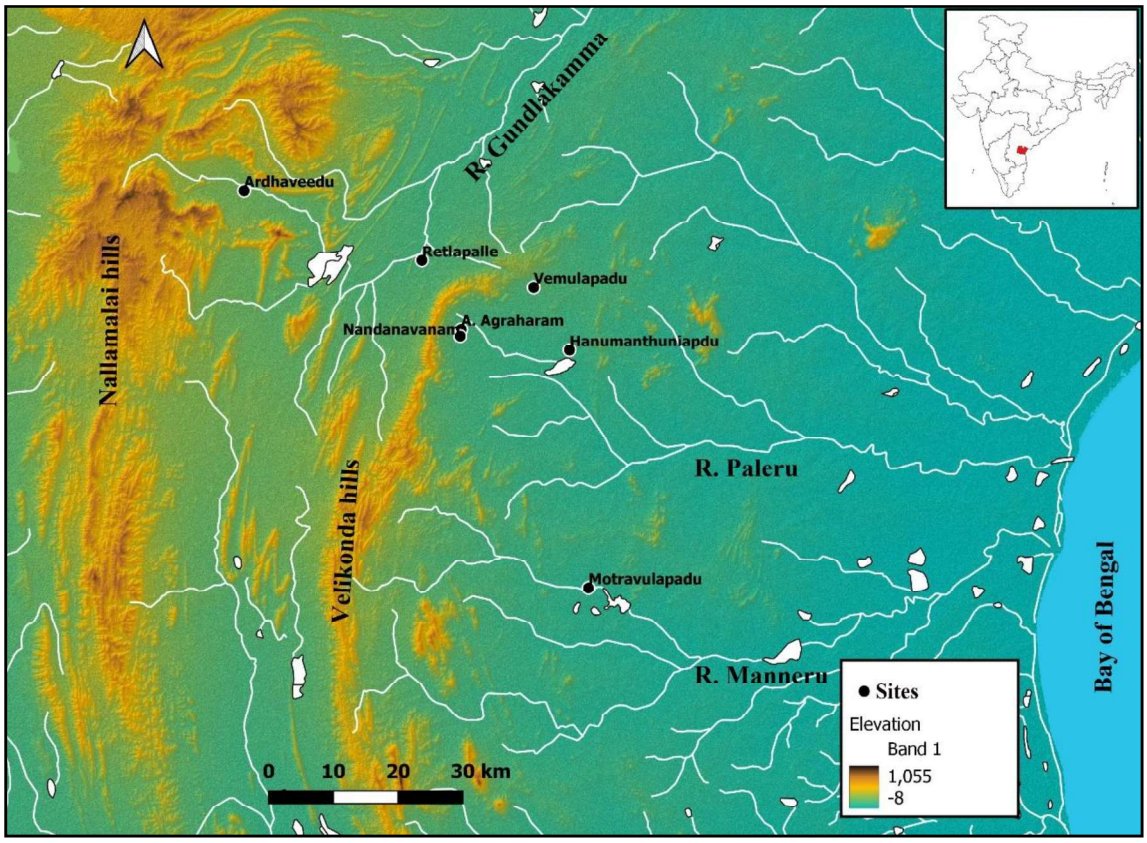

Map. 4.1.4: Map showing the location of seven sites investigated in detail and discussed in Chapter 4.

4.2 Vemulapadu (Acheulian Levels)

The site Vemulapadu (15.556370° N, 79.332440° E) is located on the foothill of the northern part of the Velikonda hills (Map. 4.2.1). A first-order stream cuts through the site by exposing good sections along a length of one kilometre. The survey was able to locate artefact-bearing sediments in the sections exposed in several places, which helped to draw up a composite stratigraphy. Section scrapings were also carried out at three places to validate the composite stratigraphy and to collect sediment samples for Luminescence age estimations. Three different artefact-bearing horizons were noted at the Vemulapadu site: 1. Acheulian (Early) being the oldest, followed by 2. the Middle Palaeolithic and 3. the Mesolithic. This chapter discusses the stratigraphy, artefacts and OSL dating of Early Acheulian levels.

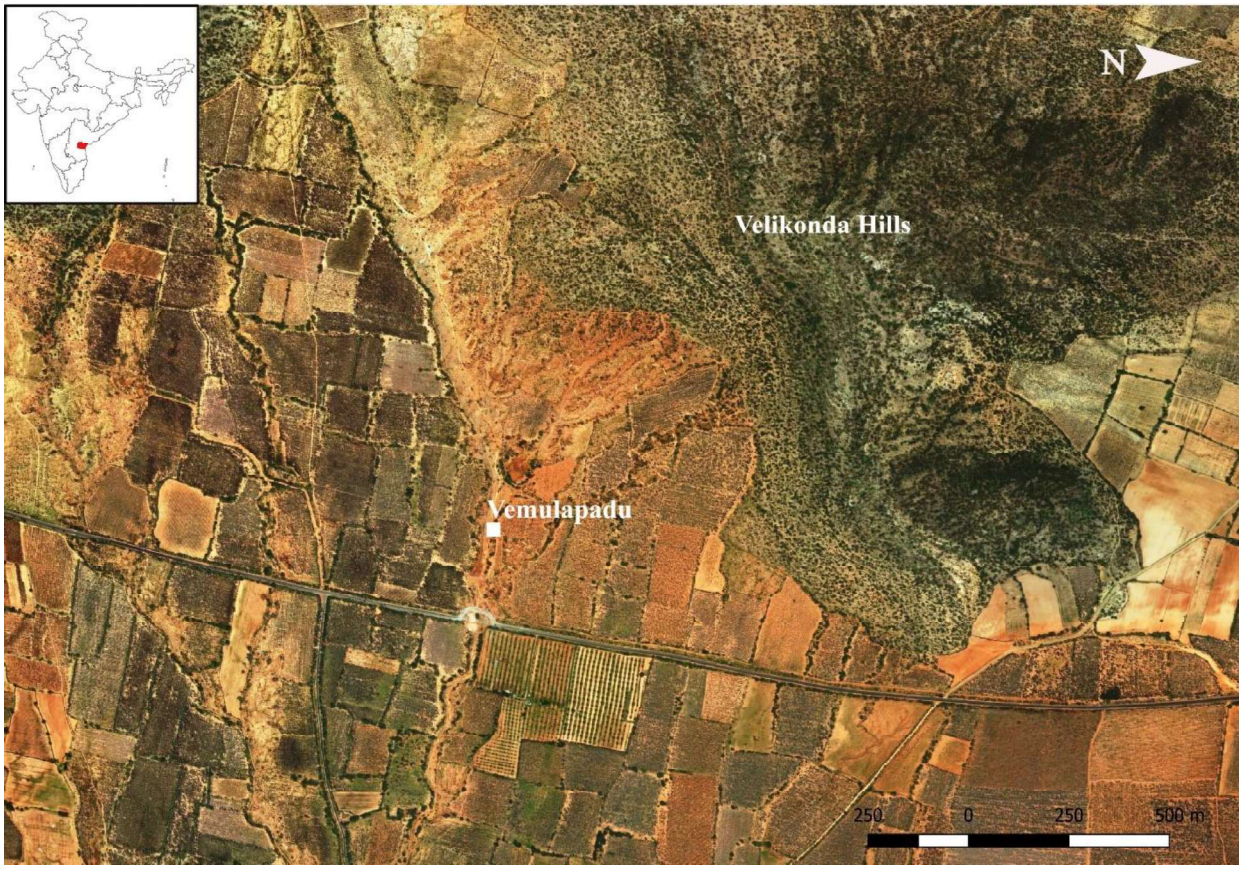

Map. 4.2.1: Map showing the location of the site Vemulapadu.

4.2.1 Stratigraphy

The composite stratigraphy consists of five discrete layers associated with three artefact horizons. This section discusses only the bottom-most two layers bearing Acheulian artefacts. The basal layer (Unit E, Fig. 4.2.1) at the site consists of a hardened calcareous bed (tufa) with a maximum thickness of ~ 1.5 m. The base of this layer is not seen in any of the exposed

sections at the site; however, based on the observations from adjacent localities, it seems that Unit E lies directly over the bedrock. This layer is overlain by a light reddish silty clay deposit of ~ 1 m thickness (Unit D) with thin carbonate crust layers (thin crusts with 2 cm maximum thickness). A few Acheulian artefacts, consisting of hand axes and cleavers, were identified as embedded within Unit-E and exposed on the surface (Fig. 4.2.2).

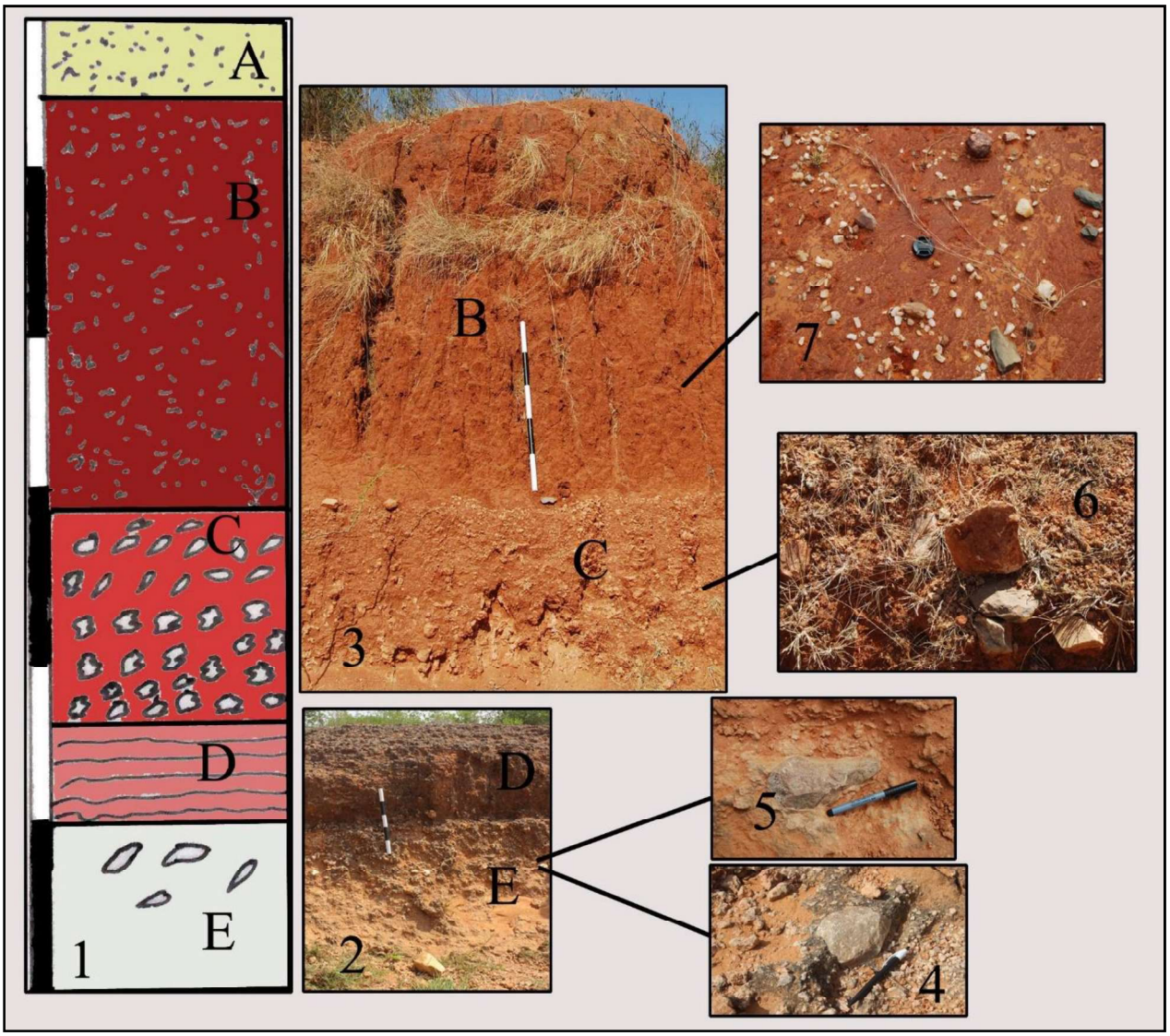

Figure. 4.2.1: Composite stratigraphy observed at Vemulapadu with artefact associations. 1: Schematic sketch of the composite stratigraphy; 2: Photograph of the Units E and D; 3: Units C and B; 4 and 5: embedded handaxes within unit E; 6: Artefacts from Unit C; 7: microlithic artefacts from Unit B.

Figure. 4.2.2: In Situ hand axe associated with Unit E sediments at Vemulapadu.

4.2.2 Luminescence Chronology

One sediment sample was collected from Unit-E to estimate the depositional age (Fig. 4.2.3). This sample was collected from a section where quartz debitage pieces were observed embedded within unit-E. The reason behind selecting this place for OSL sample collection is that the quartz debitage was observed below one meter from the currently exposed surface to eliminate the cosmogenic contamination of the luminescence signal. Post-Infrared-Infrared Stimulated Luminescence (p-IR-IRSL) protocol was applied on k-feldspar grains to obtain the last exposed time of the sediment. However, the luminescence signal of the sample saturating and actual age could not be estimated (Fig. 4.2.4b). Nevertheless, a minimum age of 410 ka was estimated, and no fading correction measurements were not done on these samples, realizing that the signal was saturating. The depositional age of Unit E goes beyond 410 ka.

Figure. 4.2.3: Sediment sample collected from Unit E for age estimations.

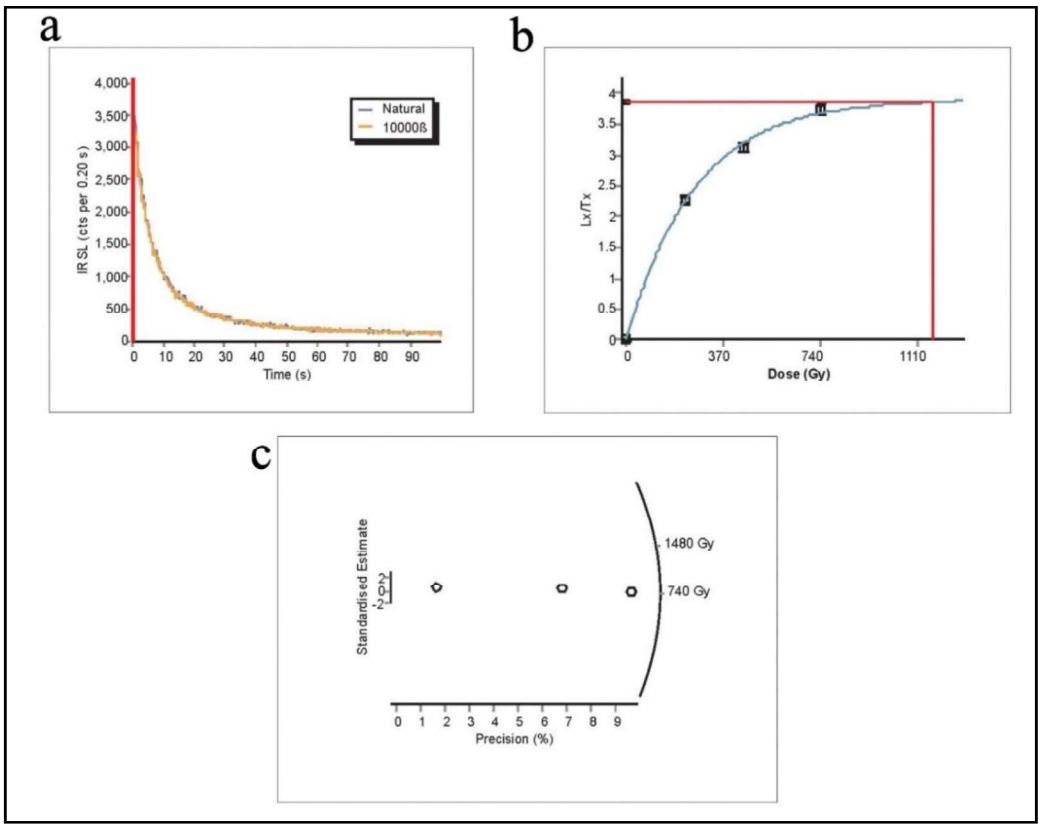

Figure. 4.2.4: Results of p-IR-IRSL analyses of sample from Unit E. a: typical feldspar shine down curve; b: typical growth curve; c: radial plot representing the estimated palaeodoses.

4.2.3 Lithic technology

Only four artefacts and quartz debitage were recovered from Unit-E at Vemulapadu. These four artefacts are hand axes made on quartzite blocks from the adjacent Velikonda hills. Technologically these hand axes are large in size and thick with minimal flake scars (Fig. 4.2.5). These features denote that these hand axes may be part of the Early Acheulian phase. However, more sample size is required to confirm the observation mentioned above.

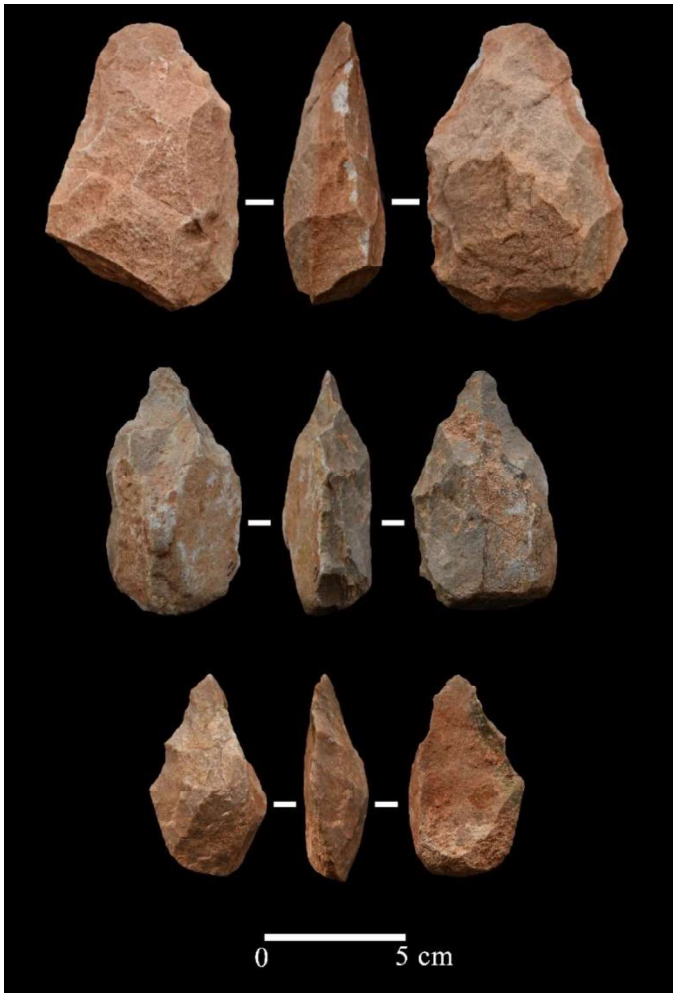

Figure. 4.2.5: Hand axes recovered from Unit E, at Vemulapadu.

4.2.4 Summary

Due to the limited number of artefacts recovered from Vemulapadu (Acheulian level), it is difficult to understand the technology of the lithic assemblage. However, with the large size of the handaxes with minimal flake scars, it can assume that these handaxes are part of the early phase of the Acheulian. The luminescence age of the artefact-bearing horizon further suggests the aforementioned observation.

4.3 Anandapuram Agraharam

The site at Anandapuram Agraharam is located three kilometres south of the site Vemulapadu, at the foothill of the northern Velikonda hill range (Map. 4.3.1).

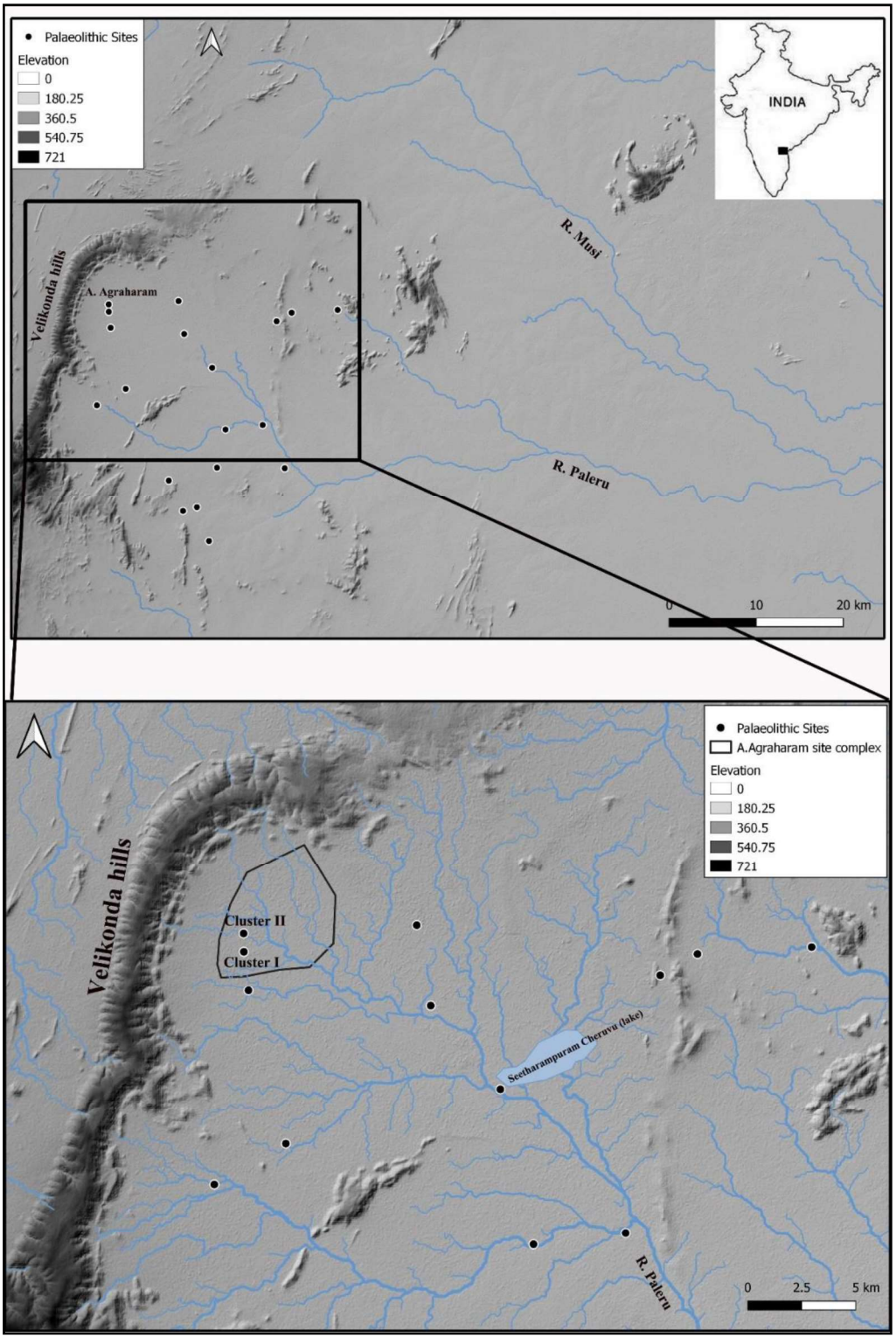

Map. 4.3.1: Map showing the location of site A. Agraharam (Source: Anil et al., 2022).

This quarzitic hill range (Velikonda) is a part of the eastern margin of the Cuddapah basin and was the primary raw material source for Palaeolithic tool making. Artefacts are quite widely spread around an area of 23 sq km to the west of the A. Agraharam village, and therefore it is appropriate to call it a site complex. Several streams (first and second order) originating from the adjacent hill cut through the site complex and expose artefacts on the surface as several discrete clusters (Fig. 4.3.1a & b). Some of the streams are relatively deep, and their channels have recently been expanded to conserve rainwater. These anthropogenic activities have exposed the artefact-bearing horizons (Fig. 4.3.1c). Our surveys were limited to the southern part (13 sq. km) of the site complex, and we identified 27 artefact clusters exposed due to natural erosion and anthropogenic activities.

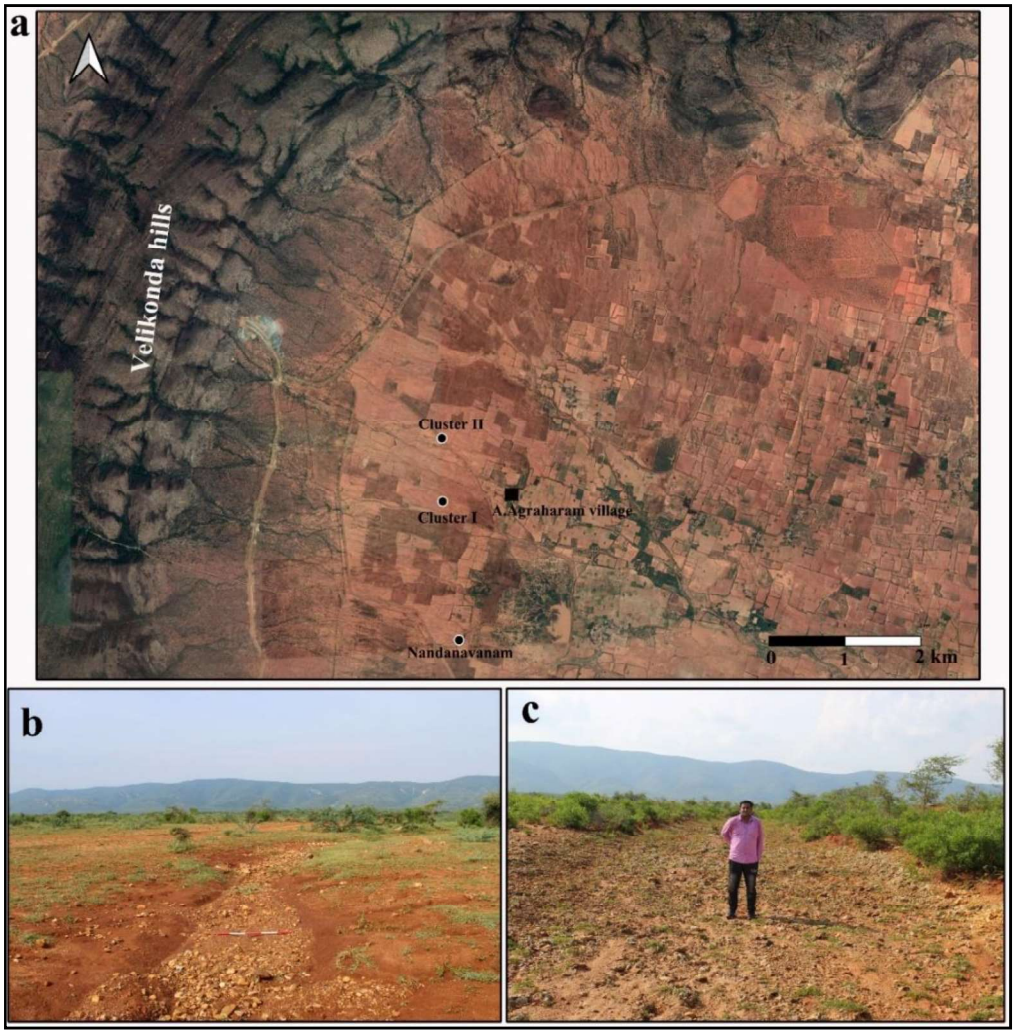

Figure. 4.3.1: Images showing the location of site A. Agraharam and exposed artefact clusters. a: several streams cut through the site; b: Artefact cluster exposed due to the stream erosion; c: Artefact cluster exposed due to anthropogenic activities.

4.3.1 Stratigraphy

Based on our observations from these clusters and other eroded areas, we identified ferricrete gravels as the geological context of the artefacts. To confirm our observation and to understand other sediments associated with the ferricrete gravels, we opened a 1 m^2 test pit (Fig. 4.3.2). The test pit yielded 27 lithic artefacts embedded within the ferricrete gravels. The test pit exposed five sedimentary units in which the tufa bed that directly overlies the bedrock forms the base of the section. On top of this tufa bed lies the ferricrete dominant gravel unit with a thickness of 25-30 cm and occurs as a discontinuous unit within the test pit. These ferricrete gravels are overlain by two sandy silt units separated by a 20 cm thick colluvial deposit. This colluvial deposit includes quartzite clasts of different sizes and a few rolled lithic artefacts. Except for the ferricrete gravels, the rest of the four units are culturally sterile. The sedimentary units from the test pit further corroborate our observation that the ferricrete gravel is the artefact-bearing horizon.

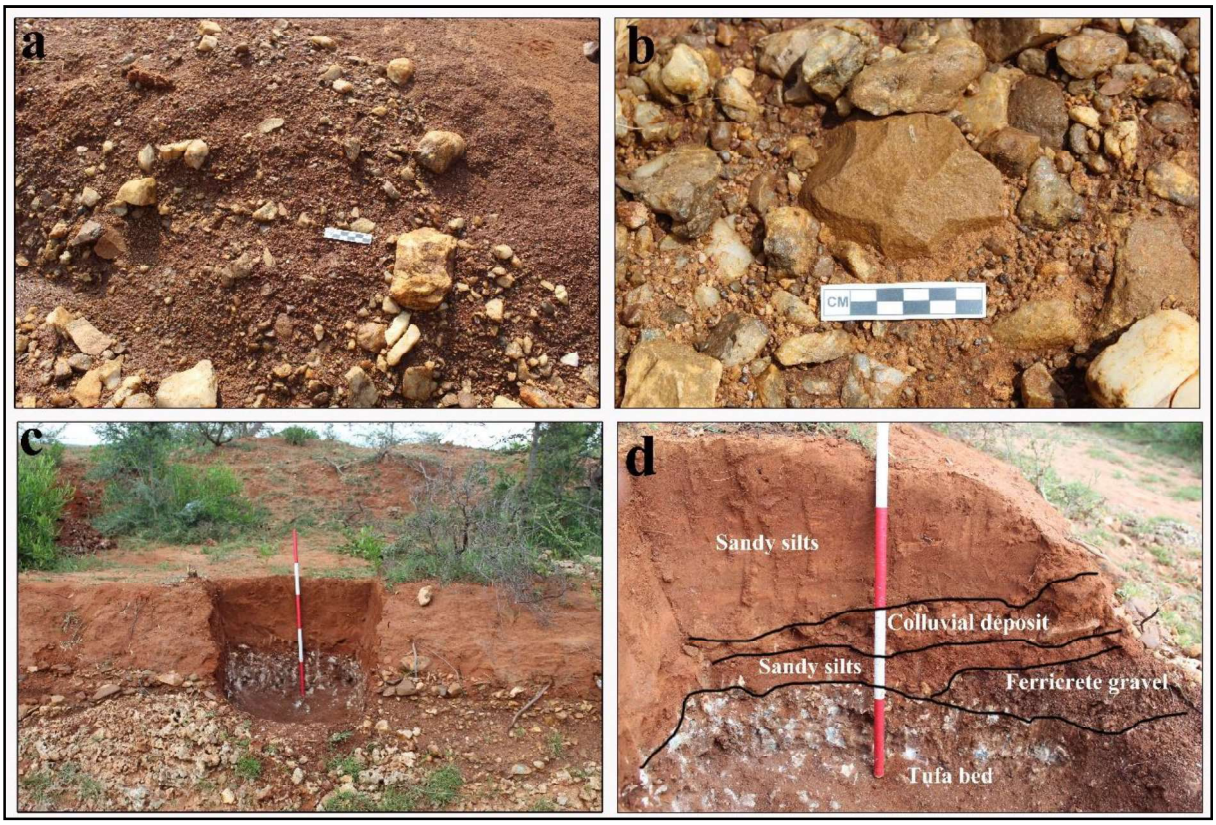

Figure. 4.3.2: Artefacts and their geological context. a and b: Artefacts embedded within the ferricrete gravels; c and d: test pit showing the stratigraphic context of sedimentary units.

4.3.2 Luminescence Chronology

Sediment sample from the artefact-bearing horizon exposed in the test pit was collected to estimate luminescence age. The k-feldspar grains were analyzed using the p-IR-IRSL protocol to estimate palaeodose. However, as in the case of Vemulapadu (Acheulian Levels), this sample showed a saturated luminescence signal (Fig. 4.3.3b). Therefore, no age estimation of the artefact-bearing horizon at Agraharam was possible. However, an equivalent dose of 955 Gy was estimated from two discs and considering the dose rate as 2 Gy per ka (this average was estimated based on dose rate measurements from other sites in the region), the burial age of artefact bearing horizon may be > 477 ka. This being the minimum age, clearly indicates the artefacts from A. Agraharam are certainly older than 477 ka.

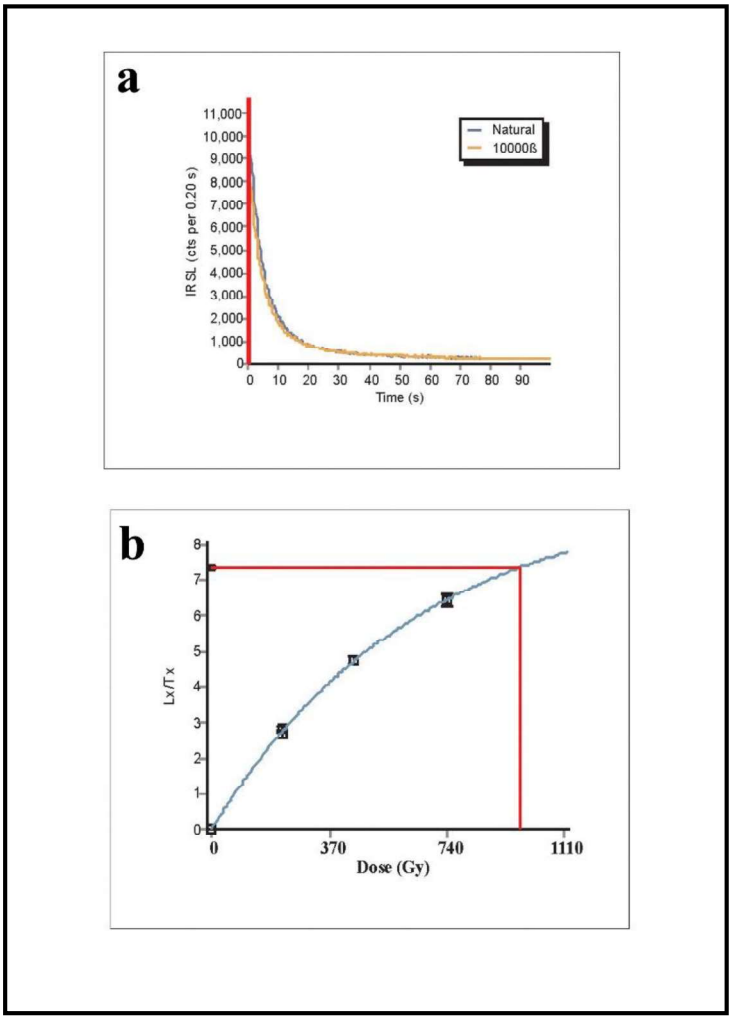

Figure. 4.3.3: Results of p-IR-IRSL analyses of sample from artefact bearing horizon. a: typical feldspar shine down curve; b: typical growth curve showing saturation of the signal.

4.3.3 Lithic Technology

The whole assemblage was made of quartzite from the adjacent Velikonda hills in the form of slabs and chunks. Except for two slightly abraded artefacts, the rest of the assemblage is in mint condition, indicating a recent exposure of the artefacts. The unretouched component consisting of flakes of varying size – large flakes (>10 cm in length) and debitage (< 2 cm in length) – dominate (59.31%) the assemblage (Table. 4.3.1). Many of the large flakes show prepared platforms and complex dorsal scar patterns probably suggesting the existence of prepared core technology on giant cores (Fig. 4.3.4). However, no such cores were noted in the assemblage except for one unprepared giant core.

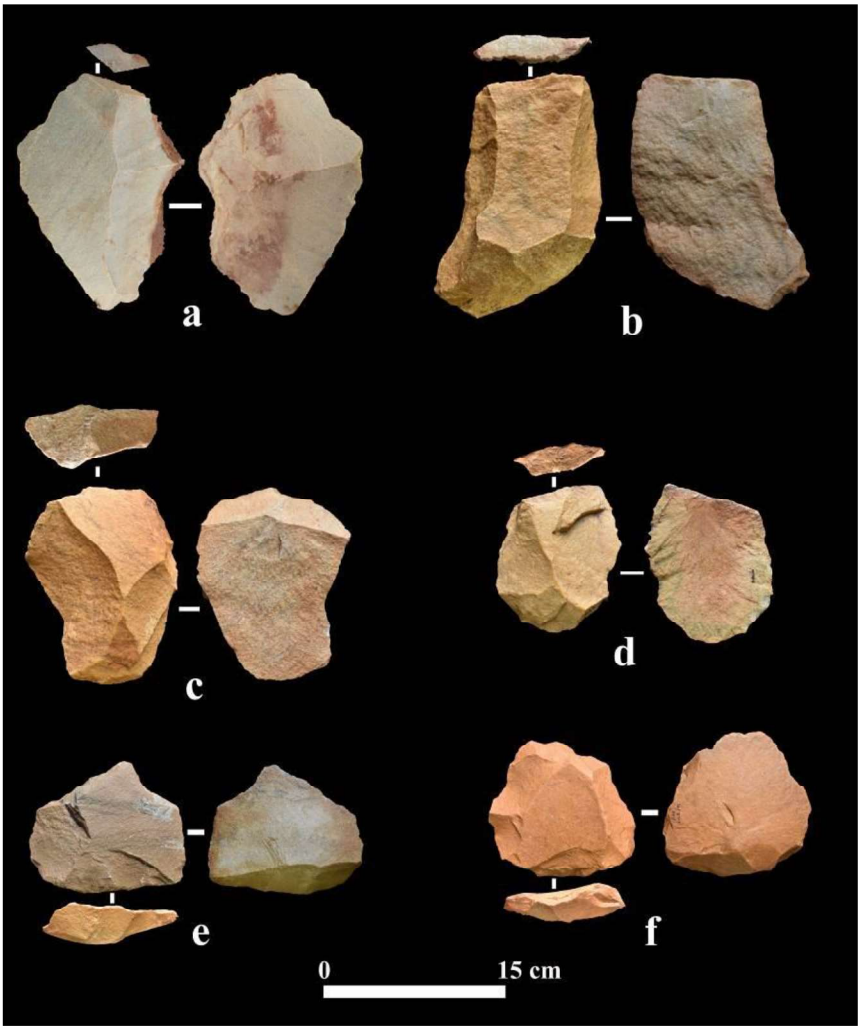

Figure. 4.3.4: Large flakes recovered from the site. a to d: large flakes with prepared platforms; e and f: retouched large flakes.

Table. 4.3.1: Composition of the assemblage from Locality I & II and test pit.

Typology	Locality I	%	Locality II	%	Test Pit	%	Total	%
Bifaces								
Handaxe	16	3.49	24	8.05	0	0.00	**40**	5.10
Cleaver	4	0.87	4	1.34	0	0.00	**8**	1.02
Biface with Invasive Flake Scar	1	0.22	6	2.01	0	0.00	**7**	0.89
Total Biface	**21**	**4.58**	**34**	**11.41**	**0**	**0.00**	**55**	**7.02**
Cores								
Preferential Surface Core	25	5.45	14	4.70	0	0.00	**39**	4.97
Discoidal core	9	1.96	7	2.35	1	3.70	**17**	2.17
Simple flake core	12	2.61	3	1.01	1	3.70	**16**	2.04
Preferential Levallois core	1	0.22	3	1.01	0	0.00	**4**	0.51
Core on a flake	1	0.22	1	0.34	0	0.00	**2**	0.26
Laminar flake core	1	0.22	0	0.00	0	0.00	**1**	0.13
Unidirectional core	1	0.22	0	0.00	0	0.00	**1**	0.13
Giant Core	0	0.00	1	0.34	0	0.00	**1**	0.13
Core fragment	15	3.27	4	1.34	1	3.70	**20**	2.55
Total Core	65	14.16	33	11.07	3	11.11	**101**	12.88
Retouched								
Bifacial Point	27	5.88	21	7.05	0	0.00	**48**	6.12
Tanged point	4	0.87	7	2.35	0	0.00	**11**	1.40
Point	4	0.87	4	1.34	1	3.70	**9**	1.15
Retouched flake	42	9.15	33	11.07	5	18.52	**80**	10.20
Scraper	6	1.31	4	1.34	0	0.00	**10**	1.28
Chopper	1	0.22	0	0.00	0	0.00	**1**	0.13
Core Scraper	0	0.00	1	0.34	0	0.00	**1**	0.13
Notch	1	0.22	0	0.00	0	0.00	**1**	0.13
Retouched core fragment	1	0.22	0	0.00	0	0.00	**1**	0.13
Knife	0	0.00	1	0.34	0	0.00	**1**	0.13
Total Retouched	86	18.74	71	23.83	6	22.22	**163**	20.79
Unretouched								
Flake	194	42.27	92	30.87	18	66.67	**304**	38.78

Large flake	4	0.87	1	0.34	0	0.00	**5**	0.64
Debitage (< 2 cm in length)	89	19.39	67	22.48	0	0.00	**156**	19.90
Total Unretouched	287	62.53	160	53.69	18	66.67	**465**	59.31
Total	**459**	**100**	**298**	**100**	**27**	**100**	**784**	**100**

Bifaces include both the handaxes and cleavers in the assemblage. Bifaces form 7.02% (n=55) of the assemblage with ~ 6:1 handaxe and cleaver ratio. Flakes were the most preferred blank types to make the bifaces, but slabs and cobbles were also used (Table. 4.3.2). Due to more intensive flaking on the flakes to produce bifaces, where attributes of platform preparations and positive bulb of percussion were modified, it became near impossible to identify the strike orientation.

Table. 4.3.2: The classification of the biface assemblage by type and blank

Biface Type	**Blank Type**			
	Flake	**Slab**	**Cobble**	**Total**
Handaxe	29	12	6	**47**
Cleaver	8	0	0	**8**
Total	**37**	**12**	**6**	**55**

Among the 37 bifaces, only 17 show clear strike orientation: nine were end-struck, and eight were side-struck flakes. Few bifaces retain original platform preparation, including single and multiple flake scars and facetted dihedral platforms. Similar platform preparations are also observed in the production of large flakes. There is moderate variation among the length of bifaces (Table. 4.3.3), as there are 11 bifaces that are less than 100 mm in length, however, width and thickness show minimal variations.

Table. 4.3.3: Mean values of the metrical attributes recorded for Bifaces.

Attributes	**Mean (mm)**	**Standard deviation**	**Min**	**Max**
Length	118.43	34.12	70.76	216.22
Width	76.36	15.4	47.20	105.33
Thickness	32.47	9.91	17.31	58.83
Elongation	1.55	0.25	1.10	2.15
Refinement	0.42	0.09	0.23	0.62
Plan Symmetry	3.53	1.43	1.82	8.80
Profile Symmetry	4.63	2.11	1.53	11.48

Elongation denotes the relation between the biface length and width. South Asian Acheulian assemblages reveal a broad spectrum of variation with long, elongated, and thick bifaces at one end and short, broad, and thin bifaces at the other end (Shipton, 2016). The mean elongation value of the A. Agraharam bifaces lie within the latter end of the spectrum (Fig. 4.3.5). Creating a thin biface requires more refinement as it is difficult to achieve thinness without losing the width. Usually, the biface thickness-to-width ratio is used as the refinement index. Bifaces from A. Agraharam are thin and well-refined and lie at one end of the distribution of mean refinement values of the known Indian assemblages (Fig. 4.3.6 & 4.3.7). Bifaces are deliberately made symmetrical by the knappers (Wynn, 2000). The mean value of plan symmetry (Table. 4.3.3) indicates that a high level of symmetry was achieved for the A. Agraharam bifaces. Plan symmetry is relatively easy to impose on bifaces, whereas imposing profile symmetry is difficult as it involves controlling biface thickness (Shipton, 2016). Moderate profile symmetry can be seen for A. Agraharam bifaces with a mean value of 4.63 as per (Hardaker & S. Dunn, 2005) scheme.

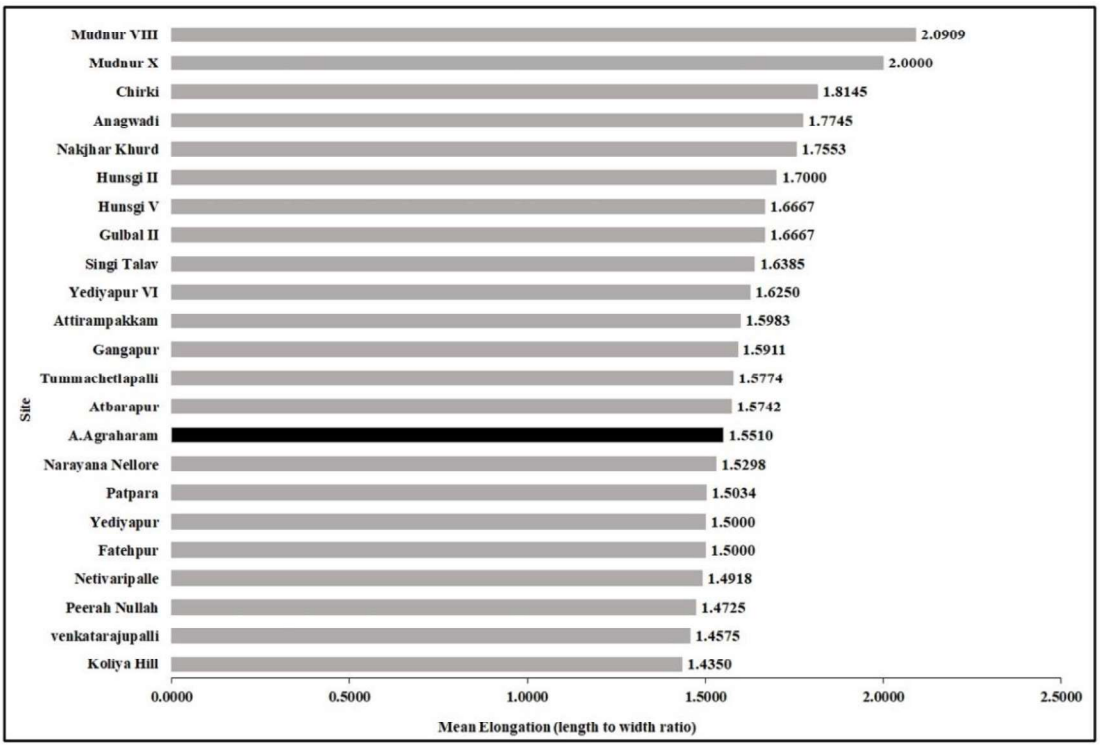

Figure. 4.3.5: Variation in mean biface elongation (length to width ratio) for Indian assemblages. Comparative data from (Chauhan, 2010; Gaillard et al., 1986, 2008; Paddayya & Petraglia, 1993).

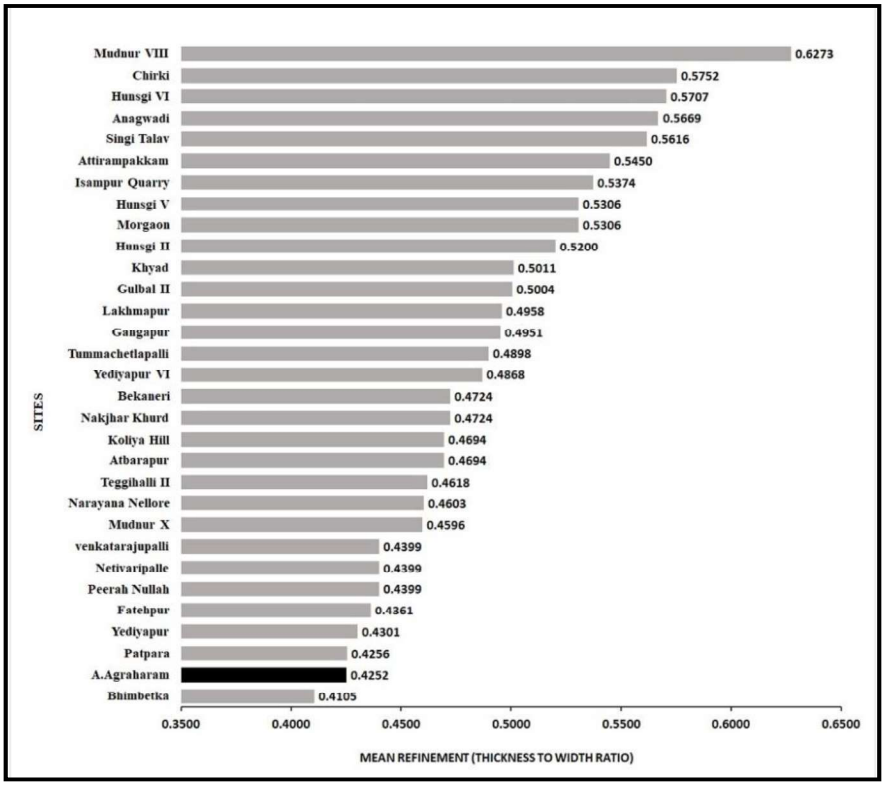

Figure. 4.3.6: Variation in mean biface refinement (thickness to width ratio) for Indian assemblages. Comparative data from (Shipton, 2016). Note that A. Agrahara, occurs next to the Bhimbetka on one end of the distribution, while assemblages with Early Pleistocene age estimates occur on the other end of the distribution.

The core component of A. Agraharam consisting of 101 pieces, forms 12.88% of the total assemblage (Table 4.3.1). The dominant category is preferential surface cores (4.97%), followed by discoidal cores (2.17%) and simple flake cores (2.07%). The other categories of cores include Levallois cores, core-on-flake, laminar flake cores, giant cores, and core fragments. The preferential surface cores are a variant of the hierarchical core reduction strategies where the core surface is exploited rather than the volume (Zaidner et al., 2018). The preferential surface cores exhibit Levallois-like volumetric conception with two hierarchical surfaces organized as flaking surface and platform surface; the fracture plane of the flakes is parallel to the plane of intersection between flaking and platform surfaces (Zaidner et al., 2018). However, the crucial aspect of the Levallois technology, i.e., the predetermination and preparation of the flaking surface (Boëda, 1995), does not seem to be standardized in the case of preferential surface cores (Fig. 4.3.8c). Also, the platform surface shows limited or no preparation to remove the flakes (Zaidner et al., 2018). The removal of flakes on the flaking surface ranges from a single removal to multiple removals radially.

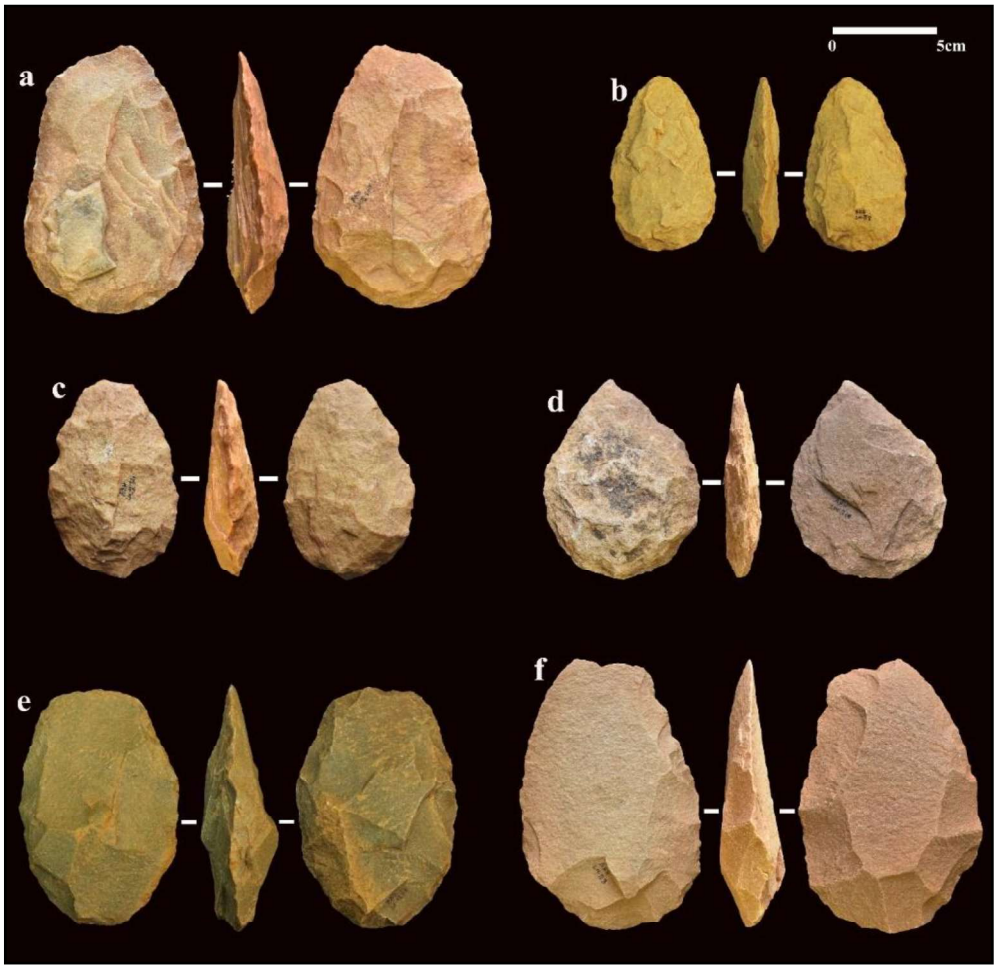

Figure. 4.3.7: Refined, symmetrical bifaces from A. Agraharam. a to d: Handaxes; e and f: Cleavers.

The second-largest category among the cores is discoidal cores. These cores were exploited on both sides resulting in a typical discoid shape (Fig. 4.3.8d and e). Simple unprepared cores with amorphous shapes are also present in the assemblages. The aforementioned three core types are the dominant categories in the assemblage. However, a few Levallois cores were recovered from the site (Fig. 4.3.8g and h). Even though there is evidence of the existence of giant core technology at the site, only one giant core was recovered from Cluster II. The cores at the site with prepared and unprepared cores and debitage form the dominant category in the assemblage.

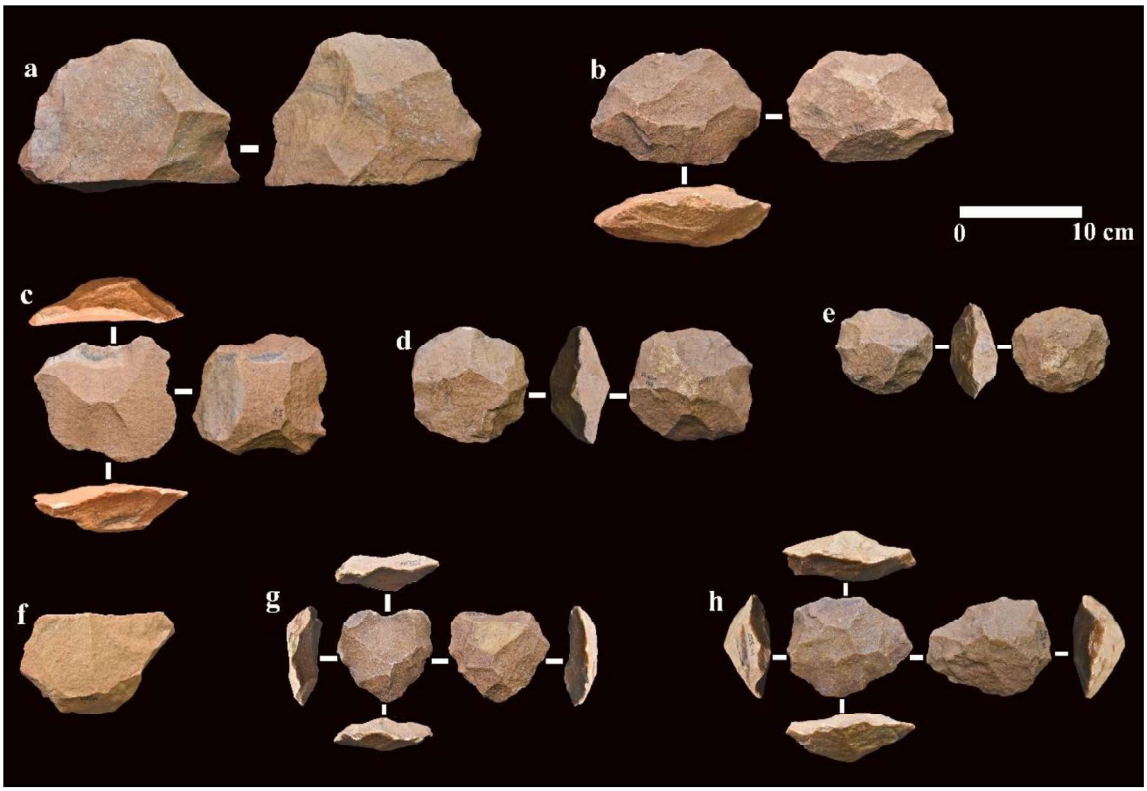

Figure. 4.3.8: Cores from the assemblage. a: Giant core; b and c: preferential surface cores; d and e: discoidal cores; f: laminar flake core; g and h: Levallois cores.

Slightly less than half of the cores (45.74%) show no cortex, whereas 25.53% in the assemblage has 10% cortex. Cores with 20%, 30%, 40%, 60% and 70% cortex are present in 9.57%, 7.45%, 7.45%, 2.13% and 2.13% respectively. The core's mean length, medial width and medial thickness are 76.29x73.72x31.26 mm when oriented along the flaking axis (last flake scar) (Table 4.3.4). The core's proximal, medial, and distal widths measured along the flaking axis are 73.85x73.72x70.02 mm, respectively indicating no significant changes in the core width. The proximal shape of the cores is relatively straight (mean 0.90 mm) whereas distal shape is tapering (mean 1.20 mm). No considerable variation in core elongation, ranging between 0.46 - 1.38, is observed; maybe because no significant variation in the cores' mean length and mean medial width. The core flatness index ranges from 1.32 to 4.55, where most cores are wider than thick. Three cores have cortical platforms, 15 cores have single conchoidal platforms, and 14 cores shows multiple conchoidal platforms. Platforms were facetted on 20 cores and in 12 instances, no preparation is observed. The last scar-face length of cores is less than the axial core length, indicating the flaking face is limited to the smaller axial surface. The last scar lengths range from 18.17-77.58 mm, with an average of 41.46 mm, and the last scar widths range between 10.84-81.90 mm, and a mean of 31.40 mm. On average, last flake scar elongation indicates that relatively square-shaped flakes were removed (mean=1.42). Half of

the of the last flake scars exhibit feather terminations (50.57%), with non-feather terminations accounting for 49.42%. A maximum of seven and minimum of one core rotations were observed on cores. Most cores show three (n=30), two (n=15) and one (n=16) major scars (more than 1/3 core length), with 11 cores exhibiting four scars. There are six cores with five scars, two cores with six scars and one core with eight scars.

Table. 4.3.4: Statistical data for the Core attributes.

Attribute	N	Mean	SD	Min.	Max.
Length	81	76.29	16.86	37.91	133.18
Proximal Width	81	73.85	20.37	35.18	177.76
Medial Width	81	73.72	21.93	22.50	156.31
Distal Width	81	70.02	19.19	37.08	121.18
Proximal Thickness	81	24.88	7.63	12.66	54.39
Medial Thickness	81	31.26	7.86	17.28	56.03
Distal Thickness	81	27.75	10.01	13.07	78.33
Proximal Shape	81	0.90	0.12	0.48	1.16
Distal Shape	81	1.20	0.12	0.89	1.57
Elongation	81	0.89	0.19	0.46	1.38
Flatness	81	2.55	0.65	1.32	4.55
No. of Core Rotations	81	3.59	1.52	1.00	7.00
Last Platform Angle	81	70.51	13.21	40.00	108.00
Last Scar Length	81	39.47	18.92	16.67	143.87
Last Scar Width	81	47.11	19.76	19.43	151.88
Last Scar Elongation	81	0.86	0.27	0.42	1.73

Flakes (n=421), including the retouched ones, form 53.69% of the assemblage (Table 4.3.5). These flakes are classified into technological types to identify the position of each flake in a reduction sequence. Distinguishing flakes from the biface reduction sequence and prepared core reduction sequence (e.g., Levallois) becomes difficult owing to the morphological similarities of the debitage between the two reduction sequences. However, following the attributes suggested by (Akhilesh & Pappu, 2015; Delagnes, 1993; Newcomer, 1971), flakes were classified into various stages of biface and core reduction sequences (Table 4.3.5). It is hard to distinguish between the biface roughout flakes and core roughout flakes, so the roughout flakes mentioned in Table 4.3.5 represent both biface and core reduction sequences. The relatively smaller number of roughout flakes in the assemblages indicates that the initial

dressing of the bifaces and cores were done at raw material procurement sites, probably the Velikonda hills.

Table. 4.3.5: Flake component of the assemblage.

Technological Type	Unretouched	%	Retouched	%	Total	%
Roughout flakes	29	9.35	7	6.31	36	8.55
Biface thinning & shaping flakes	39	12.58	16	14.41	55	13.06
Biface Finishing flakes	49	15.81	5	4.50	54	12.83
Prepared core flake	35	11.29	52	46.85	87	20.67
Core preparation flakes	150	48.39	28	25.23	178	42.28
Indeterminate	8	2.58	3	2.70	11	2.61
Total	**310**	**100**	**111**	**100**	**421**	**100**

Flakes that are part of the core reduction sequence dominate the flake component with 63% which implies the predominance of prepared core technology. Transverse flakes (flakes having wide distal end) with prepared platforms and having a distinct morphology (Fig. 4.3.9) were noted in the assemblage. Probably these flakes are struck from the sides of the core/biface which gave the flakes a transverse shape. Some of these flakes reveal long platforms that extend over to lateral margins (Fig. 4.3.9a to e). Among the 56 transverse flakes, 29 were retouched into informal retouched flakes, points, tanged points, and scrapers. Whether these flakes were produced through any of the known core reduction methods (e.g., Discoid, Levallois, etc) or any other distinct core reduction procedure is yet to be understood. Flakes of both prepared and unprepared cores were preferred for expedient retouching (Table 4.3.5). Contrasting to this, formal retouched tools are less in the assemblage. Overall, the flake component of the assemblage suggests an intentional production of flakes, however, the further modification of flakes is limited to informal retouch only.

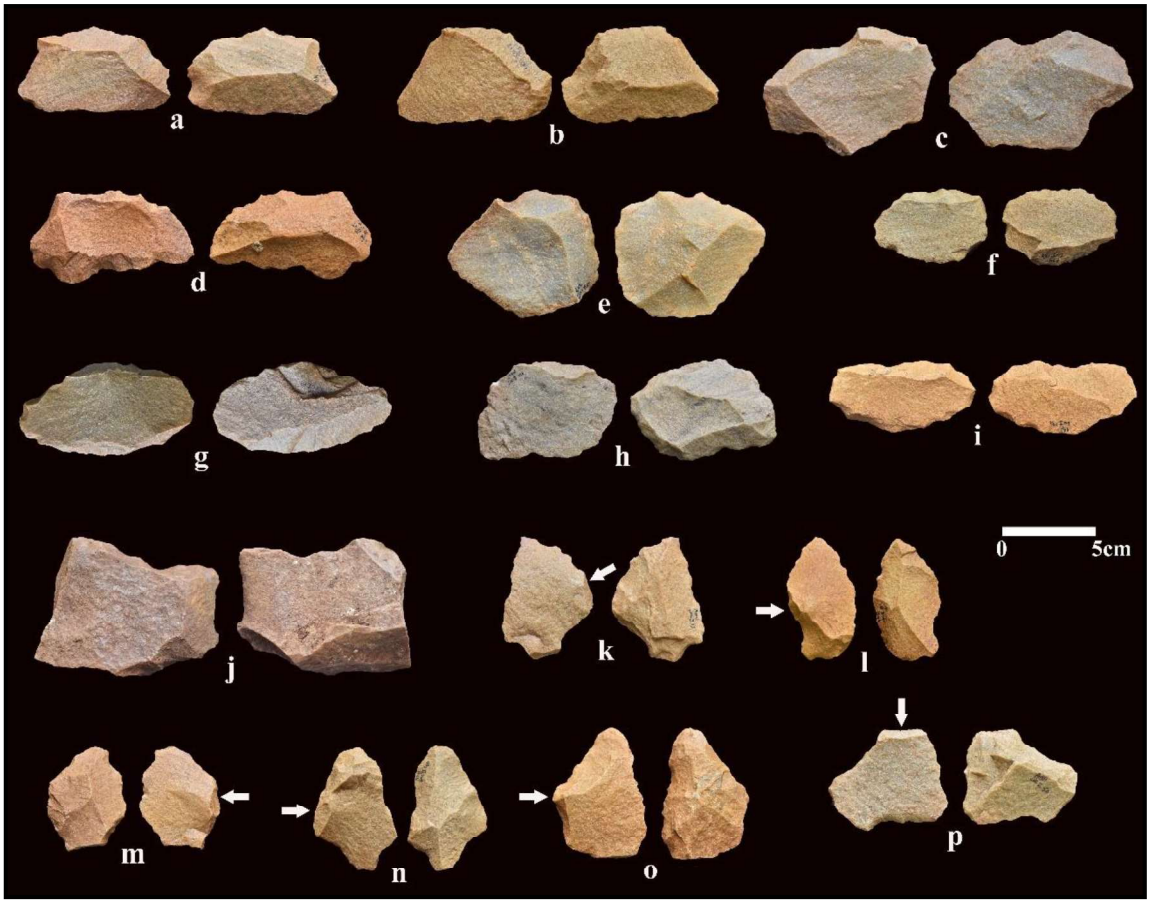

Figure. 4.3.9: Transverse flakes from the assemblage. a to e: transverse flakes with platforms extend over to lateral margins; f to i: transverse flakes with prepared platforms; j: transverse flake recovered from test pit; k to n: tang like point made on a transverse flake (arrows indicate the position of the platform); o: Bifacial point made on a transverse flake; p: notch made on a transverse flake.

Morphometrical description of the flakes are limited to intact flakes in the assemblage that are 397 in number. Wide range of technological diversity is evident amongst the flakes from biface preparation to core preparation flakes and prepared core flakes. Mean axial flake dimensions are 54.75 x 55.17 x 15.25 mm (LxWxT); on average, flakes are squarish in shape (mean elongation=1.02) (Table 4.3.6). Typical flakes are more than four times wide as they are thick (mean flatness=3.76), with a range of 1.35-8.45. 66.39% of the flakes exhibit slightly expanding proximal margins (mean proximal shape=0.79), with 33.60% exhibiting contracting proximal margins, leading to an upper proximal shape index of 1.19. In contrast, the distal shape indicates that 80.73% of the flakes exhibit distal contracting margins (mean=1.42). Multiple conchoidal (42.39%) and single conchoidal (42.80%) platforms are the most common type, followed by dihedral (11.11%), cortical (1.23%), punctiform (0.41%) and indeterminate (2.06%). Platform preparation is dominated by facetted platforms with 65.57%, followed by

overhang removal (6.14%) and none (28.27%). A wide range in platform size is evident, with platform width ranging from 4.70-92.80 mm and platform thickness ranging from 2.10-44.90 mm. The platform shape index indicates that platforms are typically elongate (mean=3.24), with 84% of platforms are two times wider than they are thick. The most common dorsal scar patterns present on complete flakes in the assemblage are weakly radial (42.85%), followed by radial (10.34%), proximal (16.74%), indeterminate (29.55%) and cortical (0.49%). Cortical coverage ranges from 0-100%, with 85.64% of flakes recorded with no cortex present and 6.44%, 1.98%, 2.48%, 1.98%, 0.50%, 0.99% with 10%, 20%, 30%, 40%, 50% and 100% cortex present respectively. Feather terminations are present on 72.06%, followed by step (21.08%) terminations and indeterminate 6.86%.

Table. 4.3.6: Statistical data for flake attributes.

Attribute	N	Mean	SD	Min.	Max.
Length	397	54.75	33.07	15.00	197.54
Proximal Width	397	48.96	18.75	4.90	125.20
Medial Width	397	55.17	19.90	17.90	122.10
Distal Width	397	44.58	18.41	10.80	104.60
Medial Thickness	397	15.25	5.35	3.60	37.58
Elongation	397	1.02	0.36	0.33	2.54
Flatness	397	3.76	1.23	1.35	8.45
Proximal Shape	397	0.90	0.23	0.15	1.51
Distal Shape	397	1.32	0.38	0.68	2.95
Platform width	397	40.23	20.11	4.70	92.80
Platform Thickness	397	13.42	6.45	2.10	44.90
Platform Shape	397	3.24	1.45	0.44	10.55
Platform area	397	633.82	551.64	15.33	2940.95
Dorsal scar count	397	2.72	1.42	0	8

Retouched tools form around 20.79% of the total assemblage (Table 4.3.7). Even though flake production through prepared and unprepared core reduction is dominant at the site, formal retouched tools are less in numbers and form only 4.3% of the assemblage. Flakes with informal retouch forms 50% of the retouched tools (Table 4.3.7). Prepared core flakes (n=46) were preferred to make these informal tools, however, unprepared core flakes and a few quantities of biface and core reduction debitage (e.g., roughout flakes, thinning & shaping flakes, etc.) were also used. The informal retouch does not show any pattern or standardization. Flakes were retouched randomly on ventral and dorsal sides, on the distal end and both lateral margins.

Table. 4.3.7: Classification of retouched artefacts.

Tool Type	Quantity	%
Bifacial point	48	29.45
Tanged point	11	6.75
Point	9	5.52
Retouched flake	80	49.08
Scraper	10	6.13
Chopper	1	0.61
Core Scraper	1	0.61
Notch	1	0.61
Retouched core fragment	1	0.61
Knife	1	0.61
Total	**163**	**100**

Scrapers (n=10; 6.3%) are few in the assemblage and are made on prepared core flakes, roughout flakes, and thinning & shaping flakes. Points are the second largest category in the retouched tool type with a frequency of 41.7%. Bifacial points are the most preferred type among the points. Flakes, small pebbles, and slabs were used to make bifacial points. The bifacial points show variability in shapes and sizes (Fig. 4.3.10). Metrical dimensions of the bifacial points are 85.06x57.52x26.86mm (LxWxT). Some of the points show basal modifications (Fig. 4.3.10a, b, h, j, and k) which must have facilitated hafting. A few flakes, particularly the transverse flakes, were also retouched into points (Fig. 4.3.9) and some of these points also show basal modifications (e.g., tang) (Fig. 4.3.9k to n and Fig. 4.3.11b to h) like bifacial points. Bifaces used as cores to remove preferential flakes are also recorded in the assemblage (Fig. 4.3.12). Overall, the tool category was dominated by informally retouched flakes and points.

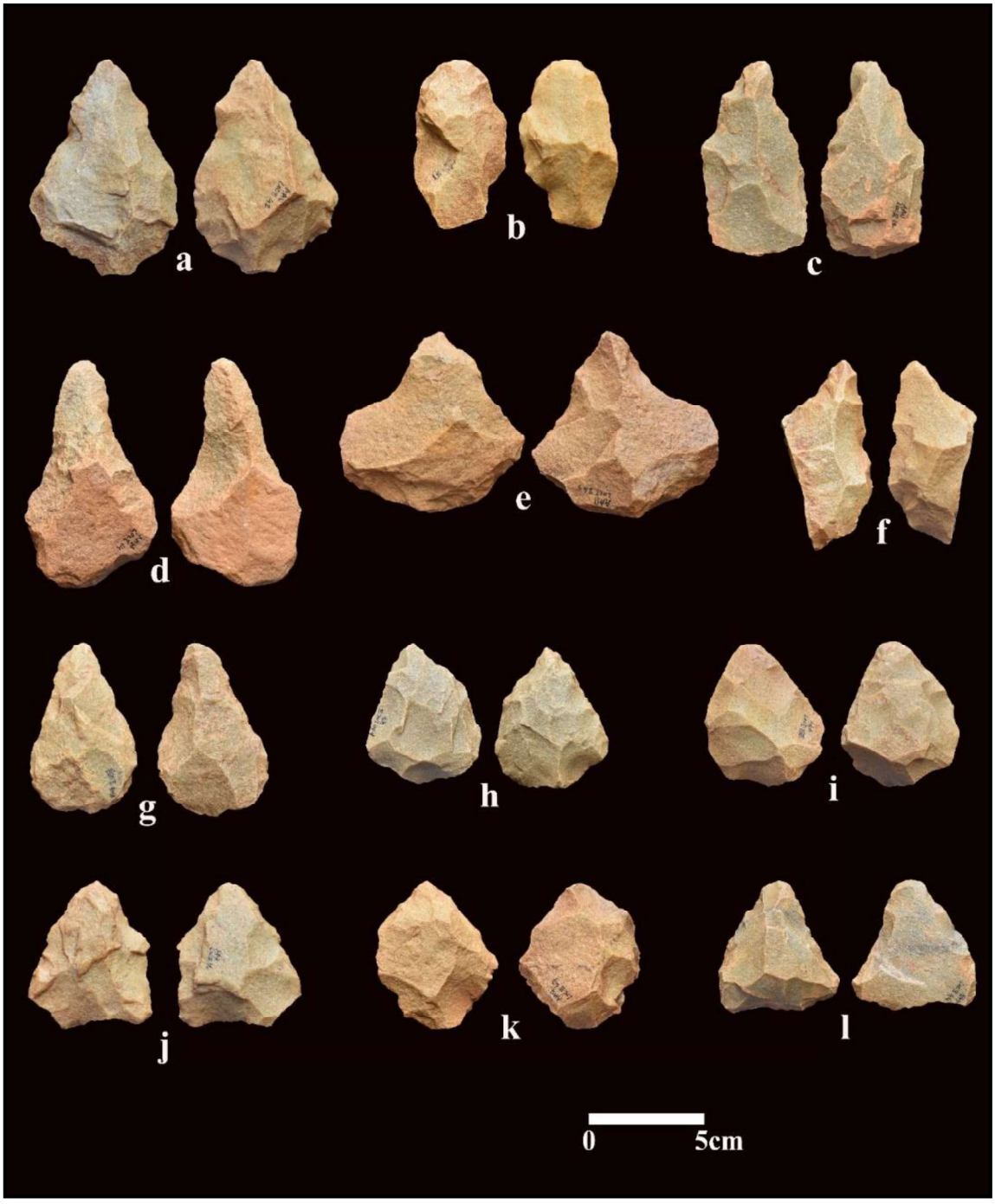

Figure. 4.3.10: Bifacial points. a, b, h, j, k: Bifacial points with basal modifications; c to g and i, l: bifacial points.

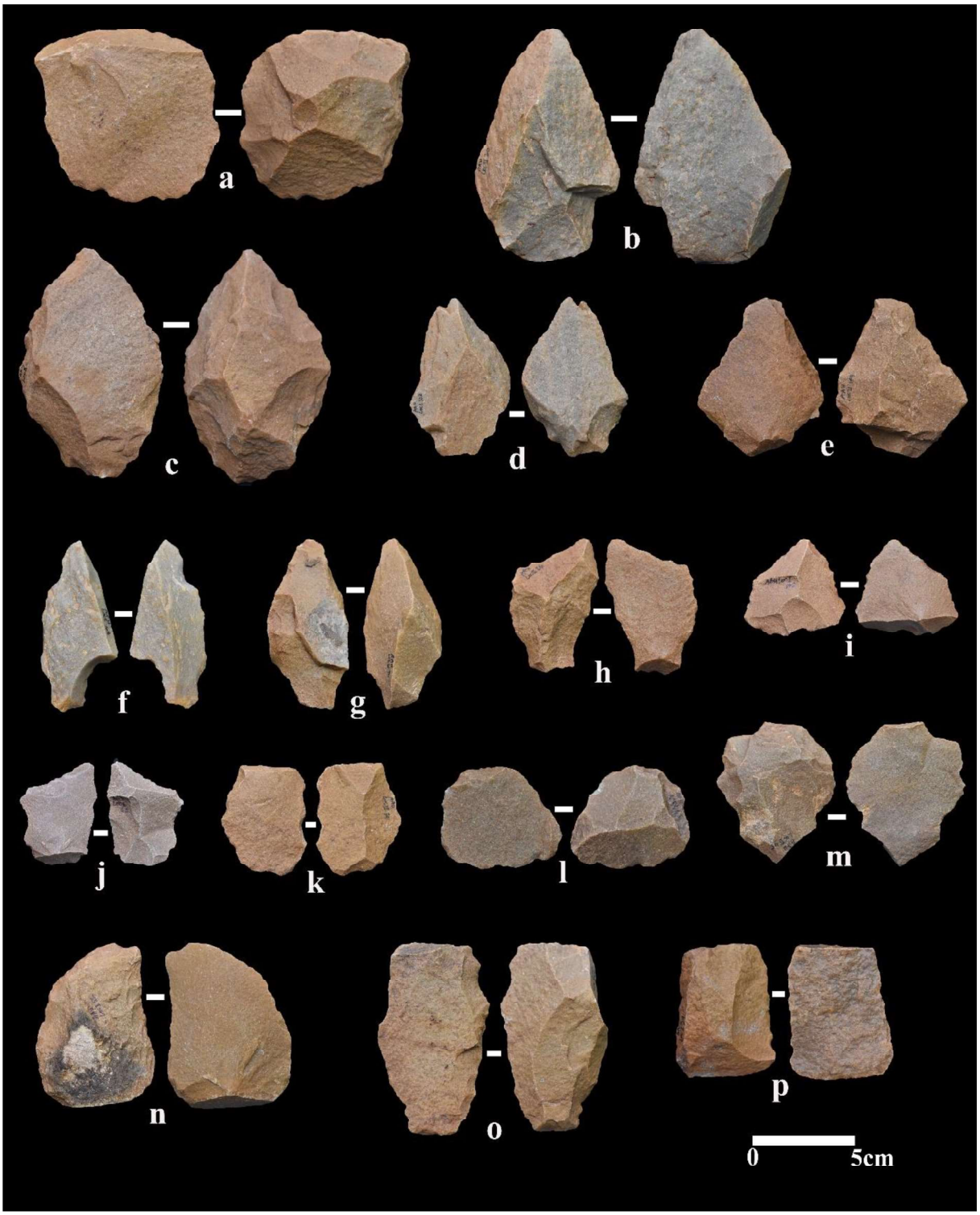

Figure. 4.3.11: Flake tools. a: Split discoidal core; b to h: points with basal modifications (tangs); I and j: points on prepared core flakes; k to m: prepared core flakes; n: Scraper; o and p: Laminar flakes.

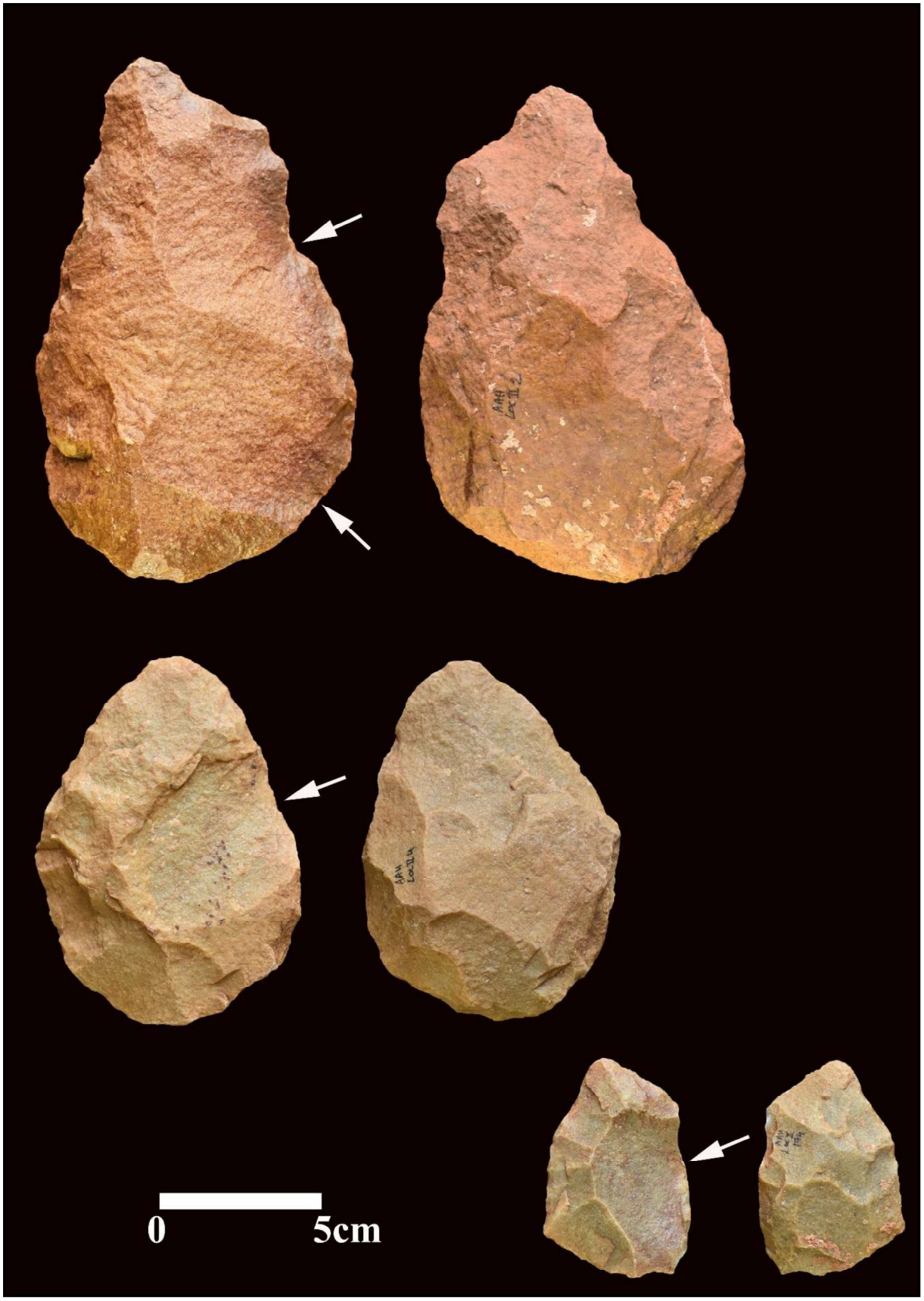

Figure. 4.3.12: Handaxes with preferential flake removals.

4.3.4 Summary

The assemblage from A. Agraharam was collected using a systematic grid laid out on the freshly exposed artefact cluster. Even though the assemblage is collected from the surface, only two artefacts are slightly abraded suggesting recent exposure of the artefacts. 86% of the assemblage shows similar patina indicating the same geological context of the assemblage. The presence of debitage less than 2 cm in length and other flakes (e.g. roughout flakes, core preparation flakes) that are part of the reduction sequence demonstrate the primary nature of the assemblage. However, The presence of a relatively high proportion of cores with no and less than 10% cortical surfaces, including platform surfaces, indicates that primary stages of core reduction sequence must have taken place at raw material sources. This observation is further supported by the dominance of formal core reductions such as Preferential and discoidal core types. The whole assemblage comes from two clusters separated by 1.2 km and they do not show any significant variations in their composition. However, artefacts from Cluster-II are less in number than artefacts from Cluster I, even though the area of Cluster II (100 sq. m) is greater than the area of Cluster I (50 sq. m). This may be due to the fact that the Cluster II was exposed by anthropogenic activities which must have caused the displacement of some portion of the assemblage. Based on the aforementioned observations it can be presumed that the whole assemblage is in primary context with little temporal variations.

The artefact assemblage from A. Agraharam shows characteristics of both the Large Flake Acheulian and Early Middle Palaeolithic, the latter being dominant. The Large Flake Acheulian is represented by the presence of large flakes (> 10 cm in length) with giant cores, well-made handaxes, and cleavers. The mean elongation, refinement, and profile & plan symmetry values of the bifaces show close similarities with the Late Acheulian assemblages reported in South Asia (Shipton, 2013, 2016; Shipton et al., 2013). There are a few instances of handaxes being used as cores to produce flakes and such examples were also noted in Europe and Levant in the terminal Acheulian contexts (Petraglia et al., 2003; Rolland, 1995; Tuffreau, 1995; White & Pettitt, 1995). Prepared core technology and its debitage dominates the assemblage at A. Agraharam with some definite evidence of Levallois core reduction. However, preferential surface cores that are a forerunner to the Levallois technology (Bolton, 2015) are abundant in the assemblage. Together with discoidal and other simple core reduction strategies, the core technology at the site is represented by a variety of core reduction strategies aimed at producing flakes. Even though the flake production was dominant at the site most of the flakes were limited with informal retouch. However, a few flakes were used to make scrapers and points.

Notably, bifacial points made on pebbles, slabs, and flakes are abundant among the retouched categories. Some portion of the points and bifacial points shows basal modifications and tangs indicating possibilities of hafting technology.

Overall, the lithic assemblage from A. Agraharam represents an overlapping of the Late Acheulian and early prepared core technologies which is a typical character of transitional assemblages. Besides, the presence of points and bifacial points with basal modifications suggest a preference for hafting which is a characteristic feature of Middle Palaeolithic. The luminescence age estimations of the artefact bearing horizon places the assemblage probably in the mid Middle Pleistocene with a minimum age of 477 ka.

4.4 Nandanavanam

The site Nandanavanam is located on the upper reaches of the Paleru river basin, Prakasam District, Andhra Pradesh (Map. 4.4.1). It is situated close to the A. Agraharam palaeolithic complex and shares similar geological and geographical setting. However, in terms of cultural material, both sites show very distinct material remains.

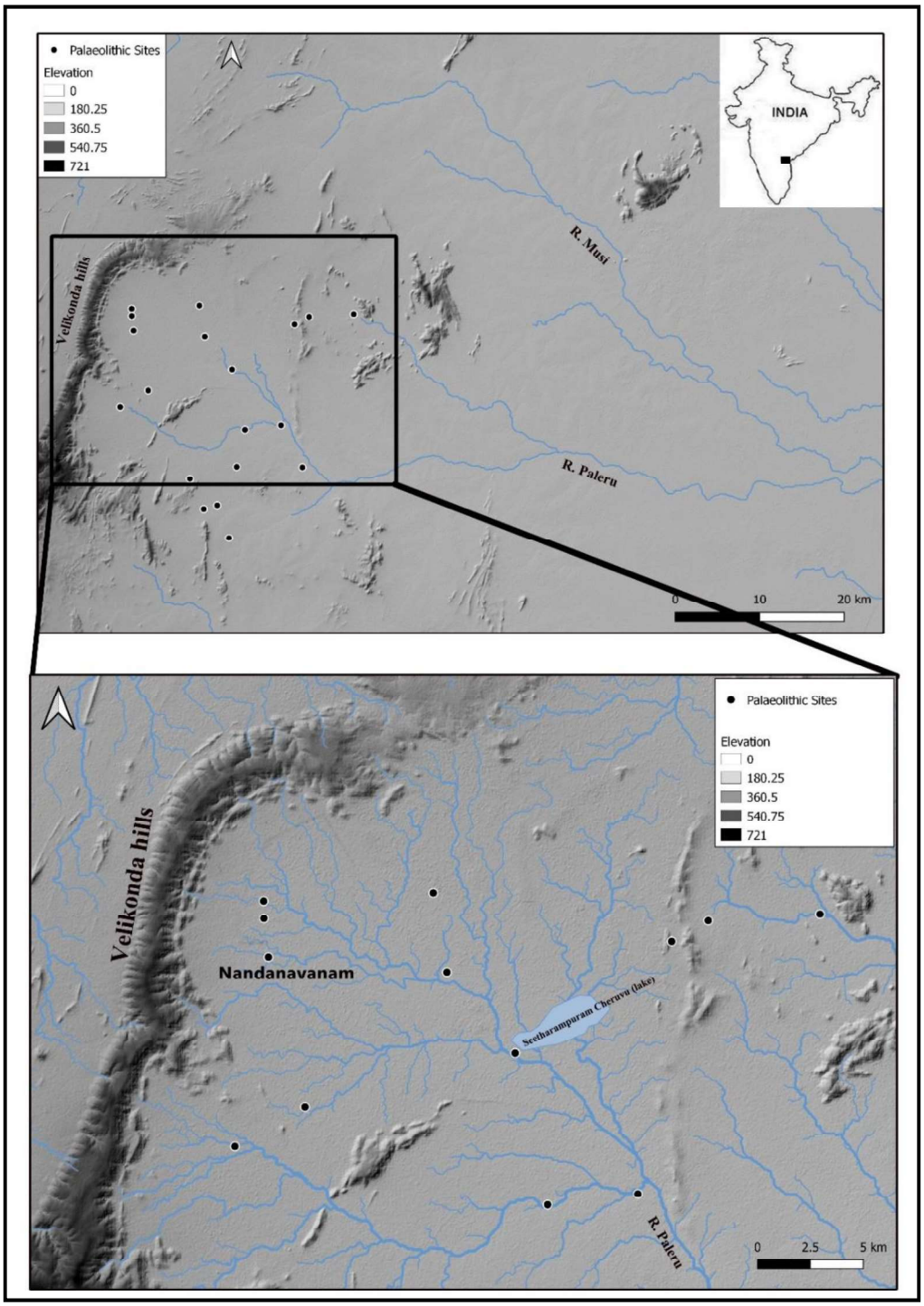

Map. 4.4.1: Map showing the location of Nandanavanam.

4.4.1 Stratigraphy

The site Nandanavanam is located at the foothills of the northern Velikonda hill range. This quarzitic hill range is a part of the eastern margin of the Cuddapah basin and was the main raw material source for tool making. Artefacts are found spread over an area of 15 sq. km to the south of the village Nanadanavanam. Several streams (1st and 2nd order) originating from the adjacent hill drains through the site complex and expose artefacts on the surface as several discrete clusters. A few of the above streams are relatively deep and are expanded in the recent past to conserve rainwater. These anthropogenic activities are also responsible for exposing the artefact bearing horizons (Fig. 4.4.1).

Figure. 4.4.1: Anthropogenic activities exposed artefacts bearing horizons at Nandanavanam.

Several such exposed sections were examined to understand the geological context of the artefacts. Shale bedrock forms the base of the lithology at the site (Fig. 4.4.2). The bedrock is overlain by tufa beds and there a few places where the tufa seems to have infiltrated into gaps in the shale bed rock. Greyish coloured silty clays, rich in carbonate nodules with gravels, rests on the tufa beds. Artefacts are observed to be eroding out from this layer (Fig. 4.4.3b and c). This artefact bearing horizon is overlain by the reddish silty sand deposit with varying thickness across the site (Fig. 4.4.3a).

Figure. 4.4.2: Shale bed rock exposed at the site.

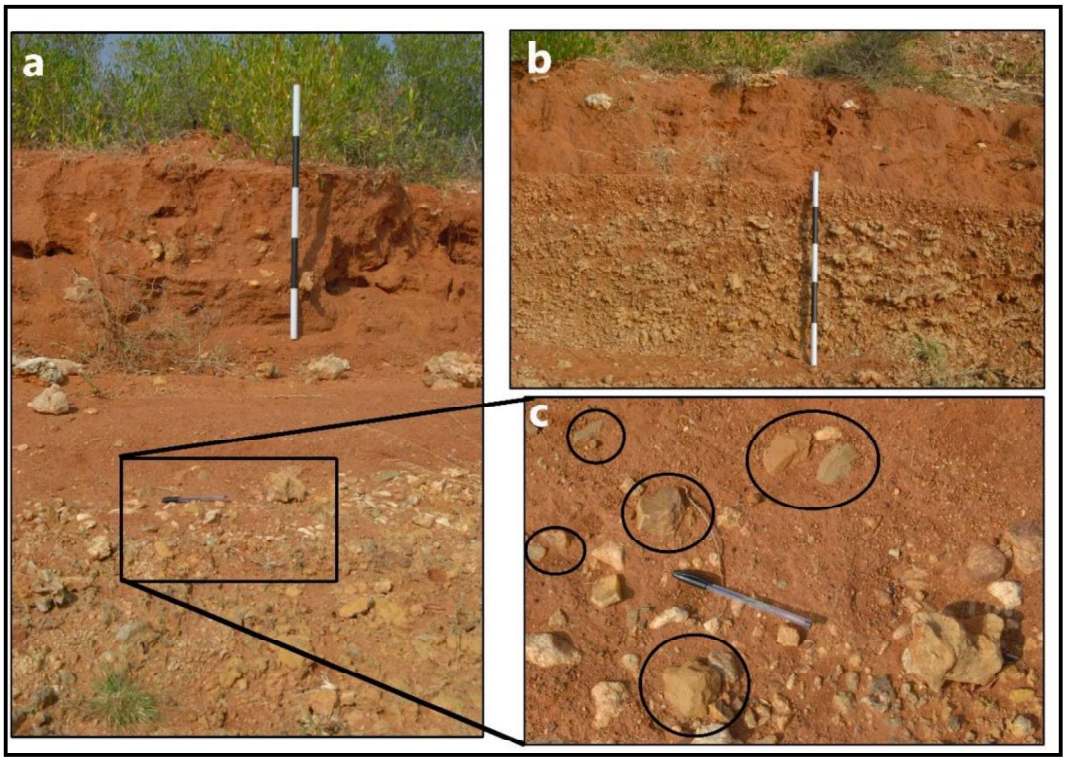

Figure. 4.4.3: Images showing the geological context of the artefacts. a: Artefact bearing horizon overlain by reddish sandy silts; b: artefact bearing horizon; c: In situ artefacts exposed.

To confirm surface observations and to collect samples for luminescence dating a small section of 50 cm width was scraped and two flakes were observed in situ within the greyish coloured sediment layer (Fig. 4.4.4) confirming the surface observations.

Figure. 4.4.4: Test pit showing the artefact bearing horizon.

4.4.2 Luminescence Chronology

Sediment sample from the artefact bearing horizon exposed in the test pit was collected to estimate luminescence ages. The k-feldspar grains were analysed using p-IR-IRSL protocol to estimate palaeodose. However, this sample also like Vemulapadu (Lower Levels) and A. Agraharam showed saturated luminescence signal (Fig. 4.4.5b). Therefore, no age estimation of the artefact bearing horizon at Nandanavanm was possible. But an equivalent dose of 964 Gy was estimated from two discs and considering dose rate as 2 Gy per ka (this average was estimated based on dose rate measurements from other sites in the region) the burial age of artefact bearing horizon may be > 482 ka. This is the minimum age, and it clearly indicates the artefacts from Nandanavanam are certainly older than 482 ka.

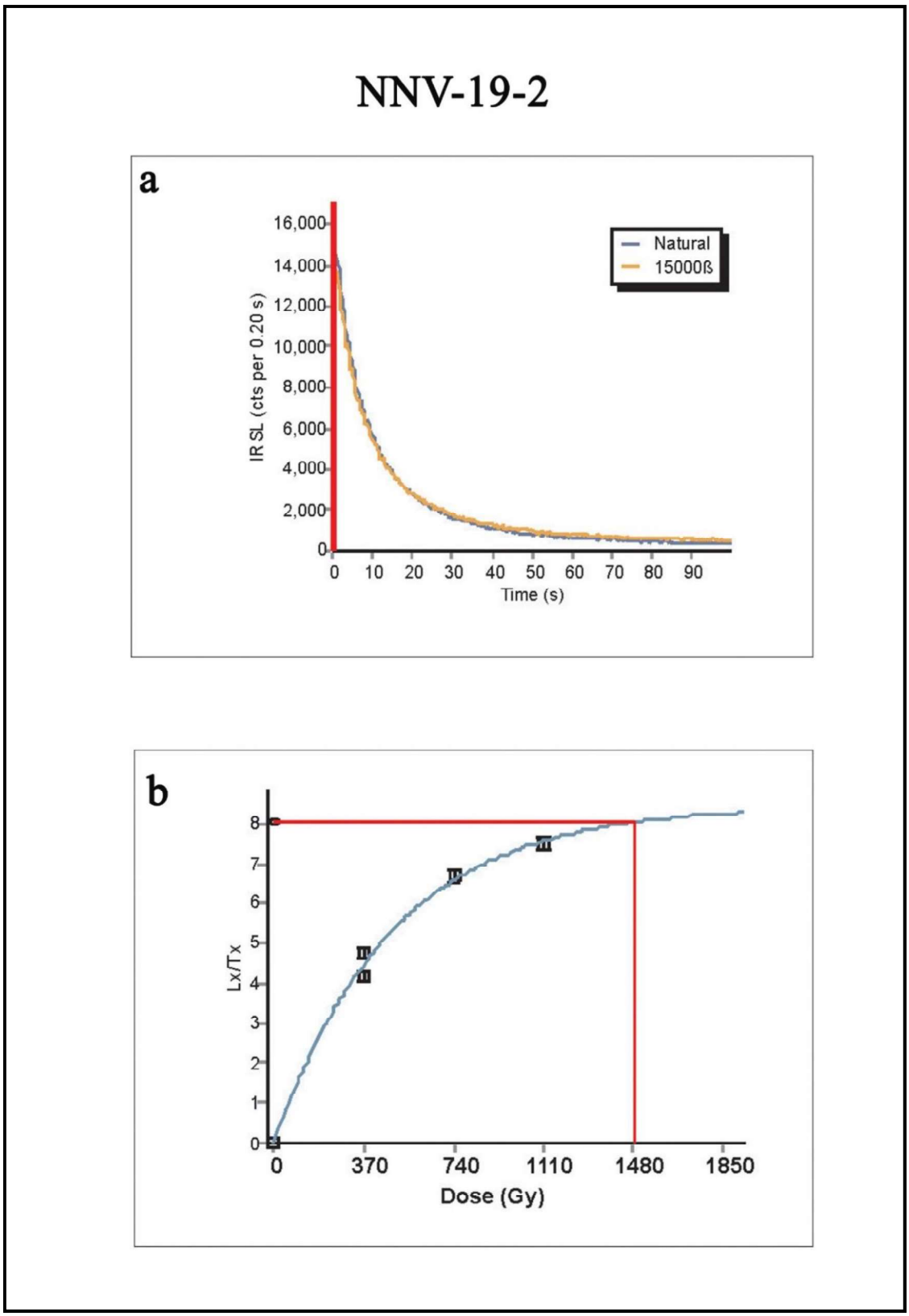

Figure. 4.4.5: Results of p-IR-IRSL analyses of sample from artefact bearing horizon. a: typical feldspar shine down curve; b: typical growth curve showing saturation of the signal.

4.4.3 Lithic Technology

A total of 241 artefacts were collected from an area measuring 50 X 50 m from the site. Natural exposures are very limited at the site unlike A. Agraharam (see Chapter 4.3). Here anthropogenic activities such as PWD works are a major factor for exposing artefacts. Due to shallow exposures the area of collection of artefacts was increased to 50 x 50 m which is five time bigger than the surface grids laid out at A. Agraharam. The artefacts were made of both fine and coarse quartzite, out of which the fine quartzite accounts for 12.30% and coarse quartzite accounts for 87.69% of the total assemblage. Artefacts were classified as broken and unbroken (intact) to identify and understand any specific breakage patterns either due to deliberate human activity or post depositional alterations. A large portion of the assemblage (88.71%) was found intact, flakes were considerably more damaged rather than cores and bifaces as flakes are usually thinner. Whereas the cores are mostly intact due to their robust nature compared to other tool types. Varying degrees of patina are noted on the artefacts; however, half of the assemblage does not show patina and 40% of the artefacts contain a low percentage of patina (Table 4.4.1).

Table 4.4.1: Percentage of Patina observed on Bifaces and Cores.

	Biface and Debitage	**Cores and Debitage**
High	2.11	2.00
Moderate	13.68	16.00
Low	41.05	40.00
Absent	43.16	42.00

The unretouched component consisting of flakes of various reduction strategies and in this category, debitage less than 2 cm in length dominate (51.87%) the assemblage (Table. 4.4.2). Four large flakes (more than 10 cm in length) were identified in the assemblage however, no giant cores were noted. Flakes (n=177), including the retouched ones, form 69.68% of the assemblage. The retouched category in the assemblage consists of a variety of finished tools (Table 4.4.2).

Table. 4.4.2: Typo-technological classification of the lithic assemblage at Nanadanavanam.

Typology	Quantity	%
Biface		
Hand Axe	16	**6.64**
Cleaver	3	**1.24**
Diminutive Handaxe	4	**1.66**
Handaxe with Preferential Flake Scar	1	**0.41**
Total Bifaces	**24**	**9.96**
Cores		
Preferential Surface core	6	**2.49**
Discoidal Core	8	**3.32**
Simple Flake Core	8	**3.32**
Radial Core	1	**0.41**
Total Cores	**23**	**9.54**
Retouched		
Side scraper	4	**1.66**
End Scraper	14	**5.81**
Round scraper	3	**1.24**
Notch	10	**4.15**
Notch cum Scraper	1	**0.41**
Retouched Point	8	**3.32**
Tanged Point	4	**1.66**
Retouched Levallois point	1	**0.41**
Bifacial Points	16	**6.64**
Bifacial Point with Tang	1	**0.41**
Borer	1	**0.41**
Retouched flake	6	**2.49**
Total Retouched	**69**	**28.63**
Unretouched		

Prepared Core Flake	17	**7.05**
Thinning & Shaping Flake	18	**7.47**
Finishing Flake	5	**2.07**
Core Preparation Flake	8	**3.32**
Flake	20	**8.30**
Debitage (< 2 cm in length)	57	**23.65**
Total Unretocuhed	**125**	**51.87**
Total	**241**	**100**

Bifaces including both handaxes and cleavers are a part of the lithic assemblage. Bifaces form 9.96% (n=24) of the assemblage with, ~ 5:1 handaxe and cleaver ratio. The mean length of bifaces are 88.52, which is less than 10 cm and there is less variation among the length of bifaces (Table 4.4.3), as there are only four bifaces, which are more than 100 mm in length, similarly, width and thickness show minimal variation.

Table. 4.4.3: Metrical values of the bifaces present in the assemblage.

Attributes	Mean (mm)	Standard deviation	Min	Max
Length	88.52	14.99	55.05	133.81
Width	57.78	8.81	40.83	83.96
Thickness	27.86	15.71	16.50	48.48
Elongation	1.54	0.2	1.18	1.94
Refinement	0.49	0.1	0.29	0.77

As mentioned earlier elongation denotes the relation between the biface length and width. South Asian Acheulian assemblages reveal a wide spectrum of variation with long, elongate, and thick bifaces at one end and short, broad, and thin bifaces at the other end (Shipton, 2016). The mean elongation value of the Nanadanavanam bifaces lies within the latter end of the spectrum (Shipton, 2016) (Fig. 4.4.6) Creating a thin biface requires more refinement as it is difficult to achieve thinness without losing the width. Usually, the biface thickness to width ratio is used as the refinement index. Bifaces from Nandanavanam are moderately thin and refined and lie at the middle of the distribution of mean refinement values of the known Indian assemblages (Fig. 4.4.7 & Fig. 4.4.8).

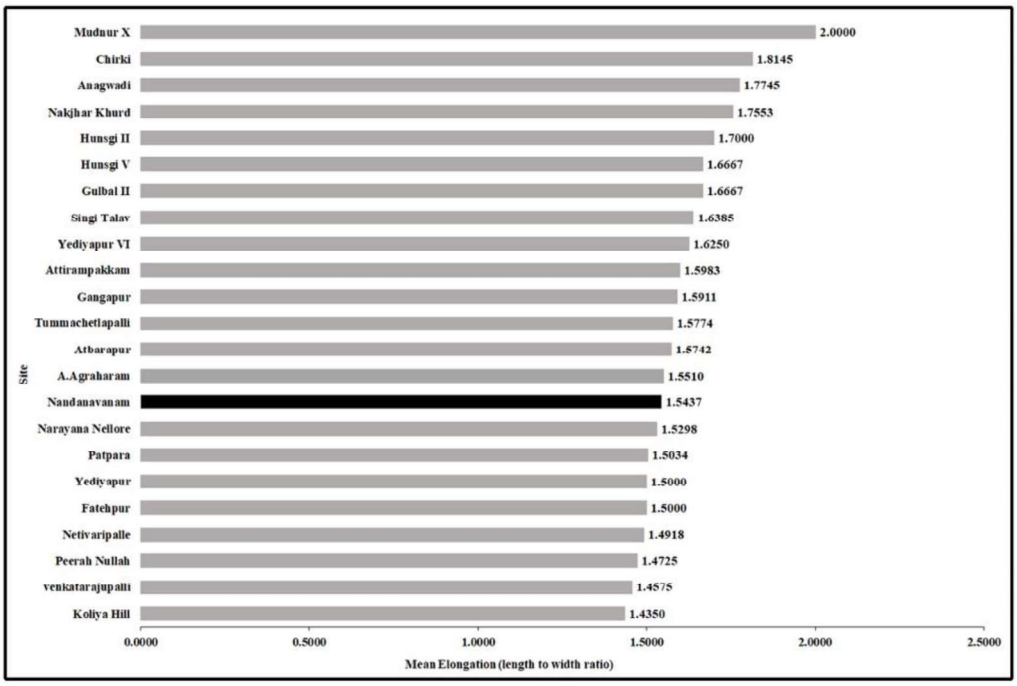

Figure. 4.4.6: Variation in mean biface elongation (length to width ratio) for Indian assemblages. Comparative data from (Chauhan, 2010; Gaillard et al., 1986, 2008; Paddayya & Petraglia, 1993).

The cores from Nandanavanam consisting of 23 pieces form 9.6% of the total assemblage (Table 4.4.2). The dominant categories are simple and discoidal cores followed by preferential surface cores. Simple cores with multiple, random flake removals from one or two sides of the cores are noted in the assemblage. The second-largest category among the cores is discoidal cores. These cores were exploited on both sides resulting in a typical discoid shape (Fig. 4.4.9). The preferential surface cores are a variant of the hierarchical core reduction strategies where a surface of the core is exploited rather than the volume (Zaidner et al., 2018) also present in the assemblage (Fig. 4.4.10). Also, the platform surface shows limited or no preparation to remove the flakes (Zaidner et al., 2018). The removal of flakes on the flaking surface ranges from a single removal to multiple removals radially. Except for three cores, the rest of them (n=20) do not show any evidence of cortex; and the three cores show a minimal percentage (< 10%) of cortex. This observation indicates early-stage core reductions were carried out off the site, probably near raw material procurement areas.

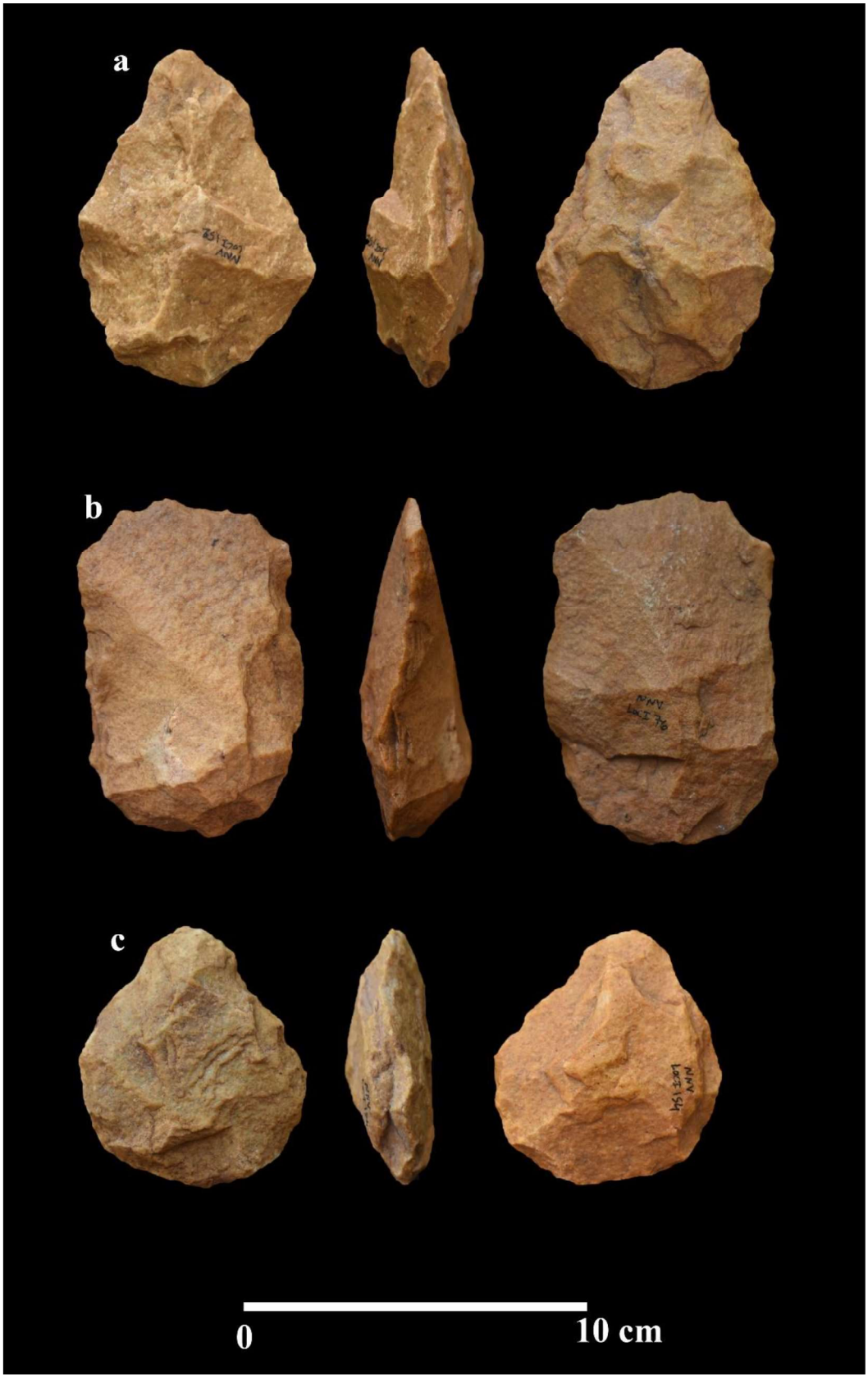

Figure. 4.4.7: Bifaces in the assemblage. a: Handaxe; b: Cleaver; c: diminutive handaxe.

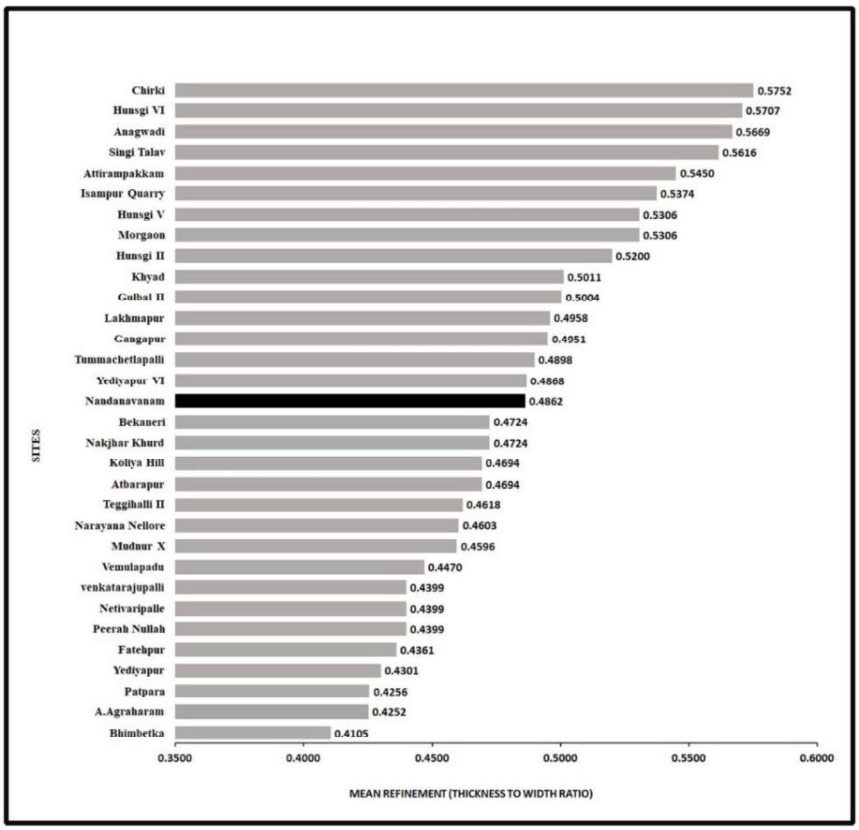

Figure. 4.4.8: Variation in mean biface refinement (thickness to width ratio) for Indian assemblages. Comparative data from (Shipton, 2016).

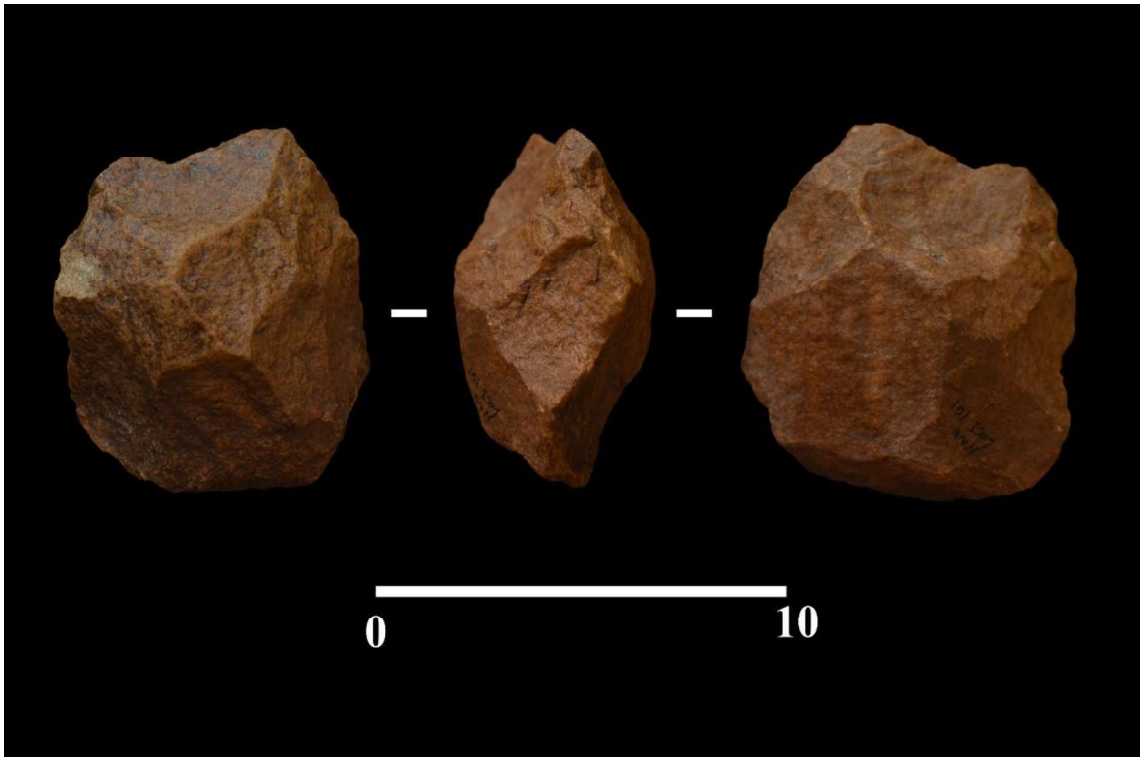

Figure. 4.4.9: Discoidal core.

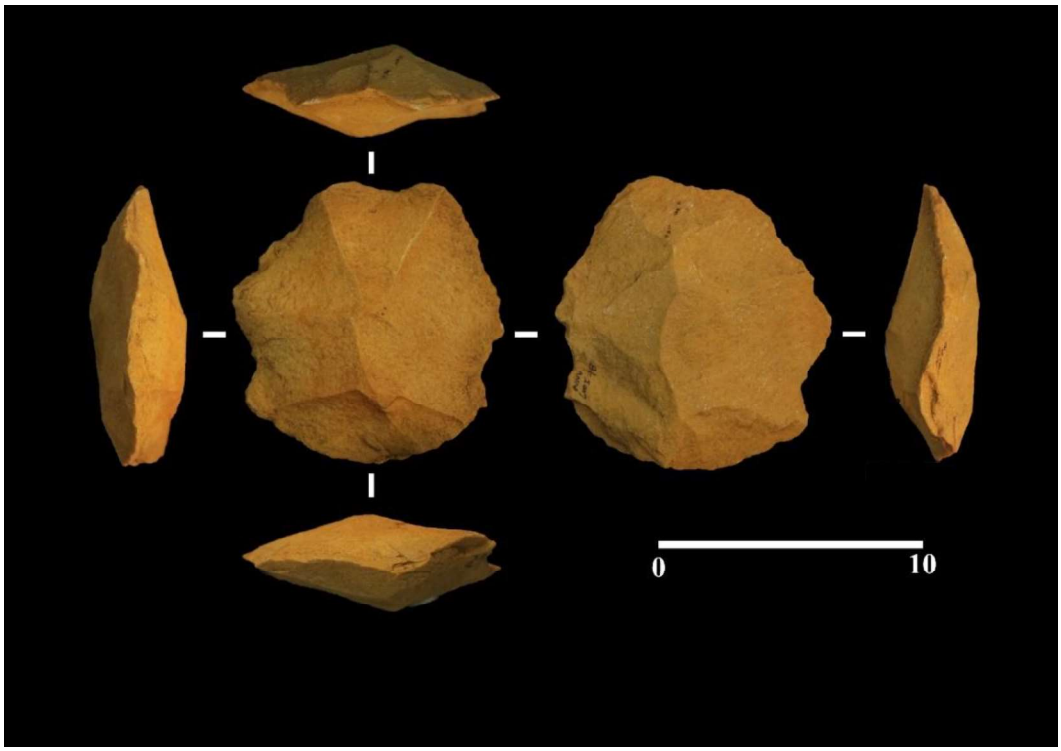

Figure. 4.4.10: Preferential Surface Core

The mean length, medial width and medial thickness of cores are 75.11x80.17x31.39 mm when oriented along the flaking axis (last flake scar) (Table 4.4.4). The core's proximal, medial, and distal widths measured along the flaking axis are 67.11x80.07x51.24 mm, respectively. The proximal shape of the cores is relatively straight (mean 0.83 mm), whereas distal shape is tapering (mean 1.62 mm). No considerable variation in core elongation (ranging between 0.79-1.23) is observed, maybe because there is no significant variation in the cores' mean length and mean medial width. The core flatness index ranges from 1.56 to 4.40, where most cores are wider than thick. Seven cores have multiple conchoidal platforms; 14 cores have single conchoidal platforms. Platforms were facetted on 7 cores and in 14 instances, no preparation is observed. The last scar face length of cores is less than the axial core length, indicating the flaking face is limited to the smaller axial surface. The last scar lengths range from 19.30-65.64 mm, with an average of 38.47 mm, and the last scar widths range between 21.20-79.41 mm, and a mean of 44.33 mm. On average, last flake scar elongation (mean=0.95) indicates that relatively square-shaped flakes were removed. Half of the last major flake scars exhibit feather terminations (51.78%), with non-feather terminations accounting for 48.21%. On average, all the cores were rotated thrice with a maximum of two and minimum of four rotations. Most cores show two (n=9) and three (n=5) major scars (more than 1/3 core length), with four cores exhibiting four, two cores with one scar and one core with five scars.

Table. 4.4.4. Statistical data for the Core attributes.

Attribute	N	Mean	SD	Min.	Max.
Length	23	75.11	15.82	53.31	103.26
Proximal Width	23	67.11	22.33	29.59	115.69
Medial Width	23	80.07	18.19	50.95	111.57
Distal Width	23	51.24	11.61	23.74	70.07
Proximal Thickness	23	21.46	8.08	9.70	35.47
Medial Thickness	23	31.39	5.82	21.34	46.70
Distal Thickness	23	22.69	6.41	10.21	33.72
Proximal Shape	23	0.83	0.17	0.55	1.23
Distal Shape	23	1.62	0.41	1.05	2.64
Elongation	23	0.95	0.13	0.79	1.23
Flatness	23	2.60	0.64	1.56	4.40
No. of Core Rotations	23	2.90	0.54	2.00	4.00
Last Platform Angle	23	67.38	9.44	50.00	80.00
No. of Major Flake Scars	23	2.67	1.06	1.00	5.00
No. of Flake Scars	23	5.05	1.28	3.00	8.00
No. of Feather terminations	23	1.29	0.96	0.00	4.00
No. of non-feather Terminations	23	1.38	0.74	0.00	3.00
Last Scar Length	23	38.47	12.29	19.30	65.64
Last Scar Width	23	44.33	16.84	21.20	79.41
Last Scar Elongation	23	0.95	0.42	0.46	2.05

Flakes, both retouched and unretouched (n=120; excluding debitage) were classified into technological types to identify the position of each flake in either biface or prepared core reduction sequence. Distinguishing flakes from the biface reduction sequence and prepared core reduction sequence (e.g., Levallois) becomes difficult owing to the morphological similarities of the debitage between the two reduction sequences. However, following the attributes suggested by (Akhilesh & Pappu, 2015; Delagnes, 1993; Newcomer, 1971), flakes were classified into various stages of biface and core reduction sequences (Table 4.4.5). Notably, no roughout flakes present in the assemblages indicate that the initial dressing of the bifaces and cores were done at raw material procurement sites, probably the Velikonda hills. Flakes that are part of the core reduction sequence (including end products) dominate the flake

component with 65.83% (Table 4.4.6), which implies the predominance of prepared core technology. Flakes of both prepared and unprepared cores were preferred for expedient retouching (Table 4.4.2) however, prepared core flakes were mostly preferred to make retouched artefacts.

Table. 4.4.5: Classification of flakes according to various stages of reduction sequences.

Technological Type	Unretouched	%	Retouched	%	Total	%
Biface thinning & shaping flakes	18	**26.47**	14	**26.92**	32	**26.67**
Biface Finishing flakes	5	**7.35**	4	**7.69**	9	**7.50**
Prepared core flake	17	**25.00**	26	**50.00**	43	**35.83**
Core preparation flakes	28	**41.18**	7	**13.46**	35	**29.17**
Levallois Flake	0	**0.00**	1	**1.92**	1	**0.83**
Total	**68**	**100**	**52**	**100**	**120**	**100**

Morphometrical descriptions are limited to intact flakes in the assemblage that are 88 in number. Wide range of technological diversity is evident amongst the flakes from biface preparation to core preparation flakes and prepared core flakes. Mean axial flake dimensions are 57.83 x 55.01 x 15.46 mm (LxWxT); on average, flakes are square in shape (mean elongation=1.08) (Table 4.4.3.6). Typical flakes are more than four times wide as they are thick (mean flatness=3.64), with a range of 2.26-5.53. 69.32% of the flakes exhibit slightly expanding proximal margins (mean proximal shape=0.82), with 30.68% exhibiting contracting proximal margins, leading to an upper proximal shape index of 1.09. In contrast, the distal shape indicates that 93.18% of the flakes exhibit distal contracting margins (mean=1.74). Multiple conchoidal platforms are the most common type (60.23%), followed by single conchoidal (24.14%) and dihedral (13.64%). Platform preparation is dominated by facetted platforms with 89.77%, followed by overhang removal (10.22%). A wide range in platform size is evident, with platform width ranging from 18.69-100.59 mm and platform thickness ranging from 3.51-33.18 mm. The platform shape index indicates that platforms are typically elongate (mean=3.06), with 92% of platforms two times wider than they are thick. The most common dorsal scar patterns present on complete flakes in the assemblage are radial (55.68%),

followed by weakly radial (25%), and weakly proximal (19.31%). Cortical coverage ranges from 0-5%, with 94.31% of flakes recorded with no cortex and 5.68% with 5% cortex present. No flakes with cortical platforms and 100% cortical cover of dorsal surface are observed. Feather terminations are present as 55.68%, followed by step terminations (44.31%).

Table. 4.4.6: Statistical data for flake attributes.

Attribute	N	Mean	SD	Min.	Max.
Length	88	57.83	17.52	30.96	132.65
Proximal Width	88	48.50	13.16	21.99	88.72
Medial Width	88	55.01	14.13	24.47	103.64
Distal Width	88	35.77	14.32	13.29	98.06
Medial Thickness	88	15.46	3.62	6.21	27.03
Elongation	88	1.08	0.33	0.50	2.15
Flatness	88	3.64	0.72	2.26	5.53
Proximal Shape	88	0.90	0.17	0.43	1.26
Distal Shape	88	1.68	0.61	0.77	4.05
Platform width	88	44.65	14.06	18.69	100.59
Platform Thickness	88	15.41	5.58	3.51	33.18
Platform Shape	88	3.06	0.90	1.44	5.87
Platform area	88	757.91	502.84	137.00	3080.43
Dorsal scar count	88	2.15	0.95	1.00	6.00

69 retouched artefacts, including bifacial points, scrapers, notches and retouched flakes, are recorded in the assemblage. Among the retouched category, points (including bifacial points) dominate with 43.48%, followed by scraper 30.43%. Stone blocks were preferred to make bifacial points whereas prepared core flakes were the most preferred type to make other retouched artefacts (e.g., Scrapers) forming 36.67% of the total retouched artefacts. however, unprepared core flakes and a few bifaces and core reduction debitage (e.g., roughout flakes, thinning & shaping flakes, etc.) were also used. Retouch length measured on the retouched artefacts shows that 8.70% are randomly retouched whereas on 91.30% of the artefacts retouch was regular. Average retouch length was 56.64%, with the length ranging between 11.58-

145.66 mm. Sixteen bifacial points and one bifacial point with tang were noted in the assemblage with Length, Width, thickness dimensions as 79.64x51.35x29.53 mm respectively. Some of the points show basal modifications which must have facilitated hafting.

4.1.4 Summary

The artefact assemblage from Nandananavanam shows characteristics of both the bifacial (Acheulian) and Prepared core technologies (Middle Palaeolithic), the latter being dominant. The Acheulian is represented by the presence of well-made handaxes, and cleavers. The mean elongation value of the bifaces shows close similarities with the Late Acheulian assemblages reported in South Asia (Shipton, 2013, 2016; Shipton et al., 2013). However, the mean refinement indicates otherwise, falling midway between Early and Late Acheulian. This mismatch between elongation and refinement indicates the absence of standardization in manufacturing bifaces. Notably, all the bifaces except four are less than 10 cm in length denoting a preference towards smaller bifaces. Such a trend of decreasing length of bifaces can be seen in Early Middle Palaeolithic assemblages or in the transitional assemblages.

Prepared core technology and its debitage dominate the assemblage at Nandanavanam with predominant evidence of discoid core reduction. However, preferential surface cores that are a forerunner to the Levallois technology (Bolton, 2015) are also present in the assemblage. Together with discoidal and other simple core reduction strategies, the core technology at the site is represented by a variety of core reduction strategies aimed at producing flakes. There is absolute evidence in the assemblage that these flakes produced through prepared core technology were used to make formally retouched artefacts. The retouched tools are dominated by the presence of scrapers and notches made flakes which is a typical character of South Asian Middle Palaeolithic culture. Some portion of the points and bifacial points shows basal modifications and tangs indicating possibilities of hafting technology. Together with the prepared cores, the dominance of flake tools and evidence for hafting clearly indicates that the assemblage can be classified as Middle Palaeolithic in nature. However, the relatively higher percentage of bifaces in the assemblage does not support the aforesaid observation. But this could be due to the biases in artefact collection methodologies. Overall, the lithic assemblage from Nandanavanam represents an early stage of prepared core technologies with a few bifacial elements.

4.5 Hanumanthunipadu

The site Hanumanthunipadu is located in the upper Paleru river basin, Prakasam District, Andhra Pradesh (Map. 4.5.1). It is situated on the northern fringes of a shallow lake named *Seetharampuram Cheruvu.* Several streams originating from the northern part of the Velikonda hill ranges drain into this lake and the tributary stream *Rallvagu* connects the lake to the river Paleru. These streams contribute to the drainage system of the upper reaches of the Paleru, although several of them were buried below the inland sand dunes. Due to the prevailing low rainfall conditions (700 mm annual average) some of the aforementioned buried streams were recently reactivated and connected to the lake to preserve rainwater. These anthropogenic activities (2010-2015) exposed the artefact bearing horizon at Hanumanthunipadu and at several places across the area. The stream that flows through the site was widened along 850 m to a width of 10 m, connecting it with lake *Seetharampuram Cheruvu.* All along this length, artefacts were found embedded in the sections exposed on either banks and on the bed of the expanded stream (Fig. 4.5.1).

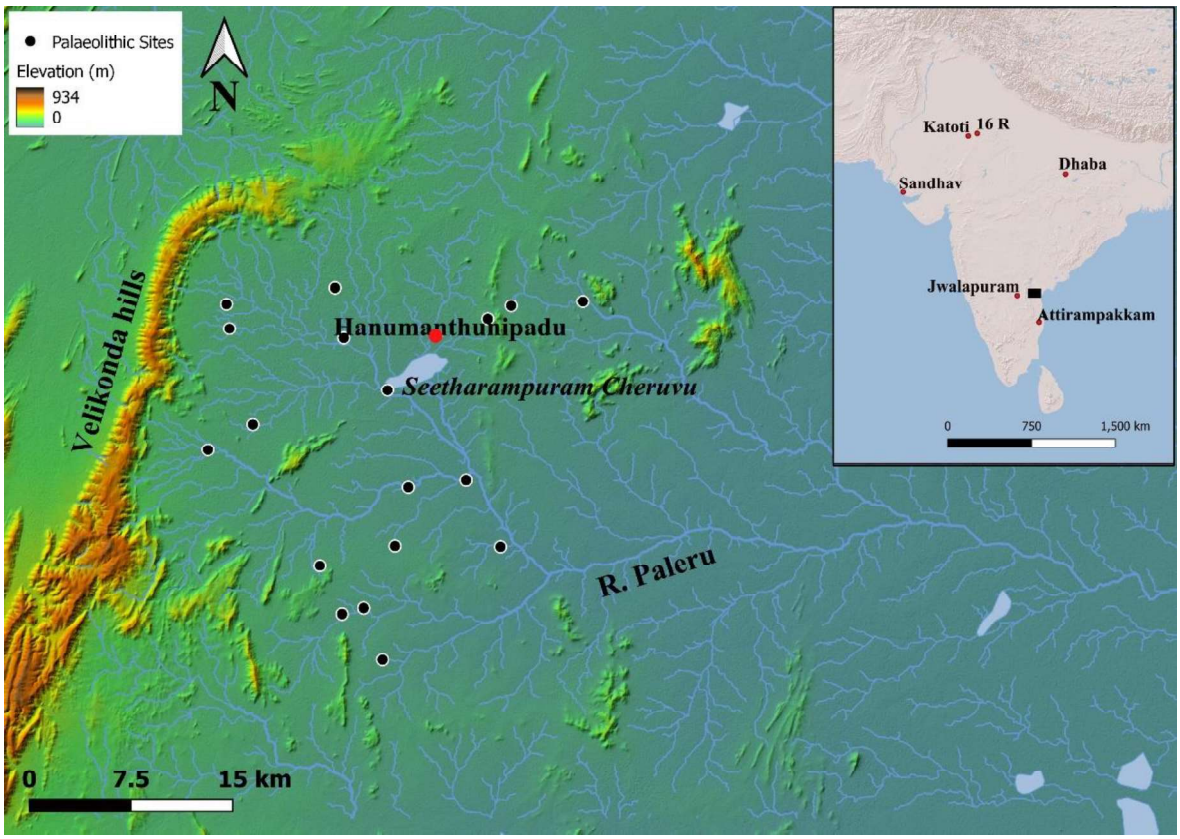

Map. 4.5.1: Map showing the location of the site Hanumanthunipadu (Source: Anil, et al., 2022).

Figure. 4.5.1: Anthropogenically exposed vertical section with artefacts at Hanumanthunipadu and location of the trench.

4.5.1 Stratigraphy

Section scrapings were conducted at the site to understand the geological context of the artefact and to collect sediment samples for luminescence dating. A 2m stretch along the newly exposed right bank of the stream was cleaned up by excavating it about 2 m inwards in order to collect relatively undisturbed samples. Overall, the section went down up to a depth of 2.65 m and at 2.20 m depth, Middle Palaeolithic *in situ* artefacts were identified associated with clayey silts rich in pedogenic carbonates (Fig. 4.5.2). The trench revealed a complex, three-phased lacustrine-fluvial-aeolian lithostratigraphic sequence (Fig. 4.5.3). Phase III, the aeolian phase, includes the top three units of fine to coarse-grained sands. The pale-yellow sands of units U1 and U2 are comparable with the A-1 type younger sand dunes described by (Mishra & Singaraju, 2009; Reddy et al., 2013). The semi-consolidated, thin, dark brown sands of unit 3 represent remnants of a palaeosoil formation. Phase II, consists of units 4 to 14, encompasses fluvial sediments that are point bar deposits comprising cross-bedded alternate layers of fine and coarse sediments. Fine sediment layers consist of sands, whereas coarse sediments contain redeposited carbonate nodules. During the time of phase II sediments deposition, the stream must have been actively draining into the lake. Units 15 and 16 denote Phase I which represents the lacustrine phase. Unit 15 is a 37 cm thick, clay-rich layer that shows desiccation cracks that

are filled by the foreign sediment deposited later (Fig. 4.5.3). These cracks are of various sizes and visible all along within unit 15 in the trench sections. Unit 16 is a clay-rich silty layer with rich carbonate nodules and shows a diffused contact with overlying unit 15. The average thickness of unit 16 is 1.5 m, observed along the exposed sections; however, in the excavated trench its thickness was only up to 50 cm. This sediment contained in situ Middle Palaeolithic artefacts.

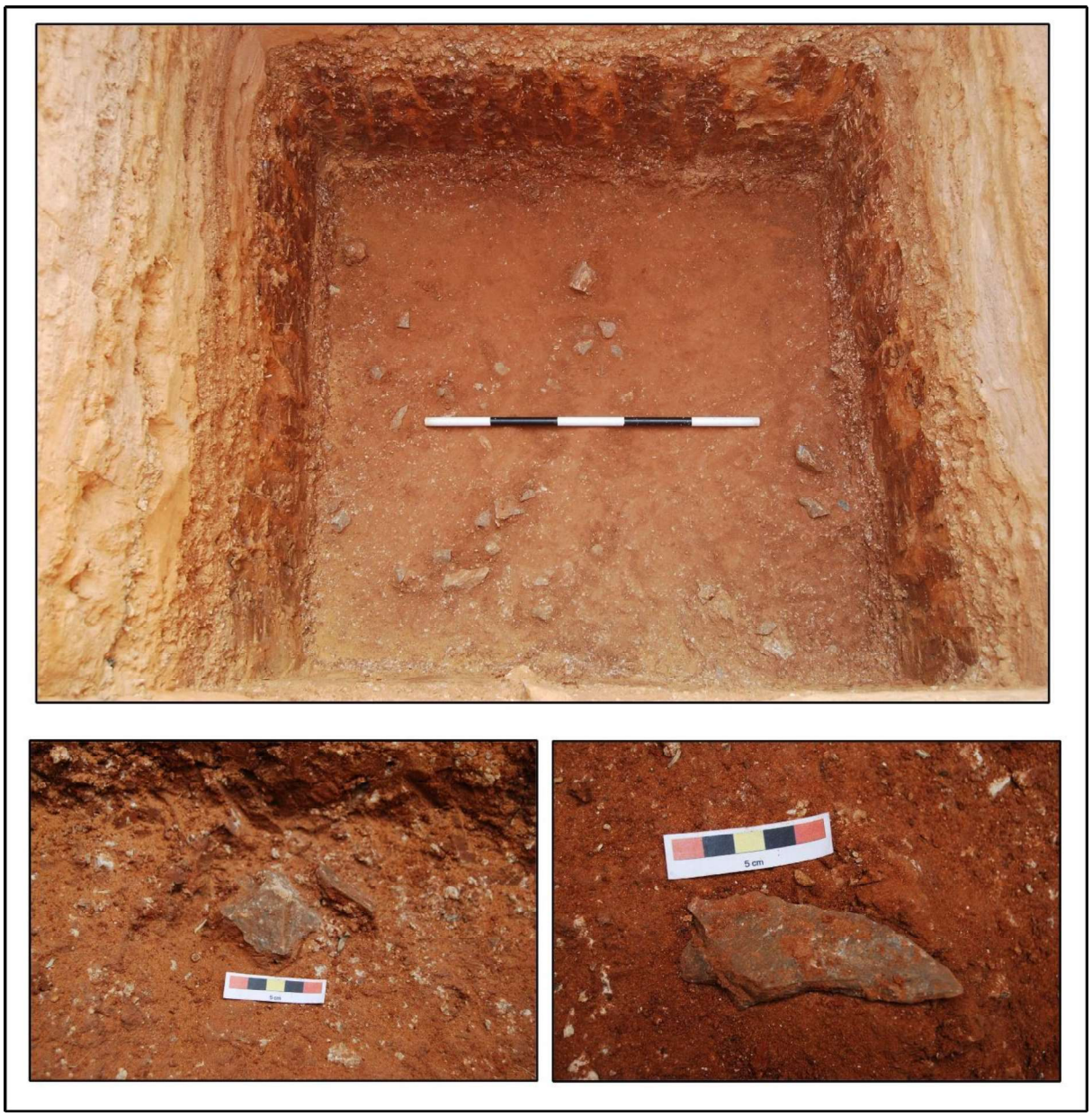

Figure. 4.5.2: Images showing exposed sections and *in situ* artefacts. a) Artefact exposures (above), *in situ* artefacts (below) (Source: Anil et al 2022).

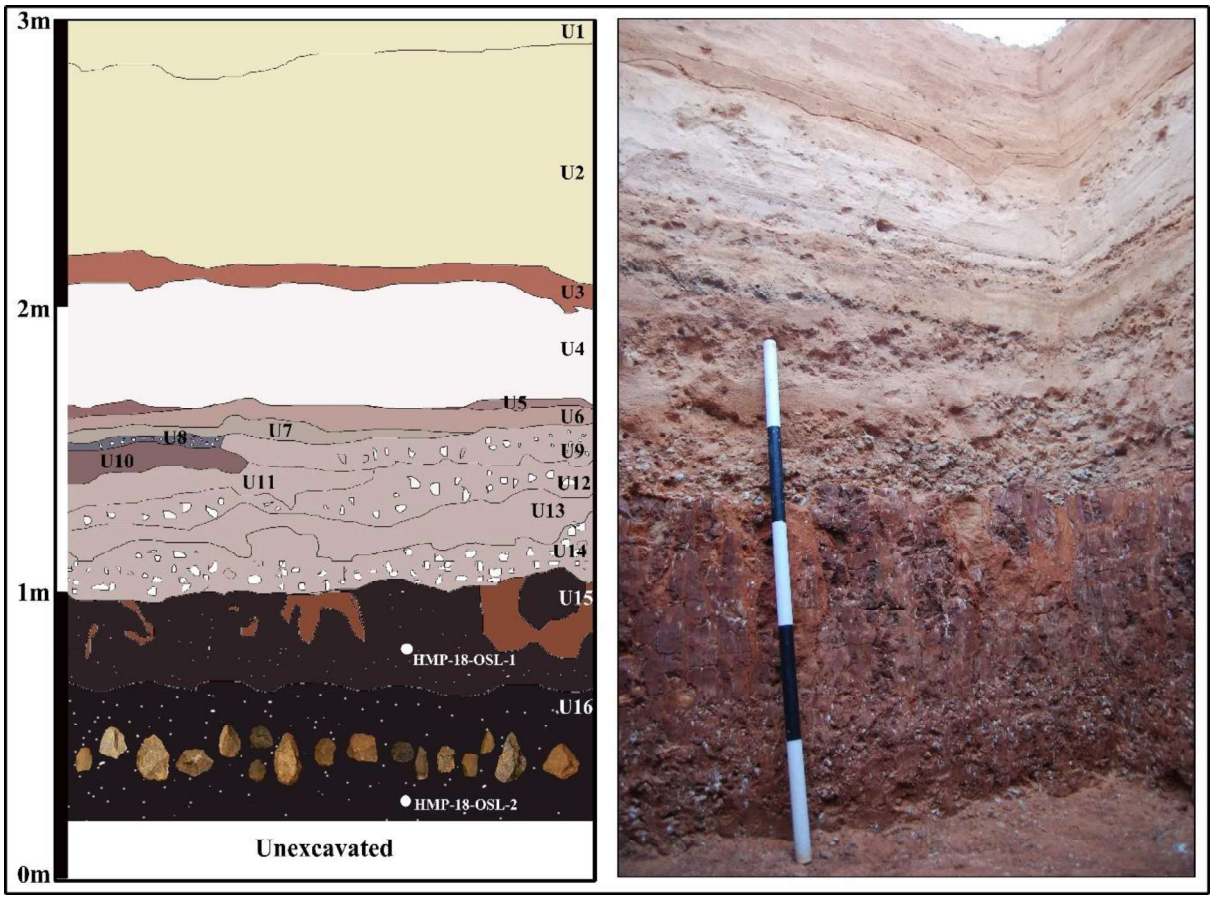

Figure. 4.5.3: Section facing north (right) and a schematic sketch of the section (left). U: identifying specific lithological units; dots and codes: positions of OSL samples (Source: Anil et al 2022).

4.5.2 Luminescence Chronology

Two sediment samples were collected from units 15 and 16 for luminescence dating. The sample of unit 16 was dated to obtain an age for the middle palaeolithic artefacts. The unit 15 sample was also processed for dating but shows post-depositional alterations resulting in a wide distribution range among the equivalent doses (D_e) (Fig. 4.5.4d). Therefore, the age of unit 15 (culturally sterile) is not further discussed here. The estimated paleo-dose for the osl sample from unit 16 was 325 ± 12 Gy (Table. 4.5.1 and Fig. 4.5.4c) and the typical shine down & growth curves of p-IR-IRSL is shown in (Fig. 4.5.4a and b). The overdispersion (OD) in the estimated D_e value was quite low (~8%) as shown in (Table. 4.5.1), indicating well bleaching of sediment before burial. Thus, for d_e estimation central age model (CAM) was used.

The fading rates (*g*-values) were estimated using the procedure outlined by (Auclair et al., 2003). It involves bleaching of the sample followed by incorporation of a known laboratory dose approximately similar to paleo-doses estimated for respective samples, preheating the

sample and then measurement of luminescence intensity for different time delays. The time delays ranged from prompt measurements to up to 3 days. Fading rate (% per decade) was estimated from the slope of the graph plotted between delayed intensities and logarithmic delayed time as shown in (Fig. 4.5.5) (Huntley & Lamothe, 2001). Obtained *g*-value was 2.9 ± 1.4 (%/decade) for the HMP sample.

The estimated paleo-dose was 325 ± 12 Gy, indicating that the dose is in a non-linear region; hence, fading correction method suggested by Huntley and Lamothe (2001) is not applicable for correction. Therefore, the model proposed by Kars and Wallinga et al. for fading correction was adopted (Kars et al., 2008)(Kars & Wallinga, 2009). This model is based on (Huntley, 2006). The model assumes that anomalous fading follows power law and depends upon the number density of recombination centres as

$$I = I_o e^{-\acute{\rho}\ln(st)^3}$$

Where ρ' is the recombination charge density, s is the attempt to escape frequency (assumed here $3*10^{15}$ s^{-1}). I and Io are the intensity of signal at time t and immediately after irradiation. After correction was applied, the natural luminescence intensity was above the simulated corrected dose response curve as shown in (Fig. 4.5.6). Therefore, we restricted ourselves to the minimum age (which is equivalent to saturation age given by $2D_0$ value) provided by the Kars model, which is 247 ± 32 ka.

Table. 4.5.1: Dose rate data, D_e values and OSL ages for the sediment sample from unit 16 at Hanumathunipadu (Source: Anil et al 2022).

Sample Code	Depth (cm)	Radionuclide activity				Equivalent doses				OSL age (ka)
		U (ppm)	Th (ppm)	K (%)	Total Dose rate [b,c] (Gy/ka)	No. of aliquots/ grains	Water content (%)	OD (%)	D_e (Gy)[d]	
HMP-18-5	255	1.9±0.4	8.2±1.4	0.50±0.06	2.0±0.12	10/ ~120	17	8	325±12	**>247±32[e] ($2D_0$ value)**

[a] Radioactivity measurement made on a dried, homogenized and powered sample by gamma-ray spectrometry and alpha counting.

[b] Includes cosmic-ray dose rate of 0.096 Gy ka^{-1}

[c] 12.5±0.5% and 200±20 ppm Rubidium (^{87}Rb) concentrations were used to estimate the internal dose rate

[d] after subtracting of a residual dose of 22 Gy

[e] fading corrected age (see the text)

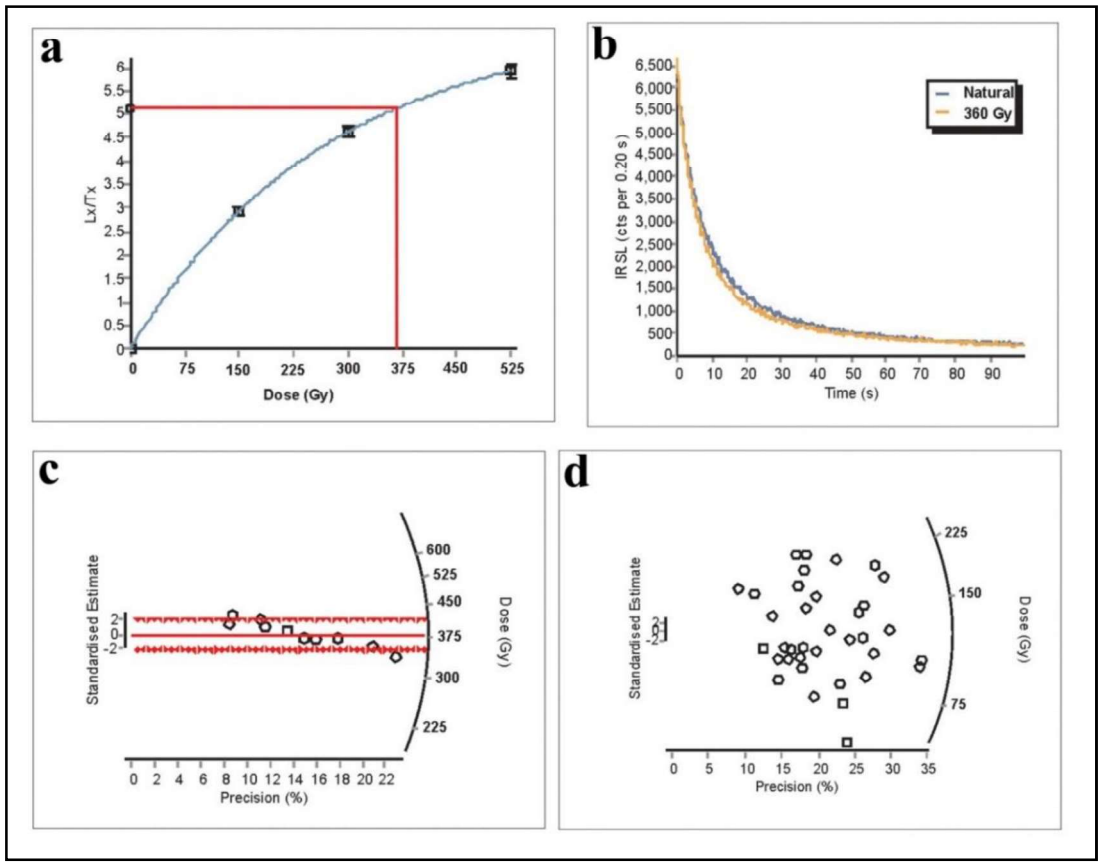

Figure. 4.5.4: a: SAR growth curve for p-IR-IRSL signal; b: luminescence decay curve for p-IR-IRSL signal; c: Radial plot of estimated D_es using p-IR-IRSL protocol indicating that dose scatter is less. Over-dispersion (OD) for all D_es is ~8%, d) Large dose scatter observed in the sample recovered from Unit 15 (Source: Anil et al 2022).

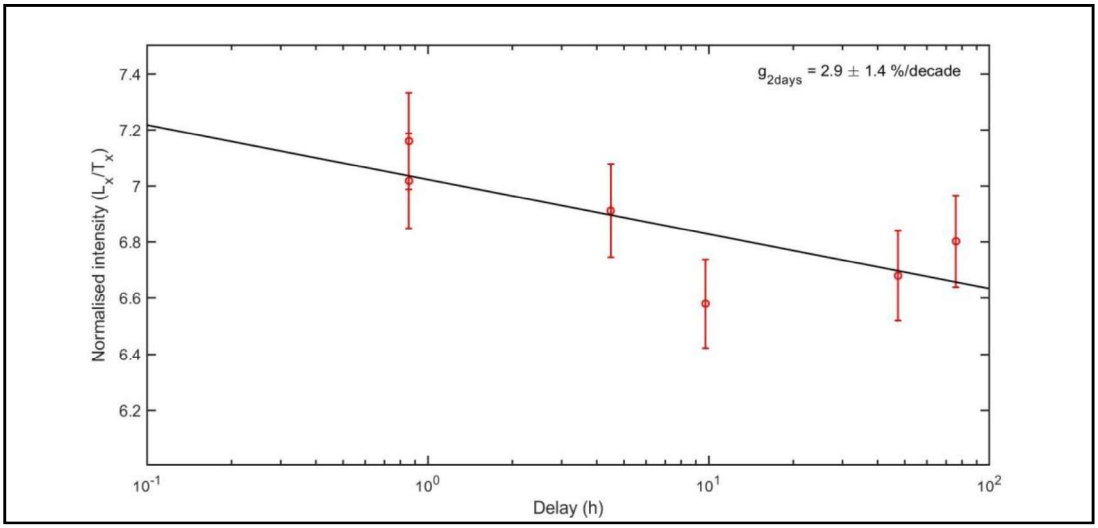

Figure. 4.5.5. Anomalous fading (g-value) measurements on a single aliquot by using a series of prompt and delayed sensitivity corrected measurements of the HMP sample (Source: Anil et al 2022).

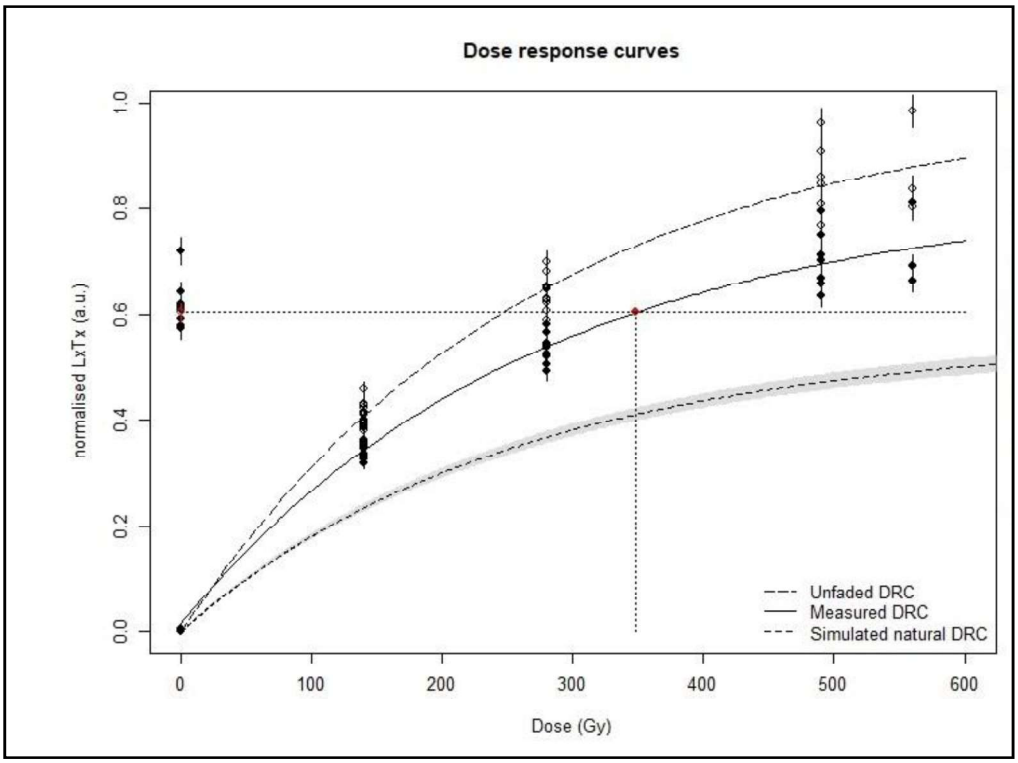

Figure. 4.5.6: The measured dose response curve (DRC), unfaded drc and the simulated natural DRC are shown **(Kars et al., 2008; Kars & Wallinga, 2009)**. The natural L_x/T_x is also shown. The natural luminescence signal is higher than the simulated natural DRC and hence gives the dose saturation value only ($2d_o = 511 \pm 1$ gy) (Source: Anil et al 2022).

4.5.3 Lithic Technology

Excavations at the HMP site yielded a total of 305 lithic artefacts. Medium to fine grained quartzite was used as raw material which was abundant in the Velikonda hill ranges situated ~ 10 km north-west of the site. Fresh condition of the artefacts and the presence of debitage from various stages of lithic reduction sequence indicate the primary context of the assemblage or minimal post depositional alteration of the assemblage (Fig. 4.5.7). The compositions of the assemblages are shown in Table 4.5.2, showing technological and typological classification. The assemblage is dominated by the debitage (flakes less than 2 cm in length) which makes up 40 percent and unretouched flakes forming 17.7%. Flaked pieces, exhibiting the characteristics of conchoidal fracture but difficult to ascertain the typo-technological classification due to the absence of diagnostic attributes, also constitute a considerable portion of the assemblage (12.1%). The variety of cores collected from the sites consist of Levallois and multi-platform core reductions (Table 4.5.2). Levallois elements including flakes, cores and finished artefacts made on Levallois flakes contribute 13% to the assemblage. Levallois is clearly the formal

reduction strategy evident across the core, debitage and retouched assemblage. Retouched flakes mostly consist of scrapers, points and bifacial tools making up 14.75% of the assemblage. The clear presence of Levallois and focus on smaller flakes, retouched tools and rare presence of Large Cutting Tools makes the assemblage part of Middle Palaeolithic technology.

Table. 4.5.2: Composition of the lithic assemblage.

Typology	Number	%
Cores		
Multi-Platform core	6	**1.97**
Levallois core	3	**0.98**
Core fragment	8	**2.62**
Retouched		
Bifacial point	2	**0.66**
Diminutive handaxe	2	**0.66**
Handaxe	1	**0.33**
Levallois point	5	**1.64**
Notch	2	**0.66**
Retouched core fragment	3	**0.98**
Retouched flake	18	**5.90**
Retouched levallois point	1	**0.33**
Retouched piece	3	**0.98**
Scraper	4	**1.31**
Scraper on levallios flake	4	**1.31**
Unretouched		
Flake	54	**17.70**
Levallois flake	4	**1.31**
Redirecting flake	1	**0.33**
Prepared core flake	6	**1.97**
Pointed flake	1	**0.33**
Flaked piece	37	**12.13**
Debitage	123	**40.33**
Broken		
Broken biface piece	2	**0.66**
Broken flake	15	**4.92**
Total	**305**	**100.00**

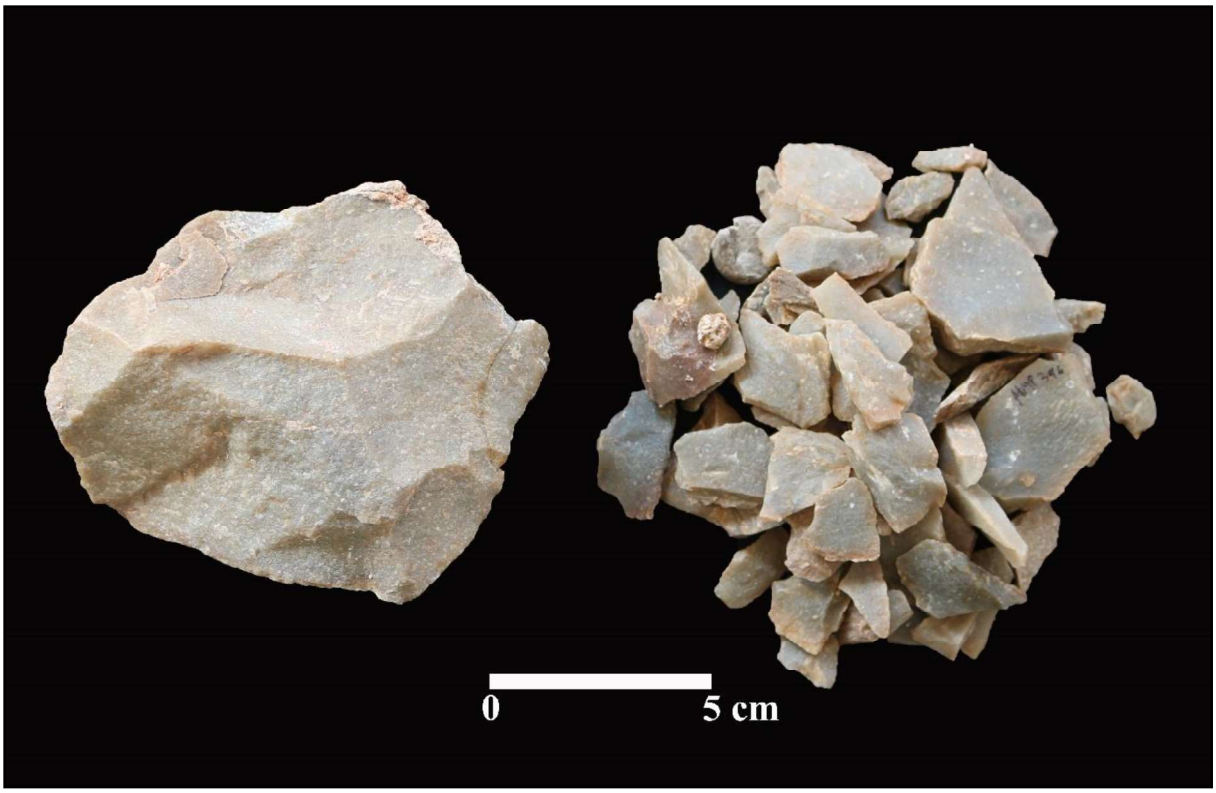

Figure. 4.5.7: Core and debitage pieces recovered from the trench (Source: Anil et al 2022).

A total of nine cores and eight core fragments have been recorded in the HMP assemblages. The majority of cores are informal in reduction (n=6) classified as multi-platform cores, and a low number of Levallois cores (n=3) are also present that are formal core reduction strategies. Two types of Levallois reduction strategies are apparent amongst the HMP assemblages, including preferential and recurrent flaking patterns (Fig. 4.5.8). All multi-platform cores have undergone numerous rotations in the flaking axis ranging from a maximum of 5 and a minimum of 3 rotations (Fig. 4.5.9). In contrast, the Levallois cores rotated twice in two instances and thrice in one example. Most cores (n=6) show two major scars (more than 1/3 core length), with three cores exhibiting one, three and four scars each. The presence of cortex on cores ranges from 0-30%, with a mean of 9%. The mean length, width and thickness of cores are 81x74x37 mm when oriented along the flaking axis (last flake scar). The core's proximal, medial, and distal widths measured along the flaking axis are 74x82x72 mm, respectively, indicating no considerable variations. Similarly, no considerable variation in core elongation (ranging between 0.69-1.48) is observed, maybe because the core's mean length and medial width are more or less similar (81x82 mm). The core flatness index ranges from 0.90-4.49, where most of the cores (n=7) are wider than they are thick. Five cores have single conchoidal platforms, three cores with multiple conchoidal platforms, and in one instance indeterminate. Six cores show facetted platforms, and in three instances, no preparation is observed. The last

scar face length of cores is less than the axial core length, indicating the flaking face is limited to the smaller axial surface. The last scar lengths range from 32-72 mm, with an average of 49 mm, and the last scar widths are also closely matched with length, with a range between 32-75 mm, and a mean of 51 mm. On average, last flake scar elongation (mean=1.0) indicates relatively square-shaped flakes were removed. Many of the last flake scars exhibit non-feather terminations (93.3%), with feather terminations accounting for 6.7%. Levallois cores exhibit a greater maximum width (mean=83.5 mm; range=78.4-98.4 mm) than multi-platform cores (mean=81.2 mm; range=42.2-100.4 mm. Whereas the axial length of multi-platform cores (mean=82.6; range=58.6-134.8 mm) are larger than Levallois cores (mean=78.9 mm; range=75.9-92.3 mm). Levallois core are significantly flatter (mean=3.4; range=2.1-3.5) than multi-platform (mean=2.1; range=0.9-3.7) cores. Beyond this, there are no significant differences in core size and shape between core types.

Figure. 4.5.8: Schematic sketches of the two (a and b) Preferential Levallois cores from the assemblages (Source: Anil et al 2022).

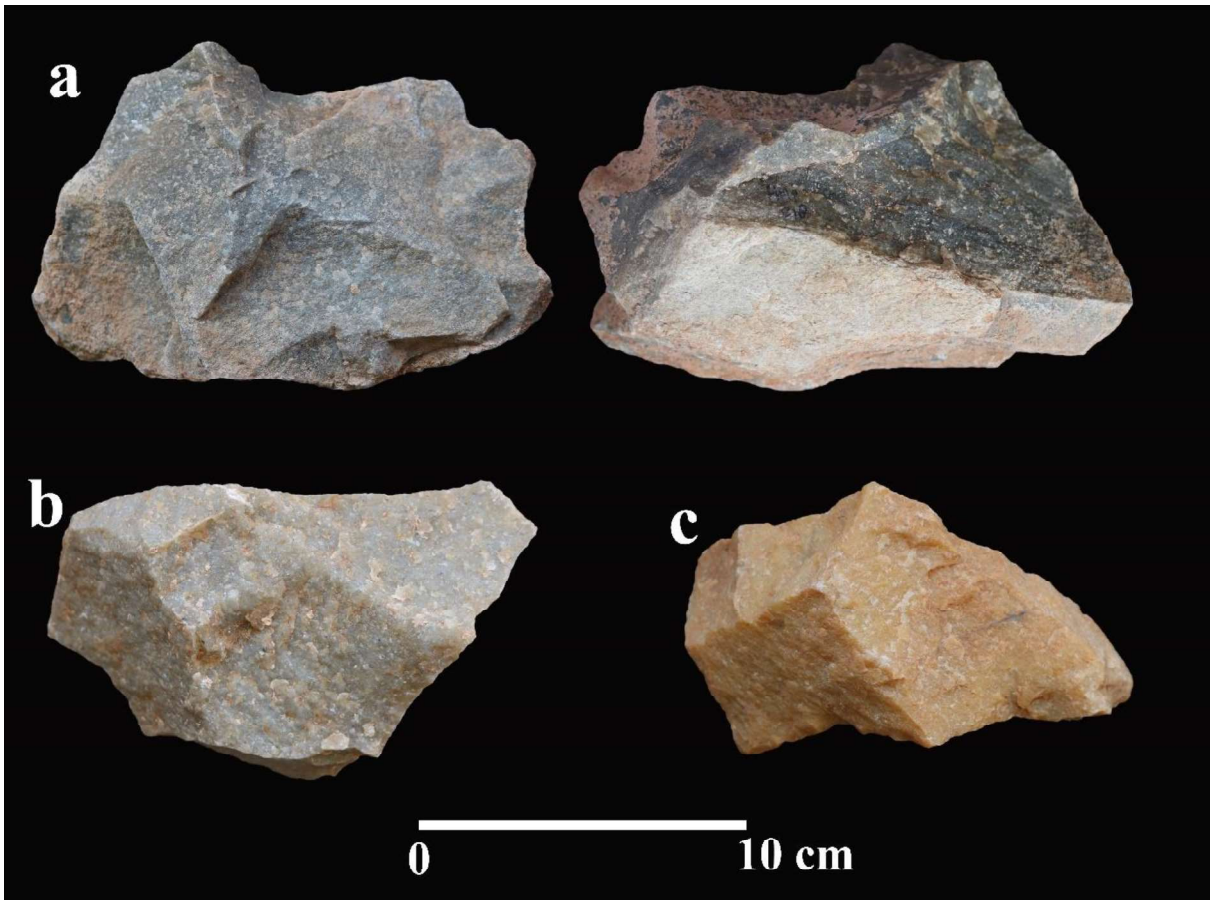

Figure. 4.5.9: Large quartzite blocks used as cores (multi-platform cores) recovered from the trench (Source: Anil et al 2022).

A total of 81 unretouched flakes have been recorded in the HMP assemblage, including 54 complete flakes. Limited typological diversity is evident amongst the flakes from HMP, with six prepared core flakes, four Levallois flakes and one redirecting and one pointed flake (Fig. 4.5.10). The most common dorsal scar patterns present on complete flakes in the assemblage are weakly radial (48.1%) followed by proximal (33.3%) and radial (18.5%). Cortical coverage ranges from 0-100%, with 75.9% of flakes recorded with no cortex present, and 18.5% of flakes with less than 50% cortex present. Low frequencies of flakes with only cortical platforms (5.5%) and 100% cortical cover of dorsal and platform surface (7.4%) are observed. The majority of flakes show feather terminations (79.6%), followed by step (16.6%) and hinge (3.7%) terminations. Mean axial flake dimensions are 54.9 x 55.3 x 13.3 mm, and on average, flakes are as long as they are wide (mean elongation=1.2). A low number of blade proportioned flakes (n=6) are present, with a maximum elongation of 3.12. Typical flakes are more than four times wide as they are thick (mean flatness=4.2), with a maximum range of 1.69-8.16. 66.6% of the flakes exhibit slightly expanding proximal margins (mean proximal shape=0.92),

with a 33.3% of flakes exhibiting contracting proximal margins, leading to an upper proximal shape index of 1.16. In contrast, the distal shape indicates that 88.8% of the flakes exhibit contracting distal margins (mean=1.36).

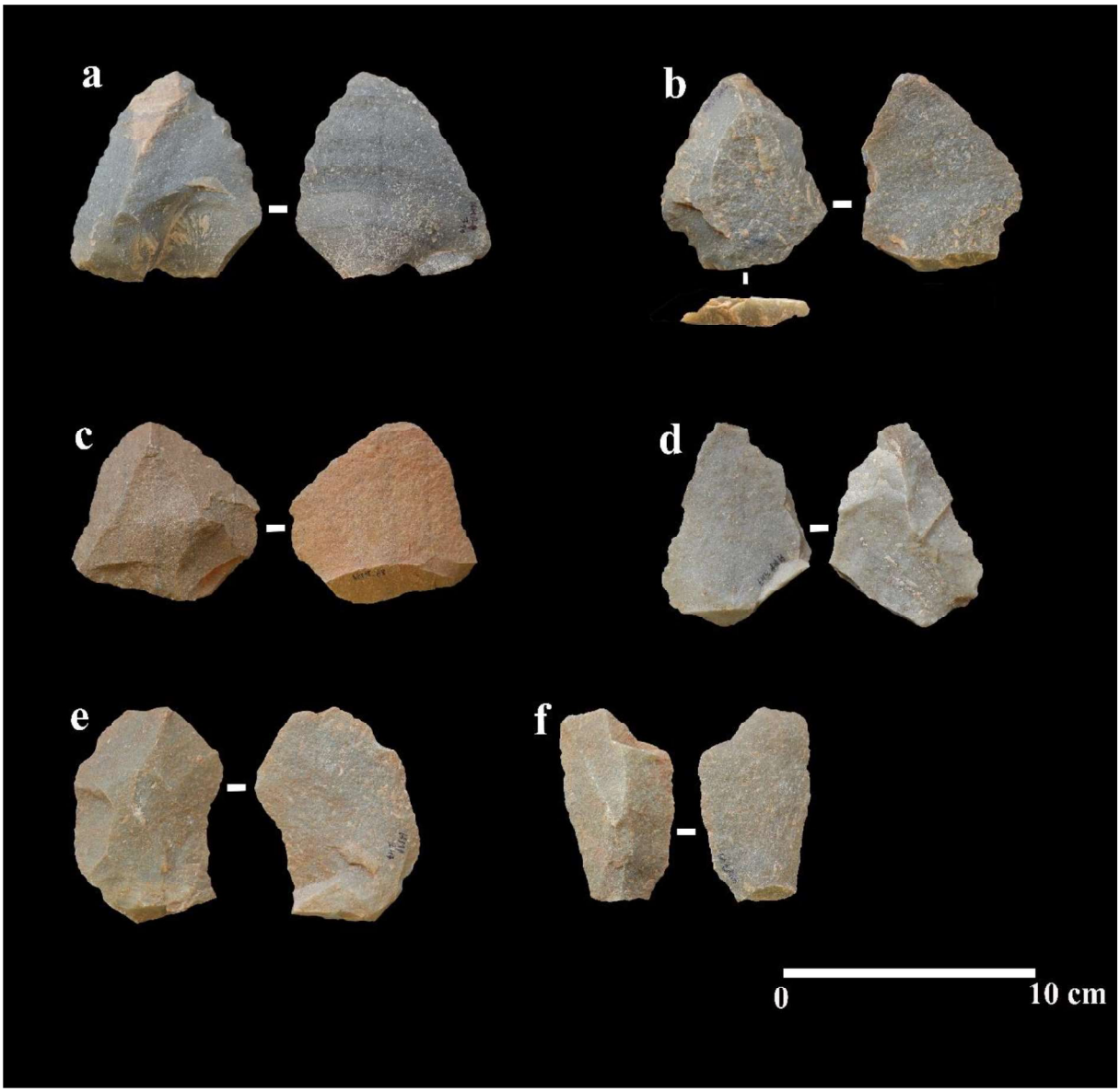

Figure. 4.5.10: Representative samples of Levallois debitage products present in the assemblage. a to d: Levallois point; e and f: Levallois flakes.

Single conchoidal platforms are the most common type (38.8%), followed by multiple conchoidal (29.6%) and cortical (14.8%), dihedral (11.1%) and punctiform (3.70%) types. Platform preparation is dominated by facetted platforms with 42.5%, followed by unprepared platforms (29.6%) and overhang removal (27.7%). A wide range in platform size is evident, with platform width ranging from 5.9-98.7 mm and platform thickness ranging from 3.9-28.1 mm. The platform shape index indicates that platforms are typically elongate (mean=3.41),

with 88% of platforms twice as wide as they are thick. A total of 37 artefacts that are categorised as flaked pieces are present, which bear no clear ventral morphologies or negative flake scars originating from the margins of the artefact but have clearly undergone some reduction.

A total of 45 retouched flakes, bifaces, bifacial points and flaked pieces are recorded at HMP (Fig. 4.5.11). A wide range of retouched artefacts are present in the assemblage including one handaxe and two diminutive handaxes. Retouched core fragments and retouched pieces are also present in small quantities. Among the retouched category informally retouched flakes dominates with 40% followed by scrapers and points present in equal quantities (17.7%). Two artefacts present simple notches, along with varying levels of further retouch. The average dimensions of all retouched flakes are 61.9 x 53.4 x 14.26 mm. Very few artefacts contain cortical coverage in low percentage and 75% of artefacts recorded are with no cortex. With regards to retouching intensity, retouch length on flakes typically ranges from 24.5-90.5 mm.

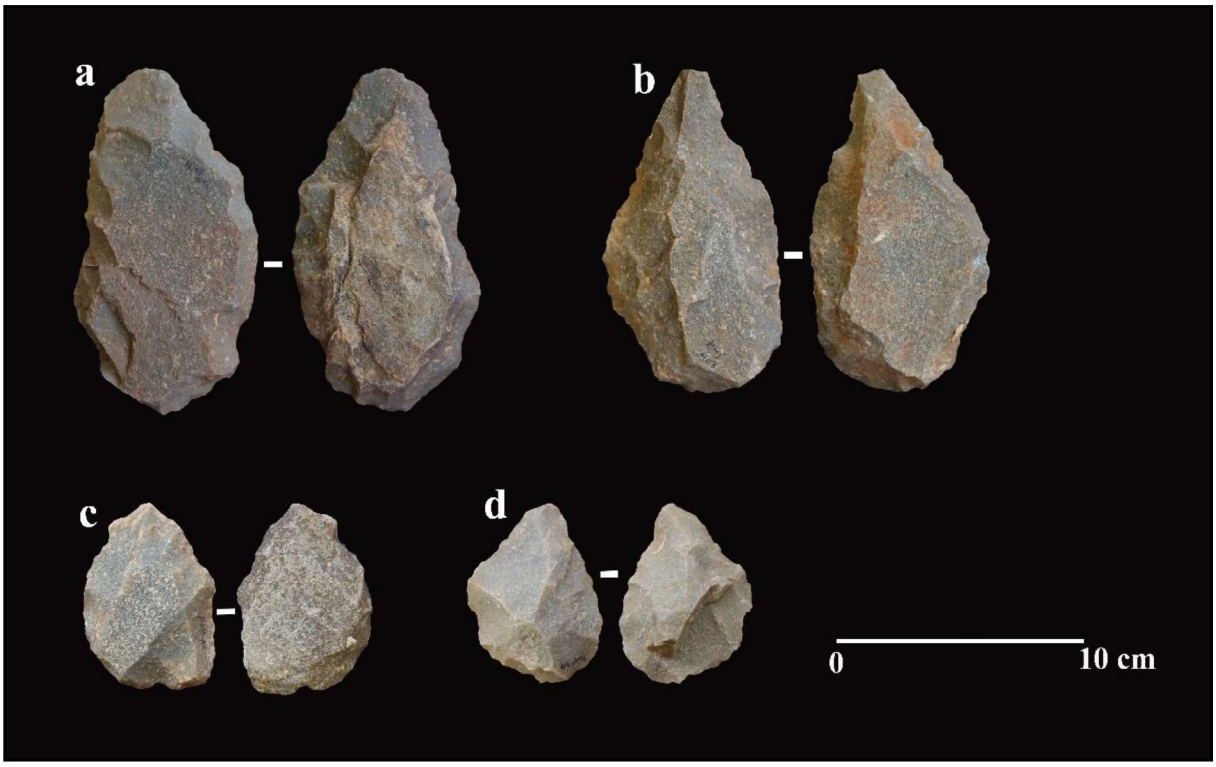

Figure. 4.5.11: Bifacial artefacts recovered from the trench. a to c: Bifacial points; d: Diminutive Handaxe.

4.5.4 Summary

Excavations at the site have yielded Middle Palaeolithic artefacts datable to > 247±32 ka. The assemblage consists of Levallois products, points, and bifacial tools which can be attributable to Middle Palaeolithic culture. The complex stratigraphy observed at the site includes lacustrine, fluvial, and aeolian depositions. Bottom layers of the trench (Unit 16 and 15) seem to be low energy fluvial deposits indicating lake-like situations. Whereas Layers from Unit 4 to 14 may have been alluvial formations including channel bar/point bar deposits. Layer 3 represents a palaeosol formation. The topmost two layers represent the aeolian sand deposits which are the characteristic of the terminal Pleistocene deposits in the upper Paleru river basin. This site represents a mosaic of fluvial and aeolian deposits which can provide significant insights into the palaeoclimate of the region.

Core attribute analysis offers several insights into reduction intensity and strategy at HMP. The presence of a relatively low proportion of cores with cortical surfaces, including platform surfaces, suggest that the primary reduction was conducted away from the site, possibly at the raw material procurement area. The presence of Levallois core types suggests that some reduction sequences were conducted principally at the site. The fewer variation in the size of flakes indicates that preliminary reduction activities were performed off the site. In addition, most of the flakes having no or minimal cortical cover support the aforesaid observation. Average flake dimensions typically fall between 20-50 mm, and the largest and smallest flakes present at the site are likely to have been by-products of reduction activity, rather than the outcome of specific reduction strategies. However, the presence of a small number of Levallois flakes and small debitage (less than 2 cm in length) indicates that some specific debitage products were produced at the site. Platform types are typically complex, and platform preparation is common. Of all scar patterns, proximal and radial flakes dominate which may indicate that radial flaking was employed to create flakes with large perimeters. Overall. there is little evidence for the targeted production of elongate flakes.

4.6. Retlapalle

Retlapalle (15.590630°N, 79.194290° E) is located on the right bank of the stream Erravagu, a tributary of the Gundlakamma River (Map. 4.6.1).

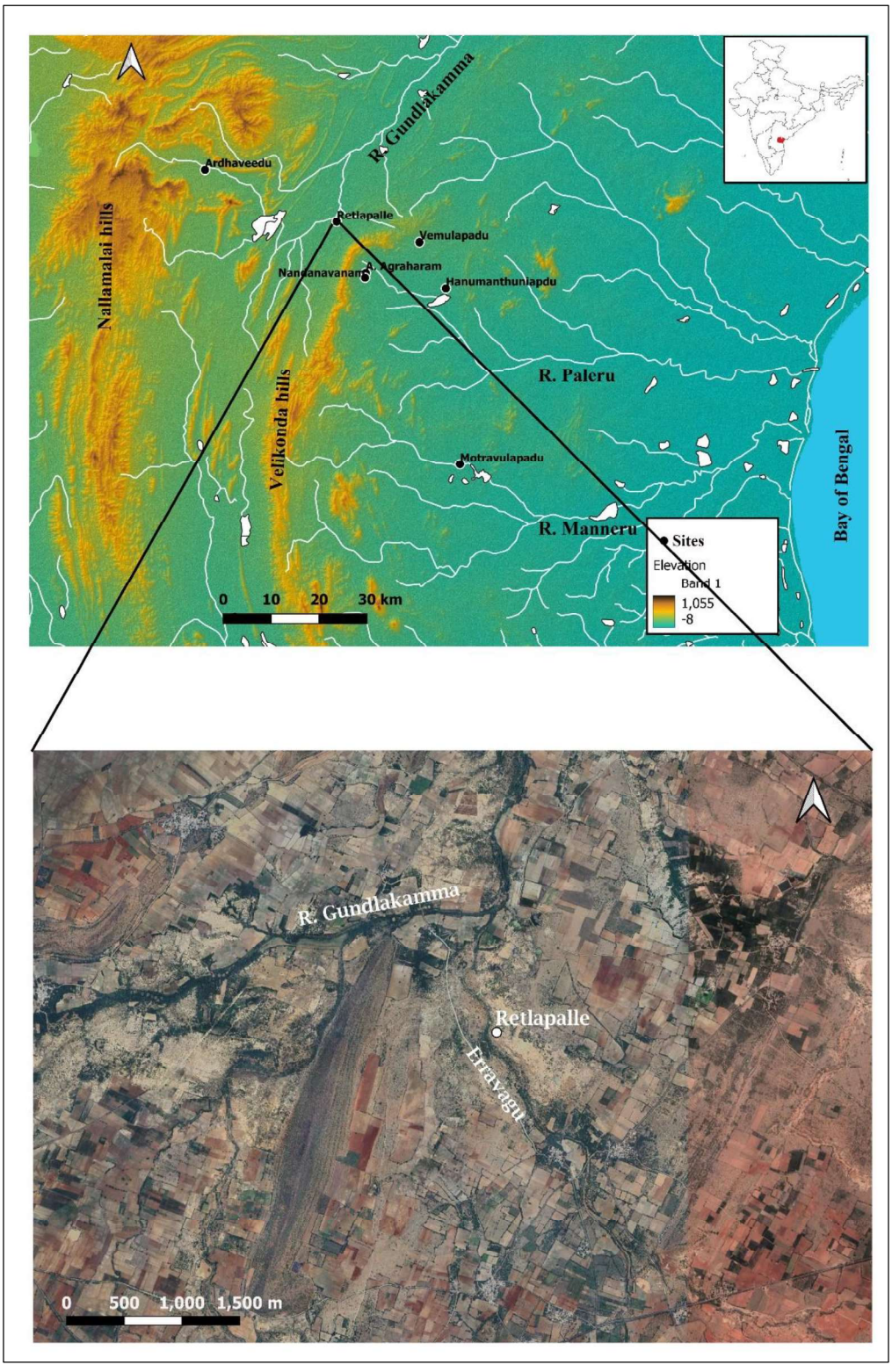

Map. 4.6.1: Map showing the location of the site Retlapalle.

4.6.1. Stratigraphy

A 1.00m wide step-trench was laid out in the stream cliff at Retlapalle to understand Youngest Toba Tuff's geological context and the surface material's stratigraphic context (Fig 4.6.1). The stream Erravagu cuts through the underlying slate bedrock, which forms the base of the stratigraphy at the site. The bedrock was overlain by 0.7 m thick calcareous sandy silt sediment (Fig 4.6.1, Unit E), where the upper part of this Unit contains colluvial material (mostly pebbles) that has Middle Palaeolithic artefacts embedded. This horizon is covered by 1.10m reddish-brown clayey silts (Unit D). This clayey silt Unit is overlain by 42cm thick ash (Unit C), which shows diffused lower contact and sharp upper contact with the overlying brown-coloured organic-rich silts (Unit B). The blade-flake and blade-based lithic assemblages collected from a number of surface sites are attributable to this horizon, but they have not been recovered in the excavation. Reddish sandy silts (Unit A, Fig 4.6.1) deposits of ~ 1.50 m overlie this brown clayey deposit.

Figure 4.6.1: 1: Step-trench section showing the lithological Units; 2: Unit A; 3: General view of the site, Retlapalle.

4.6.2. Geoarchaeology

4.6.2.1. Mineral Magnetic studies

The mineral magnetic results for the above step-trench section are described below (for the methods and raw data, see Chapter 3). The mean Xlf shows a value of 6.38, indicating ferromagnetic concentration. The median of 6.58 and variation from 9 to 1.92 further suggest moderate to high variance. The frequency dependence of susceptibility (Xfd%) shows a mean value of 12 varying between 14.55 to 7.59, depicting significant SP content in all the samples (Fig. 4.6.2). The mean SIRM of 357 varying from 479 to 137 depicts moderate variability within the ferromagnetic mineral concentration. The soft-IRM agrees well with SIRM, and Xlf depicts moderate to high variance in the ferromagnetic concentration. The coercivity of remanence B(0)R shows a mean value of 26mT with a median of 25mT, and a variation from 24 to 34mT indicates remarkably low variation, denoting unimodal ferromagnetic mineralogy with the dominance of SD-PSD domain size. The mean S-ratio of -0.62, coinciding with the same median value and variation from -0.47 to -0.74, mainly indicate SD-PSD domain size and the absence of typical MD ferrimagnets. The same is reflected in the S-ratio of 300. There is a significant positive correlation of Xlf with XARM (R^2=0.94), SIRM (0.98) & Soft-IRM (0.99), indicating overall SD ferromagnetic concentration governing all these parameters. A strong negative correlation of coercivity B(0)R for all the above parameters indicates that the higher concentration for SD ferrimagnets corroborates with more SP fraction.

Previously the Xfd% has indicated significant SP content. Therefore, a mixture of SD and SP rather than MD appears to have controlled the above relation. Due to a higher ferromagnetic influx of SD ferrimagnetism the SP content is also enhanced. The Xfd% shows a positive correlation with XARM/Xlf, confirming an influx of SD and SP ferrimagnets. XARM shows a positive correlation with SIRM and soft-IRM but a negative correlation with SIRM/Xlf, indicating SP influence of SIRM and Xlf where SIRM drops sharply with the increase in Xlf due to SP content. Therefore, the overall mineral magnetic data indicate that SD and SP content variations govern the studied parameters. The broad overall trend shows a gradual increase in the concentration of ferromagnetic minerals of almost unimodal nature, except for the topmost samples being disturbed by surface activities. Iterative matching of the variation in individual parameters allows five distinct zones closely comparable to lithologic boundaries. Zone-I falls with the basal gravely calcareous unit showing a gradual increasing trend in the ferromagnetic concentration. This fining upward unit denotes the increasing concentration of SD

ferromagnetic towards the top. There is only a minor change in the type of mineralogy (i.e. domain size in the present case), although the concentration increases gradually upwards. The Zone I is followed by Zone II, which marks an influx with a minor peak and a more gradual change in ferrimagnetic concentration. This unit falls in reddish-brown clay. Although the colour displays a hematite-like appearance, the magnetic mineralogy does not reveal any signs of ~~the~~ antiferromagnetic mineral oxides, and hematite, if at all present, may be fine-grained. This follows Zone III displaying variation in all the mineralogic parameters falling within the unit of volcanic ash occurrences.

Although no domain size change is indicated by B(0)R, the S-ratio depicts a relatively larger domain towards MD ferrimagnets in agreement with lowering Xfd, XARM, and higher HardIRM. Overall, there is a significant fluctuation in the mineralogy and concentration within this Zone of volcanic ash. After this, Zone IV maintains a trend similar to Zone II, whereas the topmost Zone with one sample appears to reflect a disturbed trend. The mineral magnetic studies show unimodal mineralogy except for a variation in the volcanic ash horizons. Although the Xfd shows significant SP content, it is mainly independent of trends indicated by Xlf and XARM. The HardIRM shows the most significant anomaly with volcanic ash (Zone III), the origin of which is not clear, since the B(0)R and S-ratio remain reasonably constant with the SD-MD ferromagnetic range. The volcanic ash, therefore, can be assumed to have deposited MD ferrimagnets of aeolian origin. The SP and SD content for the rest of the units denote floodplains-like depositional environment except for the lower unit (Zone I) depicting channel like a deposition. The remarkably gradual nature of variation indicates the almost negligible occurrence of high-energy flood events and the absence of any seasonal deposits. The abundance of SP fraction suggests pedogenic origin either by transported soils or in situ formation.

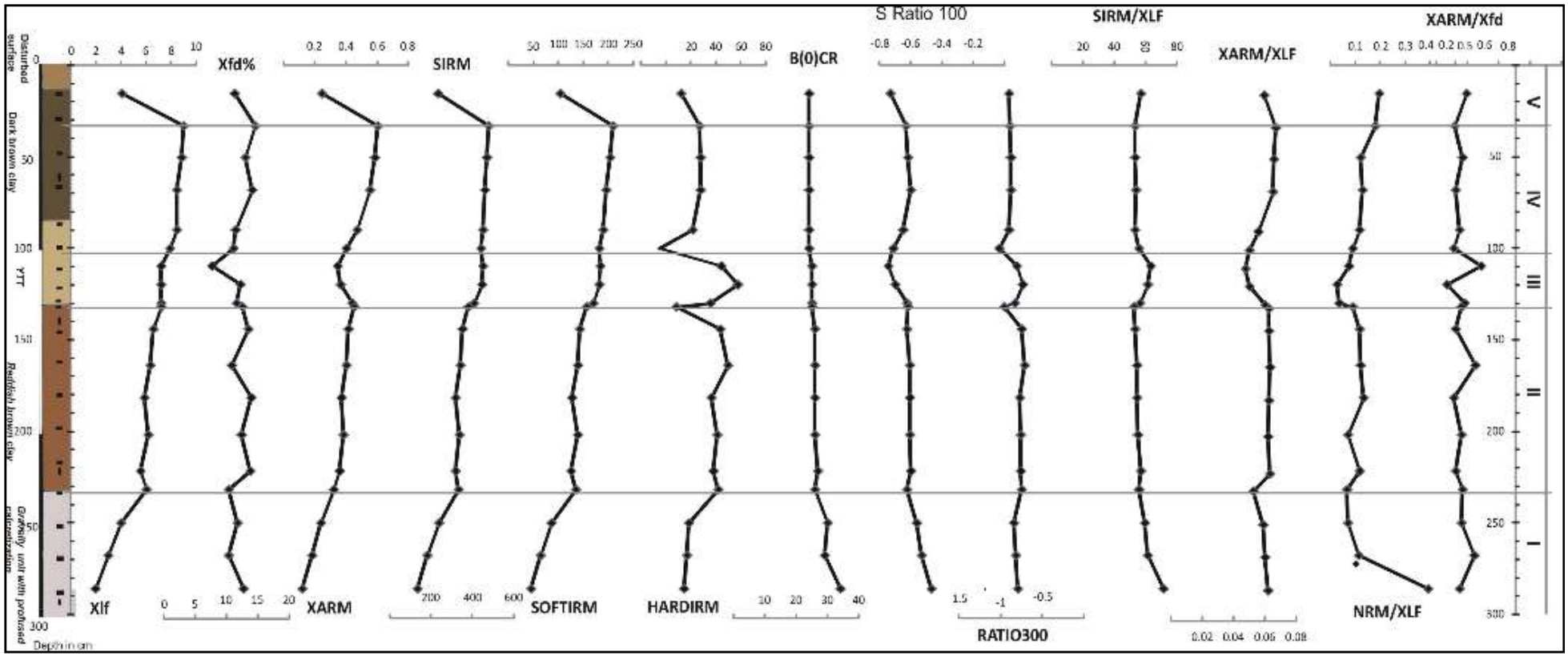

Figure 4.6.2: Rock magnetic parameters and inter parametric ratios for sediment samples from Retlapalle step trench.

4.6.2.2. Particle Size Analysis

Most of the samples from the Retlapalle section are polymodal silts, suggesting relatively low energy fluvial depositional settings (Fig 4.6.3), which is ideal archaeologically (less chance of artefact mobility). The presence of tephra changes the size distributions as the system is swamped with lots of material of the same size; however, the tephra samples were all fluvially reworked.

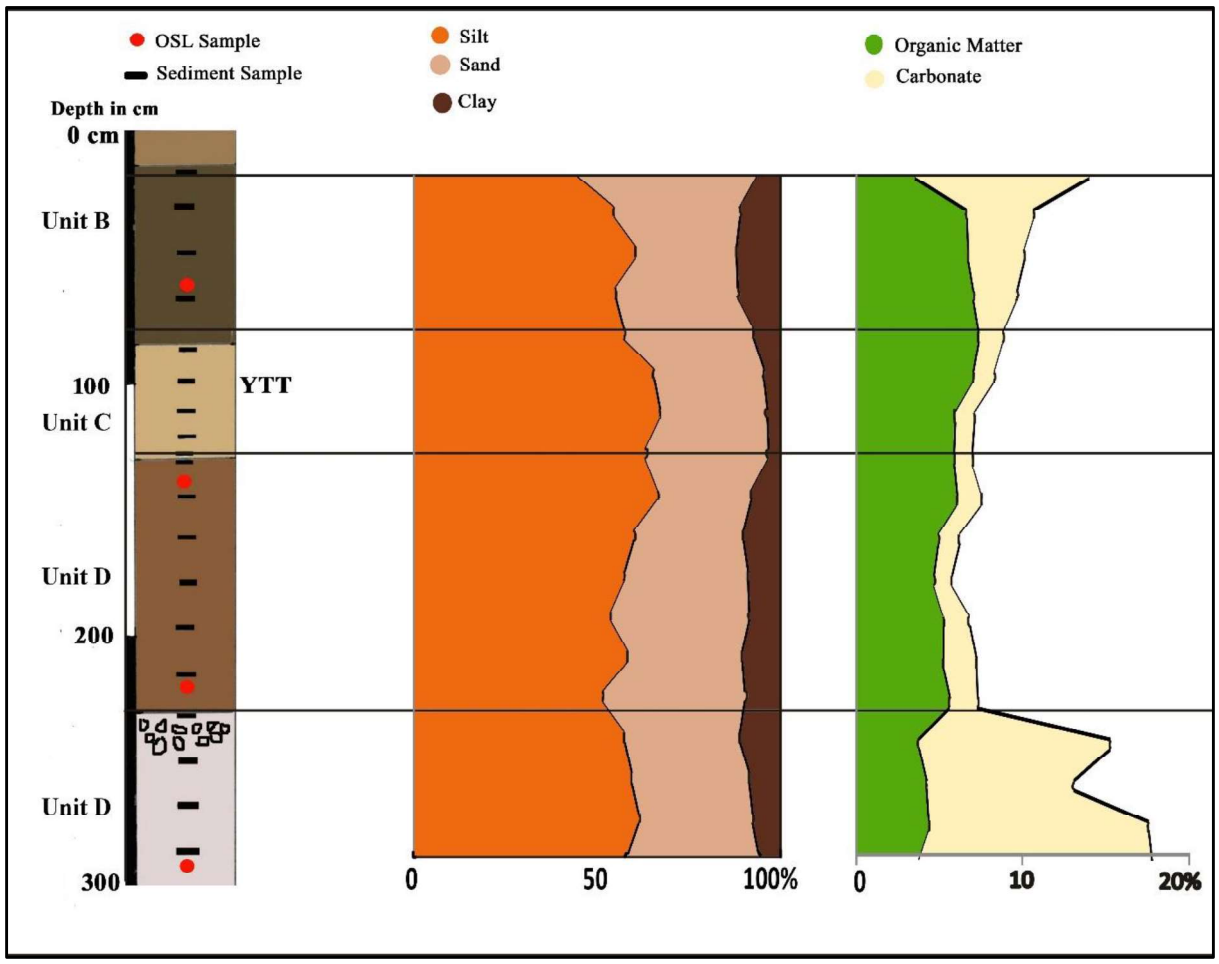

Figure 4.6.3: Particle size, organic matter, and carbonate values for the Retlpalle step trench. The sediment log shows the position of the YTT deposits and samples collected at 10 cm interval.

4.6.2.3. Geochemistry

Glass shards within the tephra samples occur as pristine colourless blocky and bubble wall shards up to 100 µm long (Fig 4.6.4). The composition of the glass shards from the Retlapalle is 70.77-73.23 wt% SiO2, 4.15-4.93 wt% K2O, 2.83-3.46 wt% Na2O, 0.67-0.90 wt% CaO, and 0.83-1.05 wt% FeOT (all Fe presented as FeO). These are similar in composition to glass shards from the tephra preserved in the Jurreru Valley, Son Valley, Lenggong, and the YTT

proximal samples (Fig 4.6.5a). Biotite occurs as tiny (up to 50 μm) thin mica sheets in the Retlapalle distal tephra. The compositional range of biotite crystals in Retlapalle distal tephra is 20.74-23.00 wt% FeOT, 9.08-9.58 wt% MgO, and 0.23-0.24 wt% F. These are similar to the biotite compositions of the distal YTT units in Malaysia and India (Son Valley, Jurreru Valley) (Fig 4.6.5b). Unlike the glass compositions, the biotite compositions of the YTT are distinct from those samples of the older, large eruptions from Toba, the OTT, and the MTT. Therefore, the similar composition of the biotite from the Retlapalle tephra (and others in India) to the YTT confirms that the deposit is associated with the last major eruptive event of Toba.

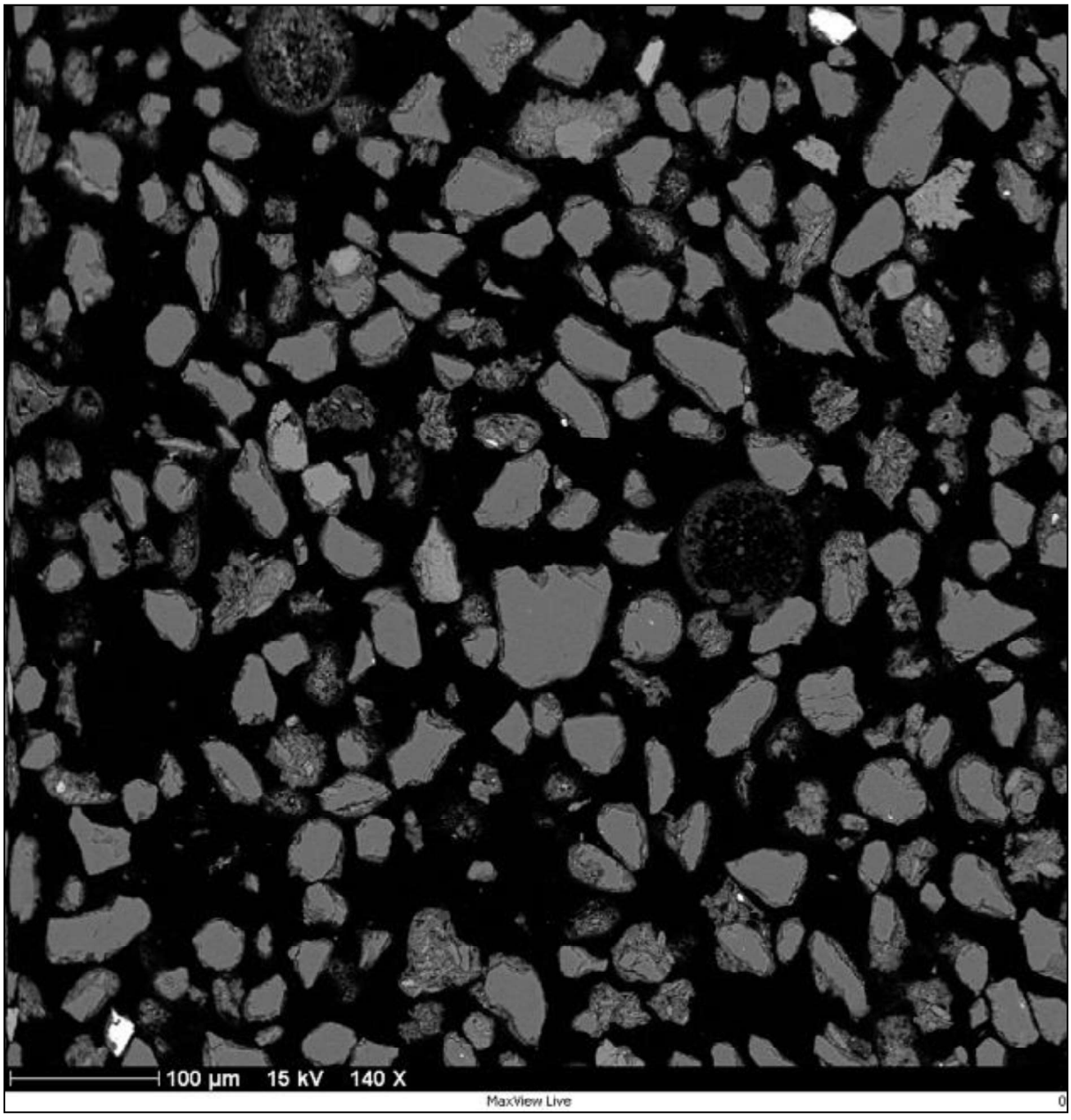

Figure. 4.6.4: A scanning electron microscope image of glass shards and (brighter) biotite grains (top right corner and bottom left corner of the image) from Retlapalle.

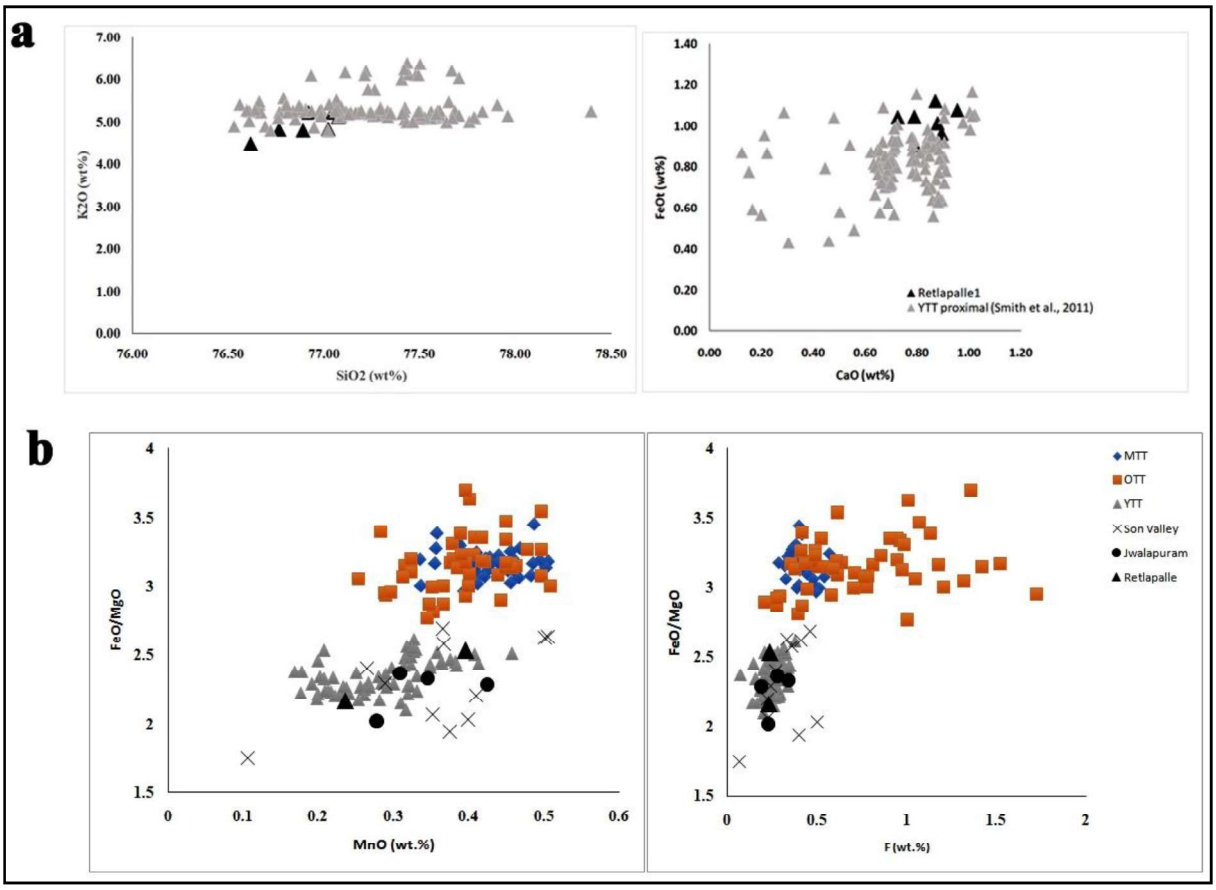

Figure. 4.6.5: a: Glass shard compositions (normalized to 100%) from Retlapalle tephra (black diamonds) compared with published proximal YTT data (grey triangles; from Smith et al., 2011); b: Biotite composition of crystals from the deposits at Retlapalle compared with those from the tephra in the Son and Jurerru valleys and proximal samples of OTT, MTT And YTT (data from Smith et al., 2011).

4.6.3. Luminescence Chronology

Sediment samples from Units B, D and E from the Retlapalle step trench were dated using the post-infrared infrared-stimulated luminescence (pIR-IRSL) method. The age of Unit B, which is above YTT, is 64.4±3.9 ka, and the age for the sample from Unit D underlying the YTT is 76.3± 5.5 ka (Table. 4.6.1). The overdispersion (OD) in estimated D_e values for Unit B and C are quite low (~8%) as shown in Table. 4.6.1 and Fig. 4.6.6c, indicating well bleaching of sediment before burial. Thus, for D_e estimation central age model (CAM) was used. The sample from Unit D shows relatively higher over-dispersion (30%) than the samples from Unit B and D. This may be due to the presence of rich carbonates. However, Unit E yielded an age of 143.6±18.1.

Table 4.6.1: Dose rate data, D_e values and OSL ages for the sediment samples from the step-trench at Retlapalle.

Sample Code	Depth (cm)	Radionuclide activity [a]				Equivalent doses				OSL age (ka)
		U (ppm)	Th (ppm)	K (%)	Total Dose rate[b,c] (Gy/ka)	No. of aliquots/ grains	Water content (%)	OD (%)	D_e (Gy)[d]	
RTP-18-1	60	2.8±0.3	8.4±1.0	1.5±0.07	3.03±0.17	19	20.6	7.1	193.8±4.5	**64.4±3.9**
RTP-18-2	110	2.6±0.6	11.7±2.2	1.4±0.09	3.07±0.21	20	20.1	8.2	233.7±5.6	**76.3±5.5**
RTP-18-4	278	4.08±0.39	5.76±1.38	0.81±0.09	2.64±0.19	10	12.65	30	378±39.2	**143.6±18.1**

[a] Radioactivity measurement made on the dried, homogenized and powered sample by gamma-ray spectrometry and alpha counting.

[b] Includes cosmic-ray dose rate

[c] 12.5±0.5% and 200±20 ppm Rubidium (^{87}Rb) concentrations were used to estimate the internal dose rate

[d] after subtracting a residual dose of 20 Gy

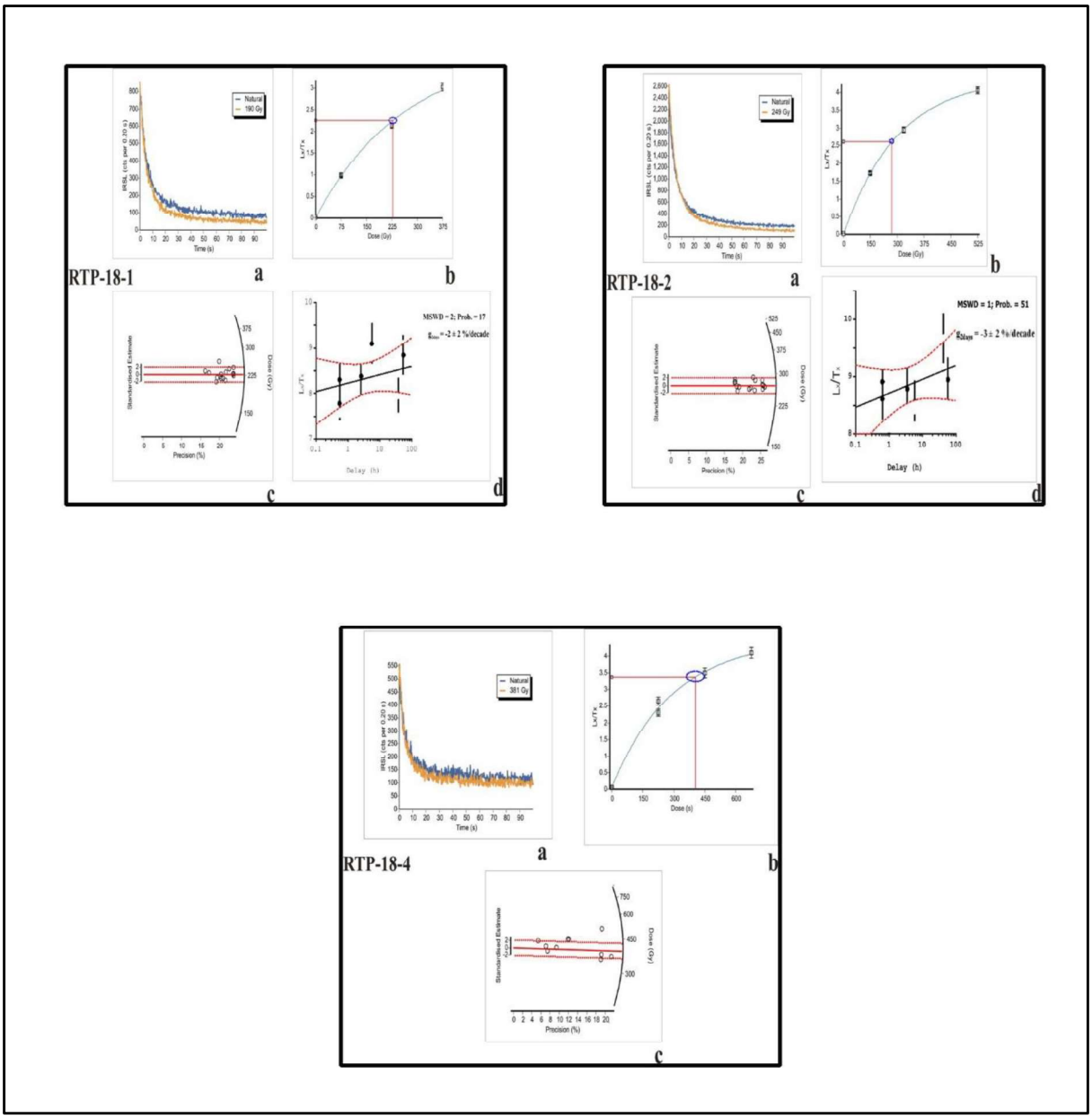

Figure. 4.6.6: Results of pIR-IRSL analyses at Retlapalle. Each panel shows a-d separately for the samples RTP-18-1, RTP-18-3, and RTP-18-4. a: typical feldspar shine down curve; b: typical growth curve; c: radial plot representing the estimated palaeodoses; d: typical *g*-value data.

The fading rate estimated for the samples shows *g* - values either less than 1% or negative with ~100% errors, suggesting the p-IR-IRSL signal is not affected by the anomalous fading (Buylaert et al., 2011). Unit D and Unit C (YTT) had a diffused contact suggesting no considerable time gap between the depositions of the two Units. However, Unit B shows a sharp contact with the underlying YTT deposit, indicating a possible unconformity. This corresponds to an age gap of 12 ka between Unit B and D. The Middle Palaeolithic artefact

bearing Unit E was dated to 143 ka, and there was an unconformity of 64 ka after the deposition of Unit E.

4.6.4. Lithic Technology

From the step-trench (within Unit E), 101 lithics were collected, most of them being the debitage, flakes and flaked pieces (79%). Finished artefacts consist of one unidirectional core, one diminutive biface, and two retouched points (Table. 4.6.2 and Fig. 4.6.7). These were embedded within the calcrete horizon, and a carbonate crust on the surface of the artefacts was observed. Informally retouched artefacts consisting of retouched flakes (n=6) and pieces (n=6) are also present in the assemblage.

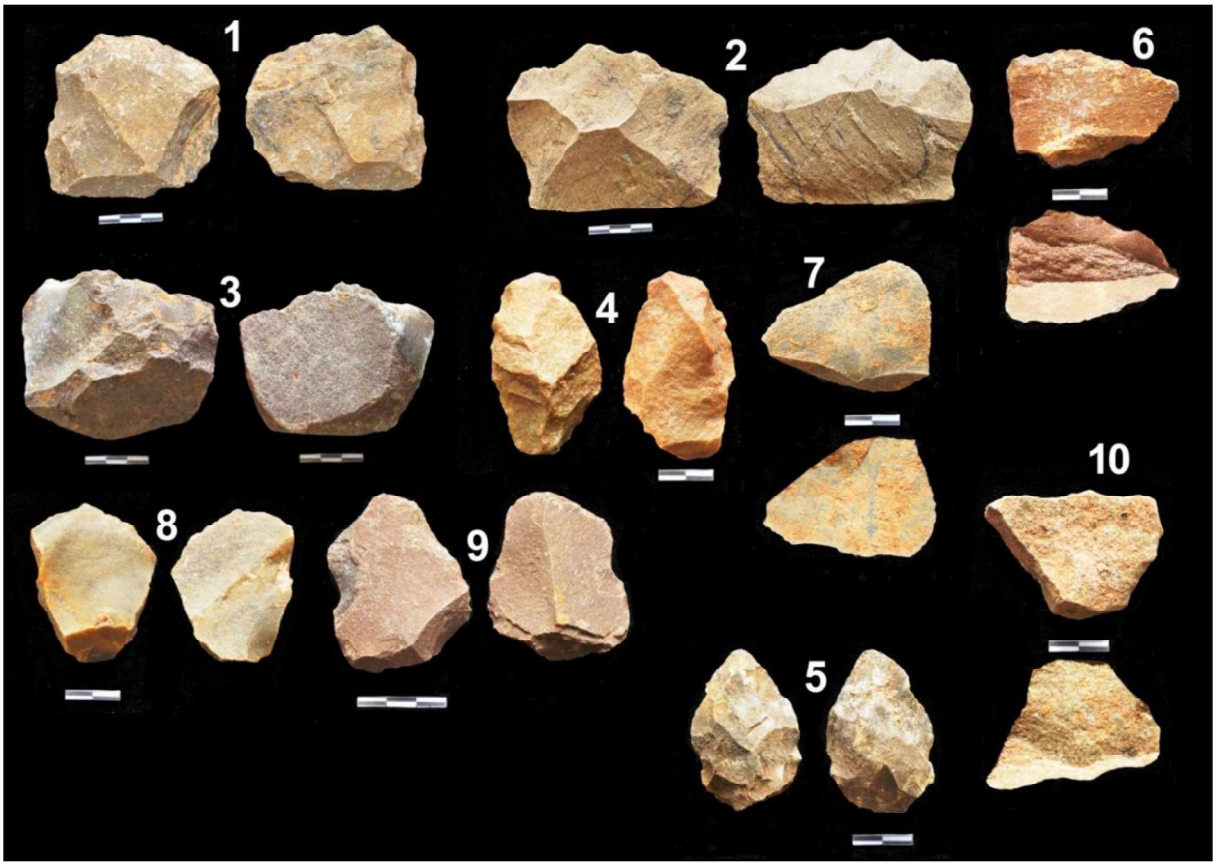

Figure 4.6.7: Representative lithic artefacts from Unit E at the Retlapalle step-trench. 1: Multiplatform core; 3: Unidirectional core; 2,8,9 and 10: flakes; 6 and 7: Prepared core flakes; 4: retouched piece; 5: diminutive hand axe.

A 10 x 10 m grid was laid out adjacent to the step-trench to increase the artefact sample size to understand the assemblage technology better. Only one artefact horizon was identified from the step-trench, and surface observations indicated the same. Therefore, artefacts collected from the surface grid and trench are treated as a single assemblage for analysis.

Table. 4.6.2: Composition of the assemblage recovered from step-trench and surface grid.

Type	Trench	%	Grid	%	Total	%
Cores						
Recurrent Levallois core	0	0.0	4	1.7	4	1.2
Preferential Levallois core	0	0.0	6	2.6	6	1.8
Levallois point core	0	0.0	1	0.4	1	0.3
Discoidal core	0	0.0	9	3.9	9	2.7
Radial Core	0	0.0	7	3.1	7	2.1
Blade core	0	0.0	4	1.7	4	1.2
Unidirectional core	1	1.0	0	0.0	1	0.3
Core fragment	5	5.0	12	5.2	17	5.2
Total Cores	**6**	**5.94**	**43**	**18.78**	**49**	**14.85**
Retouched						
Bifacial Point	0	0.0	11	4.8	11	3.3
Unifacially Retouched Point	0	0.0	2	0.9	2	0.6
Retouched Point	2	2.0	3	1.3	5	1.5
Tang Point	0	0.0	5	2.2	5	1.5
End scraper	0	0.0	3	1.3	3	0.9
Round scraper	0	0.0	2	0.9	2	0.6
Side Scraper	0	0.0	1	0.4	1	0.3
Notch	0	0.0	3	1.3	3	0.9
Retouched blade	0	0.0	2	0.9	2	0.6
Retouched flake-blade	0	0.0	2	0.9	2	0.6
Retouched flake	6	5.9	26	11.4	32	9.7
Retouched piece	6	5.9	10	4.4	16	4.8
Chopper	0	0.0	1	0.4	1	0.3
Diminutive biface	1	1.0	1	0.4	2	0.6
Diminutive Cleaver	0	0.0	4	1.7	4	1.2
Total Retouched	**15**	**14.85**	**76**	**33.19**	**91**	**27.58**
Unretouched						
Levallois flake	0	0.0	6	2.6	6	1.8
Blade	0	0.0	9	3.9	9	2.7
Flake-blade	0	0.0	3	1.3	3	0.9
Flake	30	29.7	27	11.8	57	17.3
Flaked piece	29	28.7	16	7.0	45	13.6
Debitage (< 2 cm in length)	21	20.8	49	21.4	70	21.2
Total Unretouched	**80**	**79.21**	**110**	**48.03**	**190**	**57.58**
Total	**101**	**100**	**229**	**100**	**330**	**100**

Most artefacts do not contain cortex (81%), indicating that the initial preparation of cores must have taken place off-site near raw material sources. As the site Retlapalle is located on the bank of a tributary stream, Erravagu, pebbles from the stream bed must have served as raw material sources. Except for three artefacts showing evidence of slight abrasion rest of the assemblage is in mint condition. Most of the artefacts from the step trench show a thin crust of calcrete on the surface of the artefacts, whereas this was limited only to a few artefacts collected from the surface. The number of cores in the assemblage accounts for 49, most of which belong to formal reduction strategies. The formal core reductions include Levallois, blade, discoidal, radial, and unidirectional. Notably, except for 17 core fragments, no other informal cores are present in the assemblage. Among Levallois core reduction strategies, recurrent and preferential systems are present along with one example of Levallois point core (Fig. 4.6.8; Fig. 4.6.9; Fig. 4.6.10). Nine discoidal cores are present in the assemblage, among which four cores are less than 5 cm in length (Fig. 4.6.11 and Fig. 4.6.12). Four blade cores present in the assemblage have parallel flake scars (Fig. 4.6.13). Seven radial cores display centripetal radial reduction.

Table. 4.6.3: Statistical data for Core attributes.

Attribute	N	Mean	SD	Min.	Max.
Length	32	67.56	16.78	41.20	114.45
Proximal Width	32	62.60	20.68	26.17	109.19
Medial Width	32	70.12	19.15	37.90	123.84
Distal Width	32	52.77	17.74	26.35	98.87
Proximal Thickness	32	29.77	26.99	7.81	141.83
Medial Thickness	32	34.03	20.22	13.41	119.87
Distal Thickness	32	25.91	13.53	10.46	77.86
Proximal Shape	32	0.89	0.15	0.67	1.29
Distal Shape	32	1.39	0.30	1.00	2.28
Elongation	32	0.98	0.20	0.63	1.47
Flatness	32	2.35	0.66	0.86	4.22
No. of Core Rotations	32	2.75	0.84	1.00	4.00
Last Platform Angle	32	72.34	8.71	50.00	95.00
No. of Major Flake Scars	32	2.72	1.11	1.00	6.00
No. of Flake Scars	32	4.84	1.37	3.00	8.00
No. of Feather terminations	32	1.41	0.91	0.00	4.00
No. of non-feather Terminations	32	1.34	1.15	0.00	4.00
Last Scar Length	32	41.46	16.12	18.17	77.58
Last Scar Width	32	31.40	13.53	10.84	81.90
Last Scar Elongation	32	1.42	0.44	0.65	2.45

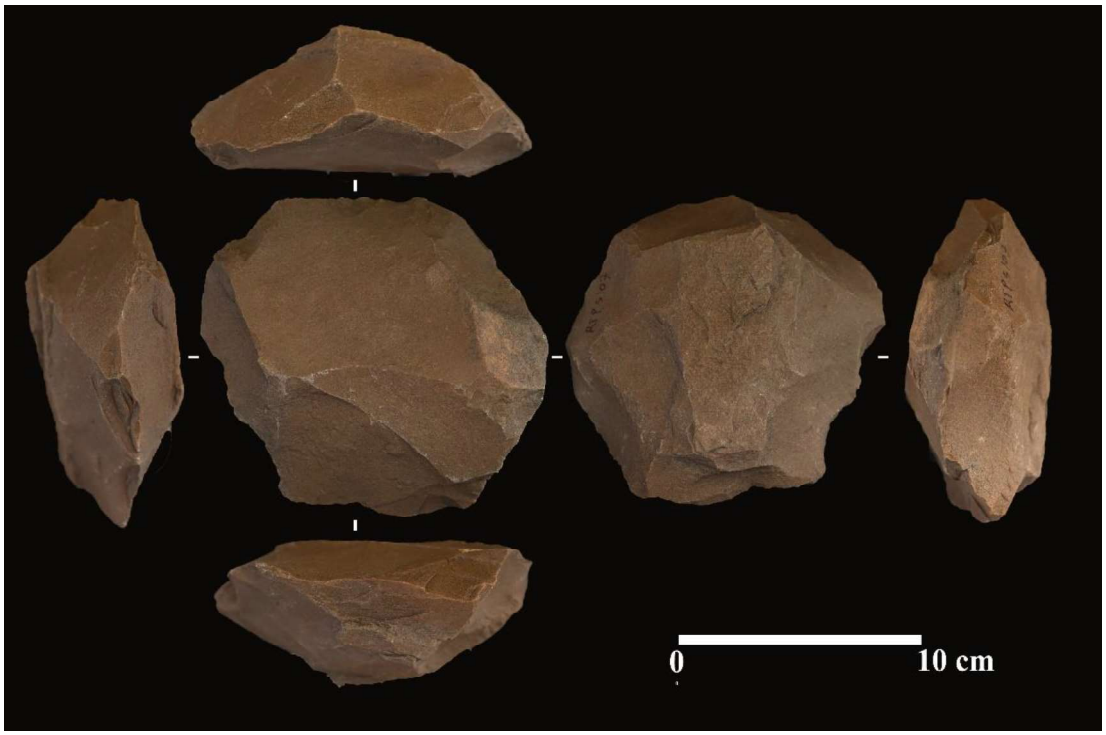

Figure. 4.6.8: Preferential Levallois core.

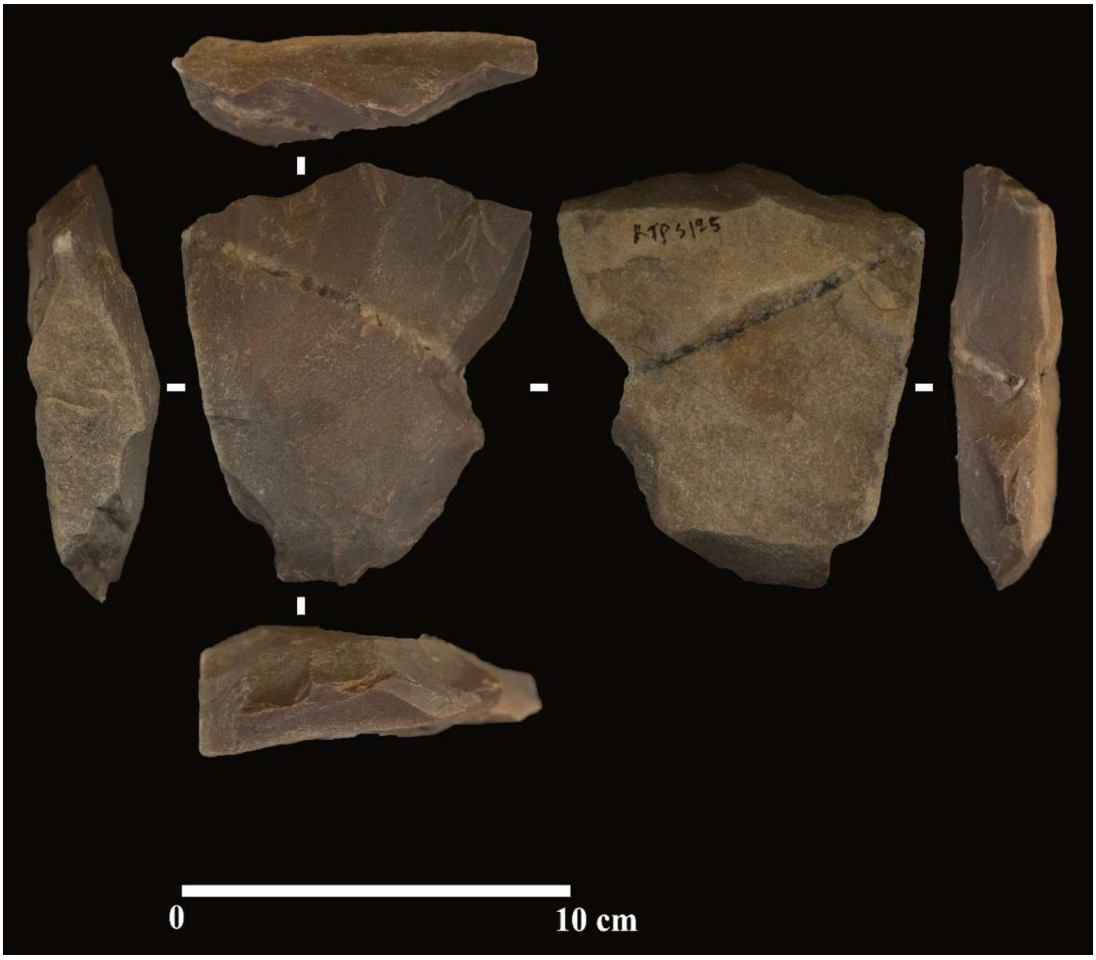

Figure. 4.6.9: Levallois point core.

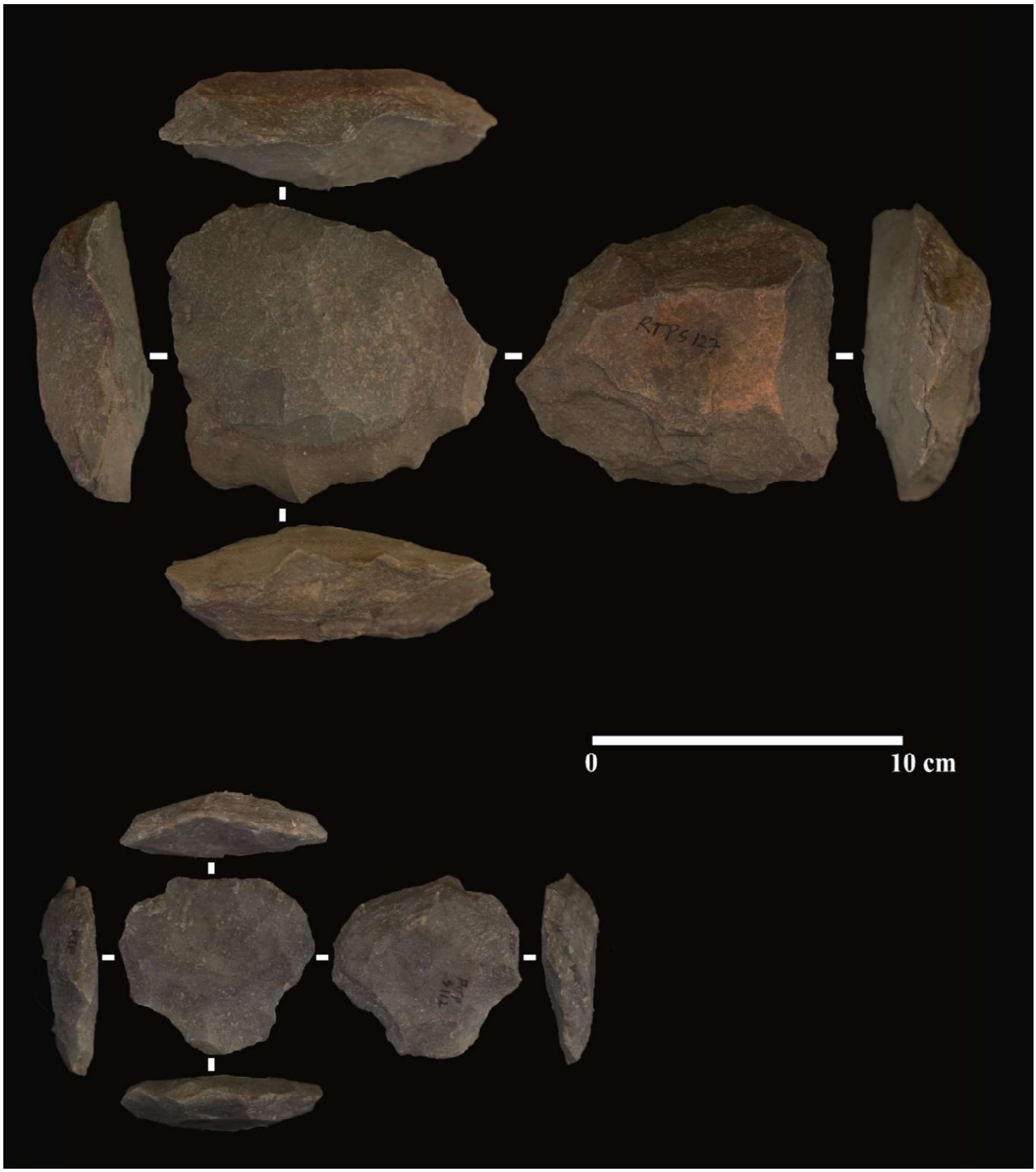

Figure. 4.6.10: Recurrent Levallois cores.

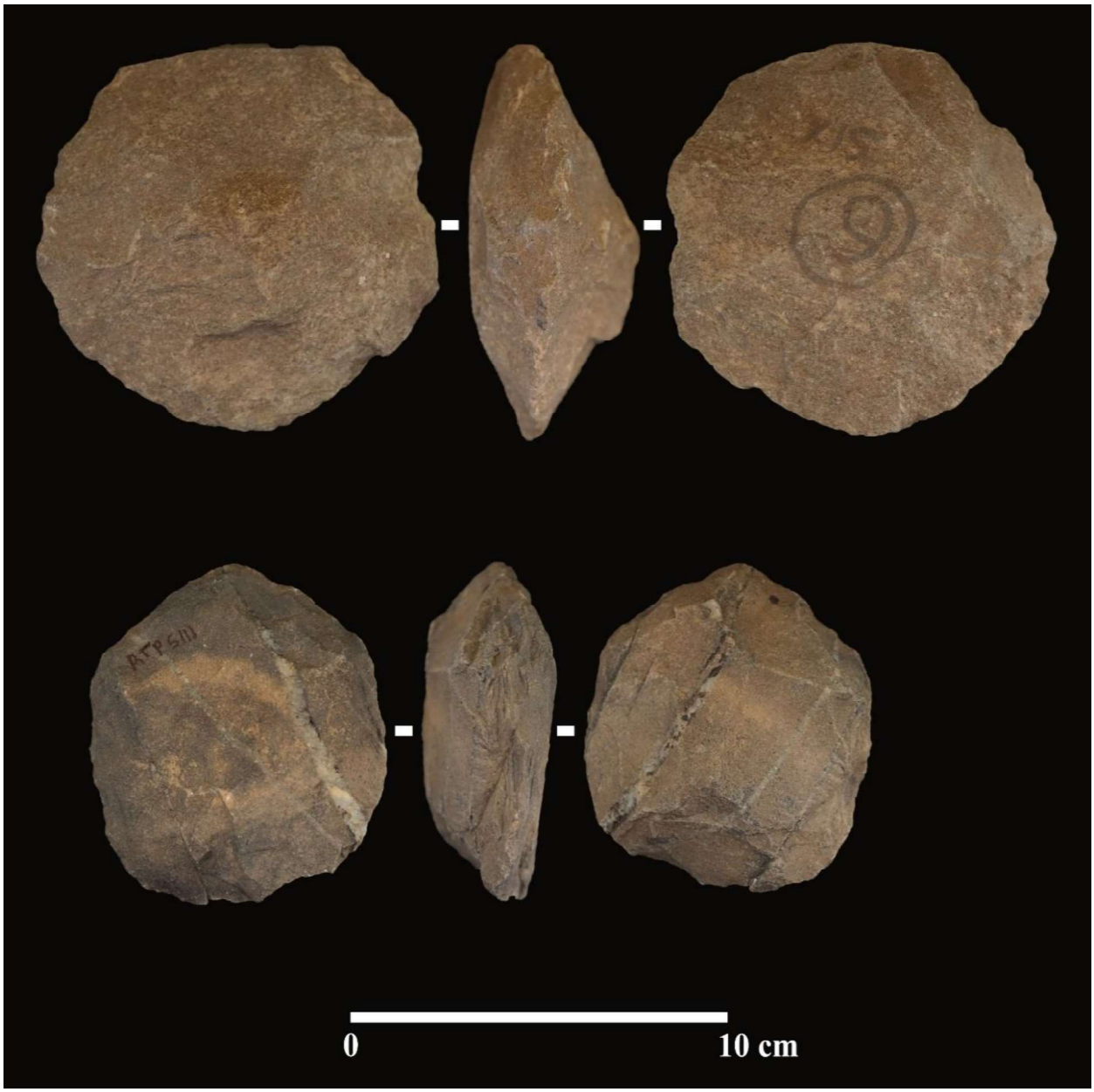

Figure. 4.6.11: Discoidal cores in the assemblage. Note the variation in the size of the cores.

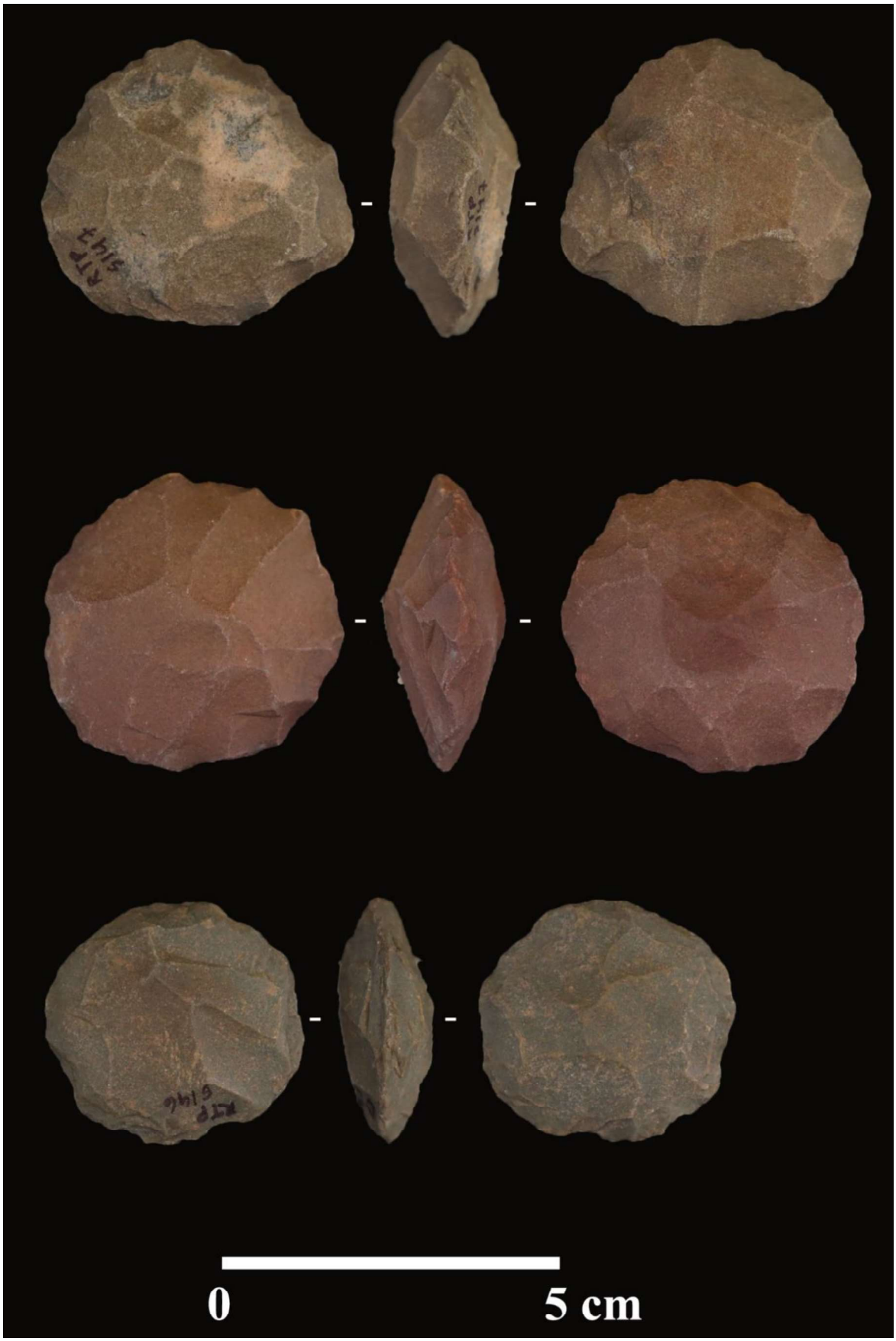

Figure. 4.6.12: Small Discoidal cores.

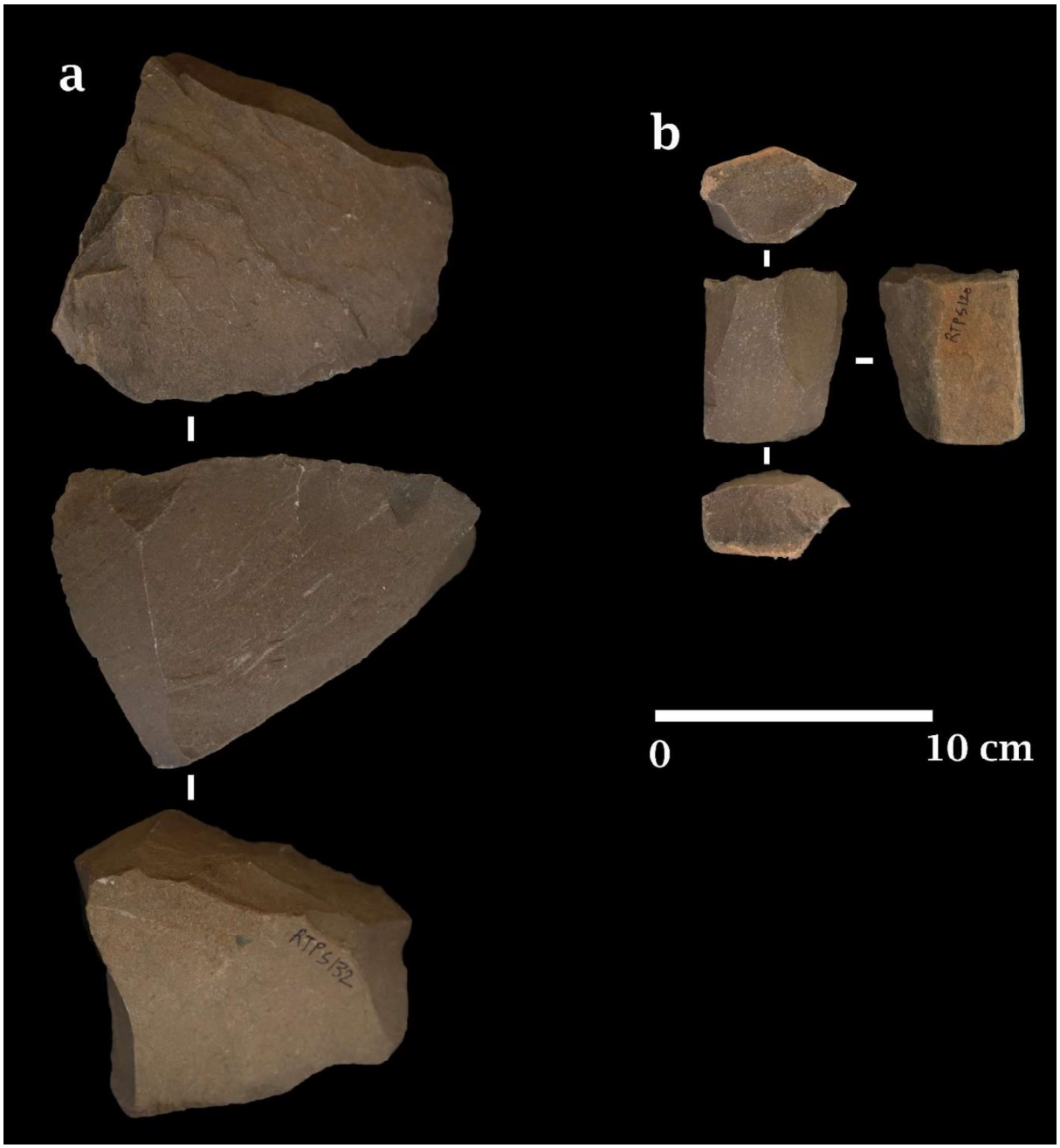

Figure. 4.6.13: Blade cores in the assemblage.

A maximum of three and a minimum of two core rotations were observed in Levallois cores, whereas discoidal and radial cores show a maximum of four and a minimum of three rotations (Table. 4.6.3). Blade and unidirectional cores show single rotation. Most cores show two (n=12) and three (n=11) major scars (more than 1/3 core length), with three cores exhibiting one, four cores with four, five, and six scars each. Cores' mean length, medial width and medial thickness are 67.56x70.12x34.03 mm when oriented along the flaking axis (last flake scar). The core's proximal, medial, and distal widths measured along the flaking axis are 62.60x70.12x52.77 mm, respectively. The proximal shape of the cores is relatively straight

(mean 0.89 mm), whereas the distal shape is tapering (mean 1.39 mm). No considerable variation in core elongation is observed, ranging between 0.63-1.47, maybe because there is no significant variation in the cores' mean length and mean medial width. The core flatness index ranges from 0.90 to 4.49, where most cores are wider than thick. Three cores have cortical platforms, 15 have single conchoidal platforms, and 14 show multiple conchoidal platforms. Platforms were facetted on 20 cores; in 12 instances, no preparation was observed. The last scar face length of cores is less than the axial core length, indicating the flaking face is limited to the smaller axial surface. The last scar lengths range from 18.17-77.58 mm, with an average of 41.46 mm, and the last scar widths range between 10.84-81.90 mm, and a mean of 31.40 mm. On average, the last flake scar elongation indicates that relatively square-shaped flakes were removed (mean=1.42). Half of the last flake scars exhibit feather terminations (50.57%), with non-feather terminations accounting for 49.42%. One hundred forty-seven flakes, including both retouched and unretouched, have been recorded in the assemblage, including 111 complete flakes. Flakes were classified according to technological type to understand their position in the reduction sequence (Table. 4.6.4). Typo-technology of the flakes was described based on the complete flakes.

Table. 4.6.4: Technological breakdown of the flakes in the assemblage.

Technological Type	Unretouched	%	Retouched	%	Total	%
Blade	7	11.86	2	3.77	9	8.04
Core preparation flake	25	42.37	18	33.96	43	38.39
Roughout flake	5	8.47	0	0.00	5	4.46
Prepared core flake	12	20.34	26	49.06	38	33.93
Levallois flake	7	11.86	5	9.43	12	10.71
Flake-blade	2	3.39	1	1.89	3	2.68
Eclat deborant	1	1.69	0	0.00	1	0.89
Kombewa flake	0	0.00	1	1.89	1	0.89
Total	**59**	**100**	**53**	**100**	**112**	**100**

A wide range of technological diversity is evident amongst the flakes, from core preparation flakes to end products. Few roughout flakes (n=5) indicate that initial preparation of the cores was done off the site; however, core preparation flakes account for 38%, suggesting that later stages of core reduction were carried out at the site. The presence of one platform rejuvenation also corroborates the observation mentioned above. End products such as Levallois flakes, and

prepared core flakes account for 55% and dominate the flake component (Fig. 4.6.14). Blades and elongated flakes also form a considerable percentage in the assemblage (3%) (Fig. 4.6.15).

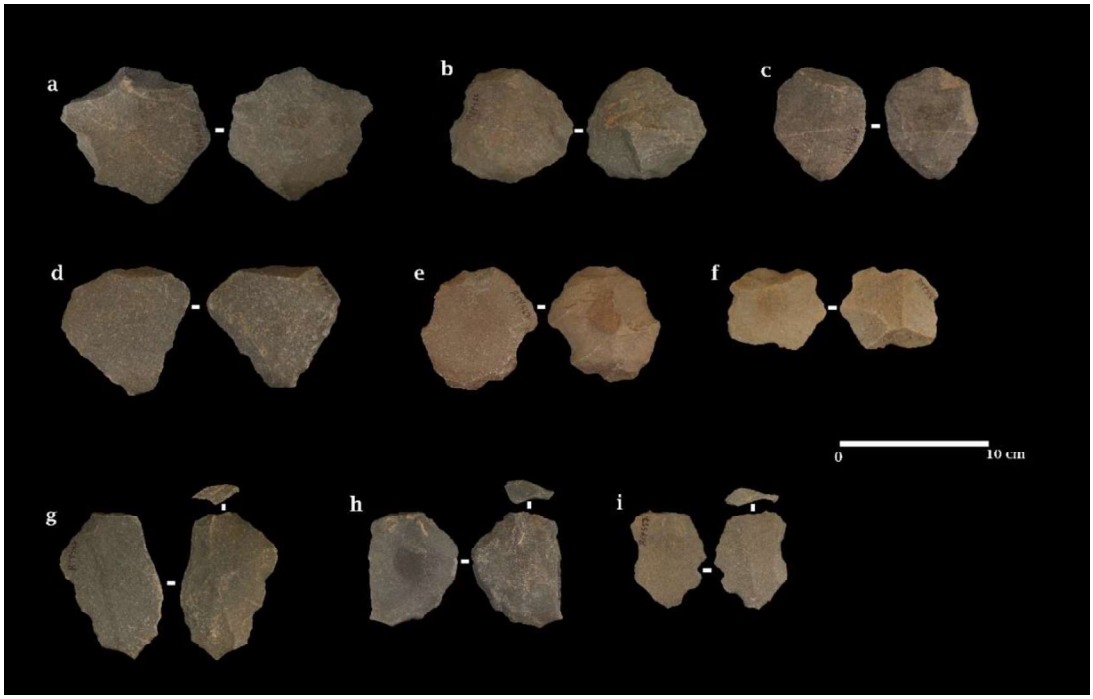

Figure. 4.6.14: Prepared core and Levallois flakes. a to e: Prepared core flakes; f to i: Levallois flakes.

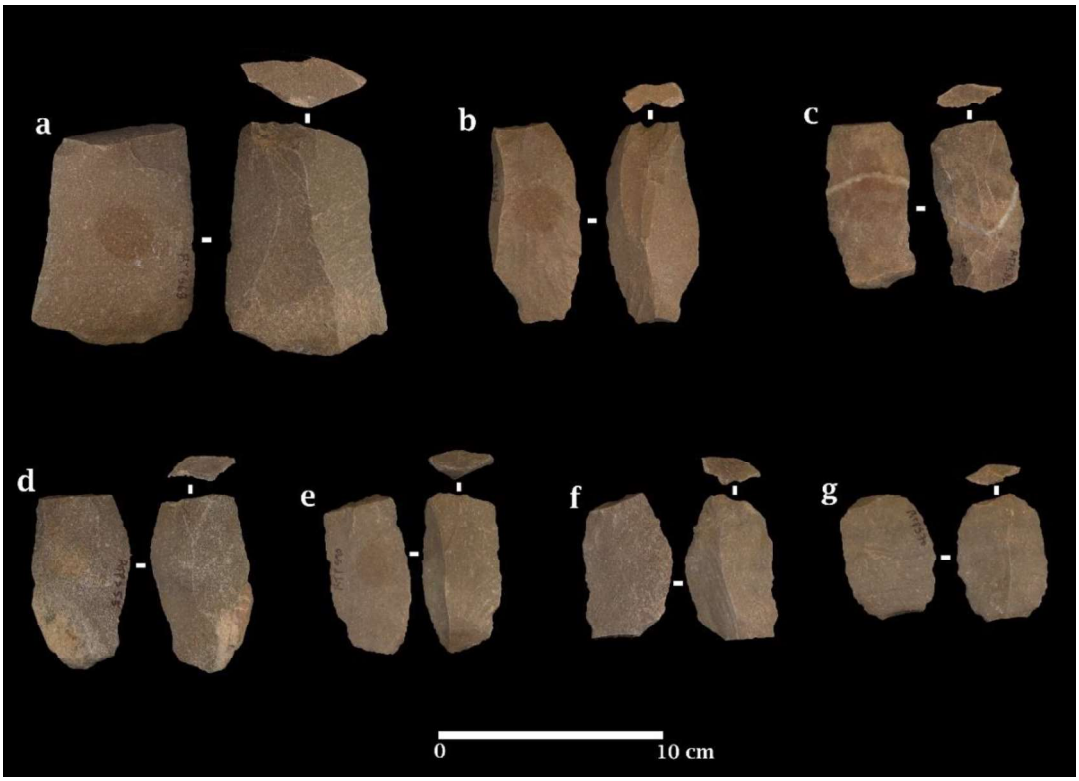

Figure. 4.6.15: Blades in the assemblage.

The most common dorsal scar patterns present on complete flakes in the assemblage are radial (32.1%), followed by proximal (31.2%) and weakly radial (25.8%). Flakes with no dorsal scars (cortical flakes) were present in 3.5%, and on 7.1% of the flakes, it was difficult to determine the dorsal scar pattern. Cortical coverage ranges from 0-100%, with 83% of flakes recorded with no cortex and 12.5% with less than 50% cortex present. Low frequencies of flakes with only cortical platforms (5.3%) and 100% cortical cover of the dorsal and platform surface (4.4%) are observed. Most flakes present feather terminations (91%), followed by step (4.4%) and indeterminate (4.4%) terminations. Mean axial flake dimensions are 57.2 x 47.7 x 13.5 mm; on average, flakes are oval/squarish in shape (mean elongation=1.30) (Table. 4.6.5).

Table. 4.6.5: Statistical data for the flake attributes.

Attribute	N	Mean	SD	Min.	Max.
Length	112	57.20	22.81	17.37	193.14
Proximal Width	112	42.32	17.68	12.67	108.77
Medial Width	112	47.73	17.56	11.39	113.05
Distal Width	112	38.42	18.08	6.54	120.49
Medial Thickness	112	13.59	4.22	5.25	28.32
Elongation	112	1.30	0.69	0.62	6.81
Flatness	112	3.59	1.01	1.10	6.97
Proximal Shape	112	0.89	0.19	0.43	1.42
Distal Shape	112	1.36	0.45	0.72	3.40
Platform width	112	35.89	17.36	5.67	110.27
Platform Thickness	112	12.53	5.10	3.53	41.26
Platform area	112	499.93	412.16	20.02	2581.42
Platform Angle	112	74.64	9.95	55.00	110.00
Dorsal scar count	112	2.84	1.25	0.00	6.00
No. Unidirectional arrises	112	0.41	0.67	0.00	2.00
No. Radial arrises	112	1.06	1.09	0.00	4.00

Typical flakes are more than four times wide as thick (mean flatness=3.59), with a maximum range of 1.10-6.97. 75.8% of the flakes exhibit slightly expanding proximal margins (mean proximal shape index=0.89), with 24.1% exhibiting contracting proximal margins, leading to an upper proximal shape index of 1.14. In contrast, the distal shape indicates that 77.6% of the flakes exhibit distal contracting margins (mean=1.48). Single conchoidal platforms are the

most common type (44.6%), followed by multiple conchoidal (41%), dihedral (6.2%), and cortical (5.3%) types. Platform preparation is dominated by facetted platforms with 47.3%, followed by overhang removal (25%), unprepared platforms (24.1%) and indeterminate (3.5%). A wide range in platform size is evident, with platform width ranging from 5.67-110.27 mm and platform thickness ranging from 3.53-41.2 mm. The platform shape index indicates that platforms are typically elongated (mean=2.91), with 90% being two times wider than thick. A total of 45 artefacts categorized as flaked pieces are present, which bear no precise ventral morphologies or negative flake scars originating from the margins of the artefacts but have clearly undergone some reduction.

Ninety-one retouched artefacts, including Levallois points, scrapers, bifacial points and retouched pieces, are recorded in the assemblage. A wide range of retouched artefacts is present in the assemblage, including one chopper, two diminutive bifaces and four diminutive cleavers. Retouched pieces are also present in small quantities. Among the retouched category, informally retouched flakes, blades, flake-blades, and pieces collectively dominate with 15.8%. Points, including bifacial, retouched, and tang points, form 7% of the assemblage's second dominant category in retouched artefacts. Scrapers and notches form 2.7% of the assemblage. Prepared core flakes were the most preferred type to make retouched artefacts forming 50% of the total retouched artefacts. Retouch length measured on the retouched artefacts shows that half of the artefacts (51.8%) are randomly retouched, whereas, on 48.2% of the artefacts, retouch was regular. The average retouch length was 63.7%, ranging between 17.6-107.6 mm. The location of the retouch was recorded and divided between distal and lateral margins, both distal and lateral margins and random. 29.6% of the artefacts were retouched on both distal and lateral margins, followed by retouched on the distal end and random locations forming similar percentages (27.7%) and lateral margins (14.8%). Retouch type was also recorded as the flake surface on which retouch was done (dorsal, ventral, or both sides). Most of the time, retouching was observed on the dorsal surface (44.4%) and both dorsal and ventral surfaces (44.4%), followed by the ventral surface (11.1%). Notably, 11 bifacial points were noted in the assemblage with Length, Width, and thickness dimensions as 72.32x50.90x20.83 mm, respectively.

4.6.5 Summary

The site Retlapalle reveals Middle Palaeolithic assemblages dated to 143 ka and 76-64 ka associated to the YTT deposits. Particle size, mineral magnetic, and LOI analyses suggest that sediments at the site deposited under low energy fluvial conditions probably represent a pond or geological depression. Mineral magnetic does not identify any rapid changes in the sediments' magnetic properties, indicating no palaeosol formations. Even though the ages bracketing the YTT deposits suggest a primary ash deposit, the thickness and composition of the ash unit suggest a considerable mixing of other sediments possible during the redeposition of ash. In the present scenario, the most plausible explanation one can suggest in the background of the given data is that; a) the ash may have been redeposited immediately after ashfall.

The bottom-most sediment, Unit E, in the step trench yielded Middle Palaeolithic artefacts dated to the terminal Middle Pleistocene epoch. Core attribute analysis offers several insights into reduction intensity and strategy at Retlapalle. A relatively low proportion of cores with cortical surfaces, including platform surfaces, suggest that the primary reduction was conducted away from the site, possibly at the raw material procurement area. Levallois core types suggest that some reduction sequences were conducted principally at the site. The fewer variation in the size of flakes indicates that preliminary reduction activities were performed off the site. In addition, most flakes present minimal cortical cover that supports the abovementioned observation. Average flake dimensions typically fall between 13-57 mm, and the largest and smallest flakes present at the site are likely to have been by-products of reduction activity rather than the outcome of specific reduction strategies. However, the presence of Levallois flakes and small debitage (less than 2 cm in length) indicates that some specific debitage products were produced at the site. Platform types are typically complex, and platform preparation is common. Of all scar patterns, proximal and radial flakes dominate, indicating that radial flaking was employed to create flakes with large perimeters. Many blade core reduction products were also present in the assemblage. Diversification in the Levallois technology was also observed in the assemblage with preferential, recurrent and point cores.

4.7 Vemulapadu (Middle Palaeolithic)

The site Vemulapadu (15.556370° N, 79.332440° E) is located on the foothill of the northeastern part of the Velikonda hills which form the common watershed ridges for the Paleru and the Gundalakamma basins in the east and northwest respectively (Map. 4.7.1).

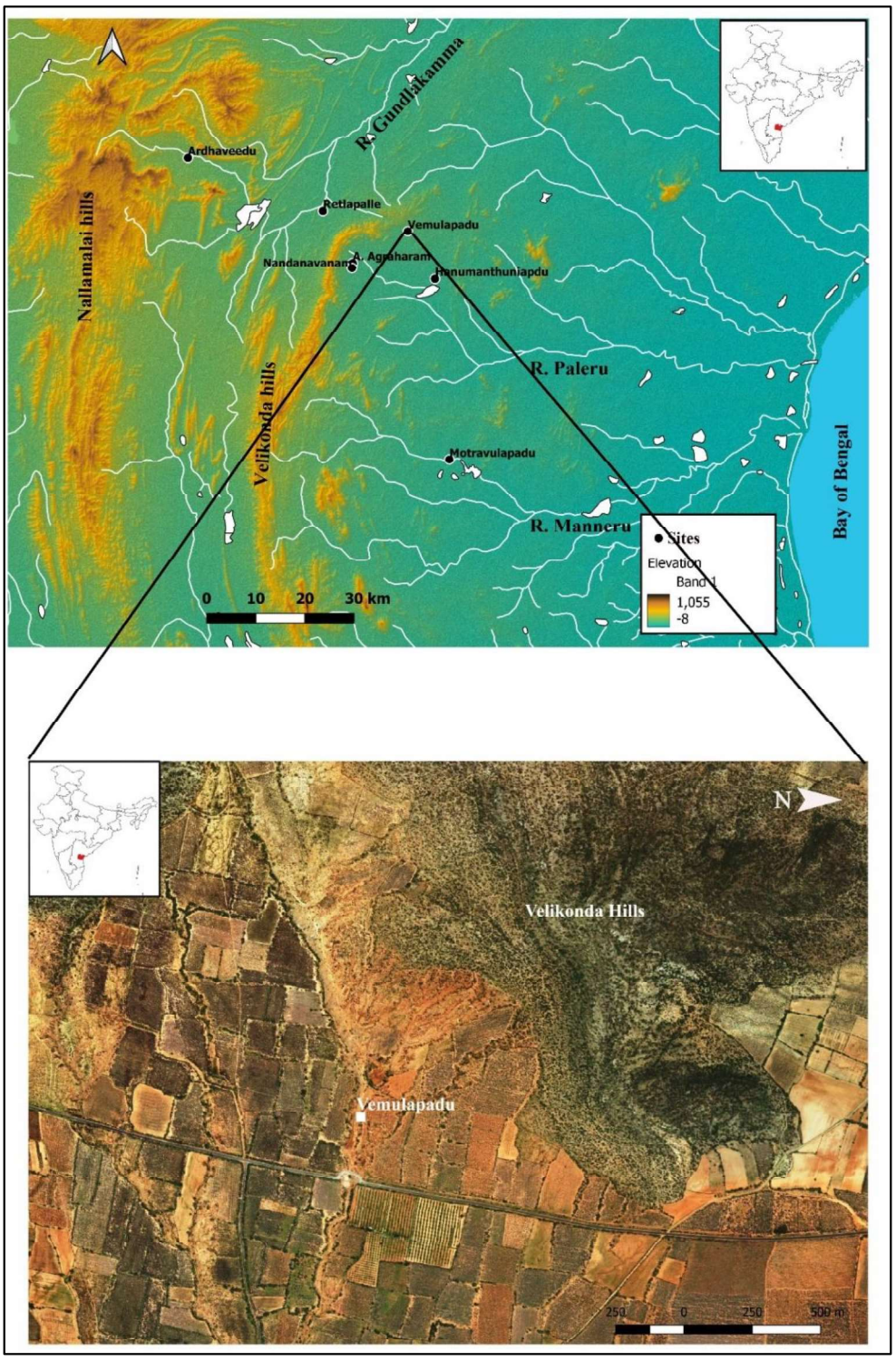

Map. 4.7.1: Map showing the location of the site Vemulapadu.

A small stream cuts through the site and exposes good sedimentary sections of the quaternary formations. Details of the composite stratigraphy of the site Vemulapadu constructed based on the surface observations and section scrapings were presented in Chapter 4.2. Further small-scale excavations at the site revealed sedimentary sequences similar to the composite stratigraphy. This chapter discusses the upper-level stratigraphy where Middle Palaeolithic artefacts were identified.

4.7.1 Stratigraphy

A 2.00 x 2.00 m 2 m wide trench was laid out at the site and excavated to a depth of 2.10 m (Fig. 4.7.1a). After this depth, excavations were limited to 1.00 x 1.00 m and reached a depth of 4.10 m by leaving steps because the sediments were compact and hard to excavate. Six discrete sedimentary units were identified in the Trench (Fig. 4.7.1b). Unit A comprises yellowish, loose sand comparable to the Unit A of the composite stratigraphy described in Chapter 4.2. This Unit has a maximum of 30 cm thickness. Unit B is of dark brown/red colour stabilized sandy Unit similar to the Unit B of Chapter 4.2 composite stratigraphy with a maximum 70 cm thickness. These two units are broadly comparable to the A1 and A2 units reported by (Mishra & Singaraju, 2009). Unit C is a dark, brown-coloured organic-rich, silt-dominated sediment with a thickness of 90 cm. A few stone blocks were observed within this sediment randomly distributed. Unit D is of ~ 30 cm thick, silty sediment with rich carbonate nodules and lithic artefacts (Fig. 4.7.2). The thickness of Unit D is uneven throughout the Trench, ranging between 10 to 30 cm. There is sharp contact observed between Unit D, and overlying Unit C. Unit E is a sandy, silty sediment with a thickness of 70 cm characterized by the presence of several thin crusts of calcrete layers alternately spread across the sediment (Fig. 4.7.3). The bottom-most Unit in the trench, Unit F, is a hard, compact layer that resembles tufa beds having a thickness of 130 cm. A biface was identified within the Unit F at a depth of 310 cm. The nature of the sediments underlying Unit F is unknown as the excavations ceased after reaching the depth of 4.10 m; however, surface observations from nearby areas indicate that Unit F directly overlies the bedrock.

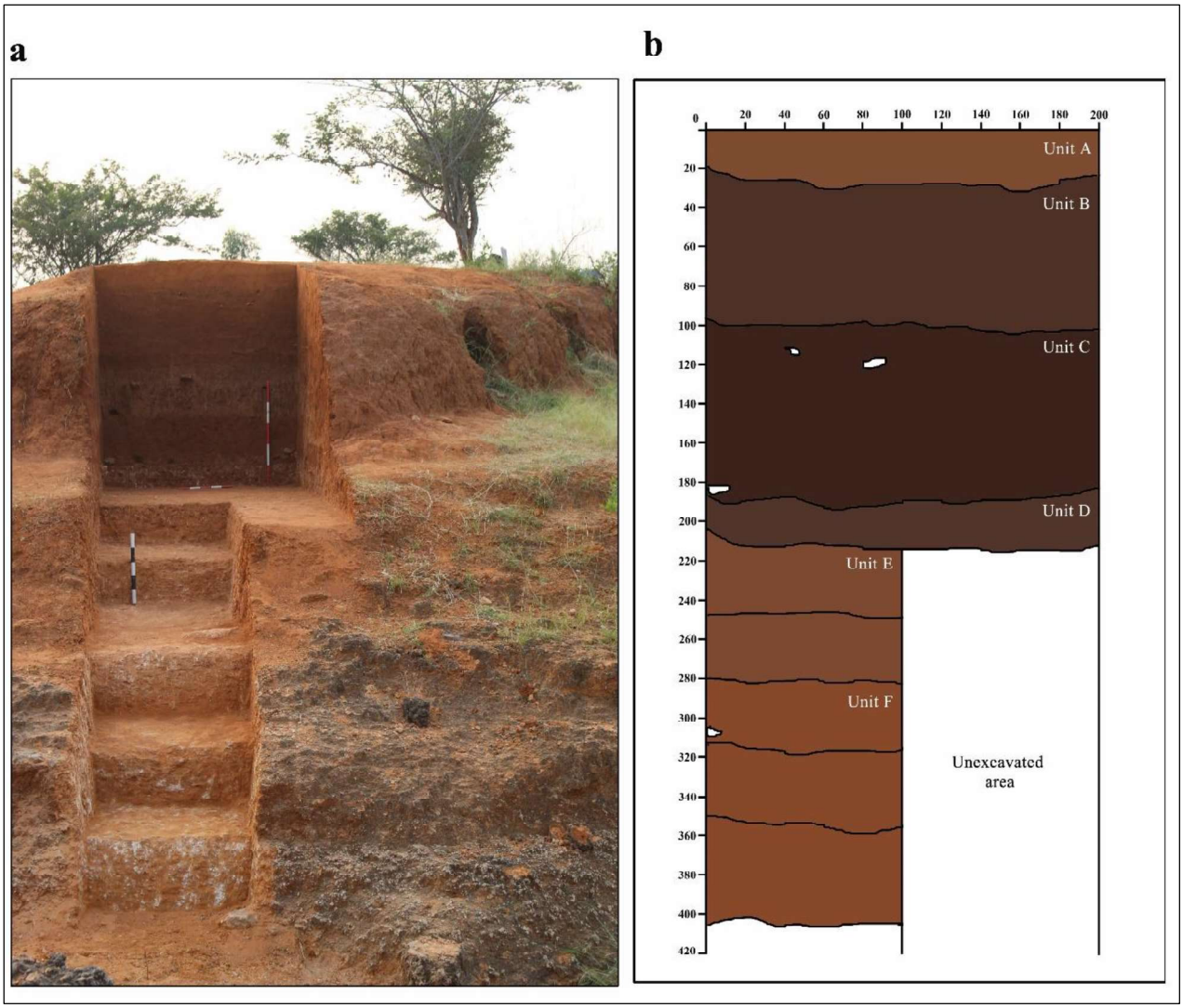

Figure. 4.7.1: Trench and a schematic sketch of the stratigraphy of Vemulapadu.

.

Figure. 4.7.2: Artefact exposures within Unit D.

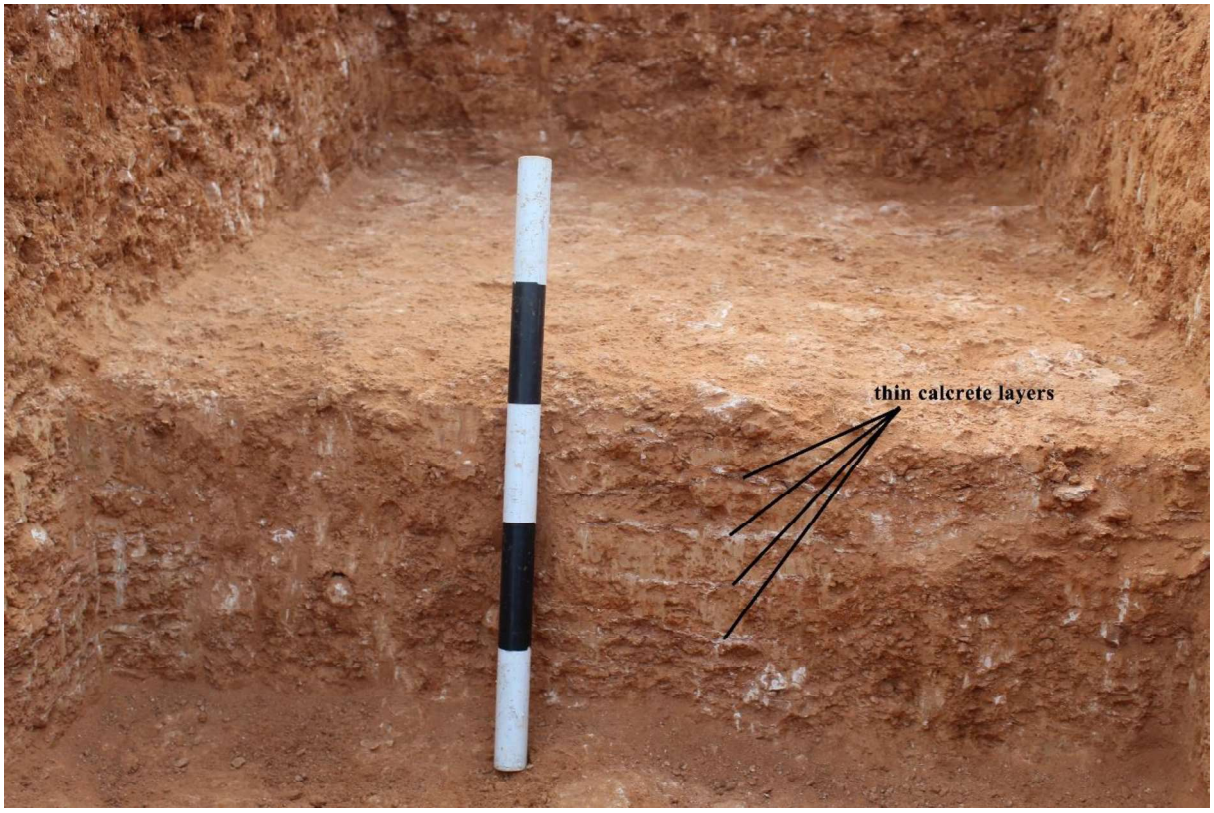

Figure. 4.7.3: Thin calcrete layers observed within Unit E.

4.7.2 Luminescence Chronology

Sediment samples were collected from each sedimentary unit for luminescence age estimations. However, the sediment sample recovered from Unit D, where the artefacts were identified, was processed for the age estimations following the p-IR-IRSL protocol. Fading measurements were carried out on this sample; however, no significant fading was observed. An age of 105±9 ka was estimated for the Unit D sediment sample (Table 4.7.1). Relatively less overdispersion value (14%) was observed, therefore CAM model was applied to estimate the equivalent dose (Fig. 4.7.4). The age of Unit D represents the final burial of the sediments and the artefacts dates to the beginning of the Late Pleistocene epoch.

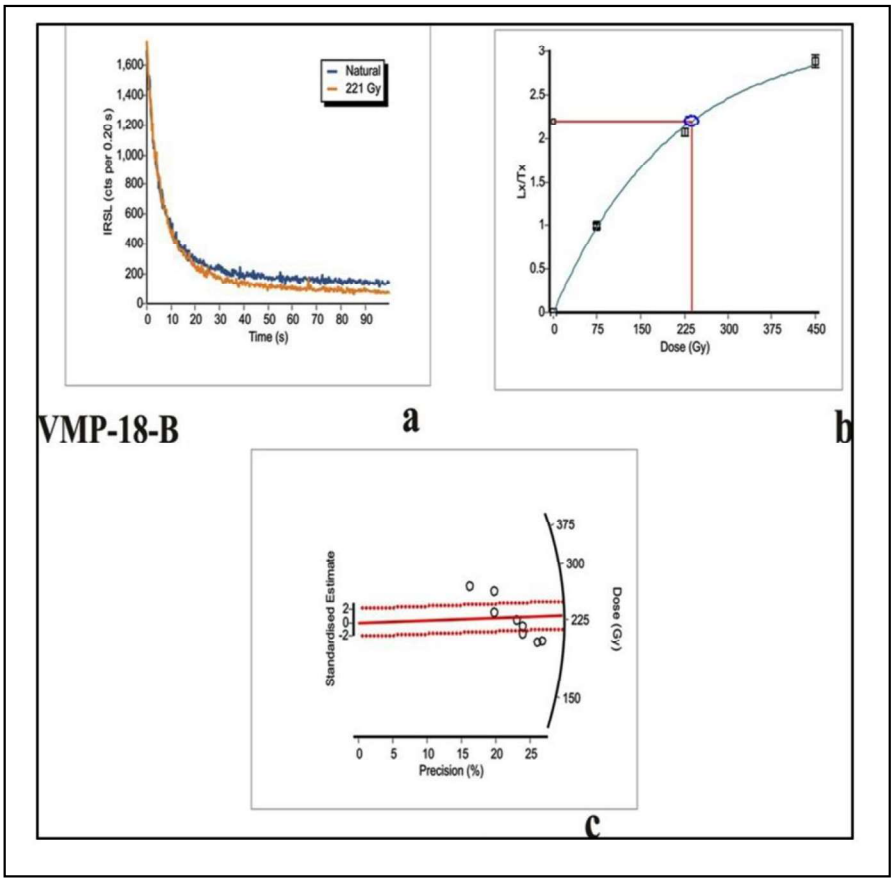

Figure. 4.7.4: Results of p-IR-IRSL analyses for sediment sample from Unit D. a: typical feldspar shine down curve; b: typical growth curve; c: radial plot representing the estimated palaeodoses.

Table 4.7.1: Dose rate data, D_e values and OSL ages for the sediment samples from Vemulapadu.

Sample Code	Depth (cm)	Radionuclide activity[a]				Equivalent doses				OSL age (ka)
		U (ppm)	Th (ppm)	K (%)	Total Dose rate[b,c] (Gy/ka)	No. of aliquots/ grains	Water content (%)	OD (%)	D_e (Gy)[d]	
VMP-1-18-B	285	1.1±0.2	4.9±0.7	0.7±0.05	1.9±0.16	8/~100	11.0	14	201.1±4.9 [f]	**105.1±9.3**

[a] Radioactivity measurement made on a dried, homogenized and powered sample by gamma-ray spectrometry and alpha counting.

[b] Includes cosmic-ray dose rate of 0.107 Gy ka^{-1}

[c] 12.5±0.5% and 200±20 ppm Rubidium (^{87}Rb) concentrations were used to estimate the internal dose rate for the sample VMP-1-18-B

[d] after subtracting a residual dose of 20 Gy

4.7.3 Lithic Technology

The lithic assemblage of the Vemulapadu (upper levels) consists of the collection from the Trench and systematic surface, grid collection (Fig. 4.7.5). A Trench was laid out on the right bank of the small stream that cuts through the site, and the grid was placed 20m away on the opposite side of the Trench on the left bank of the stream. Natural erosional activities here have resulted in the exposure of Unit D sediments on the left bank of the stream. It was observed throughout the extent of the site that natural activities were able to erode layers A to C and expose layer D (artefact horizon). This may be because layer D and the underlying layers are compact and difficult to erode and expose. However, along the stream, the sedimentary layers underlying layer D are also exposed due to anthropogenic activities involving the renovation of the stream to preserve rainwater.

Figure. 4.7.5: Location of the Trench and Grid.

Based on these observations and the absence of artefacts in layer A to C, it is fairly accurate to assume that the surface exposure of sediments at the site are eroded out of layer D and to confirms its stratigraphic association. The Trench has yielded 424 artefacts, most of which are debitage, forming 75% (Table 4.7.2) of the trench collection. To increase the sample size and

to understand the nature of lithic technology at the site, a grid measuring 15m x 10 m was laid out. Considering the similar stratigraphic context of the artefacts recovered from the Trench and the grid, the lithic assemblage was considered as a single assemblage for the typo-technological descriptions. The lithic assemblage from Vemulapadu consists of two distinct reduction sequences, i.e., biface and prepared core reductions that are characteristic of Late Acheulian and Middle Palaeolithic cultures, respectively. A total of 1147 artefacts were identified in the Vemulapadu lithic assemblage (Table. 4.7.2).

Table. 4.7.2: Composition of the lithic assemblage from the Trench and Grid collection.

Type	Trench	%	Grid	%	Total	%
Bifaces						
Hand Axe	5	**1.18**	34	**4.70**	39	**3.40**
Cleaver	0	**0.00**	16	**2.21**	16	**1.39**
Diminutive Hand axe	0	**0.00**	12	**1.66**	12	**1.05**
Total Biface	5	**1.18**	62	**8.58**	67	**5.84**
Cores						
Preferential Levallois	0	**0.00**	11	**1.52**	11	**0.96**
Recurrent Levallois	0	**0.00**	4	**0.55**	4	**0.35**
Bidirectional Recurrent Levallois	0	**0.00**	1	**0.14**	1	**0.09**
Unidirectional Recurrent Levallois	0	**0.00**	4	**0.55**	4	**0.35**
Levallois point core	0	**0.00**	1	**0.14**	1	**0.09**
Discoidal core	0	**0.00**	21	**2.90**	21	**1.83**
Blade core	0	**0.00**	1	**0.14**	1	**0.09**
Unidirectional core	0	**0.00**	3	**0.41**	3	**0.26**
Multiple platform core	1	**0.24**	1	**0.14**	2	**0.17**
Single platform core	3	**0.71**	7	**0.97**	10	**0.87**
Radial core	2	**0.47**	4	**0.55**	6	**0.52**
Core fragment	8	**1.89**	6	**0.83**	14	**1.22**
Modified blank	3	**0.71**	0	**0.00**	3	**0.26**
Total Core	17	**4.01**	64	**8.85**	**81**	**7.06**
Retouched						
Bifacial point	3	**0.71**	8	**1.11**	11	**0.96**
Bifacial Tanged Point	0	**0.00**	1	**0.14**	1	**0.09**
Retouched point	0	**0.00**	16	**2.21**	16	**1.39**
Tanged Point	0	**0.00**	2	**0.28**	2	**0.17**
Borer	0	**0.00**	2	**0.28**	2	**0.17**
Notch	0	**0.00**	3	**0.41**	3	**0.26**

Retouched flake	2	**0.47**	23	**3.18**	25	**2.18**
Retouched flaked piece	1	**0.24**	9	**1.24**	10	**0.87**
Retouched flake-blade	0	**0.00**	1	**0.14**	1	**0.09**
Retouched core fragment	0	**0.00**	1	**0.14**	1	**0.09**
Total Retouched	6	**1.42**	66	**9.13**	**72**	**6.28**
Unretouched						
Levallois flake	0	**0.00**	1	**0.14**	1	**0.09**
Levallois Point	0	**0.00**	6	**0.83**	6	**0.52**
Flake	78	**18.40**	287	**39.70**	365	**31.82**
Blade	0	**0.00**	12	**1.66**	12	**1.05**
Flaked piece	21	**4.95**	91	**12.59**	112	**9.76**
Debitage	283	**66.75**	134	**18.53**	417	**36.36**
Unworked fragments	14	**3.30**	0	**0.00**	14	**1.22**
Total Unretouched	396	**93.40**	531	**73.44**	**927**	**80.82**
Total	424	**100**	723	**100**	**1147**	**100**

Most of the artefacts were made of quartzite (both fine and coarse grained), which formed 79.5% of the assemblage and quartz accounted for the remaining 20.5%. Outcrops of quartzite and quartz are exposed extensively along the Velikonda hill ranges, which are likely to be the raw material procurement area. Patterns of exploitation of different raw materials between the products of two distinct reduction sequences give insights into the nature of lithic assemblage (Table. 4.7.3). Coarse quartzite was equally used to make both biface (n=132) and prepared core products (n=110). However, there was a high preference for fine quartzite to make prepared core products (n=168) than the biface products (n=68). This indicates that coarse quartzite is predominantly used to make biface products, and fine quartzite is mainly preferred during the prepared core reduction. The presence of patina on the artefact surface also provides insights into the burial conditions of the lithic assemblage (Table. 4.7.4). Majority of the bifaces and their products show the presence of patina (n=152).

In contrast, products from the core reduction sequence show minimal patina presence, limited to n=57. Differences in raw material preference and patterns of patina on artefacts indicate two distinct reduction sequences, one dominated by bifaces and the other by prepared core products. Flakes were classified as broken and intact to identify any unusual breakage patterns. Most flakes are intact, forming 68.5%, whereas 31.6% of the flake's breakage is on distal and lateral margins. Bifaces include the handaxes (including diminutive) and cleavers in the assemblage. Bifaces form 5.8% (n=67) of the assemblage with ~ 4:1 handaxe and cleaver ratio.

Table. 4.7.3: Raw material exploitation between Bifacial products and Prepared core products.

Type	Fine Quartzite	%	Coarse Quartzite	%	Quartz	%
Biface	10	4.24	52	21.49	5	16.67
Bifacial Points	5	2.12	6	2.48	1	3.33
Flakes from Biface Reduction*	53	22.46	74	30.58	2	6.67
Total Biface	**68**	28.81	**132**	54.55	**8**	26.67
Levallois Cores	11	4.66	9	3.72	1	3.33
Other Cores*	20	8.47	18	7.44	5	16.67
Flakes from Core reduction*	137	58.05	83	34.30	16	53.33
Total Core Products	**168**	71.19	**110**	45.45	**22**	73.33
Total	**236**	100	**242**	100	**30**	100

Table. 4.7.4: Distribution of patina on the artefacts.

Type	With Patina	%	Without Patina	%
Biface	51	24.40	16	5.35
Bifacial Points	4	1.91	8	2.68
Flakes from Biface Reduction*	97	46.41	32	10.70
Total Bifaces &Products	**152**	72.73	**56**	18.73
Levallois Cores	6	2.87	15	5.02
Other Cores*	18	8.61	25	8.36
Flakes from Core reduction*	33	15.79	203	67.89
Total Cores & Products	**57**	27.27	**243**	81.27
Total	**209**	100	**299**	100

There is moderate variation among the length of bifaces (Table. 4.7.5), as there are 12 bifaces that are less than 100 mm in length; however, width and thickness show minimal variations. Elongation denotes the relation between the biface length and width. South Asian Acheulian assemblages reveal a broad spectrum of variation with long, elongated, and thick bifaces at one end and short, broad, and thin bifaces at the other end (Shipton, 2016). The mean elongation value of the Vemulapadu bifaces lies within the latter end of the spectrum (Fig. 4.7.6). Creating a thin biface requires more refinement as it is difficult to achieve thinness without losing the width. Usually, the biface thickness-to-width ratio is used as the refinement index. Bifaces from

Vemulapadu are thin and well-refined and lie at one end of the distribution of mean refinement values of the known Indian assemblages (Fig. 4.7.7).

Table. 4.7.5: Mean values of the metrical attributes recorded for bifaces.

	Mean (mm)	Standard deviation	Minimum	Maximum
Length	112.10	26.45	62.56	176.56
Width	70.37	15.31	37.65	104.89
Thickness	31.24	7.56	11.97	48.39
Elongation	1.56	0.28	1.15	2.46
Refinement	0.44	0.10	0.22	0.66

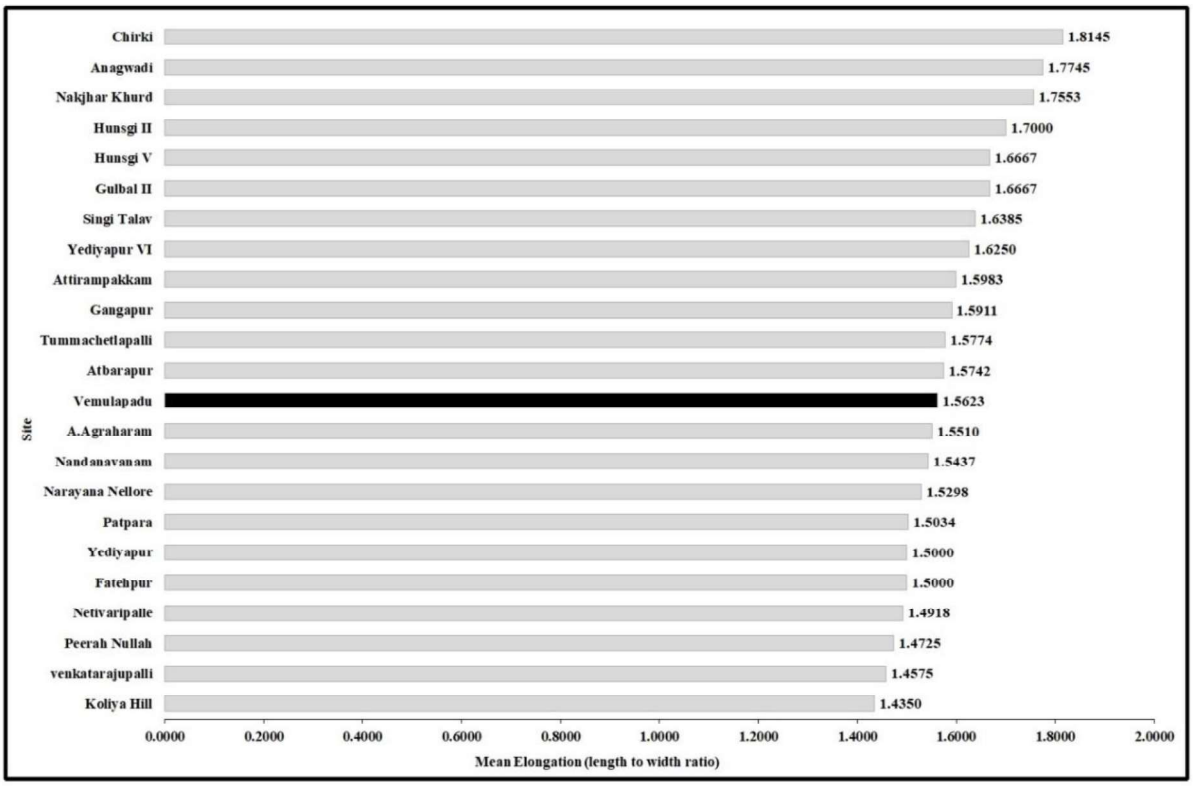

Figure. 4.7.6: Variation in mean biface elongation (length to width ratio) for Indian assemblages. Comparative data from (Chauhan, 2010; Gaillard et al., 1986, 2008; Paddayya & Petraglia, 1993).

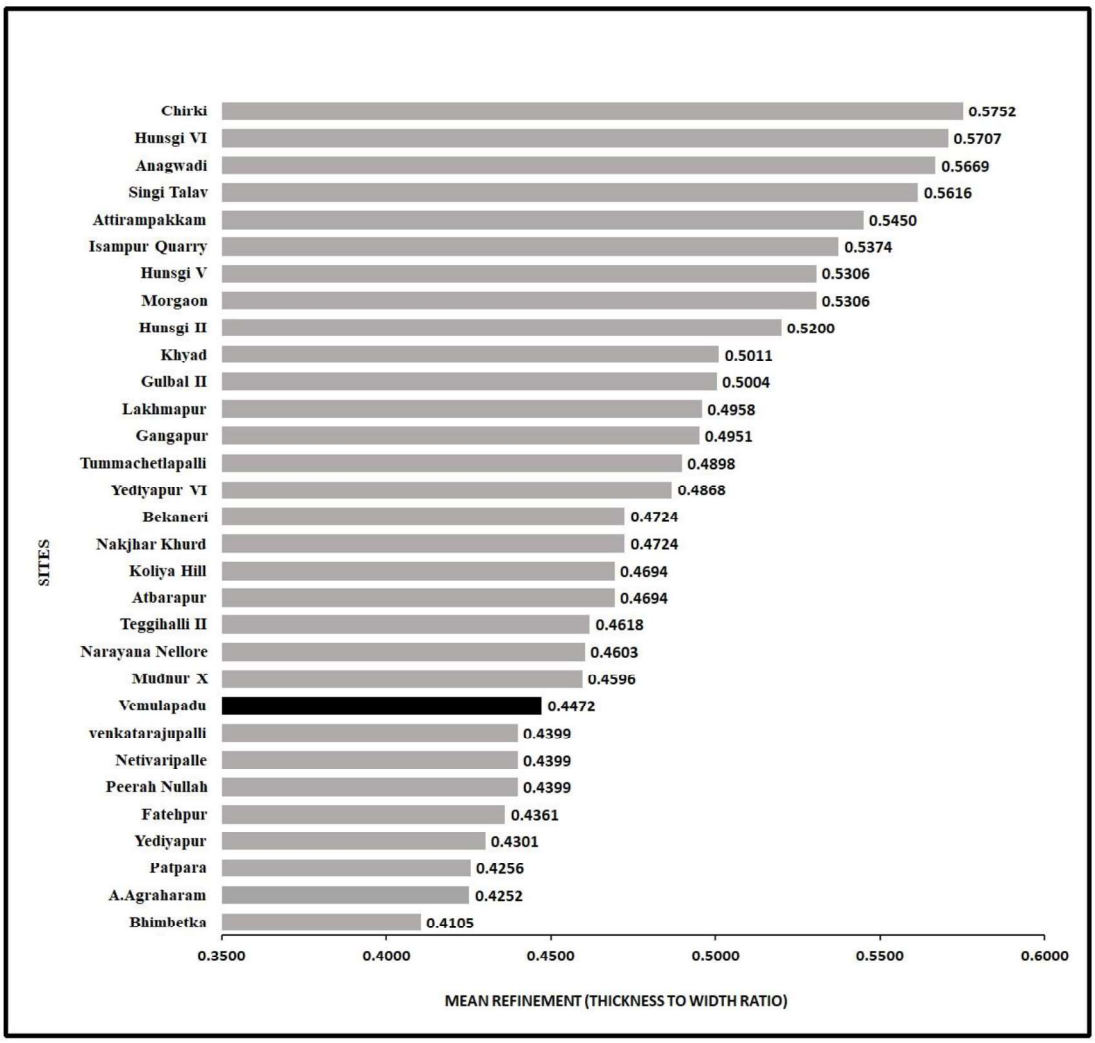

Figure. 4.7.7: Variation in mean biface refinement (thickness to width ratio) for Indian assemblages. Comparative data from (Shipton, 2016). Note that Vemulapadu occurs on the lower end of the distribution, while assemblages with early Pleistocene age estimates occur on the other end.

The cores in the collection of Vemulapadu, consisting of 81 pieces, forms 7.06% of the total assemblage. The dominant categories are Levallois cores (1.83%) and discoidal cores (1.83%), followed by single platform cores (0.87%). The other categories of cores include multi-platform cores, radial cores, blade cores, unidirectional cores, and core fragments. The Levallois cores show diverse methods of debitage surface preparation and exploitation that includes preferential, recurrent, uni and bi-directional recurrent methods (Fig. 4.7.8; Fig. 4.7.9; Fig. 4.7.10 and Fig. 4.7.11). The other largest category among the cores is discoidal cores. These cores were exploited on both sides resulting in a typical discoid shape (Fig. 4.7.12). Few numbers unidirectional and blade cores are also present in the assemblage.

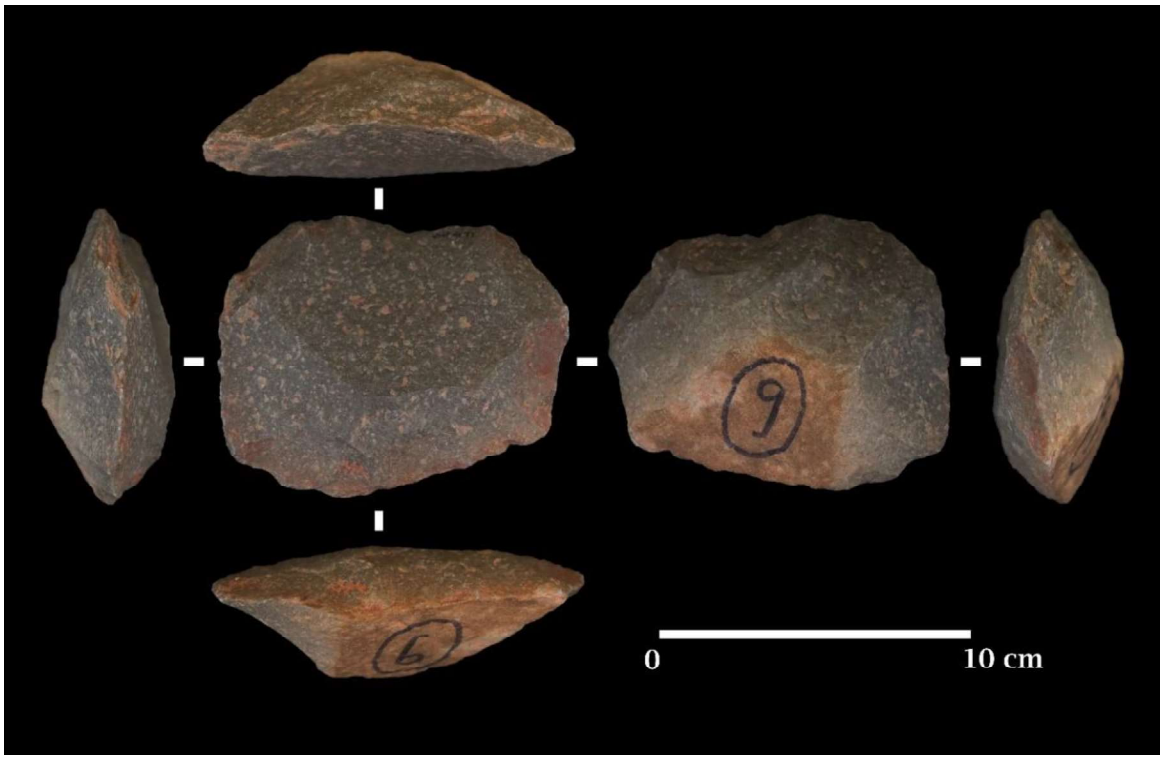

Figure. 4.7.8: Preferential Levallois core.

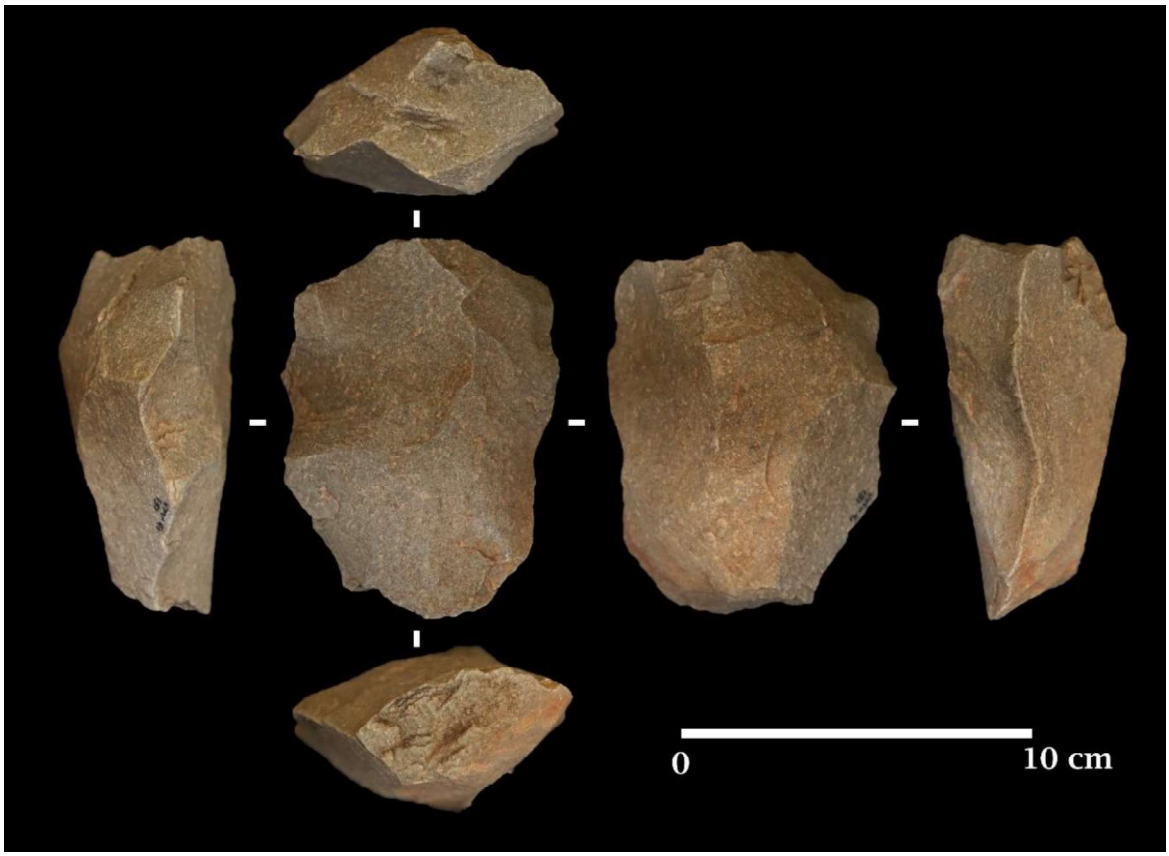

Figure. 4.7.9: Recurrent Levallois core.

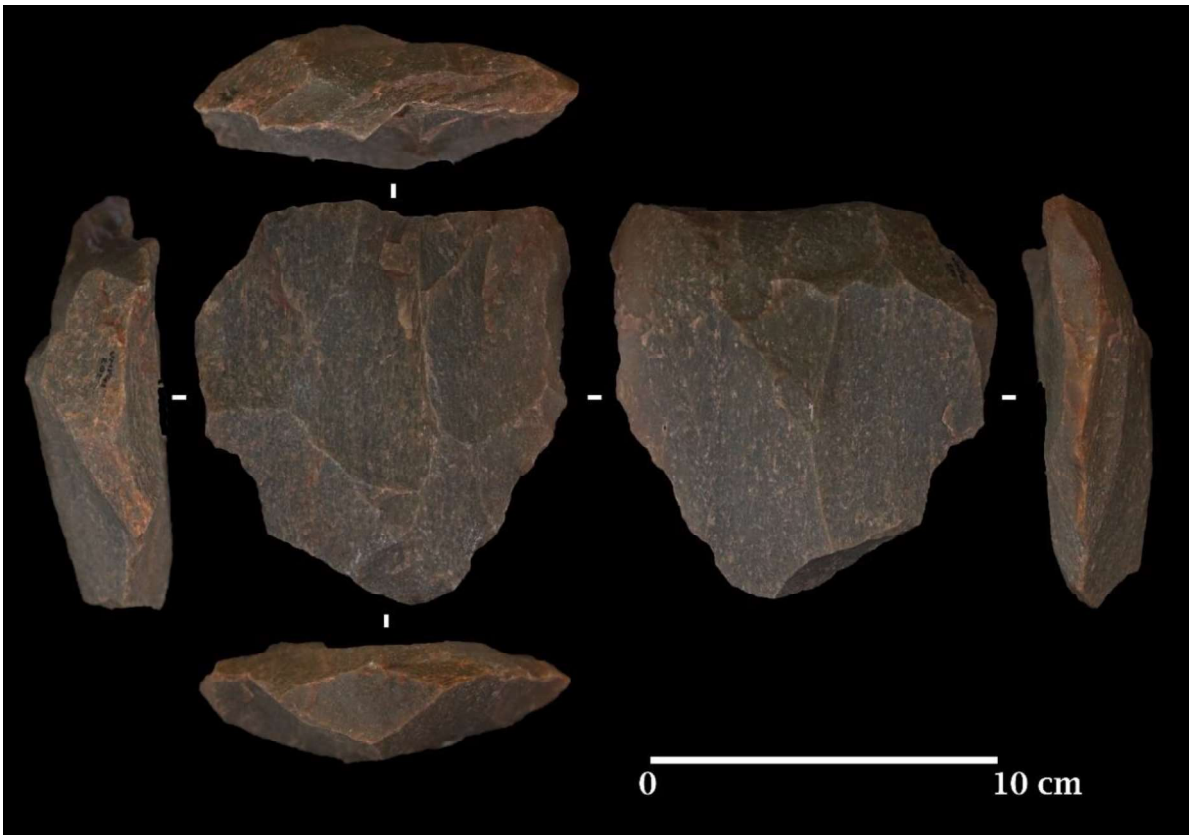

Figure. 4.7.10: Uni-directional Recurrent Levallois core.

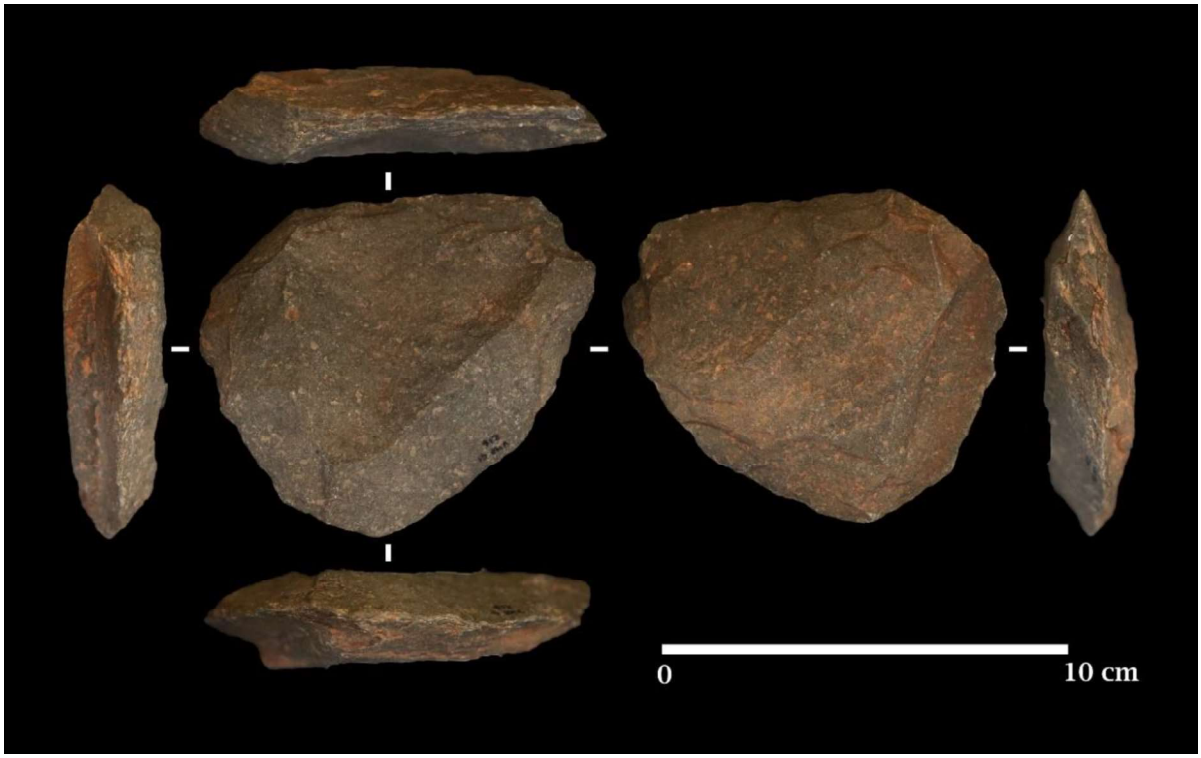

Figure. 4.7.11: Levallois point core.

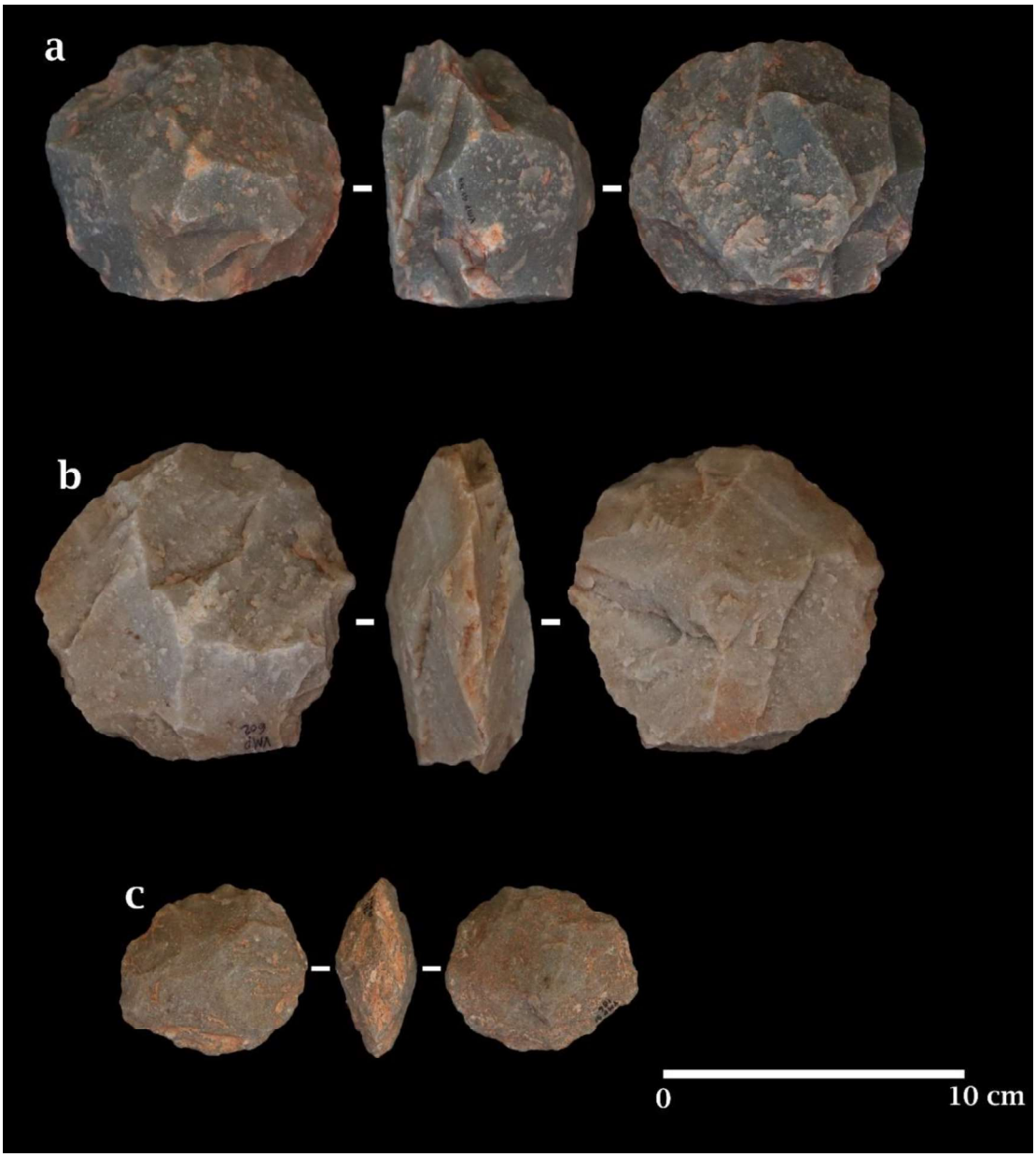

Figure. 4.7.12: Discoidal cores.

Three-quarters of the cores (73.44%) show no cortex, and cores with 10%, 20%, and 50% cortex are present in 18.75%, 6.25% and 1.56%, respectively. Cores' mean length, medial width and medial thickness are 73.04x75.40x33.99 mm when oriented along the flaking axis (last flake scar) (Table. 4.7.6). The core's proximal, medial, and distal widths measured along the flaking axis are 64.22x75.40x57.32 mm, respectively indicating cores are wider in the middle and narrower at both proximal and distal ends. The proximal shape of the cores is relatively straight (mean 0.85 mm), whereas the distal shape is tapering (mean 1.34 mm). No considerable variation in core elongation (ranging between 0.52-1.46) is observed, maybe because there is no significant variation in the cores' mean length and mean medial width. The core flatness

index ranges from 0.83 to 5.15, where most cores are wider than thick. Two cores have cortical platforms (3.13%), 30 cores have single conchoidal platforms (46.88%), 19 cores show multiple conchoidal platforms (29.69%), seven cores have dihedral platforms (10.94%), and in six instances, the platform type is indeterminate (9.38%). Platforms were facetted on 35 cores (54.69%), and overhang removal was observed on 16 cores (25%); in 12 instances, no preparation was observed, and in two instances, the platform preparation was indeterminate. The last scar face length of cores is less than the axial core length, indicating the flaking face is limited to the smaller axial surface. The last scar lengths range from 21.80-88.90 mm, with an average of 46.32 mm, and the last scar widths range between 18.40-72.30 mm, and a mean of 41.67 mm. On average, the last flake scar elongation indicates that relatively squarish or oval flakes were removed (mean=1.19). More than half of the last major flake scars exhibit feather terminations (59.34%), with non-feather terminations accounting for 40.66%. A maximum of six and a minimum of one core rotations were observed on cores. Most cores show one (n=26) or two (n=25) major scars (having more than 1/3 core length), while 11 cores exhibit three scars. There are two cores with four scars and one core with five scars.

Table. 4.7.6: Statical data for Core attributes.

Attribute	N	Mean	SD	Min.	Max.
Length	64	73.04	17.48	43.30	113.00
Proximal Width	64	64.22	19.12	39.40	117.25
Medial Width	64	75.40	20.04	40.89	144.23
Distal Width	64	57.32	15.67	30.36	101.50
Proximal Thickness	64	24.58	17.19	10.31	123.27
Medial Thickness	64	33.99	15.73	13.45	106.36
Distal Thickness	64	24.89	14.92	10.11	104.59
Proximal Shape	64	0.85	0.14	0.53	1.22
Distal Shape	64	1.34	0.20	0.86	1.77
Elongation	64	1.00	0.22	0.52	1.46
Flatness	64	2.49	0.95	0.83	5.15
No. of Core Rotations	64	2.72	1.50	1.00	6.00
Last Platform Angle	64	82.81	24.34	50.00	150.00
No. of Major Flake Scars	64	1.94	0.96	1.00	5.00
No. of Flake Scars	64	4.44	1.63	3.00	8.00
No. of Feather terminations	64	1.10	0.84	1.00	5.00
No. of non-feather Terminations	64	3.58	2.60	0.00	3.00
Last Scar Length	64	46.32	13.97	21.80	88.90
Last Scar Width	64	41.67	12.19	18.40	72.30
Last Scar Elongation	64	1.19	0.42	0.61	2.55

Flakes, including the retouched ones, form 37.75% of the assemblage with 433 specimens (Table. 4.7.7). These flakes were classified into technological types to identify the position of each flake in a reduction sequence. Distinguishing flakes from the biface reduction sequence and prepared core reduction sequence (e.g., Levallois) becomes difficult owing to the morphological similarities of the debitage between the two reduction sequences. However, following the attributes suggested by (Akhilesh & Pappu, 2015; Delagnes, 1993; Newcomer, 1971), flakes were classified into various stages of biface and core reduction sequences (Table. 4.7.7). It is difficult to distinguish between the biface roughout flakes and core roughout flakes, so the roughout flakes mentioned in Table. 4.7.3.6 represent both biface and core reduction sequences. A smaller number of roughout flakes in the assemblages indicates that the initial dressing of the bifaces and cores was done at raw material procurement sites, probably the Velikonda hills. Flakes that are part of the core reduction sequence dominate the flake component with 55.89%, implying the predominance of prepared core technology.

Table. 4.7.7: Technological classification of Flake component.

Technological Type	Number	%
Roughout flakes	69	15.94
Biface thinning & shaping flakes	94	21.71
Biface Finishing flakes	28	6.47
Prepared core flake	58	13.39
Core preparation flakes	179	41.34
Indeterminate	5	1.15
Total	**433**	**100**

Transverse flakes (flakes having wide distal end) with prepared platforms and a distinct morphology (Fig. 4.7.13) were noted in the assemblage, similar to the flakes observed in the lithic assemblage of A. Agraharam (see Chapter 4.3). Probably these flakes are struck from the sides of the core/biface, which gave the flakes a transverse shape. Some of these flakes reveal long platforms that extend over to lateral margins (Fig. 4.7.13). Whether these flakes were produced through any of the known core reduction methods (e.g., Discoid, Levallois) or any other distinct core reduction procedure is yet to be understood. Overall, the flake component of the assemblage suggests the presence of products from both biface and prepared core reduction sequences.

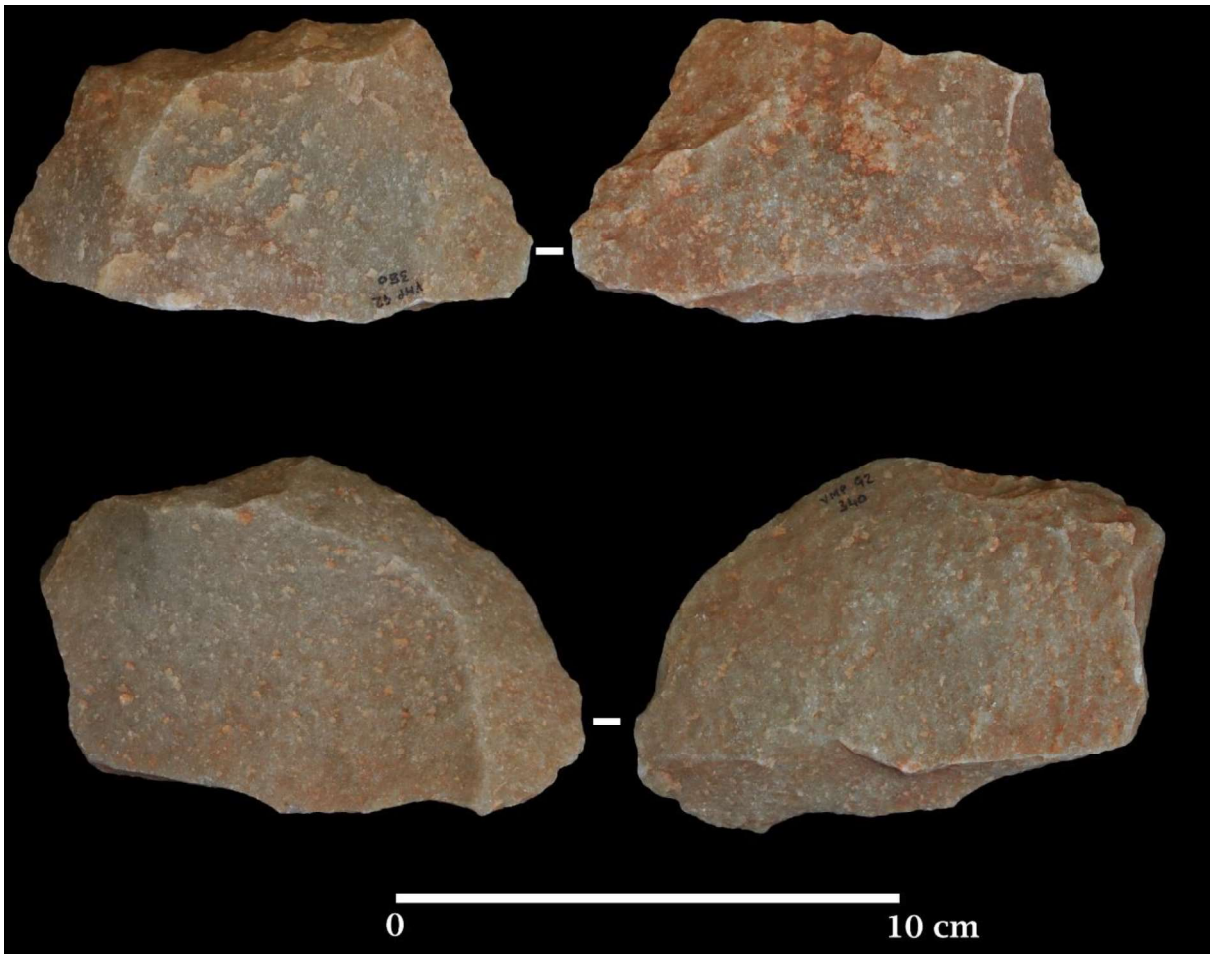

Figure. 4.7.13: Transverse flakes.

Morphometrical descriptions were limited to intact flakes in the assemblage that are 301 in number. A wide range of technological diversity is evident amongst the flakes, from biface preparation to core preparation flakes and prepared core flakes. In addition, Levallois flakes, blades, elongated flakes, and platform rejuvenation flakes are present in the assemblage (Fig. 4.7.14 & Fig. 4.7.15). Mean axial flake dimensions are 49.69 x 50.90 x 13.41 mm (LxWxT); on average, flakes are squarish or oval (mean elongation=1.28) (Table. 4.7.8). Fakes are typically more than four times as wide as they are thick (mean flatness=3.97), with the flatness ranging from of 0.61 to15.17. Three-quarters (71.1%) of the flakes exhibit slightly expanding proximal margins (mean proximal shape=0.79), with 28.90% exhibiting contracting proximal margins, leading to an upper proximal shape index of 1.22. In contrast, the distal shape indicates that 85.38% of the flakes exhibit distal contracting margins (mean=1.52). Single conchoidal (41.20%) and multi-conchoidal (39.53%) platforms are the most common type, followed by dihedral (9.97%), indeterminate (4.65%), cortical (2.33%), crushed (1.33%) punctiform (1%).

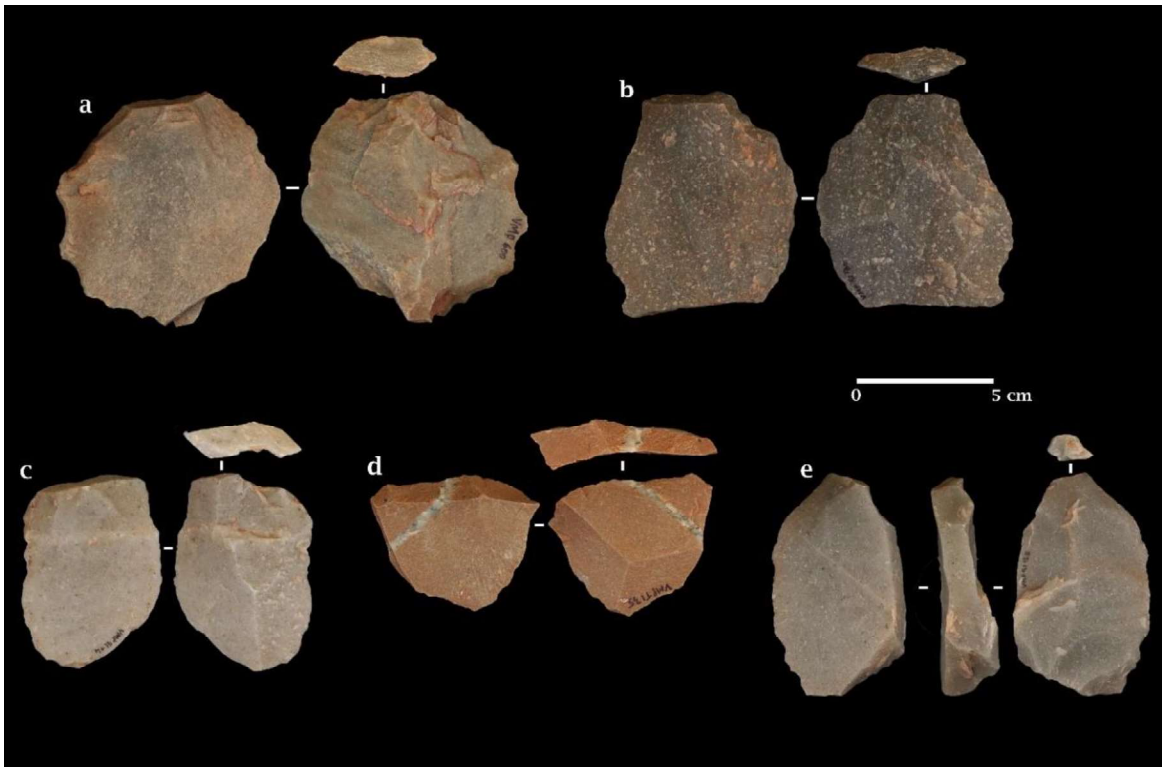

Figure. 4.7.14: Levallois flakes in the assemblage. a to d: Levallois flakes (d is from Trench); e: platform rejuvenated flake.

Figure. 4.7.15: Blades in the assemblage.

Platform preparation is dominated by facetted platforms with 49.83%, followed by no preparation (24.58%), overhang removal (19.27%) and indeterminate (6.31%). A wide range in platform size is evident, with platform width ranging from 9.18-116.73 mm and platform thickness ranging from 2.92-104.97 mm. The platform shape index indicates that platforms are typically elongated (mean=3.15), with 90% being two times wider than thick. The most common dorsal scar patterns present on complete flakes in the assemblage are weakly radial (51.16%), followed by radial (20.60%), proximal (18.27%), indeterminate (9.63%) and bidirectional (0.33%; n=1). Cortical coverage ranges from 0-30%, with 87.38% of flakes having no cortex and 8.64%, 2.33%, and 1.66% with 10%, 20%, and 30% cortex, respectively. Feather terminations are present at 86.38%, followed by step terminations (10.63%) and indeterminate (2.99%).

Table. 4.7.8: Statistical data for Flake attributes.

Attribute	N	Mean	SD	Min.	Max.
Length	301	49.69	18.53	18.75	160.34
Proximal Width	301	44.83	18.81	13.44	165.54
Medial Width	301	50.90	21.37	0.74	149.17
Distal Width	301	51.75	186.40	6.57	3252.00
Medial Thickness	301	13.41	4.85	5.25	37.60
Elongation	301	1.28	3.50	0.36	61.19
Flatness	301	3.97	1.50	0.61	15.17
Proximal Shape	301	1.22	5.23	0.37	91.38
Distal Shape	301	1.42	0.65	0.01	5.60
Platform width	301	36.84	17.42	9.18	116.73
Platform Thickness	301	12.40	7.22	2.92	104.97
Platform Shape	301	3.15	1.21	0.74	9.97
Platform area	301	520.99	622.91	46.28	8155.12
Dorsal scar count	301	2.89	1.21	0.00	7.00

Retouched tools form around 6.28% of the total assemblage (Table. 4.7.3.1). Although flake production through prepared and unprepared core reduction is dominant at the site, formal retouched tools are less in numbers and form only 3.05% of the assemblage. Flakes with informal retouch form 50% of the retouched tools. The informal retouch does not show any pattern or standardization. Flakes were retouched randomly on the ventral and dorsal sides, the

distal end, and both lateral margins. Points are the largest category in the retouched tool type, with a frequency of 41.6% (n=30). Retouched points are the most preferred type, followed by bifacial points and Levallois points (Fig. 4.7.16). Flakes, small slabs and broken biface pieces were used to make bifacial points. The bifacial points show variability in shapes and sizes (Fig. 4.7.17a to d). The metrical dimensions of the bifacial points are 88.34x53.38x23.76 (LxWxT) mm. Some points show basal modifications (similar to tanged points), which must have facilitated hafting (Fig. 4.7.17e to g).

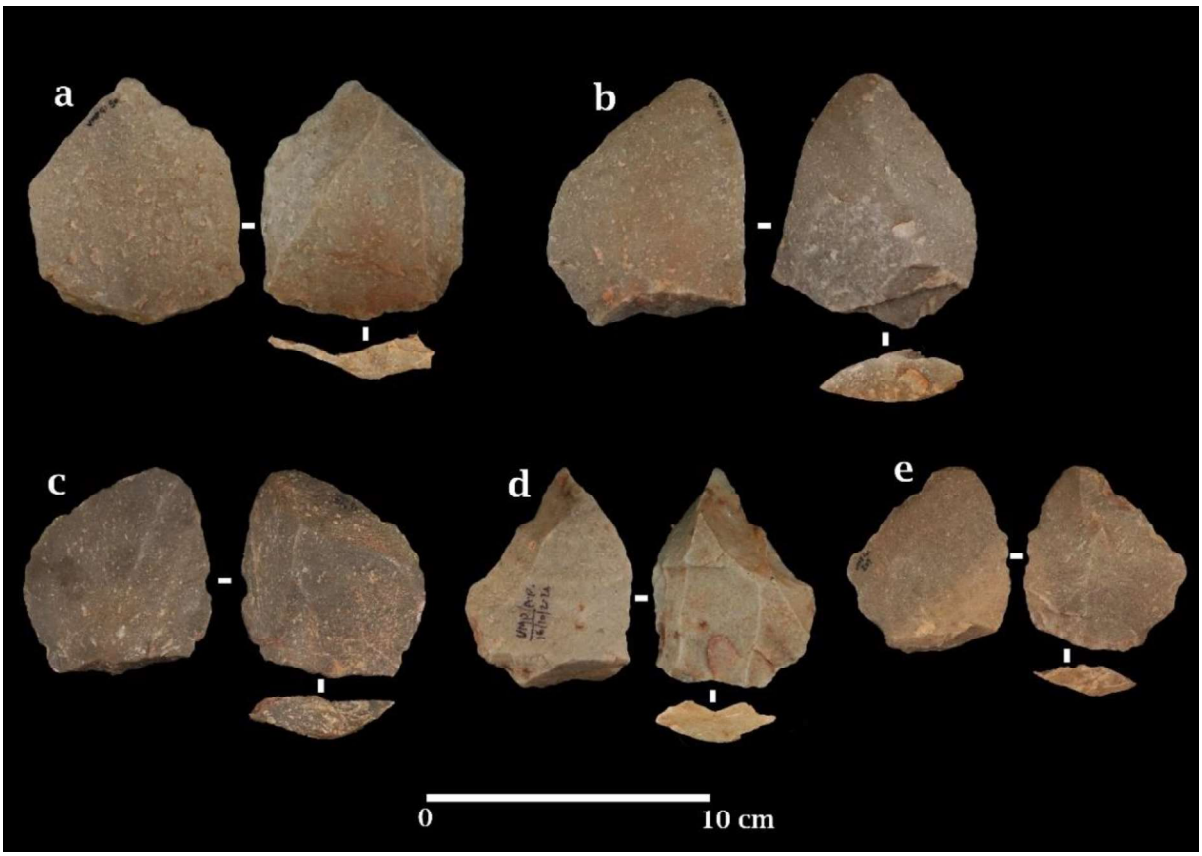

Figure. 4.7.16: Levallois points in the assemblage.

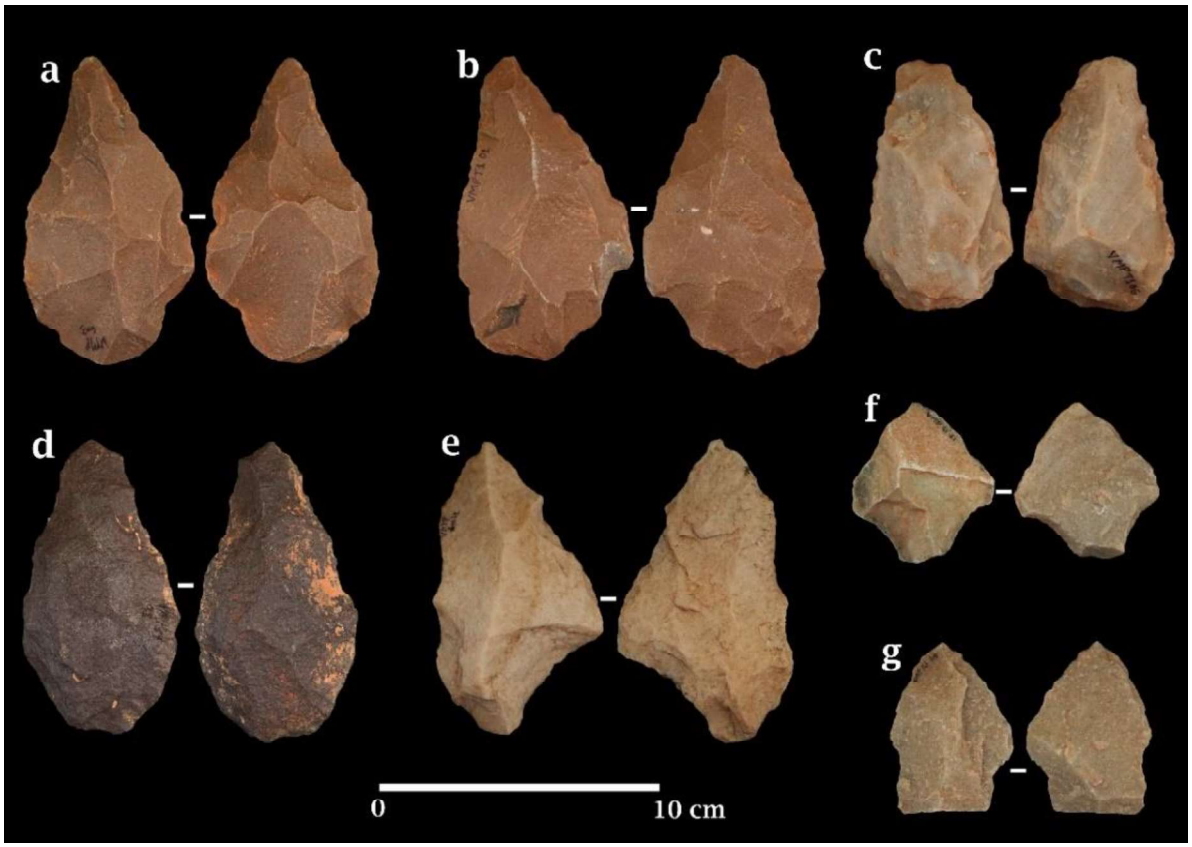

Figure. 4.7.17: Bifacial and Tanged points. a to d: bifacial points; e to g: tanged points.

4.7.4 Summary

The assemblage from Vemulapadu was collected in the small excavation and using a systematic grid laid out on the freshly exposed artefact cluster. The presence of debitage less than 2 cm in length and other flakes (e.g., roughout flakes, core preparation flakes) that are part of the reduction sequence demonstrate the primary nature of the assemblage. However, the presence of a relatively high proportion of cores with no and less than 10% cortical surfaces, including platform surfaces, indicates that the primary stages of the core reduction sequence must have taken place at raw material source itself. This is further supported by the dominance of formal core reductions such as preferential and discoidal core types and biface making. The presence of Late Acheulian bifacial artefacts and classic Levallois artefacts associated with a single sedimentary layer poses serious questions regarding the nature of the assemblage. The assemblage may belong to a transition period between Late Acheulian and Middle Palaeolithic. However, classic Levallois products (Uni and bidirectional recurrent Levallois cores and Levallois points) are not reported from Late Acheulian to Middle Palaeolithic transitional industries elsewhere and are not expected (Anil, Chauhan, et al., 2022a; Pappu et al., 2011). The second possible scenario could be that both Late Acheulian and Middle Palaeolithic

populations coexisted or shared the same landscape in and around the Vemulapadu site. However, this scenario seems unlikely, as the currently available chronometric ages imply that the Late Acheulian and classic Middle Palaeolithic technologies are separated by vast temporal differences. The third scenario could be the site forming a palimpsest of floors foccupied by Late Acheulian and Middle Palaeolithic knappers. If this is true the scenario, different patination patterns are expected between bifaces and prepared core elements (e.g., Levallois), which is evident in the assemblage. Bifacial products show more patina than the Levallois and other prepared core products. In addition, the assemblage shows differences in the raw material exploited for making bifacial and Levallois products, which was dominated by fine-grained quartzite over the coarse variety that was preferred for the biface products. However, it is unclear for now the exact reasons why these two temporally distinct lithic assemblages are associated with a single sedimentary layer in the excavated Trench. Further micromorphological and sedimentological analyses are required to investigate and understand this issue.

The artefact assemblage from Vemulapadu shows characteristics of the Large Flake Acheulian and Early Middle Palaeolithic. The Large Flake Acheulian is represented by the presence of well-made handaxes and cleavers. The mean elongation, refinement, and profile & plan symmetry values of the bifaces show close similarities with the Late Acheulian assemblages reported in South Asia (Shipton, 2013, 2016; Shipton et al., 2013). There is little evidence of handaxes being used as cores to produce flakes, and such examples were also noted in Europe and the Levant in the terminal Acheulian contexts (Petraglia et al., 2003; Rolland, 1995; Tuffreau, 1995; White & Pettitt, 1995). Prepared core technology and its debitage present in the assemblage indicate Levallois core reduction. Notably, various Levallois core preparation and exploitations were observed in the assemblage, including preferential, recurrent, uni and bidirectional recurrent methods. Notably, bifacial points made on slabs and flakes are abundant among the retouched categories. Some portion of the points and bifacial points shows basal modifications and tangs, indicating possibilities of hafting technology.

Overall, the lithic assemblage from Vemulapadu consists of the Late Acheulian and Middle Palaeolithic prepared core technologies that are characteristic of traditional Middle Palaeolithic culture. The luminescence age estimations of the artefact-bearing horizon place the assemblage at the beginning of the Late Pleistocene with an age of 105 ka.

4.8 Motravulapadu

Motravulapadu (15° 8'10.82" North latitudes, 79°25'16.08" East longitudes) is situated on the banks of Nachua vagu, a tributary of the Manneru River (Map. 4.8.1). The stream flows for 15 kilometres before joining the Manneru River and draining into the Mopadu reservoir. The site was initially reported by (Srinivasulu, 2012) as a part of his PhD thesis. The current researcher conducted a thorough investigation of the site, recording stratigraphy and palaeolithic material at various locations. Motravulapadu is a large, 4 x 2 km, site where rill and sheet erosional events have uncovered artefacts, fossilised faunal remains and several vertical sections of Quaternary formations. Furthermore, current mining activities have exposed parts of the bedrock in a few spots. The site has several artefact clusters on the surface that date from the Middle Palaeolithic to the Microlithic. The site also has volcanic ash deposits from the 74 ka Toba super-eruption.

Excavations were conducted at this site for one field-season in 2020. Trenches were opened at six localities within an area of 0.5 x 0.6 km (Map. 4.8.2). These localities were chosen with the intention of understanding the relationship between the sediments exposed at these localities and building a complete history of sediments at the site. However, in this chapter four trenches will be discussed in detail i.e., Trench 1, 2, 4 and 5. The stratigraphy, luminescence chronology and lithic and faunal assemblage recovered from these trenches are discussed below in detail.

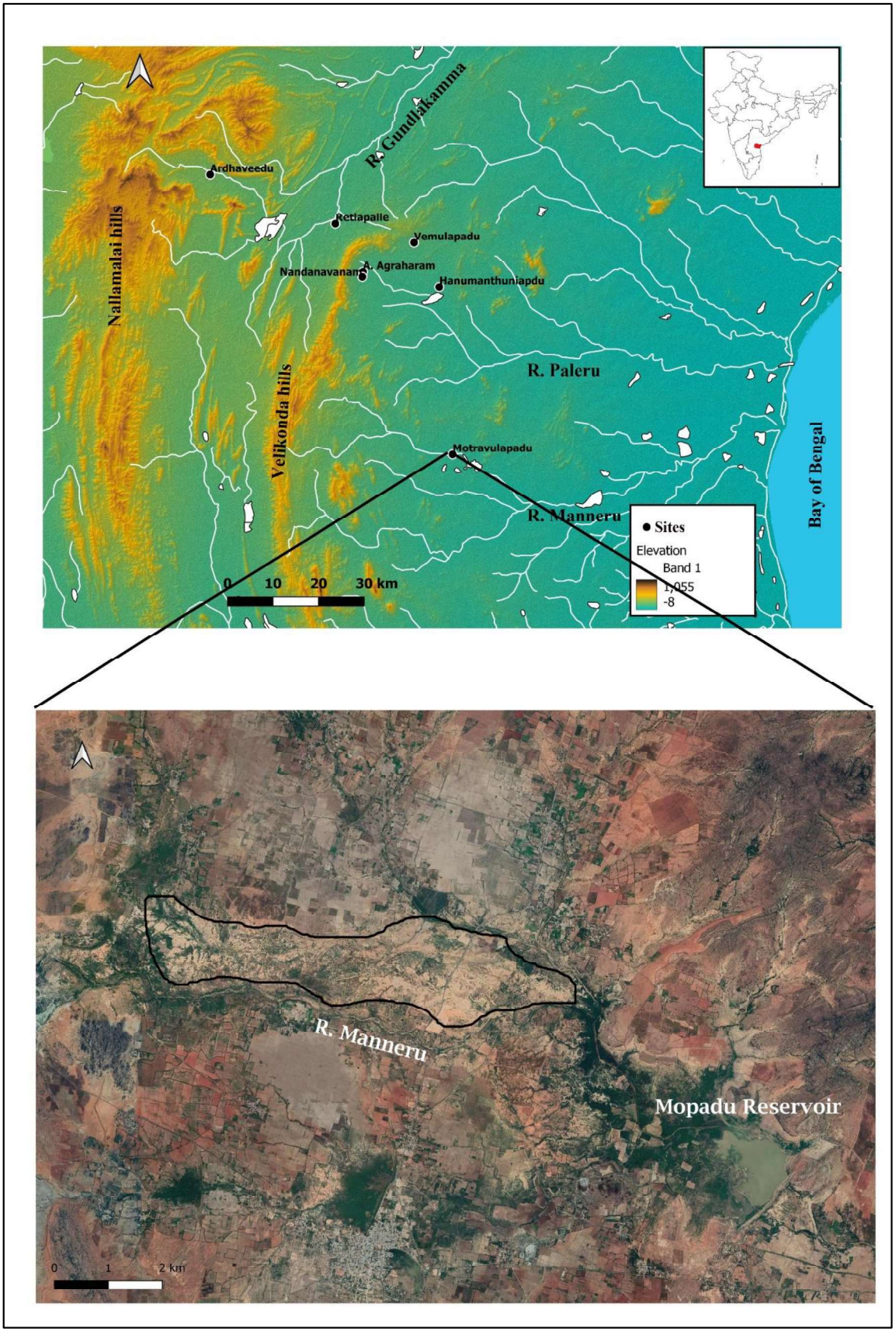

Map. 4.8.1: Map showing the location of the site Motravulapdu.

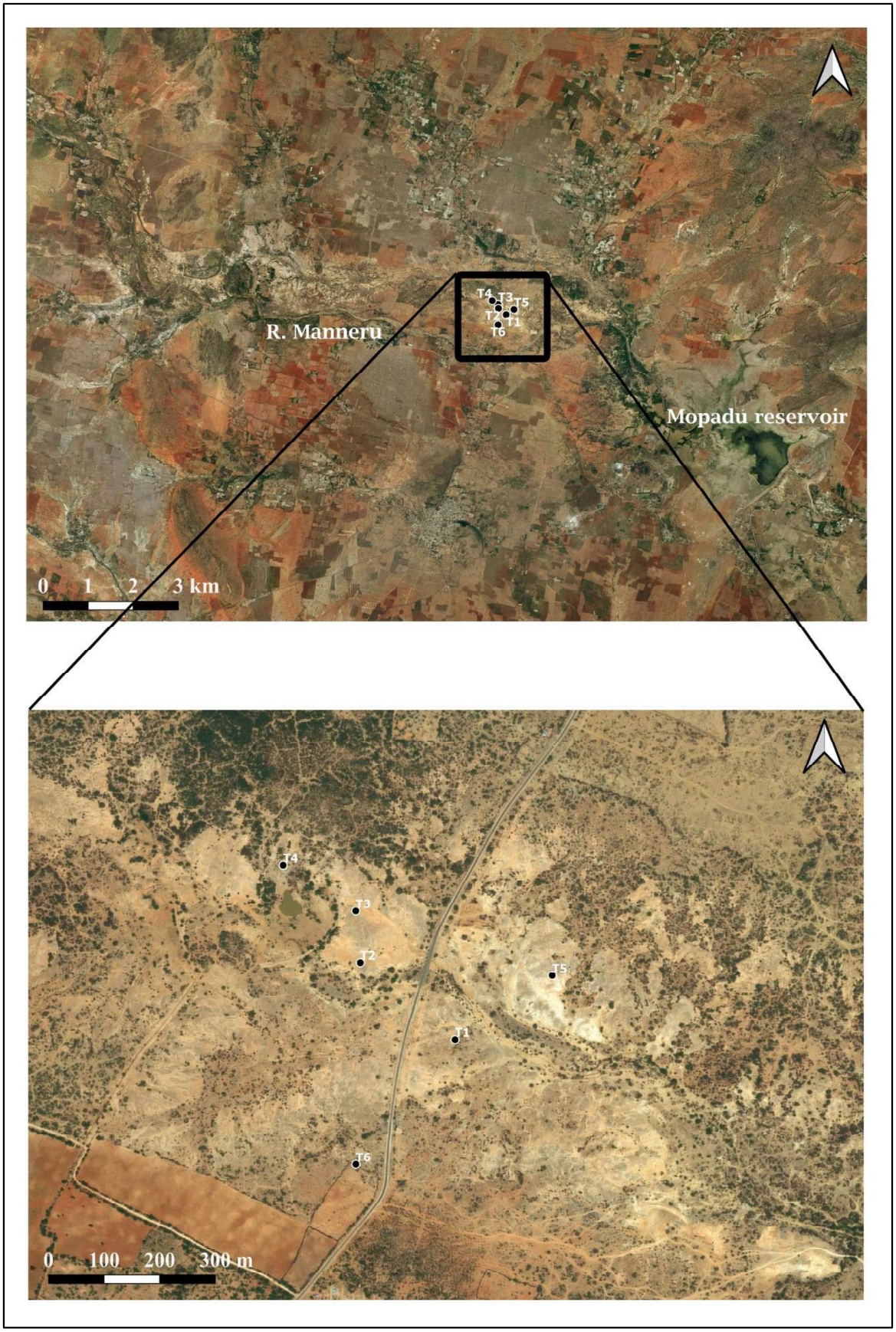

Map. 4.8.2: Map showing the locations of excavated trenches.

4.8.1 Trench 1

4.8.1.1 Stratigraphy

This trench is the largest among the six trenches that measures 4 X 3.5 m (Fig. 4.8.1). Excavations were conducted to reach a depth of 3.5 m where the digging was ceased after encountering the water table. Six distinct stratigraphic units were identified in Trench 1 (Fig. 4.8.2). The bottom most Unit (Unit 5) in the trench is of a brownish red colored silty sandy sediment with relatively high moisture content and only the top 40 cm of this Unit was excavated below which water table was encountered. Unit 5 is overlain by ~ 80 cm thick, dark brownish red coloured sandy silt sediment (Unit 4). This Unit has yielded Middle Palaeolithic artefacts. A light brown coloured clayey silt Unit (Unit 3) of uneven thickness overlays the Unit 4 throughout the trench. Lithic artefacts were recovered from the topmost part of this Unit. Unit 3 is overlain by (Unit 2), a pale yellow coloured sandy silty sediment distributed unevenly throughout the trench.

Figure. 4.8.1: Trench 1 excavations.

Notably at least three different episodes of high energy erosional events represented by coarse material consisting of small sized pebbles, carbonate nodules were observed within Unit 2 (Fig. 4.8.3). Interestingly, these subunits within the Unit 2 yielded microlithic artefacts. Unit 1 is a yellow-coloured, silt dominated Unit that represents topsoil. The stratigraphy of the Trench 1 is dominated by the presence of fine-grain sediments primarily consist of silt and with less

percentage of sand and clay. However, these observations are field based and can only be confirmed through particle size analysis of the sediments. Except the artefacts in Unit 4, 3 and 2 no other pebbles or any other coarse material was observed in the trench. Such nature of the sediments indicates low energy depositional conditions, which are archaeologically ideal for better preservation of site/occupational features.

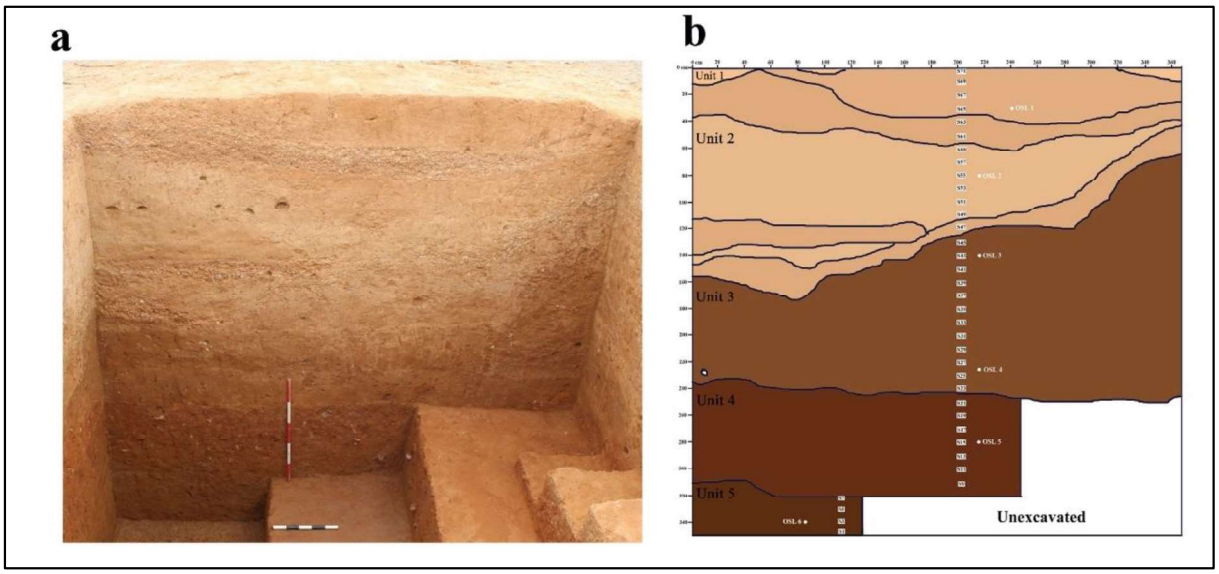

Figure. 4.8.2: a: Section facing west, trench 1; b: Schematic sketch of the section.

Figure. 4.8.3: Coarse sediments within Unit 2.

4.8.1.2 Luminescence Chronology

Six samples were collected for OSL dating (Fig.4.8.2b). However, only three of them were processed for age estimation, as the artefacts were found only in these Units. The above three dated samples were collected at the depths of 1.40 m and 2.25 m from the Unit 4, and 2.80 m from the Unit 5. The dates for Unit 4 are 49.52±2.50 ka and 33.82±1.64 ka, and Unit 5 is dated to 59.65±3.03 ka (Table 4.8.1). Luminescence age estimations were done using p-IR-IRSL protocol. All the three samples showed less overdispersion indicating well bleaching before the burial (Fig. 4.8.4; Fig. 4.8.5 and Fig. 4.8.6). No significant fading was observed in the fading estimations therefore ages were not corrected.

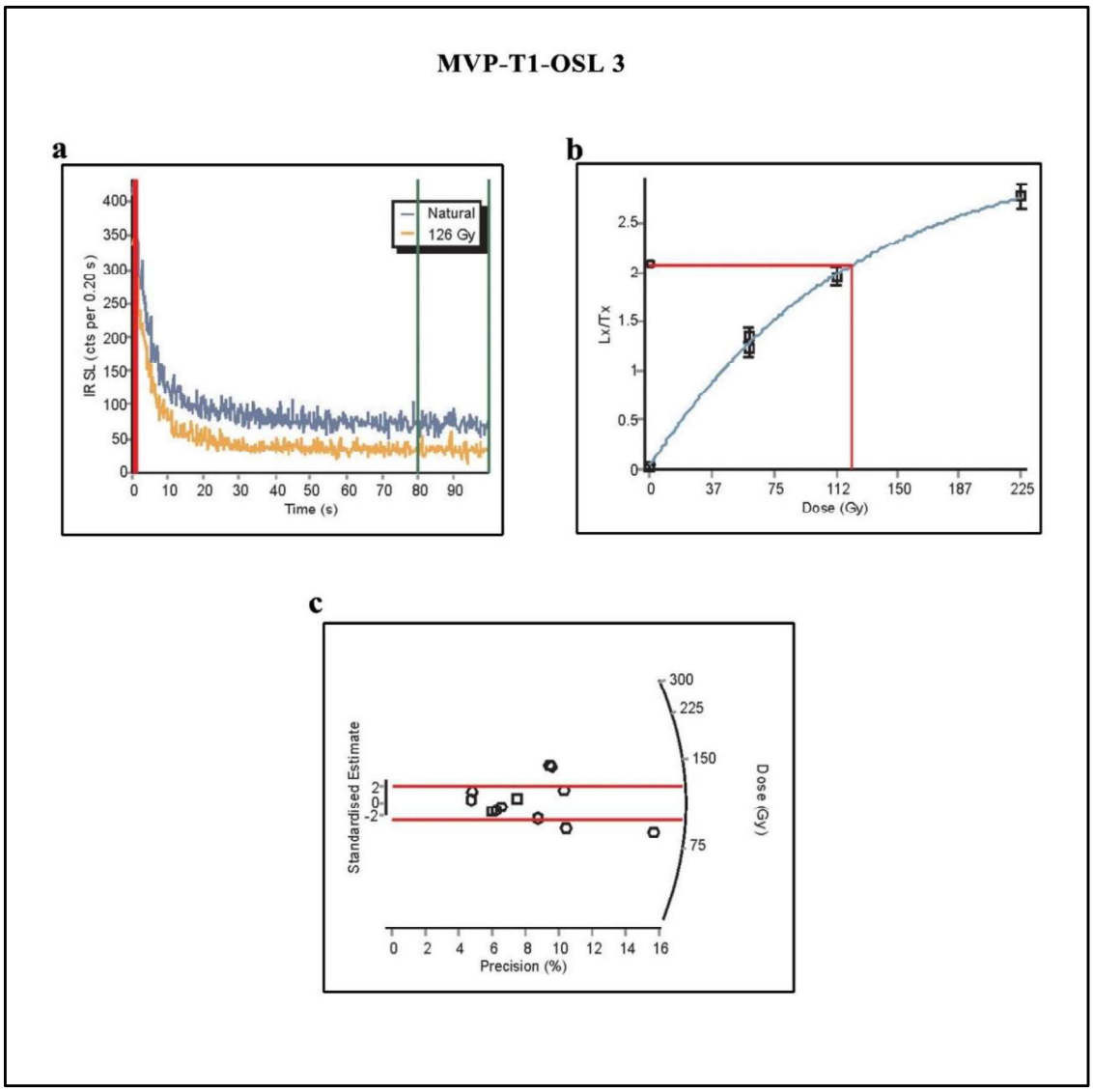

Figure. 4.8.4: Results of p-IR-IRSL analyses for sediment sample from Unit 3. a: typical feldspar shine down curve; b: typical growth curve; c: radial plot representing the estimated palaeodoses.

Table. 4.8.1: Dose rate data, D_e values and OSL ages for the sediment samples from Trench 1, Motravulapadu.

Sample Code	Depth (cm)	Radionuclide activity				Equivalent doses				OSL age (ka)
		U (ppm)	Th (ppm)	K (%)	Total Dose rate [b,c] (Gy/ka)	No. of aliquots/ grains	Water content (%)	OD (%)	D_e (Gy)[d]	
MVP-T1-OSL 3	140	2.55±0.04	14.65±0.27	2.4±0.04	3.74±0.11	12/ ~120	22.04	12.30	126.58±4.85	**33.82±1.64**
MVP-T1-OSL 4	225	1.66±0.05	10.72±0.26	1.55±0.04	2.69±0.11	10/ ~120	20.98	7.20	133.63±3.95	**49.52±2.50**
MVP-T1-OSL 5	280	2.07±0.05	9.62±0.24	1.41±0.03	2.60±0.10	12/ ~120	20.60	8.31	155.20±4.47	**59.65±3.03**

[a] Radioactivity measurement made on a dried, homogenized and powered sample by HPG detector

[b] Includes cosmic-ray dose rate of 0.096 Gy ka^{-1}

[c] 12.5±0.5% and 200±20 ppm Rubidium (^{87}Rb) concentrations were used to estimate the internal dose rate

[d] after subtracting of a residual dose of 12 Gy

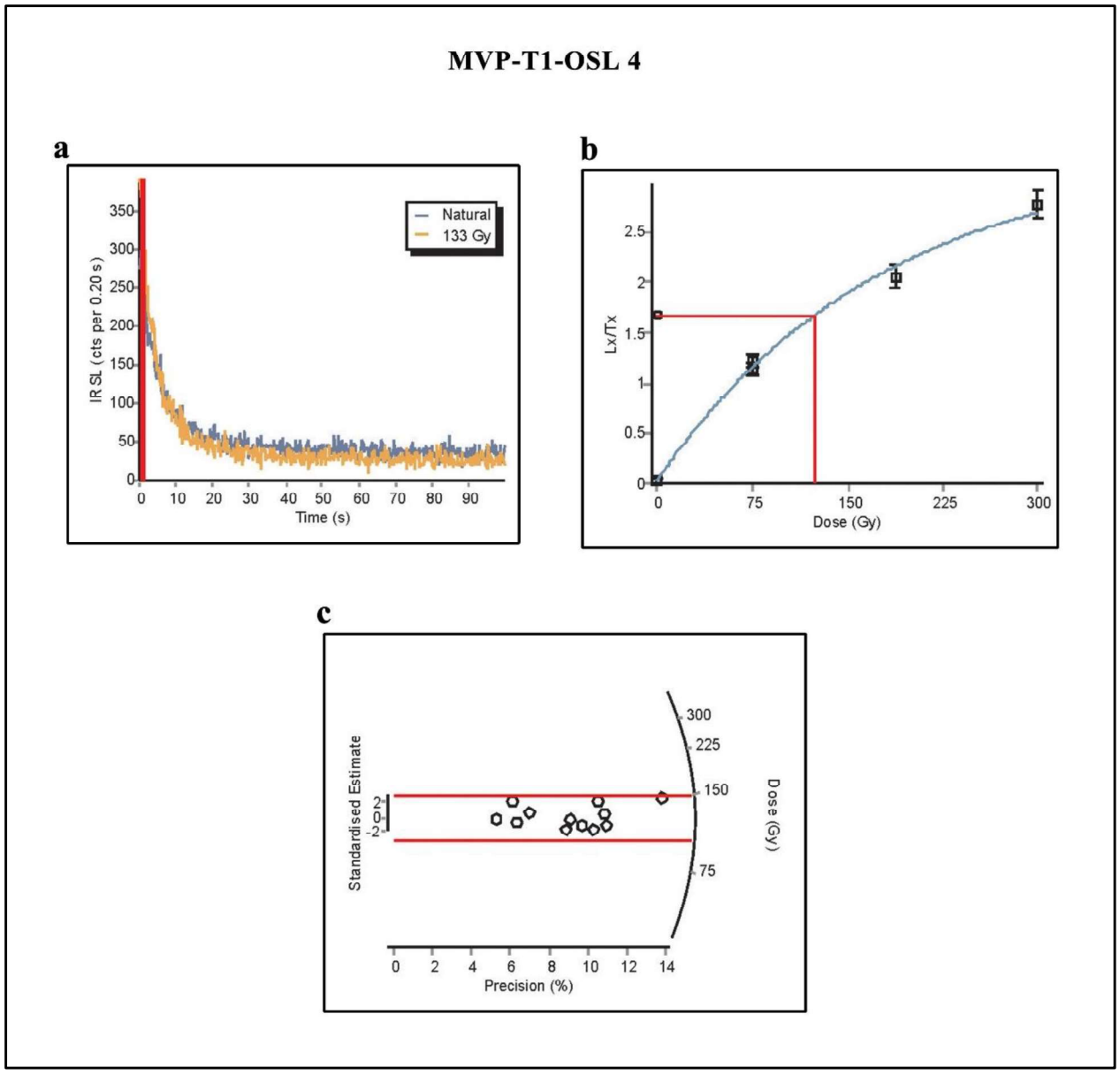

Figure. 4.8.5: Results of p-IR-IRSL analyses for sediment sample from Unit 3. a: typical feldspar shine down curve; b: typical growth curve; c: radial plot representing the estimated palaeodoses.

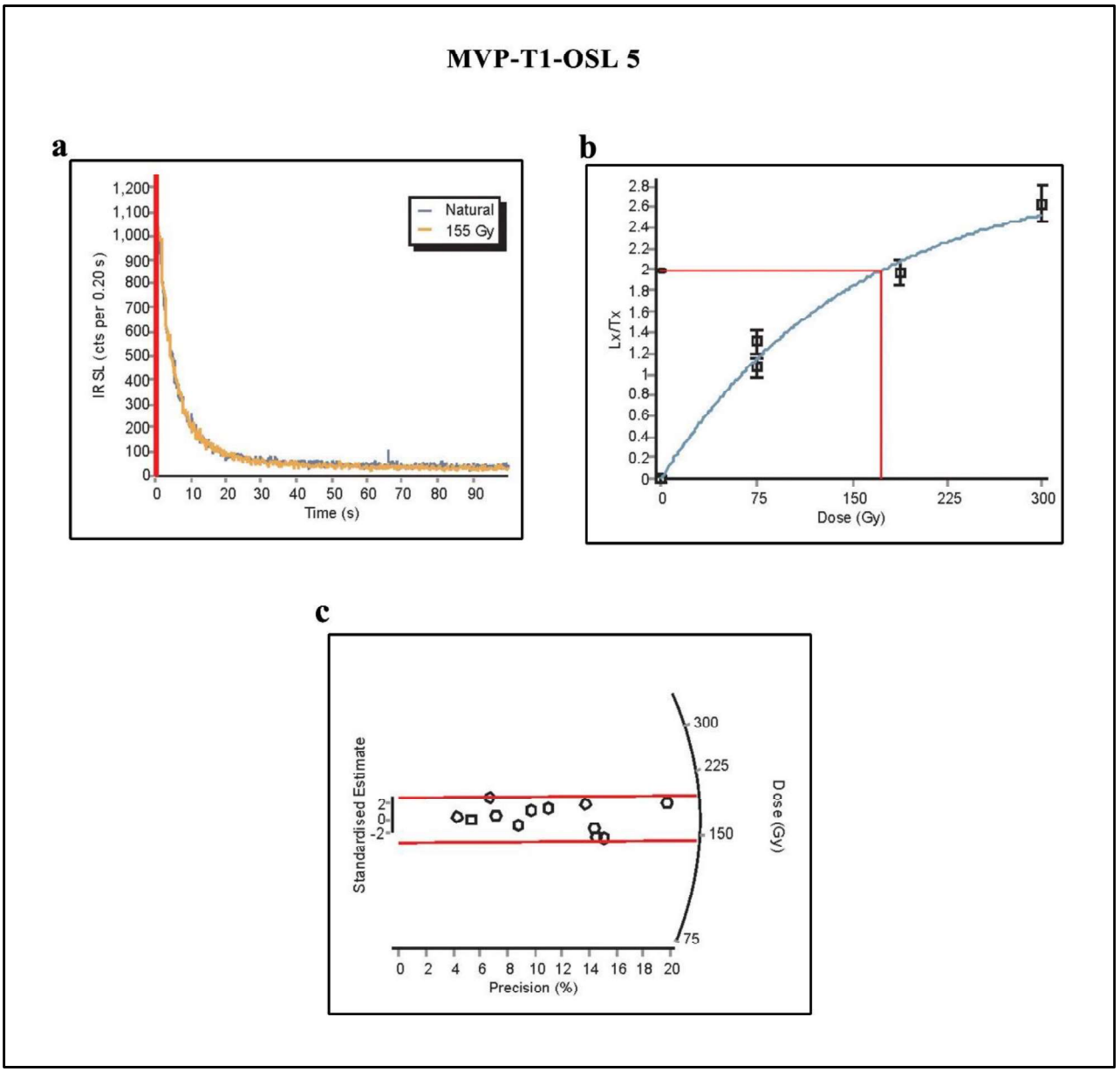

Figure. 4.8.6: Results of p-IR-IRSL analyses for sediment sample from Unit 4. a: typical feldspar shine down curve; b: typical growth curve; c: radial plot representing the estimated palaeodoses.

4.8.1.3 Lithic technology

Trench 1 has yielded three artefact bearing horizons: Unit 2, 3 and 4. Unit 2 artefacts are not discussed here as no luminescence age of this sediment was assessed. Besides, the artefacts from Unit 2 are of microlithic in nature consisting of microblade cores and blades, backed blades, geometric microliths such as lunates, triangles, and trapeziums. Artefacts from Unit 3 and 4 are discussed below, in detail. No surface collections were included in the analysis as the site is a multi-cultural site and there are high chances of considerable mixing of artefacts from different sedimentary units. Unlike the other sites discussed in previous chapters which are single cultural sites, the Motravulapadu lithic assemblage comes only from excavated trenches. The typo-technology of the artefact assemblages of Unit 3 and Unit 4 is discussed below.

Unit 3 yielded 121 artefacts within the top 35 cm associated with fine grain sediments (Fig. 4.8.7). All the artefacts were made of fine grain quartzites that are easily available in the Nachuvagu/Manneru stream bed. Among the 121 artefacts recovered, 47 are of debitage, 17 flaked pieces, and 4 are of worked nodule (Table. 4.8.2).

Figure. 4.8.7: In situ artefacts excavated from the Unit 3 of Trench 1.

The three categories which are a crucial part of the lithic reduction sequence form 56.20% of the total assemblage. All the below-mentioned lithic analyses and technological descriptions are based on these rest of 53 artefacts.

Table. 4.8.2: Composition of the Lithic assemblage from Unit 3, Trench 1.

Typology	Unit 3	%
Core		
Uni-directional core	4	3.31
Core fragment	5	4.13
Split Pebble	1	0.83
Total Cores	**10**	8.26
Retouched		
Retouched flaked piece	1	0.83
Total Retouched	**1**	0.83
Unretouched		
Flake	39	32.23
Blade	1	0.83
Cortical blade	2	1.65
Flaked piece	17	14.05
Worked Nodule	4	3.31
Debitage (< 2 cm. length)	47	38.84
Total Unretouched	**110**	90.91
Total	**121**	**100**

Lithic debitage (< 2 cm in length) constituted a large portion (38.8%, n=47) of the assemblage. Unretouched flakes, both complete and broken, are the next common class (32.23%, n=39) followed by flaked pieces (14.05%, n=17). Core component in the assemblage consists of only four unidirectional cores (Fig. 4.8.8), five core fragments and one split pebble (Fig. 4.8.9). Overall, 80 % of the assemblage, mostly cores (19.23%) and flakes (61.54%), retain cortex. The cortex is of cobble cortex type indicating the riverine source.

Generally, discarded flakes with cortex would indicate the early-stage reduction of cores and the subsequent use of unidirectional core technology. Initial stages of reduction sequences in the assemblage are evident by the presence of cortex on flake platforms, the dorsal surface, and lateral margins, which account for half of the complete flakes (n=15). Intact flakes with two or more dorsal flake scars (n=28) are dominated by the flakes with radial and weakly radial scarring forming 71.42% (n=20). Examples of unidirectional flake scarring (from proximal) makes up 28.57% (n=8). Three-quarters of the flakes have cortical platform, and a few instances of faceting (14.28%) and overhang removal (10.71%) are also observed. Flakes from different stages of the reduction sequence such as cortical flakes having cortical platforms and entire dorsal surface with cortex, flakes having cortical platforms with a few preparation scars on the dorsal surface, flakes having prepared platforms with cortex on the dorsal surface, and platform rejuvenation flakes are present in the assemblage (Fig. 4.8.10). The presence of aforementioned flake types along with high percentage of debitage indicates the primary nature of lithic assemblage. The lithic assemblage recovered from Unit 3 of trench 1 lacks characteristic diagnostic features that would allow it to be assigned to any known specific reduction sequence. However, the presence of unidirectional cores and debitage similar to Trench 4 artefacts and the luminescence age of 33 ka, which is the same as the age of the Trench 4 artefact bearing horizon, indicate the assemblage is part of the blade core reduction process. Due to the small and undiagnostic nature of the lithic assemblage from Unit 3 of Trench 1, the metrical description of artefacts is not discussed here.

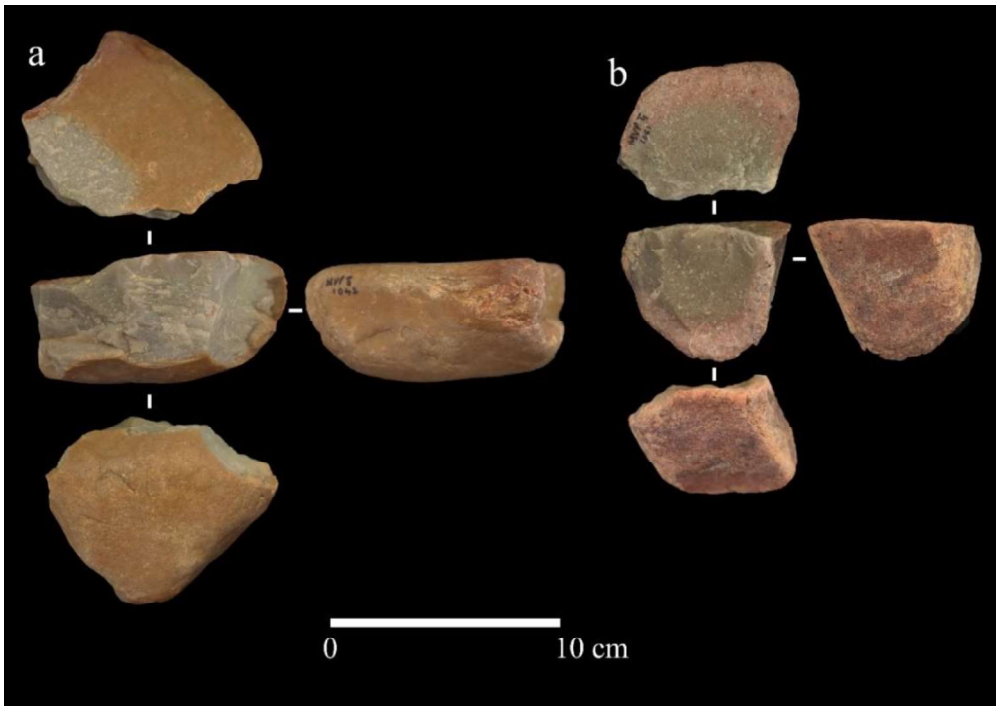

Figure. 4.8.8: Unidirectional cores**.**

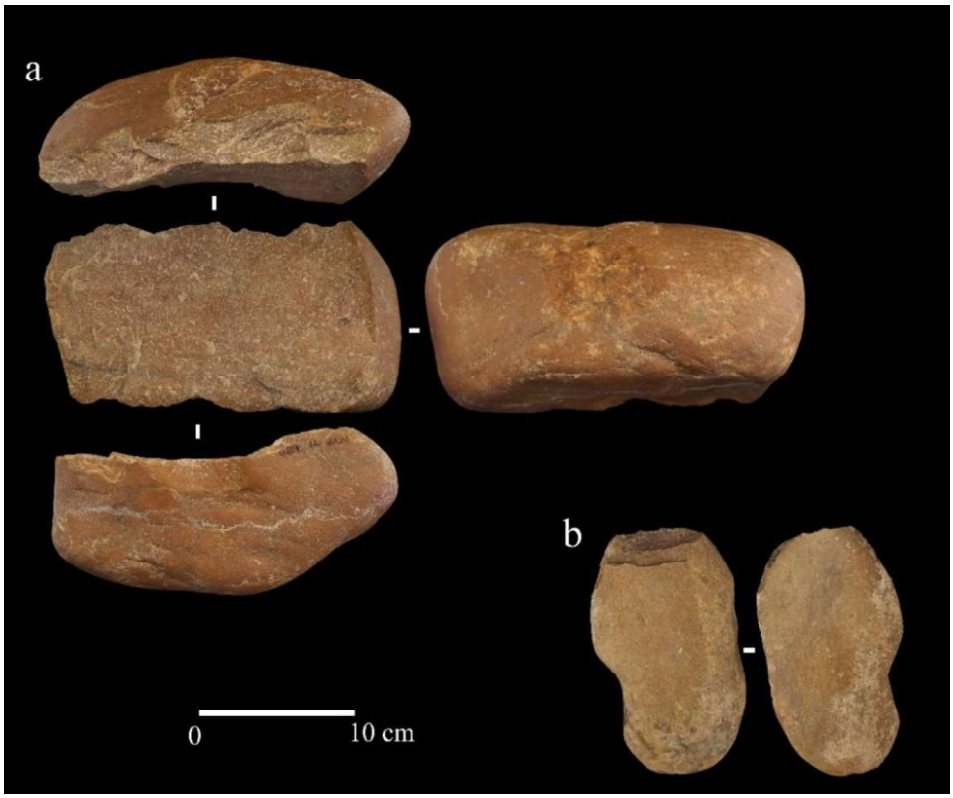

Figure. 4.8.9: Worked pebbles. a; split cobble with platform preparation; b: worked nodule.

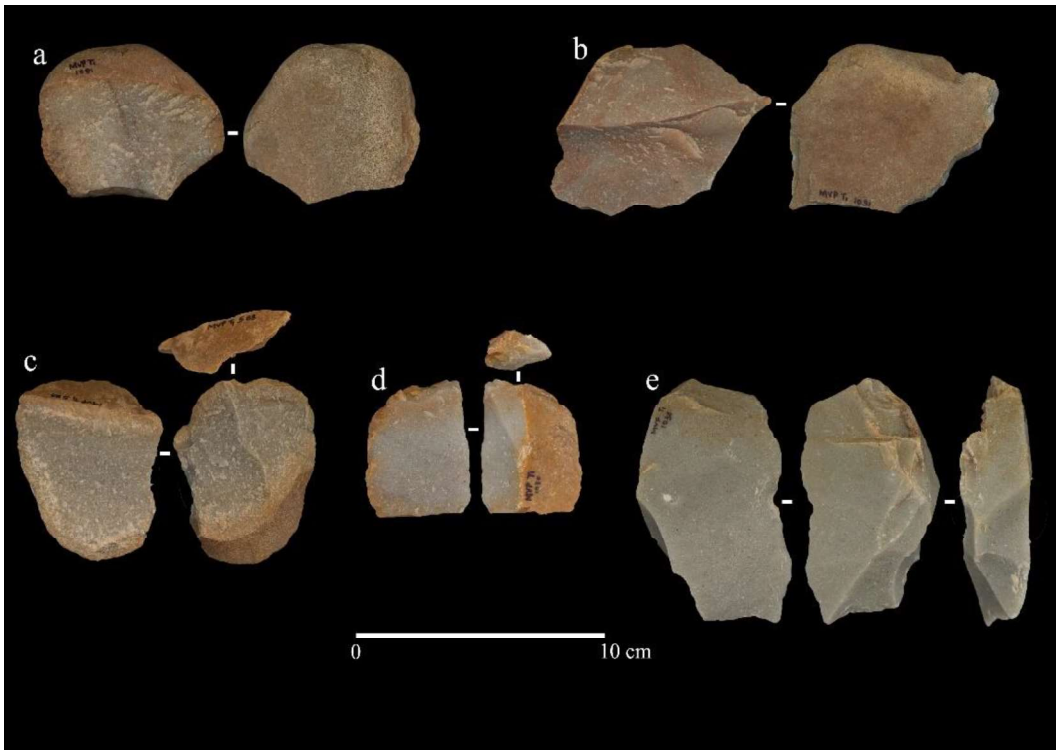

Figure. 4.8.10: Flake component in the assemblage. a and b: flakes with cortical platform and dorsal surface with 100% cortex; c: Flake with cortical platform with flake scars on the dorsal surface; d: flake with prepared platform and prepared dorsal surface; e: platform rejuvenation flake.

Unit 4 has yielded 357 artefacts dominated by the products of Levallois reduction (Table. 4.8.3). Most artefacts retain cortex (65.47%), indicating that the initial preparation of cores must have taken place on-site. As the site is located on the bank of a tributary stream, pebbles from the stream bed must have served as a raw material source. The cortex type is observed to be cobble type, which further corroborates the aforesaid observation. None of the artefacts show any evidence abrasion and are in mint condition.

Table. 4.8.3: Composition of the lithic assemblage from Unit 4 of Trench 1.

Typology	Unit 4	%
Core		
Preferential Levallois core	3	0.84
Unidirectional Recurrent Levallois core	2	0.56
Bi-directional Recurrent Levallois core	1	0.28
Levallois Point Core	3	0.84
Uni-directional core	3	0.84
Radial core	2	0.56
Core fragment	9	2.52
Total Core	**23**	**6.44**
Retouched		
Retouched point	1	0.28
Total Retouched	**1**	**0.28**
Unretouched		
Blade	6	1.68
Cortical blade	2	0.56
Levallois flake	9	2.52
Prepared core flake	12	3.36
Core preparation flake	57	15.97
Roughout flake	45	12.61
Platform Rejuvenation Flake	3	0.84
Levallois point	10	2.80
Flaked piece	95	26.61
Manuport	10	2.80
Worked Nodule	5	1.40
Debitage (< 2 cm length)	79	22.13
Total Unretouched	**333**	**93.28**
Total	**357**	**100**

The number of cores in the assemblage accounts for 23; all belong to formal reduction strategies. The formal core reductions include Levallois, radial, and unidirectional. Notably, except for 9 core fragments, no other informal cores are present in the assemblage. Among Levallois core reduction strategies, recurrent and preferential systems are present along with Levallois point cores (Fig. 4.8.11; Fig. 4.8.12; Fig. 4.8.13). Three unidirectional and two radial cores are present in the assemblage.

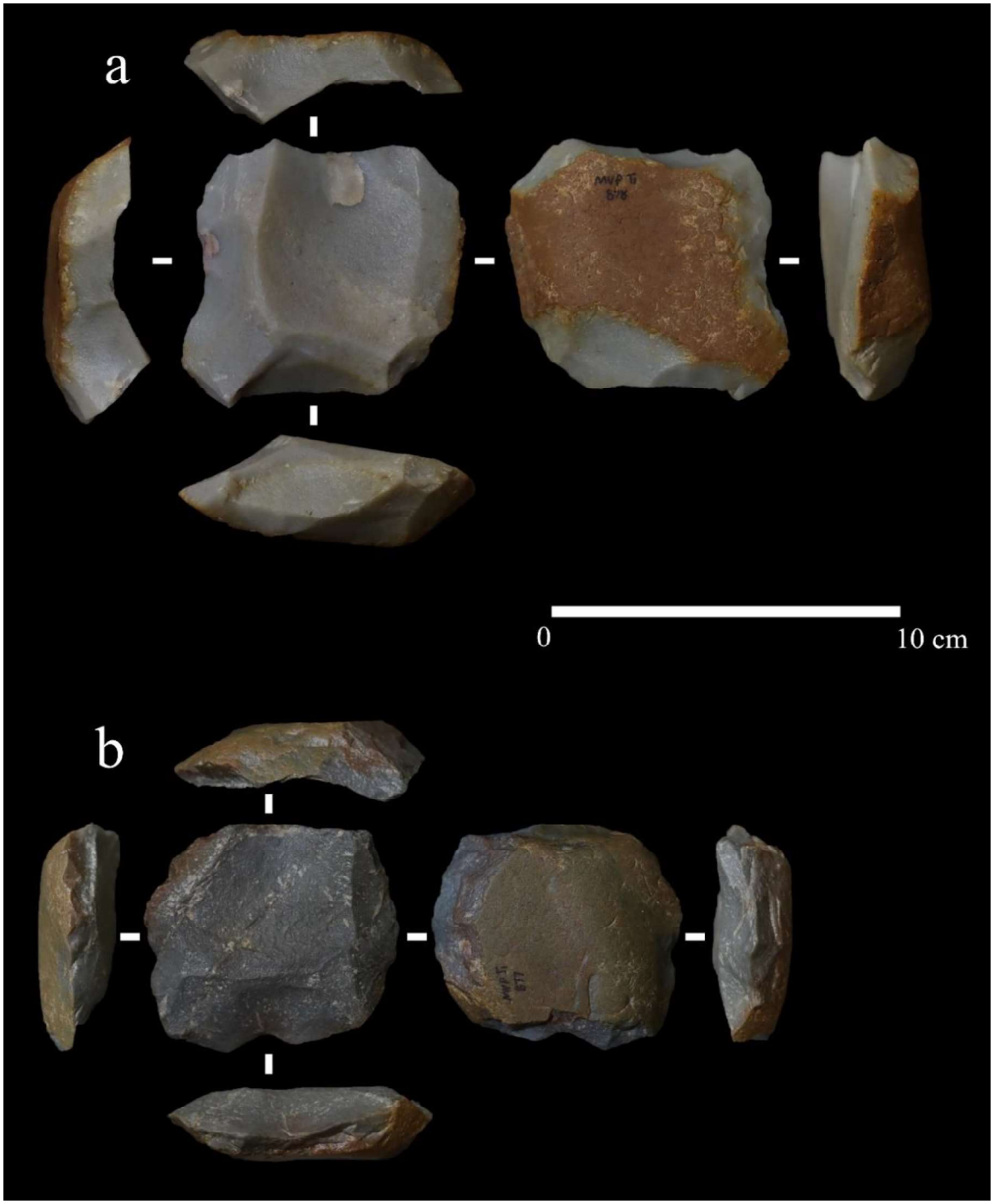

Figure. 4.8.11: Levallois cores. a: Preferential Levallois core; b: Recurrent Levallois core.

Figure. 4.8.12: Levallois point cores.

A maximum of two and a minimum of one core rotations are observed in Levallois cores, whereas unidirectional and radial cores show a maximum of three and a minimum of one rotation. Most cores show one (n=6) and two (n=11) major scars (> 1/3 core length), with two cores exhibiting three and four scars each. Cores' mean length, medial width and medial thickness are 56.35x66.11x32.35 mm when oriented along the flaking axis (last flake scar) (Table. 4.8.4).

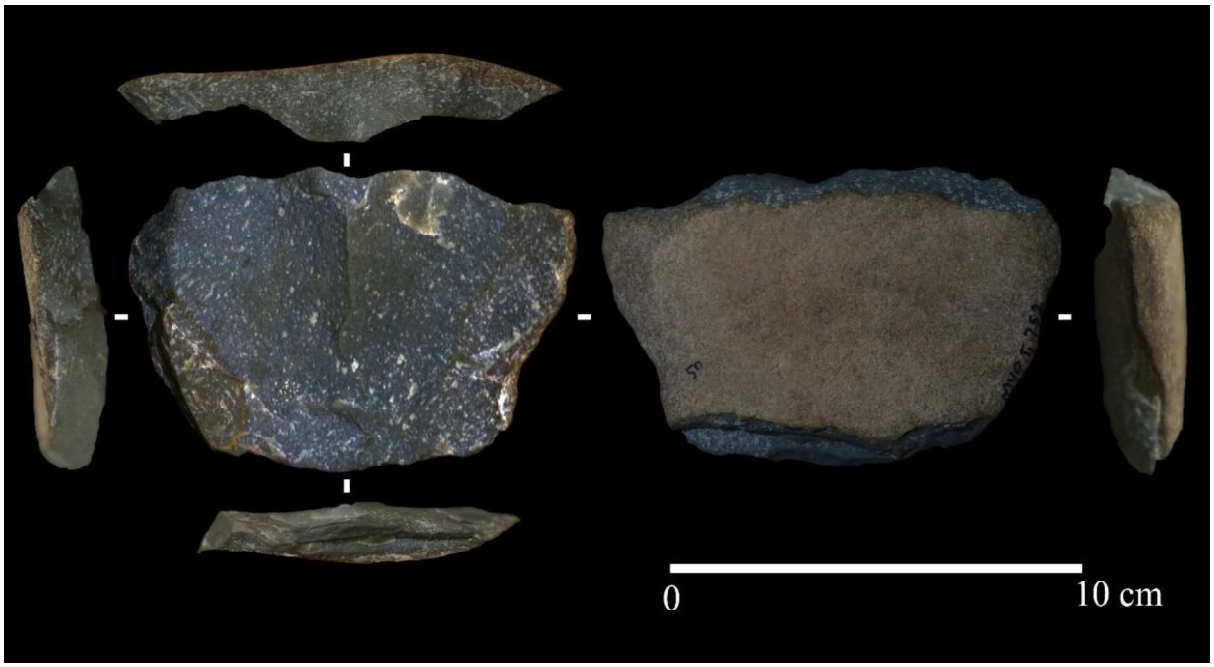

Figure. 4.8.13: Unidirectional Recurrent Levallois core.

Table. 4.8.4: Statistical data for core attributes.

Attribute	N	Mean	SD	Min.	Max.
Length	14	56.35	14.06	39.47	87.24
Proximal Width	14	64.68	11.68	49.64	84.20
Medial Width	14	66.11	9.60	53.01	82.38
Distal Width	14	46.85	16.26	24.22	76.93
Proximal Thickness	14	30.42	23.39	11.61	77.95
Medial Thickness	14	32.35	16.14	17.08	70.31
Distal Thickness	14	22.39	14.83	8.51	56.50
Proximal Shape	14	0.98	0.12	0.83	1.17
Distal Shape	14	1.55	0.39	0.90	2.41
Elongation	14	0.89	0.20	0.63	1.22
Flatness	14	2.40	0.88	0.88	3.69
No. of Core Rotations	14	1.60	0.63	1.00	3.00
Last Platform Angle	14	70.33	10.08	60.00	85.00
No. of Major Flake Scars	14	1.87	0.92	1.00	4.00
No. of Flake Scars	14	4.67	0.49	4.00	5.00
No. of Feather terminations	14	1.40	0.63	1.00	3.00
No. of non-feather Terminations	14	0.47	0.83	0.00	3.00
Last Scar Length	14	39.18	9.87	26.42	61.61
Last Scar Width	14	32.64	5.64	23.57	40.75
Last Scar Elongation	14	1.26	0.39	0.81	1.98

The core's proximal, medial, and distal widths measured along the flaking axis are 64.68x66.11x46.85 mm, respectively. The proximal shape of the cores is relatively straight (mean 0.98 mm), whereas the distal shape is tapering (mean 1.55 mm).

No considerable variation in core elongation (ranging between 0.63 and 1.22) is observed, maybe because there is no significant variation in the cores' mean length and mean medial width. The core flatness index ranges from 0.88 to 3.69, where most cores are wider than thick. Five cores have cortical platforms, six have single conchoidal platforms, and 3 show multiple conchoidal platforms. Platforms were facetted on 9 cores; in 5 instances, no preparation was observed. The last scar-face-length of cores is less than the axial core length, indicating the flaking face is limited to the smaller axial surface. The last scar lengths range from 26.42 to 61.61 mm, with an average of 39.19 mm, and the last scar widths range between 23.57 and 40.75 mm, and a mean of 32.64 mm. On average, the last flake scar elongation (mean=1.26) indicates that relatively squarish flakes were removed. Majority of the last major flake scars exhibit feather terminations (73.33%), with non-feather terminations accounting for 26.66%.

One hundred forty-five flakes, including both retouched and unretouched, have been recorded in the assemblage, including 92 complete flakes. Flakes were classified according to technological type to understand their position in the reduction sequence (Table. 4.8.5). The typo-technological description of the flakes below is based on the complete flakes in the assemblage.

Table. 4.8.5: Technological classification of flake component.

Technological Type	Number	%
Roughout flake	45	31.03
Core preparation flake	57	39.31
Prepared core flake	12	8.28
Levallois flake	20	13.79
Blade	8	5.52
Platform Rejuvenation flake	3	2.07
Total	**145**	**100**

A wide range of technological diversity is evident amongst the flakes, from core preparation flakes to end products. Considerable number of roughout flakes (31.03%) along with core

preparation flakes (39.31%) overall forming 70.34% of the flake component indicate that initial preparation of the cores was done on the site. Flakes from different stages of the core reduction sequence are noted in the assemblage, from complete cortical flakes to end products such as Levallois points and flakes (Fig. 4.8.14; Fig. 4.8.15). The presence of one platform rejuvenation (Fig. 4.8.16f) also corroborates the observation mentioned above. End products such as Levallois flakes (including Levallois points), prepared core flakes and blades account for 27.59% of the flake component (Fig. 4.8.16).

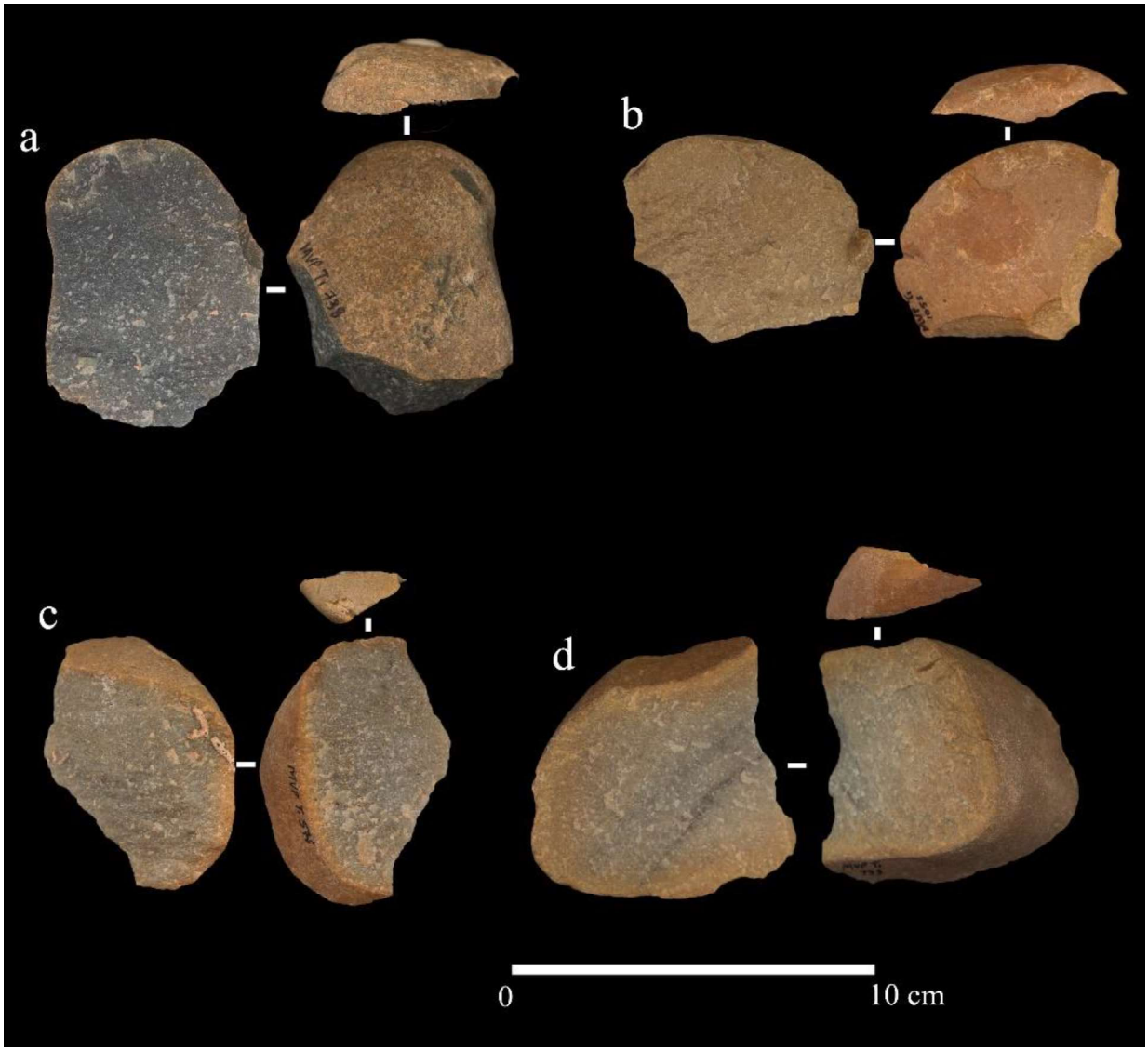

Figure. 4.8.14: Cortical flakes with cortical platform.

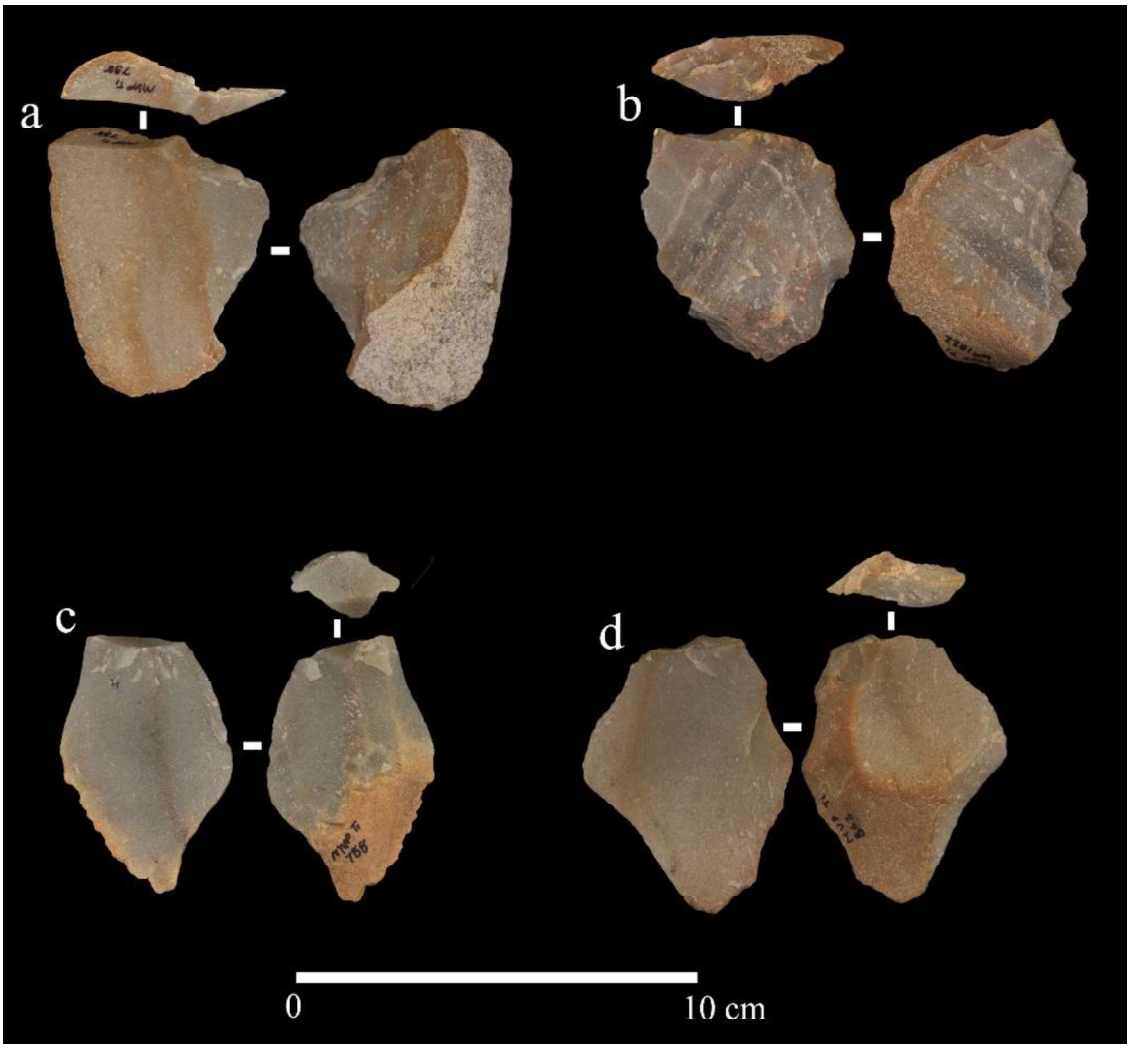

Figure. 4.8.15: Cortical flakes with prepared platforms.

The most common dorsal scar patterns present on complete flakes in the assemblage are proximal (41.30%), followed by weakly radial (32.61%) and radial (14.13%). Flakes with no dorsal scars (cortical flakes) were present in considerable numbers forming 11.96%. Cortical coverage ranges from 0-100%, with 45.65% of flakes recorded with no cortex and 28.26% with less than 50% cortex present and 9.78%, 4.35%, 11.96% with 60%, 80% and 100% cortex respectively. Considerable number of flakes with only cortical platforms (28.63%) and 100% cortical cover of the dorsal and platform surface (11.96%) are observed. Notably all the complete flakes shows feather terminations. Mean axial flake dimensions are 48.20 x 37.77 x 11.72 (LxWxT)mm; on average, flakes are squarish/oval (mean elongation=1.44) (Table. 4.8.6). Typically, flakes are more than four times as wide as they are thick (mean flatness=3.52), with a flatness range of 1.44 - 6.82. 75% of the flakes exhibit slightly expanding proximal margins (mean proximal shape=0.80), with 25% exhibiting contracting proximal margins, leading to an upper proximal shape index of 1.12. In contrast, the distal shape indicates that 84.78% of the flakes exhibit distal contracting margins (mean=2.23).

Figure. 4.8.16: Prepared core products. a to c: Levallois flakes; d and e: blades; f: platform rejuvenation flake.

Table. 4.8.6: Statistical data for Flake attributes.

Attribute	N	Mean	SD	Min.	Max.
Length	92	48.20	16.03	19.97	99.37
Proximal Width	92	32.75	13.35	11.79	79.31
Medial Width	92	37.77	14.63	12.77	96.39
Distal Width	92	29.48	16.66	2.81	95.13
Medial Thickness	92	11.72	4.86	3.86	30.38
Elongation	92	1.44	0.52	0.42	3.05
Flatness	92	3.52	1.16	1.44	6.82
Proximal Shape	92	0.89	0.18	0.50	1.26
Distal Shape	92	2.03	1.48	0.70	9.17
Platform width	92	25.61	11.03	7.57	64.32
Platform Thickness	92	10.31	5.10	3.03	29.30
Platform area	92	307.93	293.21	27.71	1694.42
Platform Angle	92	78.64	10.65	50.00	110.00
Dorsal scar count	92	2.51	1.12	0.00	6.00
No. Unidirectional arises	92	0.56	0.74	0.00	2.00
No. Radial arrises	92	0.59	0.75	0.00	3.00

Single conchoidal platforms are the most common type (38.04%), followed by cortical (28.26%), multiple conchoidal (23.91%), dihedral (7.61%), and crushed (2.17%) types. While half of the flakes (51.09%) have no platform preparation, faceting and overhang removal were seen on 35.87% and 13.04% respectively. A wide range in platform size is evident, with platform width ranging from 7.57 to 64.32 mm and platform thickness ranging from 3.03 to 29.30 mm. The platform shape index indicates that platforms are typically elongated (mean elongation=2.90), with 81.52% being two times wider than thick. A total of 95 artefacts categorized as flaked pieces are present, which bear no precise ventral morphologies or negative flake scars originating from the margins of the artefacts but have clearly undergone some reduction. Except for one retouched point, no other retouched artefacts are noted in the assemblage. However, considerable number of Levallois points (n=9) are present in the assemblage (Fig. 4.8.17).

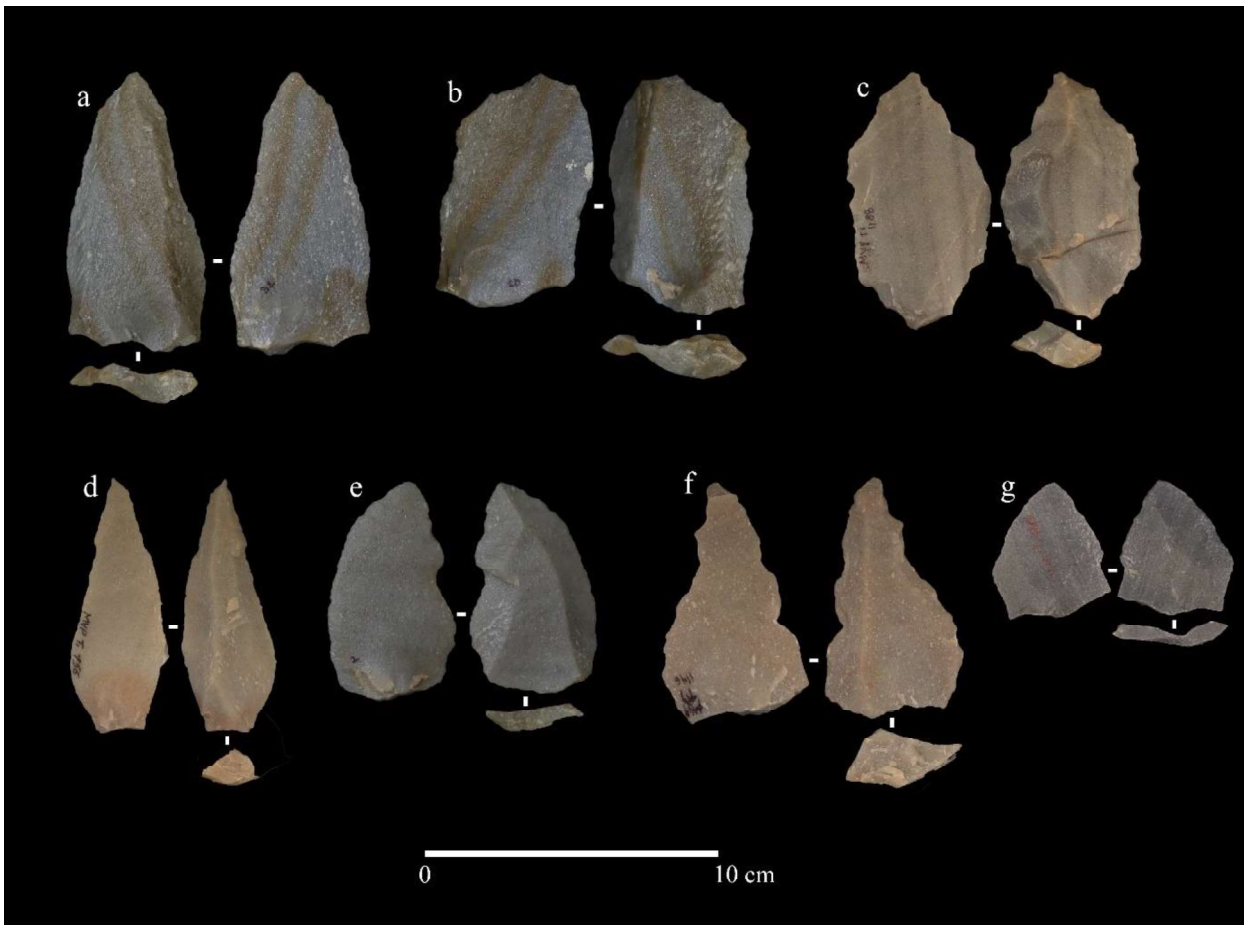

Figure. 4.8.17: Levallois points.

4.8.1.4 Summary

Trench 1 reveals two or three artefact bearing horizons belonging to distinct lithic reduction sequences. Microlithic artefacts in Unit 2 include micro-blade cores, backed blades, and geometric microliths. No chronometric age for Unit 2 was generated in this study; but based on the sediment composition and observations around the landscape indicates the Holocene age of the sediment. Unit 3 has lithic assemblage aimed at producing elongated flakes and blades dated to 33 ka. Even though, the assemblage from Unit 3 is undiagnostic, based on the presence of debitage that resembles the debitage of Trench 4 lithic assemblage dated 30 ka, it is reasonable to assume that the former is a blade technology-based assemblage.

Unit 4 from Trench 1 reveals lithic assemblages consisting of Levallois and prepared core reduction strategies dated to 59 ka. Presence of debitage smaller than 2 cm in length and flakes from different stages of core reduction indicates the in-situ nature of the assemblage. Variations in Levallois core reductions including Preferential, Recurrent, Uni and Bi-directional recurrent Levallois and Levallois point cores are present in the assemblage. Pebbles and cobbles available from the adjacent riverbeds were exploited to make artefacts. Most of the Levallois cores have cortex on the platform surface side. The pebbles were split in to two halves which resulted in each half having natural hierarchical surfaces, exploited further as Levallois and other prepared cores. Typical examples of Levallois points and Levallois flakes are present in the assemblage, indicating widespread use of Levallois technology by 59 ka at the site. A few samples of blade elements are also noted in the assemblage, though retouched artefacts are minimal.

4.8.2 Trench 2

4.8.2.1 Stratigraphy

Trench 2 measuring 2 x 2 m was laid out 110 m west of the trench 1 and excavated to reach a depth of 2.8 m (Fig. 4.8.18). The trench was excavated with the intention of understanding the stratigraphic and chronological context of the Youngest Toba Tuff deposits. Nine discrete sedimentary units were observed within 2.8 m in the trench 2. (Fig. 4.8.19). Top six units (Unit 1 to 6) are thin silty clay sediments with redeposited carbonate nodules and flakes of undiagnostic nature. Unit 7 is reddish brown coloured silt dominated sediment with large carbonate concretions.

Figure. 4.8.18: Trench 2 with YTT as a distinct Unit.

Unit 8 is YTT horizon with a maximum thickness of 40 cm spread unevenly throughout the trench. The ash Unit becomes thinner towards the east and disappears in the eastern section of the trench. Unit 9 underlying the YTT Unit is reddish brown silty sediment with high moisture content and large carbonate concretions like the ones observed in Unit 7. Compositionally Unit 7 and 9 are similar in nature except high water percentage in the latter. The presence of YTT sandwiched between Unit 7 and 9 seems to be a short event during the formation of Unit 7 and

9. The Presence of a thin, uneven lens of reddish-brown sediment was observed with YTT horizon along with the presence of large carbonate concretions (Fig. 4.8.20). In addition, YTT sediment has diffused contact with the underlying and overlying sediments (Fig. 4.8.21).

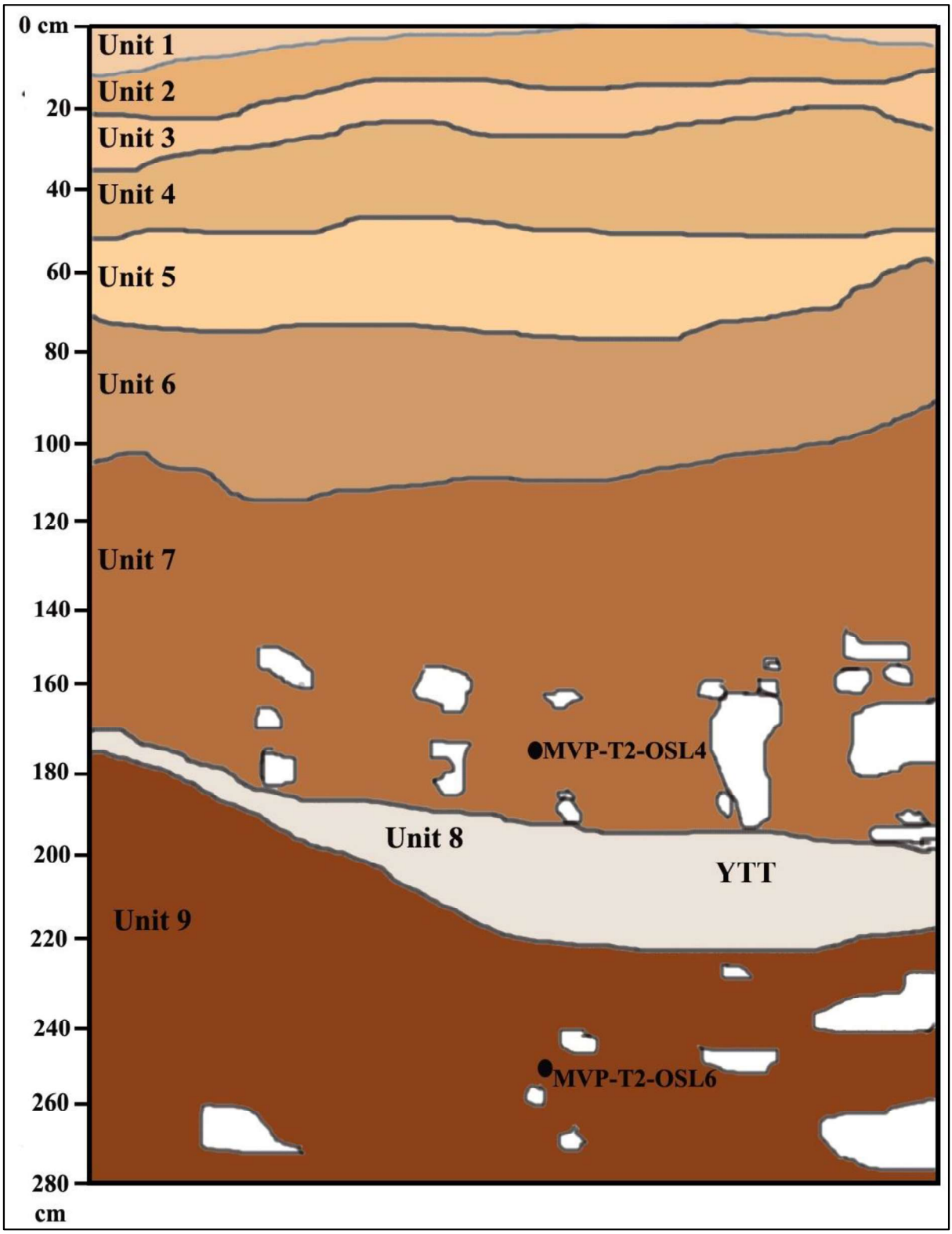

Figure. 4.8.19: Schematic sketch of section facing north of Trench 2, Motravulapadu.

Figure. 4.8.20: YTT horizon in the western section of the trench 2.

Figure. 4.8.21: Close view of the YTT sediment with diffused contact with underlying and overlying sediments.

4.8.2.2 Luminescence Chronology

Sediment samples overlying and underlying the Youngest Toba Tuff Unit, were collected to constrain the last burial age of ash deposits. Fading measurements on the samples indicates the g value is less than 1 therefore no fading corrections were applied. Both the samples yielded an p-IR-IRSL age of 29 ka and 33 ka for the overlying and underlying the YTT sediments (Table. 4.8.7). These ages are statistically indistinguishable therefore indicating an age of ~ 30 ka for the last burial of the ash. Samples are well bleached with less than 10% of overdispersion (Fig. 4.8.22 and Fig. 4.8.23) therefore central age model (CAM) was applied to estimate the palaeodose.

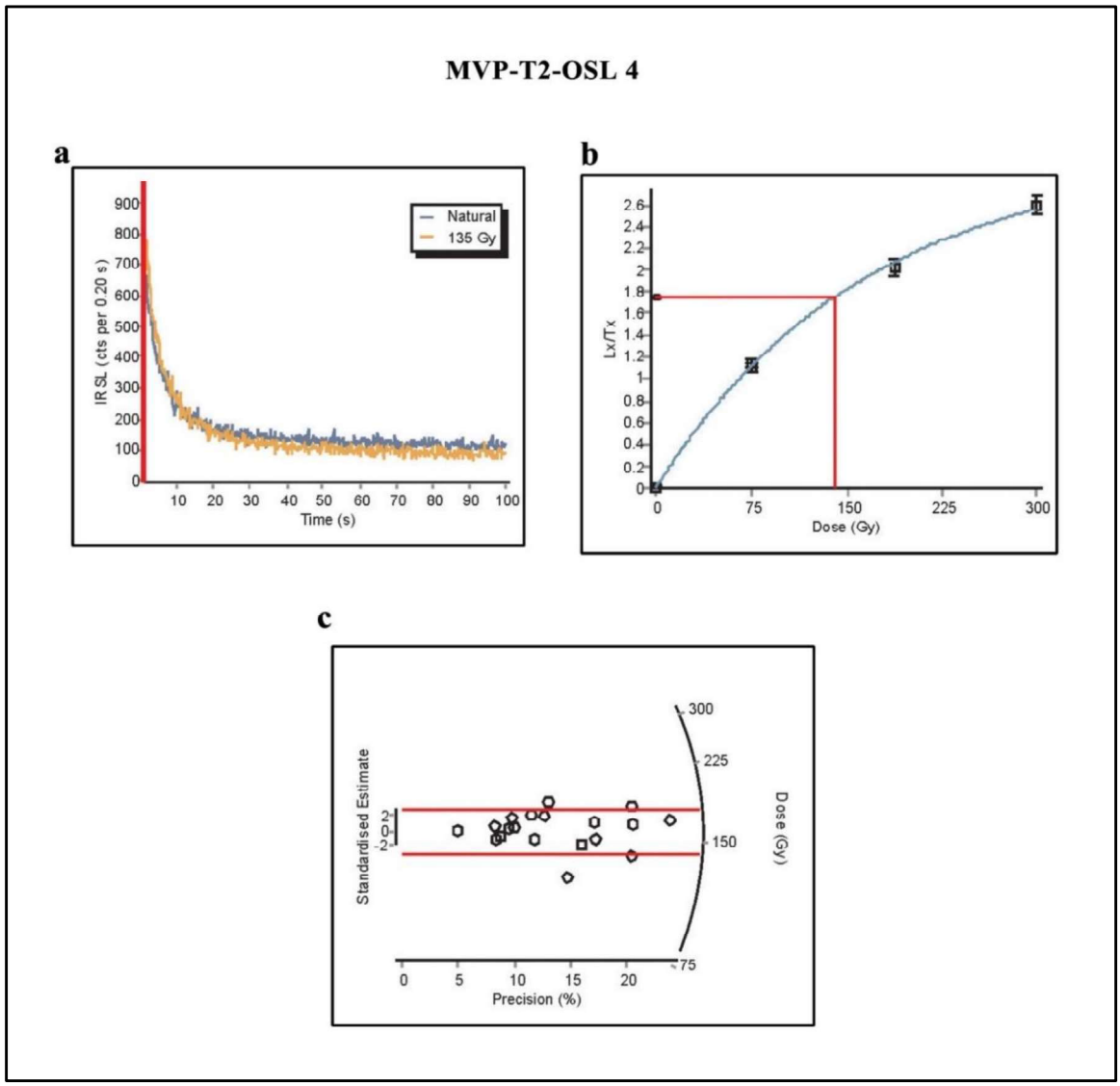

Figure. 4.8.22: Results of p-IR-IRSL analyses for sediment sample overlying the YTT horizon. a: typical feldspar shine down curve; b: typical growth curve; c: radial plot representing the estimated palaeodoses.

Table. 4.8.7: Dose rate data, D_e values and OSL ages for the sediment samples from Trench 2, Motravulapadu.

Sample Code	Depth (cm)	Radionuclide activity				Equivalent doses				OSL age (ka)
		U (ppm)	Th (ppm)	K (%)	Total Dose rate [b,c] (Gy/ka)	No. of aliquots/ grains	Water content (%)	OD (%)	D_e (Gy)[d]	
MVP-T2-OSL 4	175	3.56±0.09	23.65±0.50	2.38±0.05	4.64±0.11	22/ ~120	15.64	13.44	135.80±4.56	**29.22±1.23**
MVP-T4-OSL 6	250	2.21±0.05	10.77±0.27	1.57±0.04	2.98±0.11	23/ ~120	13.89	9.79	101.21±2.62	**33.96±1.54**

[a] Radioactivity measurement made on a dried, homogenized and powered sample by HPG detector

[b] Includes cosmic-ray dose rate of 0.096 Gy ka^{-1}

[c] 12.5±0.5% and 200±20 ppm Rubidium (^{87}Rb) concentrations were used to estimate the internal dose rate

[d] after subtracting of a residual dose of 12 Gy

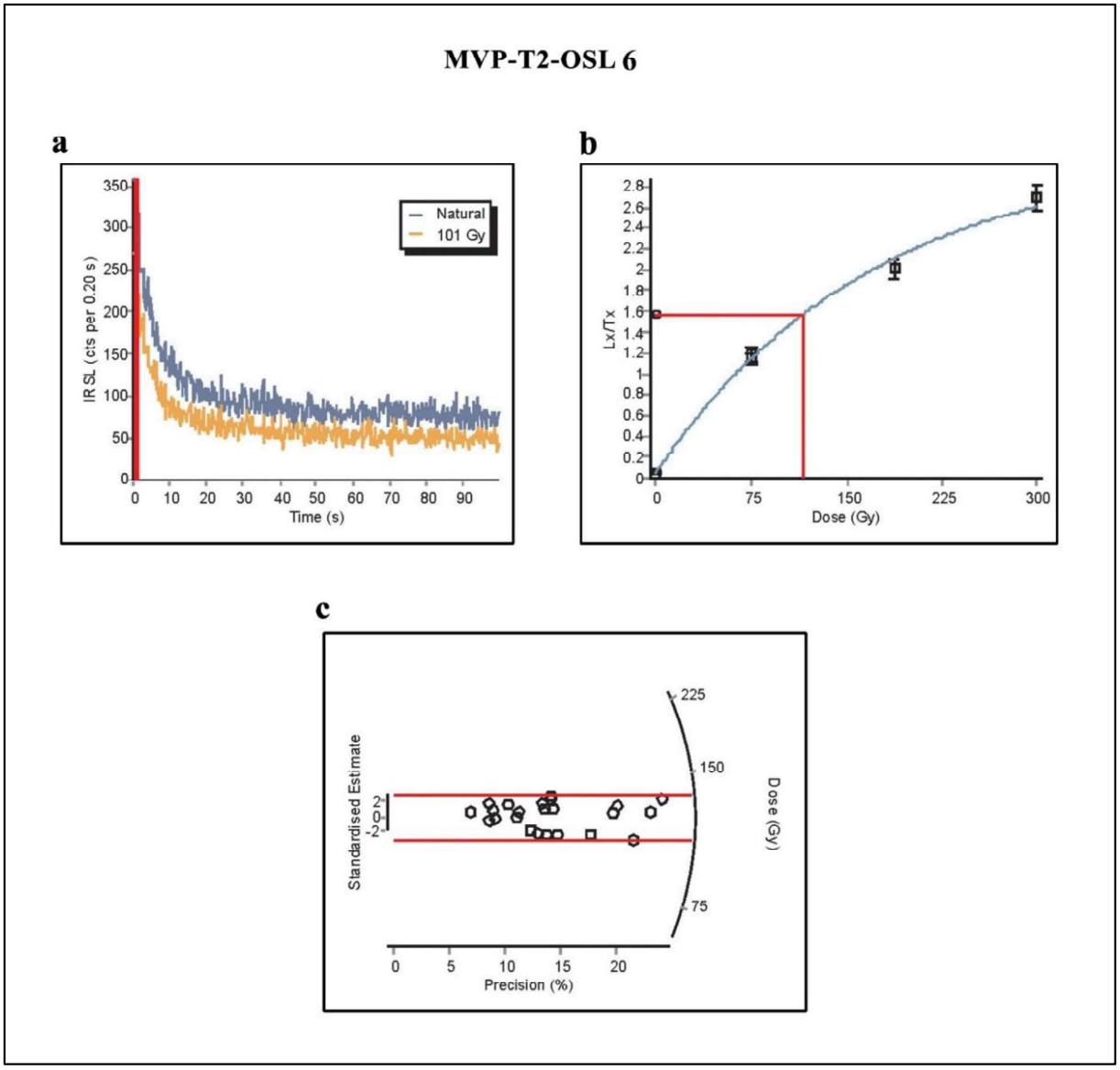

Figure. 4.8.23: Results of p-IR-IRSL analyses for sediment sample underlying the YTT horizon. a: typical feldspar shine down curve; b: typical growth curve; c: radial plot representing the estimated palaeodoses.

4.8.2.3 Summary

The YTT horizon identified in Trench 2 seems to be buried between 33 and 29 ka. Notably, the ash horizon is not considerably mixed with other foreign sediments before the burial, as indicated by the colour and composition. However, the ash horizon is discontinuing in the trench and appears to be present in lens. Probably the ash was redeposited consequent to a high energy fluvial action around 30 ka. But, in such scenarios mixing of other sediments along with the ash is expected which is not observed in this case. Further micrmorphological and site-specific geomorphological analysis are required to assess the depositional conditions of the YTT at Motravulapadu.

4.8.3 Trench 4

4.8.3.1 Stratigraphy

Trench 4 measures 2 m width (NE-SW) and 4 m length (SE-NW) and excavated up to a depth of 2.30 m. Two sedimentary Units were observed in the trench 4 excavations (Fig. 4.8.24). Unit 1 is brown coloured clay rich silty sediment of 0.55 to 0.60 m thickness with carbonate nodules. Unit 2 is light brown coloured silty sandy sediment with carbonate nodules increasing in numbers downwards. This Unit is of 1.70 m in thickness and the bottom of the Unit contains high percentage of moisture. Artefacts are found embedded at the top portion of the Unit 2, at the depth of 0.72 m from surface (datum point), and they continued to occur up to the depth of 96 cm. Artefacts are fresh in condition and through 2 mm sieve debitage less than < 1 cm was also recovered. Embedded in situ artefacts were observed within the Unit 2 (Fig. 4.8.25) and the artefact horizon is of 0.25 m.

Figure. 4.8.24: Trench 4: Sedimentary units and the location of luminescence samples and artefacts.

Figure. 4.8.25: In situ blade exposed during the excavation.

4.8.3.2 Luminescence Chronology

Four sediment samples were collected for luminescence age estimations; however, only two samples were processed. The samples named as MVP T4 OSL 2 and MVP T4 OSL 3 are collected at the depths of 0.70 m and 1.30 m respectively (Table. 4.8.8). The former sample directly overlies the artefact horizon, and the latter is at a depth of 0.35 m below the base of the artefact horizon. The two samples are therefore expected to provide the age range of the artefact horizon. Sample above the artefact horizon showed relatively high overdispersion and dated 30.7±1.9 ka and below the sample yielded an age of 29.3±1.2 ka (Fig. 4.8.26 and Fig. 4.8.27). Both ages are statistically indistinguishable indicating an age of 30 ka for the burial of artefact bearing horizon.

Table. 4.8.8: Dose rate data, D_e values and OSL ages for the sediment samples from Trench 4, Motravulapadu.

Sample Code	Depth (cm)	Radionuclide activity				Equivalent doses				OSL age (ka)
		U (ppm)	Th (ppm)	K (%)	Total Dose rate [b,c] (Gy/ka)	No. of aliquots/ grains	Water content (%)	OD (%)	D_e (Gy)[d]	
MVP-T4-OSL 2	70	2.31±0.04	15.62±0.25	2.33±0.03	3.72±0.11	23/ ~120	21.63	26.25	114.45±6.46	**30.73±1.96**
MVP-T4-OSL 3	130	2.73±0.06	17.6±0.33	2.54±0.04	4.20±0.11	23/ ~120	17.70	12.80	123.28±3.82	**29.33±1.21**

[a] Radioactivity measurement made on a dried, homogenized and powered sample by HPG detector

[b] Includes cosmic-ray dose rate of 0.096 Gy ka^{-1}

[c] 12.5±0.5% and 200±20 ppm Rubidium (^{87}Rb) concentrations were used to estimate the internal dose rate

[d] after subtracting of a residual dose of 12 Gy

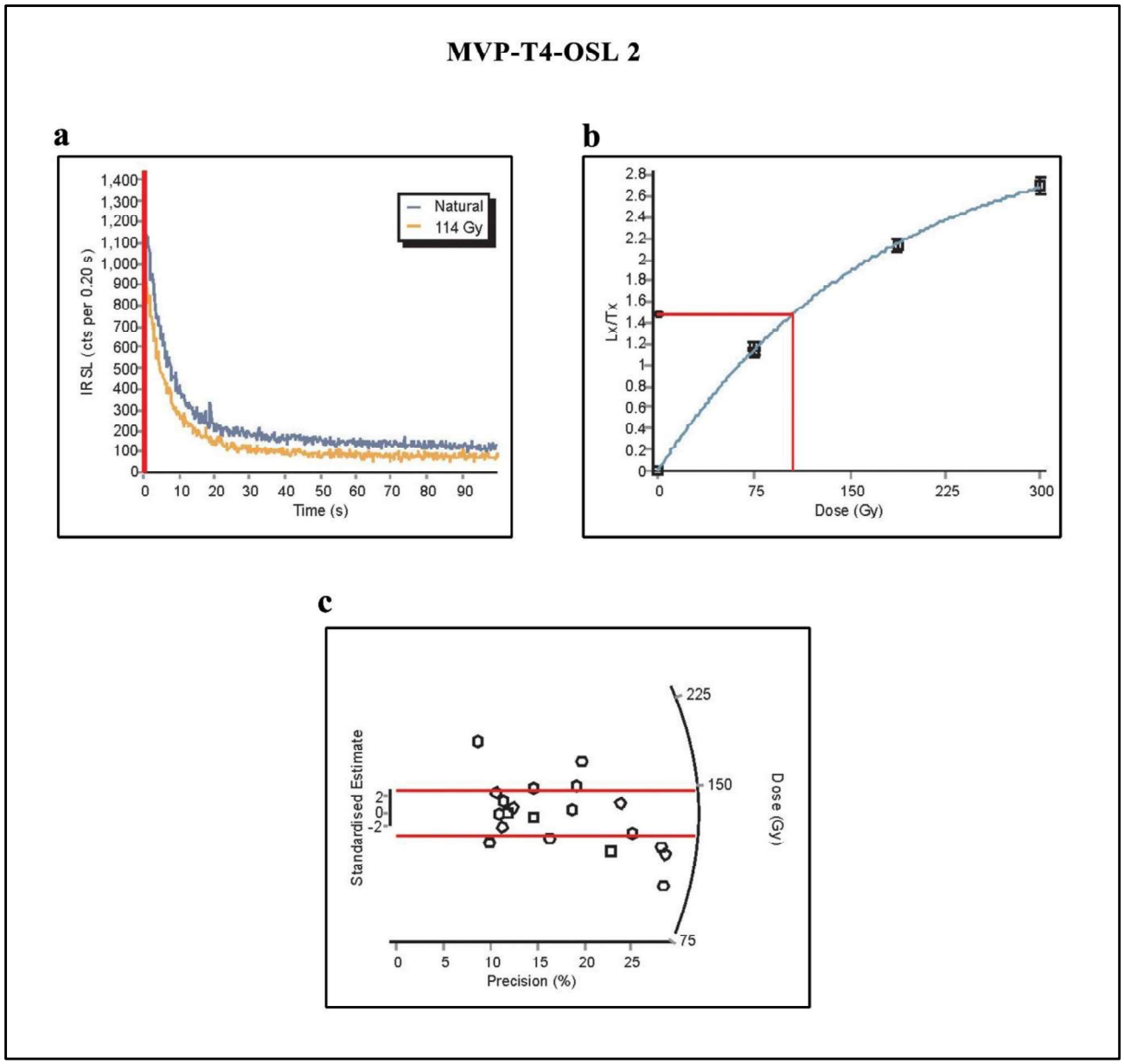

Figure. 4.8.26: Results of p-IR-IRSL analyses for sediment sample from Unit 2 above the artefact horizon. a: typical feldspar shine down curve; b: typical growth curve; c: radial plot representing the estimated palaeodoses

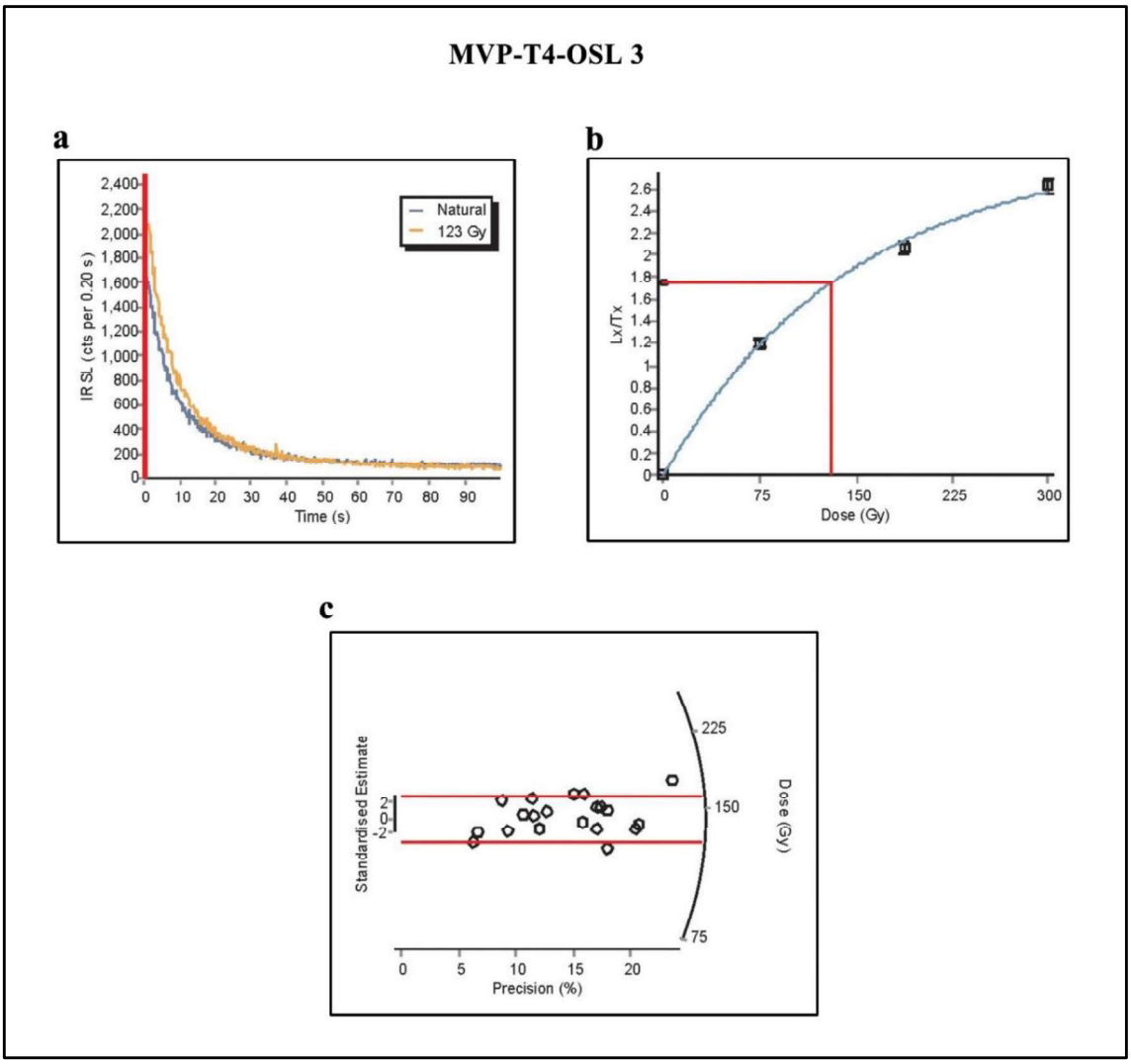

Figure. 4.8.27: Results of p-IR-IRSL analyses for sediment sample from Unit 2 below the artefact horizon. a: typical feldspar shine down curve; b: typical growth curve; c: radial plot representing the estimated palaeodoses.

4.8.3.3 Lithic Assemblage

A total of 155 lithics were recovered from a sedimentary volume of 2 cubic meter (2 x 4 x 0.25 m) in the Trench 4 (Table. 4.8.9). The of them (64.52%) are debitage, core preparation flakes, and flaked pieces. Most of the artefacts (71.23%) are without cortex and only the remaining 28.76% have just 20% or less cortex. The core assemblage consists of two specimens; one is a bidirectional blade core and the other a radial core. The blade core dimensions are 77.8x92.28x38.11mm (LxWxT) and its platform is faceted with a platform angle of 90 degrees (Fig. 4.8.28). The radial core dimensions are 57.92x71.84x30.89mm (LxWxT). Both the cores are made of fine grain quartzite available as pebbles in the adjacent riverbed of Manneru river and Nachu vagu stream. Rest of the core assemblage consists of eight core fragments and 3 manuports.

Table. 4.8.9: Composition of the assemblage from trench 4, Motravulapadu.

Type	Quantity	%
Core		
Blade Core	1	0.65
Radial Core	1	0.65
Core Fragments	8	5.16
Manuports	3	1.94
Total Cores	**13**	**8.39**
Retouched		
Retouched Broken Blade	1	0.65
Point	1	0.65
Total Retouched	**2**	**1.29**
Unretouched		
Blade	21	13.55
Cortical Blade	3	1.94
Core preparation flake	23	14.84
roughout flake	2	1.29
Eclat deborant	2	1.29
broken blade fragments	12	7.74
flaked piece	22	14.19
Debitage (<2 cm in length)	55	35.48
Total Unretouched	**140**	**90.32**
Total	**155**	**100**

Figure. 4.8.28: Cores from Trench 4. a: Blade core; b: Manuport.

The flake component forms 91.61% with both retouched and unretouched flakes. A total of 53 flakes (excluding debitage and flaked pieces) have been recorded in the assemblage, including 32 complete flakes. Limited typological diversity is evident amongst the flakes, with 15 blades, 13 core preparation flakes, two roughout flakes, 1 point and 1 platform rejuvenation flake. Among the 15 blades 3 cortical blades, 1 retouched blade and 11 blades of different stages of the blade core reduction sequence are present (Fig. 4.8.29 and Fig. 4.8.30). Notably, all the lithics from Trench 4 are products of the reduction of two pebbles only. This indicates the integrity of the site as primary context. Among the three cortical blades one has cortical platform and the two have prepared platforms. In addition, several broken blade pieces were observed in the assemblage probably due to intentional snapping of the blades.

The most common dorsal scar patterns present on complete flakes in the assemblage are weakly radial (48.1%) followed by proximal (33.3%) and radial (18.5%). Cortical coverage ranges from 0-100%, with 75.9% of flakes recorded with no cortex present, and 18.5% of flakes with less than 50% cortex present. Low frequencies of flakes with only cortical platforms (5.5%) and 100% cortical cover of dorsal and platform surface (7.4%) are observed.

Figure. 4.8.29: Blades in the assemblage. a and b: Cortical blade with cortical platform; c and d: Cortical blades with prepared platforms; d to f: Blades.

Figure. 4.8.30: Flakes and broken blades. A: Pointed blade; b: Point; c: Platform rejuvenation flake; d to i: Broken blades.

The majority of flakes (79.6%), present feather terminations followed by step (16.6%) and hinge (3.7%) terminations. Mean axial flake dimensions are 54.9 x 55.3 x 13.3 mm (Table. 4.8.10), and on average, flakes are as long as they are wide (mean elongation=1.2). A low number of blade proportioned flakes (n=6) are present, with a maximum elongation of 3.12. Typically, flakes are more than four times wide as they are thick (mean flatness=4.2), with the flatness ranging from 1.69 to 8.16. 66.6% of the flakes exhibit slightly expanding proximal margins (mean proximal shape=0.92), with a 33.3% of flakes exhibiting contracting proximal margins, leading to an upper proximal shape index of 1.16. In contrast, the distal shape indicates that 88.8% of the flakes exhibit contracting distal margins (mean=1.36).

Table. 4.8.10: Statistical data for flake attributes.

Attribute	N	Mean	SD	Min.	Max.
Length	32	47.63	21.01	20.49	99.03
Proximal Width	32	26.01	10.88	9.97	68.63
Medial Width	32	29.44	10.18	13.05	57.53
Distal Width	32	22.22	11.84	6.67	66.79
Medial Thickness	32	9.32	4.19	2.69	20.19
Elongation	32	1.80	0.76	0.43	3.92
Flatness	32	3.63	1.34	1.28	7.56
Proximal Shape	32	0.86	0.20	0.53	1.40
Distal Shape	32	1.76	0.92	0.74	5.25
Platform width	32	20.73	7.76	7.73	47.66
Platform Thickness	32	7.84	3.23	2.74	18.04
Platform area	32	205.60	149.78	37.62	689.49
Platform Angle	32	76.60	8.59	60.00	95.00
Dorsal scar count	32	2.68	0.92	1.00	5.00
No. Unidirectional arrises	32	1.28	0.86	0.00	3.00
No. Radial arrises	32	0.32	0.75	0.00	3.00

Single conchoidal platforms are the most common type (38.8%), followed by multiple conchoidal (29.6%) and cortical (14.8%), dihedral (11.1%) and punctiform (3.70%) types. Platform preparation is dominated by facetted platforms with 42.5%, followed by unprepared platforms (29.6%) and overhang removal (27.7%). A wide range in platform size is evident, with platform width ranging from 5.9 to 98.7 mm and platform thickness ranging from 3.9 to 28.1 mm. The platform shape index indicates that platforms are typically elongate (mean=3.41), with 88% of platforms being twice as wide as they are thick. A total of 37 artefacts that are categorised as flaked pieces are present, which bear no clear ventral morphologies or negative flake scars originating from the margins of the artefacts but have clearly undergone some reduction.

4.8.3.4 Summary

Trench 4 yielded blade-based assemblages associated with sedimentary contexts dated to 30 ka. Typo-technological aspects of the assemblage suggest that the site functioned as a production site mainly focused on the reduction of quartzite nodules/cobbles recovered from the stream bed of the adjacent Nachuvagu and Manneru. The presence of flakes and cores that are part of different stages of the lithic reduction sequence and high proportions of cortex on flakes and cores indicate the characteristics of a lithic production site. Further, none of the artefacts show any signs of abrasion, and no major edge damage patterns are observed. All these aforesaid observations indicate that the lithic assemblage analysed from Trench 4 is an *in-situ* assemblage associated with fine grain sediments.

It is obvious from the technological features of the assemblage at the site, the main objective of lithic reduction was to produce elongated flakes and blades. The presence of blade cores and the dorsal flake scar patterns on full flakes suggest that a unidirectional reduction seems to be the most preferred strategy at the site. Notably, the assemblage contains small portions of retouched artefacts; limited to one retouched broken blade and a point. The dearth of artefacts could be because of the limited excavation and small sample size. Therefore, increasing the sample size by further excavation may provide better insights into the retouched tool types of this assemblage. Overall, the assemblage from trench 4 indicates the practice of blade technology in the region at 30 ka.

4.8.4 Trench 5 (Fossil Trench)

4.8.4.1 Stratigraphy

Excavations at Trench 5 was conducted to understand the stratigraphic association of fossil remains exposed at the site. The excavation uncovered in situ fossil remains of a *Bos* sp. with articulated skeletal elements (Fig. 4.8.31). Stratigraphically, Trench 5 revealed three discrete Units (1, 2, and 3) and the fossils were identified within Unit 3 (Fig. 4.8.32). Unit 1 comprises of coarse material consisting of redeposited carbonate nodules and artefacts of undiagnostic character. Unit 2 is silt dominated sediment with carbonate nodules and of having a ~60 cm thickness. Unit 3 is of brown coloured organic-rich silty sediments of 1 m thickness. Excavations were stopped after reaching 2 m depth. Fossil remains were observed to be associated with Unit 3. Similar stratigraphic associations between fossils and Unit 3-like sediments were noted from two test pit as well (Fig. 4.8.33).

Figure. 4.8.31: In situ and articulated skeletal remains of *Bos* sp.

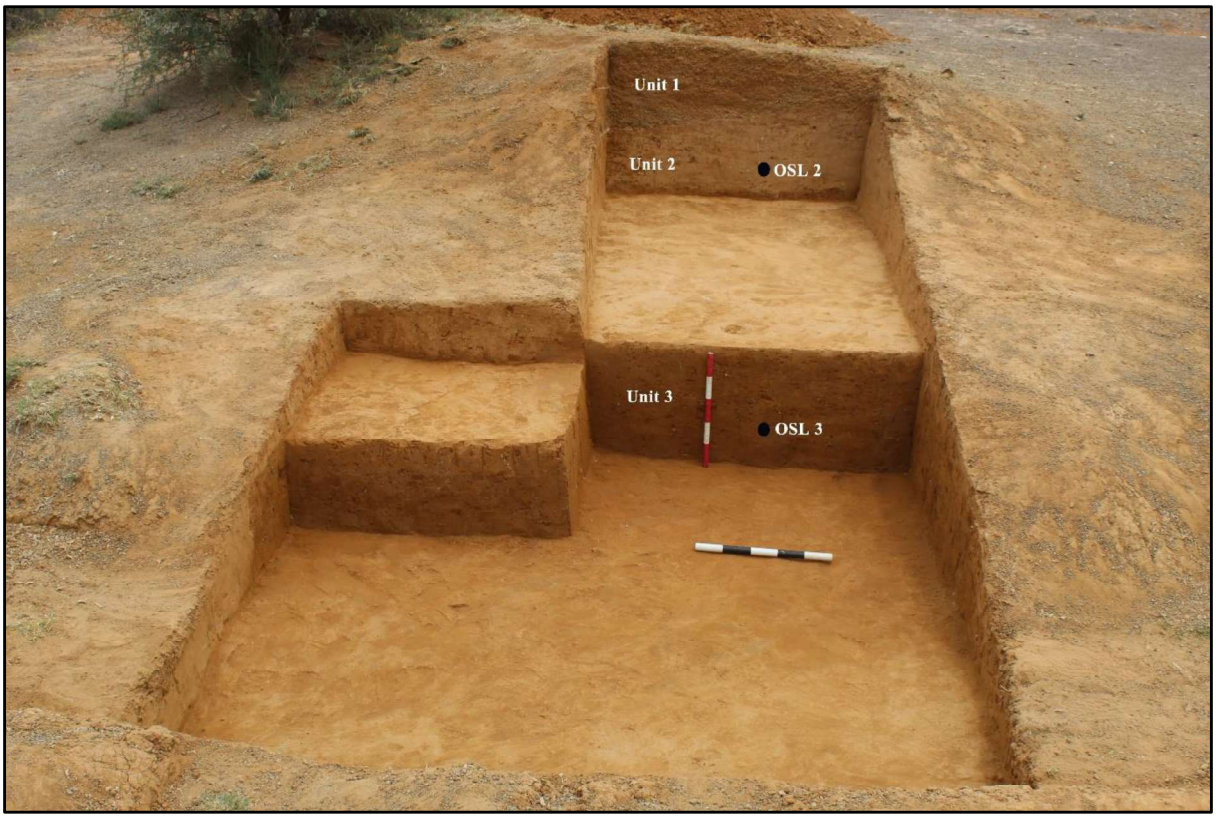

Figure. 4.8.32: Stratigraphy and position of the sediment samples used for Luminescence age estimations.

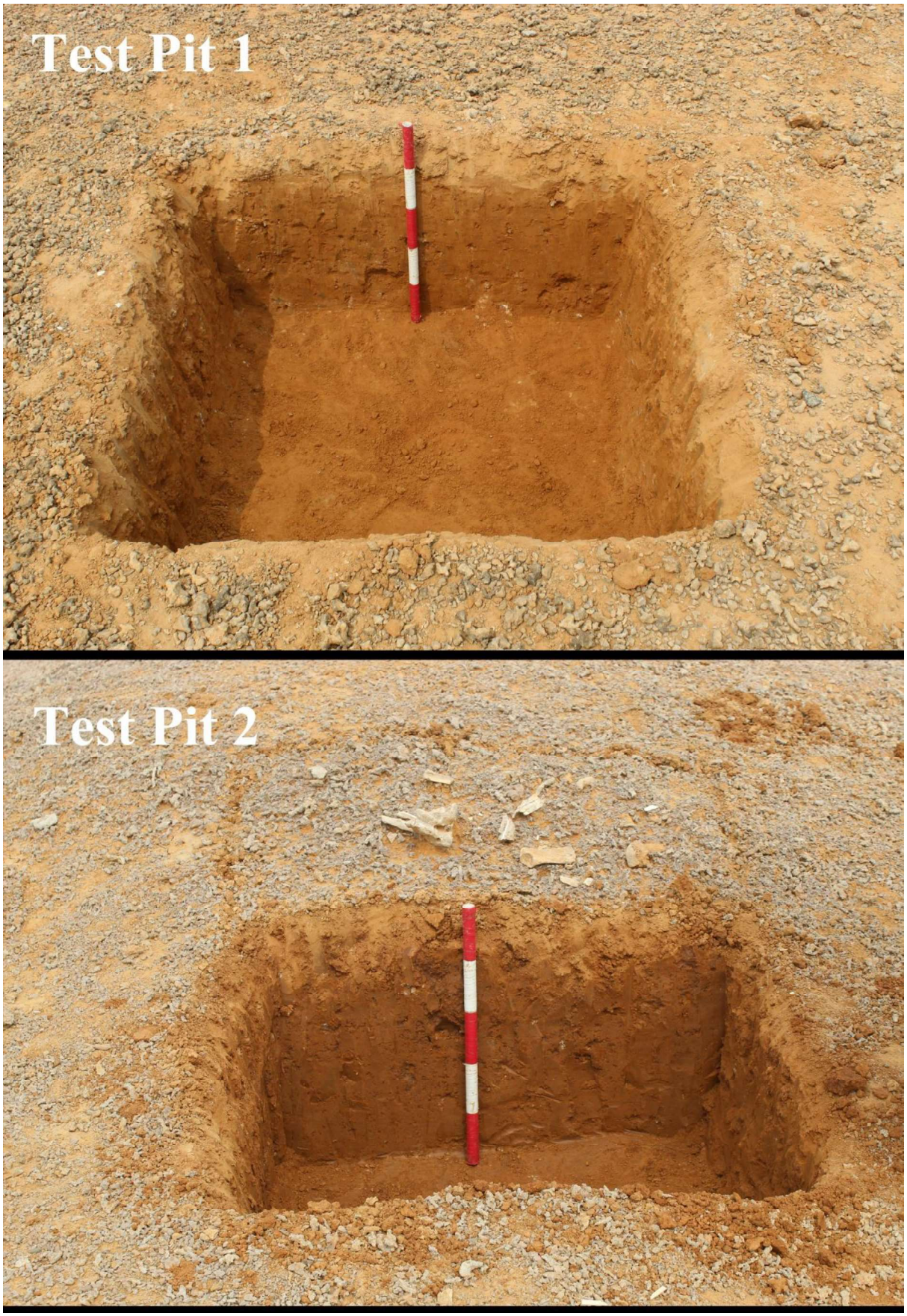

Figure. 4.8.33: Test pits excavated below surface exposures of fossil remains.

4.8.4.2 Luminescence Chronology

Two sediment samples were collected underlying and overlying the fossil remains to estimate the age of burial of the faunal remains. Both the samples showed less overdispersion values suggesting good bleaching of the samples (Fig. 4.8.34 and Fig. 4.8.35). The sample underlying the fossil horizon yielded an age of 45 ka and the overlying Unit 39 ka (Table 4.8.11). Both these ages are statistically indistinguishable, and the fossil remains were buried around the time of 42 ka.

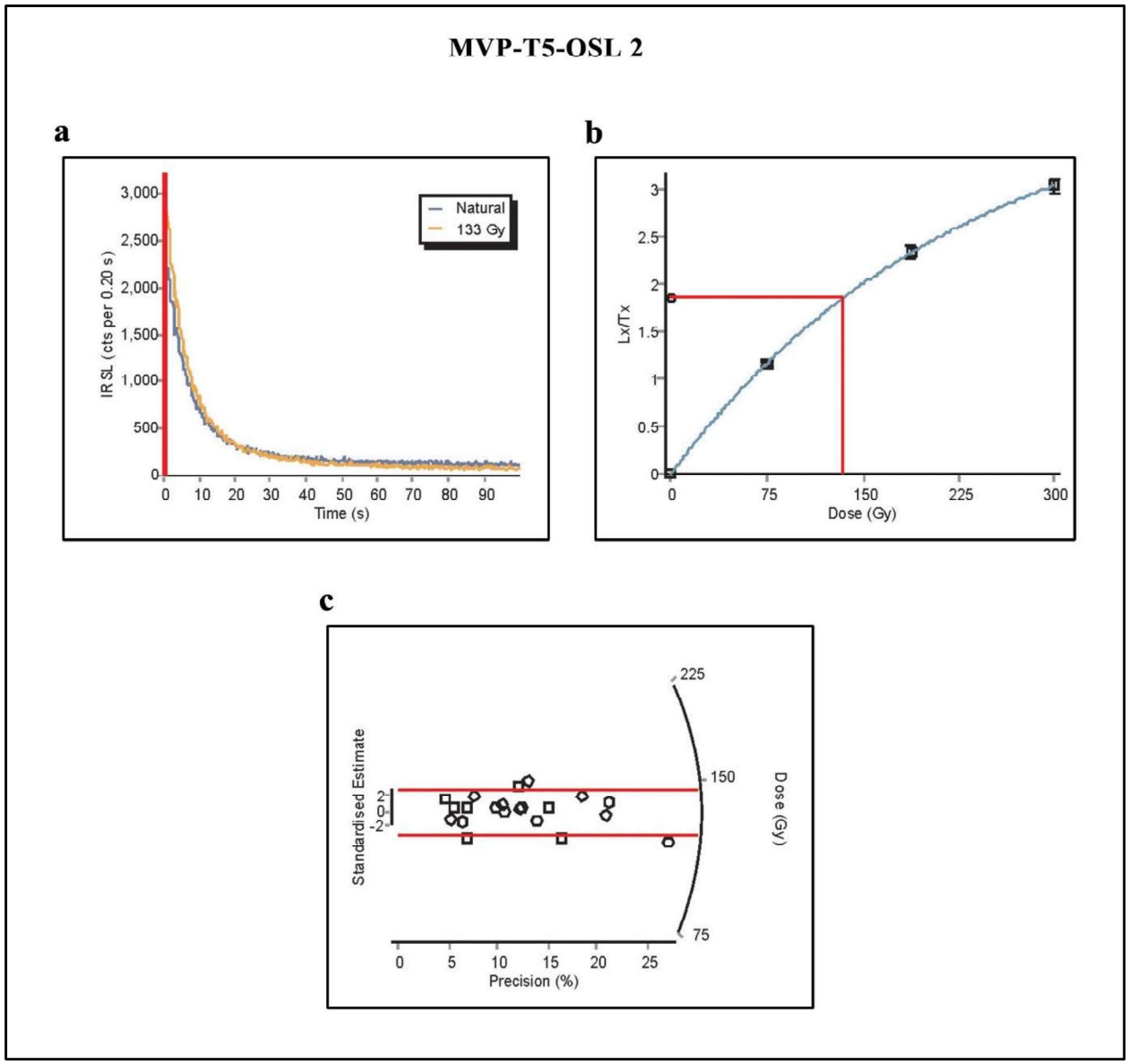

Figure. 4.8.34: Results of p-IR-IRSL analyses for sediment sample from Unit 2 above the fossil horizon. a: typical feldspar shine down curve; b: typical growth curve; c: radial plot representing the estimated palaeodoses.

Table. 4.8.11: Dose rate data, D_e values and OSL ages for the sediment samples from Trench 4, Motravulapadu.

Sample Code	Depth (cm)	Radionuclide activity				Equivalent doses				OSL age (ka)
		U (ppm)	Th (ppm)	K (%)	Total Dose rate [b,c] (Gy/ka)	No. of aliquots/ grains	Water content (%)	OD (%)	D_e (Gy)[d]	
MVP-T5-OSL 2	72	2.44±0.07	13.99±0.37	2.17±0.05	3.38±0.11	24/ ~120	26.99	12.90	133.49±4.39	**39.37±1.85**
MVP-T5-OSL 3	132	1.91±0.05	8.89±0.23	1.49±0.03	2.57±0.10	15/ ~120	22.95	12	118.52±4.60	**45.99±2.64**

[a] Radioactivity measurement made on a dried, homogenized and powered sample by HPG detector

[b] Includes cosmic-ray dose rate of 0.096 Gy ka^{-1}

[c] 12.5±0.5% and 200±20 ppm Rubidium (^{87}Rb) concentrations were used to estimate the internal dose rate

[d] after subtracting of a residual dose of 12 Gy

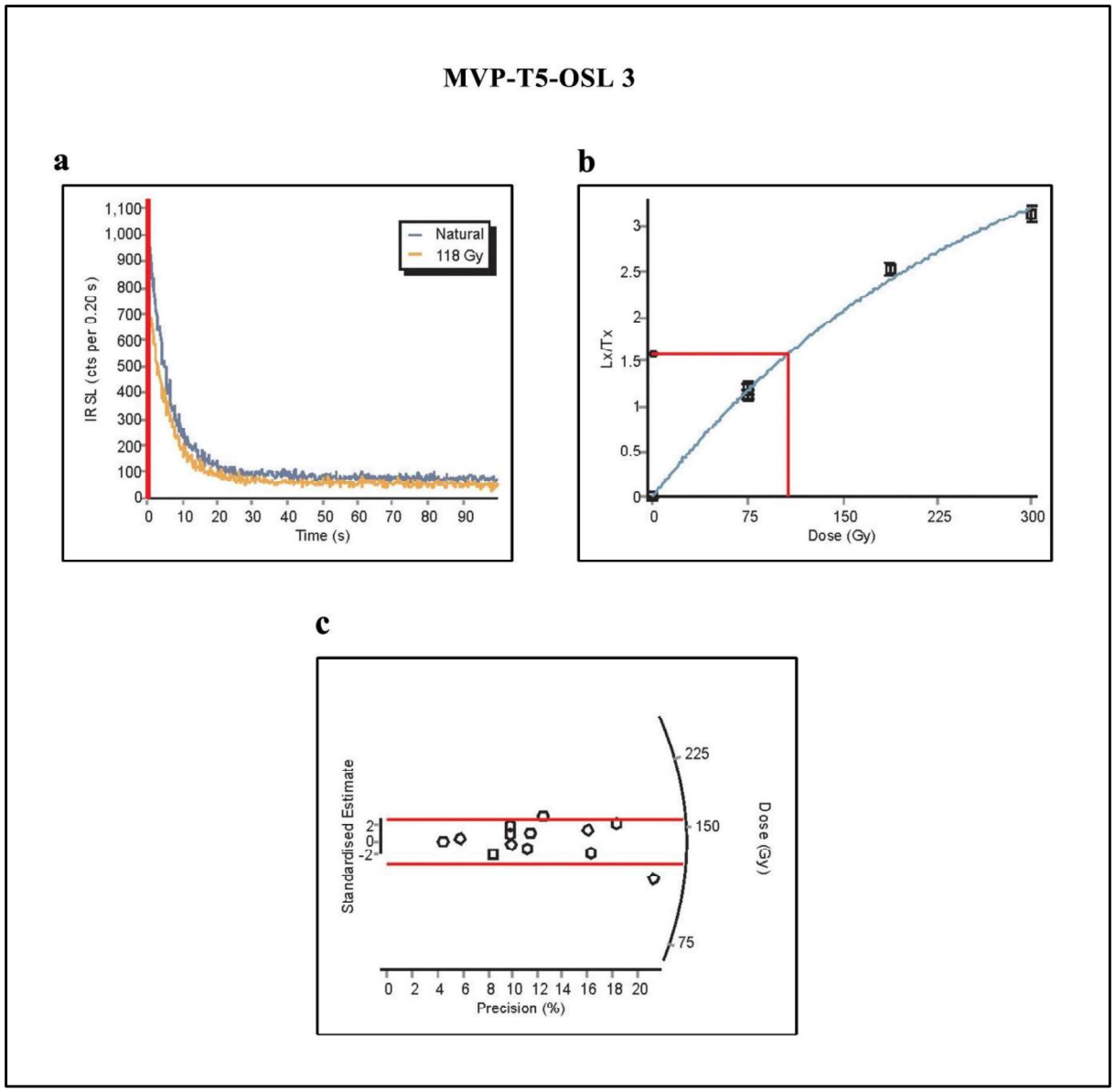

Figure. 4.8.35: Results of p-IR-IRSL analyses for sediment sample from Unit 3 below the fossil horizon. a: typical feldspar shine down curve; b: typical growth curve; c: radial plot representing the estimated palaeodoses.

4.8.4.3 Uranium-Series Chronology

A few samples of the surface collected teeth were analysed to extract the U-series ages (Table. 4.8.12). The dating was conducted at Australian Research Centre for Human Evolution (ARCHE), School of Humanities, Languages and Social Sciences, Griffith University, Australia. Six teeth samples belongs to three different species were processed for the age calculations.

Teeth were sectioned to expose dental tissues using a diamond blade-rotating saw with a thickness of 300um. Measurements were obtained by laser ablation, using an NW213 ESI laser coupled to a MC-ICPMS Neptune XT at Southern Cross University, GARG facility. Several areas for each samples were analysed using the LA-MC-ICPMS setting with 750microns rasters using a 110um spots size at a 5micron per second translation speed and a fluence of ~4.88J.cm^2. Concentration and isotopic ratio for the enamel were measured several parts of the dentine and the enamel. Values are averaged for each rasters, then average for each dental tissue. Baseline and drifts were corrected using NIST 610 and 612 glass standard, while two corals as well as a fossil Rhinoceros tooth were used to correct $^{234}U/^{238}U$ and $^{230}Th/^{238}U$ ratios and assess the accuracy of measurements.

Table. 4.8.12: U-series age for the six teeth samples collected from surface.

Sample Code	Species	U/Th	R 34/38	Err (2s)	TR 30/38	Err (2s)	Age (ka)	Err (2s)
MVPF42	*Equus nomadicus*	12	1.777	0.044	0.886	0.105	71	11.49
MVPF43	*Equus nomadicus*	1963	1.979	0.047	1.283	0.081	102.47	10.66
MVPF75	*Antelope cervicapra*	57680	2.086	0.035	1.187	0.042	84.14	4.68
MVPF106	*Sus scrofa*	15153	1.99	0.01	0.983	0.014	69.65	1.37
MVPF107	*Sus scrofa*	135460	1.988	0.007	0.568	0.009	35.62	0.65
MVPF117	*Antelope cervicapra*	26076	1.966	0.006	0.643	0.009	41.78	0.71

The U series ages of animal teeth samples forms three temporally distinct clusters 1) 102-84 ka; 2) 71-69 ka; 3) 41-35 ka indicating three distinct horizons of fossil beds spanning Late Pleistocene epoch. However, the samples are collected from exposed surfaces, there are a few issues associated with the sample processing concerning the contamination and diagenesis of the samples. Besides, since U-series date accounts only the minimum age, the samples are at least that much old and could in fact be older. Further, luminescence ages can corroborate the U-series ages for cross checking the date. However, U-series ages suggests that at Motravualapdu there are fossil horizons that are as old as 120 ka or older than this age. Luminescence age from the Trench 5 indicates fossil remains dated to 40 ka suggesting at least two temporally separable fossil horizons at the site.

4.8.4.4 Taxonomy

A total of 383 vertebrate fossil specimens had been collected from the site Motravalupadu. The 310 specimens were collected from the surface (seven clusters), while 73 specimens were recovered in the excavation from Trench 5. Specimens from the surface collection represent eleven taxa.

1. *Equus* c.f. *E namadicus* (extinct horse)
2. *Bos namadicus* (extinct cattle)
3. *Sus* sp. (Pig)
4. *Cervus* sp. (Deer species)
5. *Axis axis* (spotted deer)
6. *Antilope cervicapra* (blackbuck)
7. *Gazella gazella* (chinkara)
8. *Varanus* sp. (Monitor lizard)
9. *Trionyx* sp (Common softshell turtle)

Specimens from the Trench 5 represent a few postcranial skeletal elements, some of them in articulate position, of *Bos* sp. In the surface exposure, the number of identified postcranial specimens are 65 and the cranial specimens are 57, representing various taxa. Half of the specimens (188) among the total sample, are long bone fragments that are only preserved less than one-fourth of the whole representing the shaft portion. Specimens of vertebrae and ribs dominate in the postcranial category of fossils collected from the surface. Scapulae (n=11) of different species were the second highest among the recovered elements, which showed an abundance of the distal portion with medium to high encrustation. There are 6 specimens of tibia; all of which are unique and belong to six different taxa ranging from *Bos sp.*, antelopes and other species of medium artiodactyls. In each specimen only the distal portion was recovered, some long portions of the shaft and some without it. A total of 14 phalanges were recovered. Long bones including 3 radius, 2 ulnae, 10 femur, 2 humerus, 3 metatarsal, 2 metacarpal, 2 astragalus, and 3 metapodial were identified in the faunal assemblage (Fig. 4.8.36). Cranial specimens recovered from surface exposure indicate maximum preservation of ramus (15), and mandibles (11), of different taxa (Fig. 4.8.37 & Fig. 4.8.38). The collection included several isolated specimens of tooth (n=21), a rather well preserved horncore of blackbuck (*Antelope cervicapra*), and 5 specimens of cervid antlers.

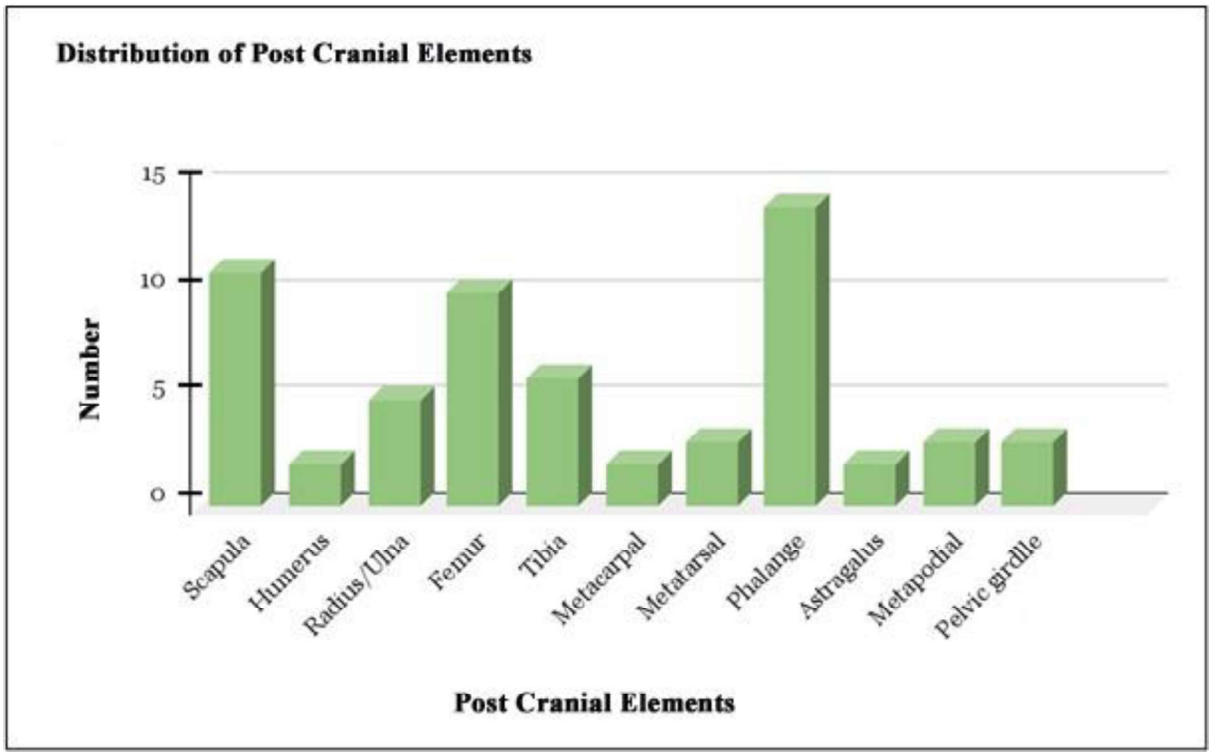

Figure. 4.8.36: Postcranial elements from surface collection.

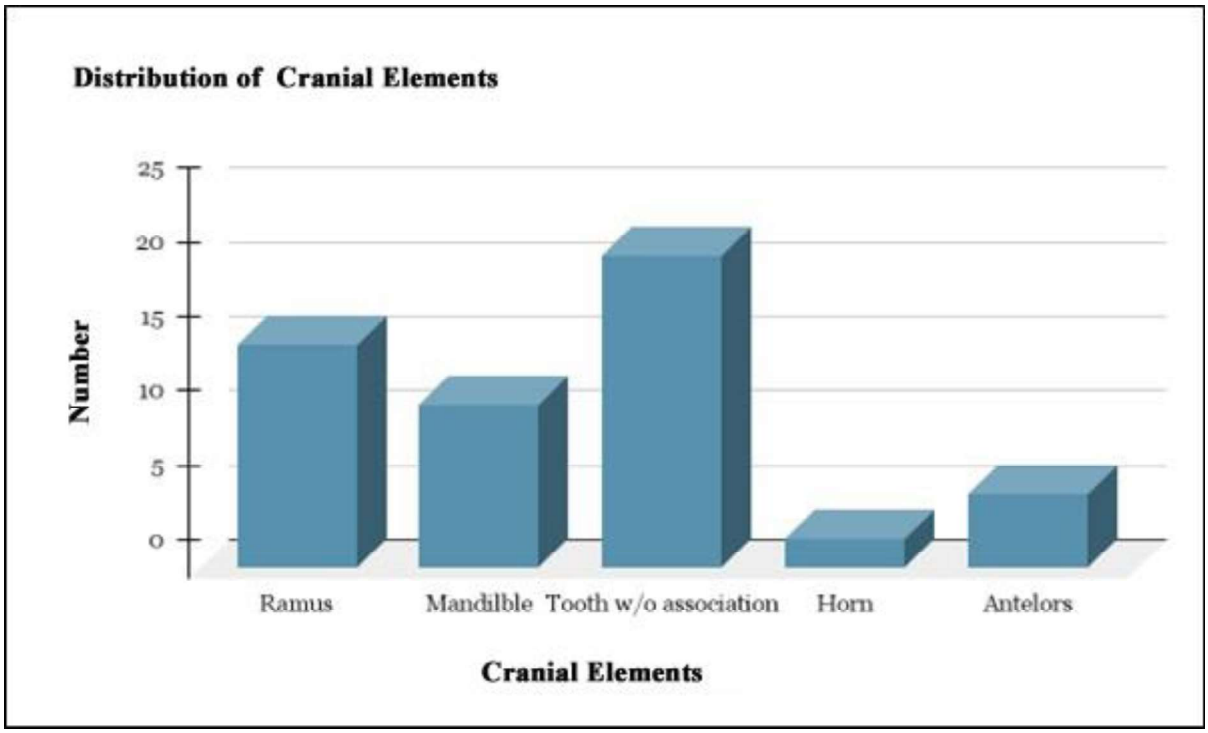

Figure. 4.8.37: Cranial elements from surface collection.

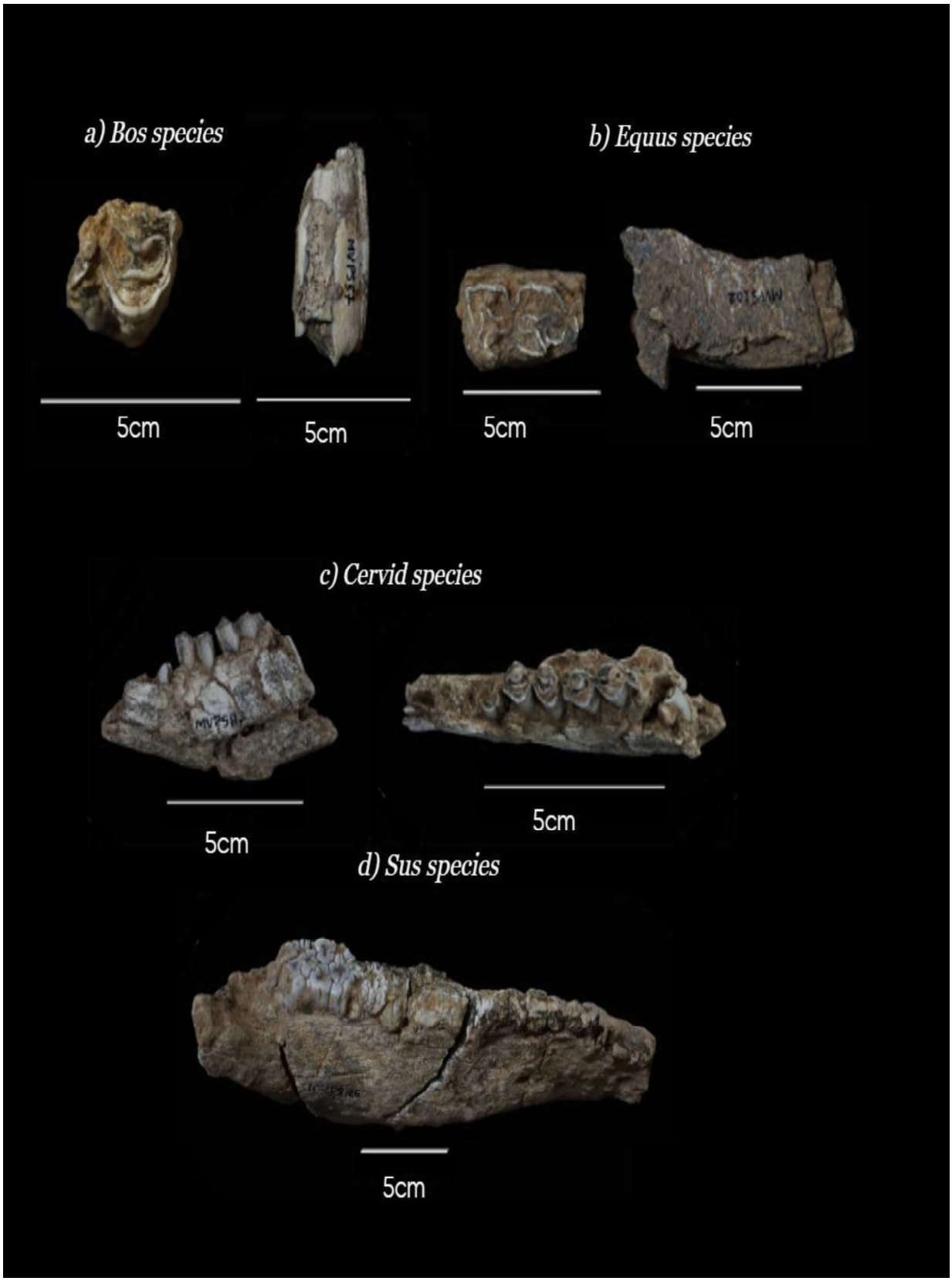

Figure. 4.8.38: Cranial elements from surface collection.

Further, the comparative taxonomic study of the specimens from cranial and postcranial suggests that both categories represent the presence of similar species. The majority of the long bone fragments and unidentified specimens were classified into mammalian taxonomy 21, for the lack of diagnostic features. Large bovines 7, small bovids 19, Large bovids 5, Large Artiodactyla 2, Small Artiodactyla 2, *Bos* sp 9, *Equus sp* 14, *Antelope cervicapra* 27, *Cervus* sp. 10, *Sus sp.* 2, *Varanus salvator* 1, *Bubalus bubalis*, Tortoise 1, *Trionyx* sp. 1 (Fig. 4.8.39). Two specimens with unfused epiphyseal ends in the fossil collection are of young cattle (*Bos* sp.). Other than this, epiphyseal fusion is visible in 7 specimens.

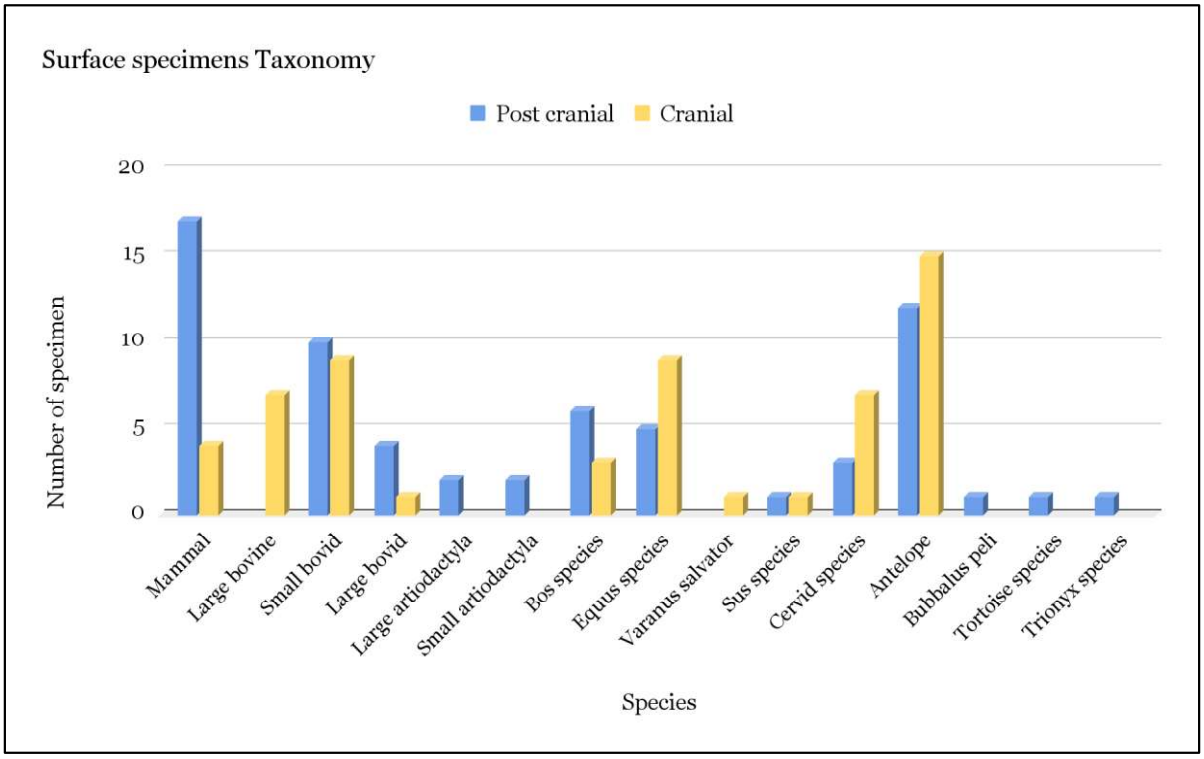

Figure. 4.8.39: Taxonomy of the surface collected fossil remains.

Almost all the specimens from trench 5 are of Bos species. Out of a total of 73 specimens, 59 of the elements were identified as postcranial (Fig. 4.8.40). The excavated specimens from the Trench 5 indicated high preservation of vertebrae and ribs. They also showed one humerus and a femur preserved intact with their respective lower articular elements: the radius, ulna, and metacarpal (with the humerus); and calcaneus, navicular, metapodial, and phalanges (with the femur). Except for phalanges and metapodials, which are relatively intact, all other specimens are fragmented skeletal elements.

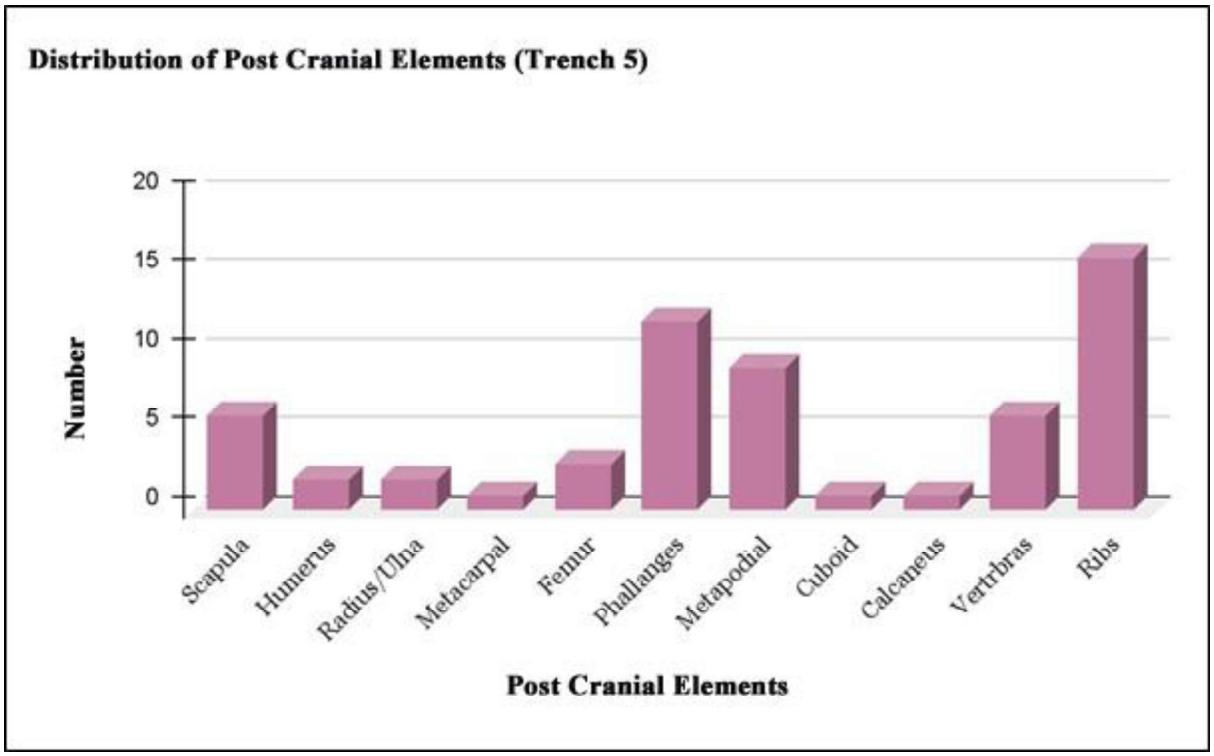

Figure. 4.8.40: Identified specimens from trench 5.

4.8.4.5 Summary

Postcranial elements – especially limb bones, vertebrae, and ribs – outnumber other skeletal elements in the fossil collection from Motravulapadu. Cranial elements are very rare in the collection. There are a few isolated teeth and a few complete mandibles with teeth preserved, allowing age estimation based on dental wear. Most of the limb bones are represented either by the diaphysis or the proximal and distal ends. Epiphyseal fusion indicates unfused or just fused state, suggesting young and subadult population (though there are a few adults too). Surprisingly, gastropods are conspicuously missing in the assemblage. As far as the status of preservation is concerned, the fossil assemblage represents predominantly incomplete skeletal elements, which also includes tiny skeletal and taxonomically unidentifiable splinters. Generally, all the bones are found to have covered with a thin film of calcretised fine sediments. Many have a thick coat of it, which persisted despite the protocol of sample processing using mild acid and water treatment. The long bones mostly do not have proximal and distal ends, and the diaphyses often show weathered surfaces. Out of four important taphonomic modifications which influence the information loss prior to burial, viz. weathering, abrasion, trampling bone breakage (biologically or naturally induced) and bioturbation; weathering is the most common factor that has impacted the assemblage. The horizontal deeper cracks or loss of ramus corpus, deep cracks along the vertical axis of long bones sometimes leading to breakage,

disappearance of proximal and distal ends of adult or just fused long bones, *in situ* breakage and yet the intact state of shafts, differential degree of pulverisation clearly indicates that the carcasses were exposed to prolonged sub aerial exposures before its final burial into the sediments. The weathering stages range from 3 to 6, which are adequate to impact the completeness of the assemblage. Interestingly the abrasion by fluvial currents is moderate to dismal. It is possible that the carcasses have been away from the water bodies for a longer period and hence post weathering fluvial dispersal may have compounded the completeness of the fossil record. However, the fluvial dispersal of select skeletal elements too can be attributed to the hydrodynamic sorting prior to burial and fossilisation. There are a couple of radii, femora and humerii whose shafts have spiral to oblique breakage that hints at carnivore or any intentional breakage. However, this is open to revision in the face of the fact that the present assemblage is a tiny representation of the entire skeletal material that awaits further excavations at the site. The absence of freshwater molluscs or the terrestrial snails' points to the lack of standing water bodies which are invariably preferred habitats of these animals. Their absence makes the sedimentological analysis imperative to better understand the deposition and burial history of the skeletal elements. Voohries' perspective of fluvial sorting based on the small but diverse collection suggest that large elements are lesser compared to the transportable ones. However, the weathered state of the material shows that perhaps most of the information losses may have occurred before the bones moved into the lithosphere. Lack of transportation and the localised nature of fragmentation may suggest the semi-primary context of their occurrence. Future excavations and detailed field taphonomy complimented by bone microstructure (process of fossilisation and diagenesis) will help explain the life histories of the fossils.

4.9 Ardhaveedu

Ardhaveedu (15°41'15.10" North latitudes 78°56'51.54" East longitudes) is located on the left bank of the stream Jampaleru, which originates from the Nallamalai hills and drains into Cumbum lake. (Map. 4.9.1). The stream Jampaleru is a seasonal river having a length of 32 km and flows parallel to the inter ridge valley formed between the Erra Konda and the Bhairavuni Konda hills. The physiography of the upper reaches of the Gudlakamma river basin is controlled by lithology, with quartzite forming long ridges and domes, whereas slates and phyllite occupy plains and inter-ridge valleys. The area falls in the zone of semi-arid tropics with an average rainfall of 60-75 cm/annually. Previous studies in the region by (Issac, 1960; Kumari, 1987)had reported Lower and Middle Palaeolithic sites. The region shows a rugged landscape mostly occupied by hill ridges and shallow depressions along Gundlakamma and its tributaries. These shallow depressions undergo erosional activities at several places through rill and sheet erosions exposing thick sections and artefact-bearing horizons.

The site occupies an area of 48,000 sq. m (300x160m) with several artefact clusters exposed due to rill and sheet erosion. Thirty-one such clusters were identified (Map. 4.9.2), and at a few places, artefacts embedded within the sediments were found in situ. At one such place, small-scale excavations were conducted with a view of unearthing the complete stratigraphy of the depositions that occurred at the Site. Explorations along the upper reaches of Gundlakamma and the stream Jampaleru resulted in identifying 11 sites with blade-based assemblages (Anil et al., 2022). Sediments associated with these assemblages are found to be uniform throughout the region. Notably, at two sites, Vemulapeta and JP Cheruvu, YTT deposits were found underlying the sediments mentioned above. Preliminary analyses of the lithic assemblages from all these 11 sites showed close similarities in technology and typology. In a few places, the sediment is as thick as 5 to 6 m suggesting a long deposition duration.

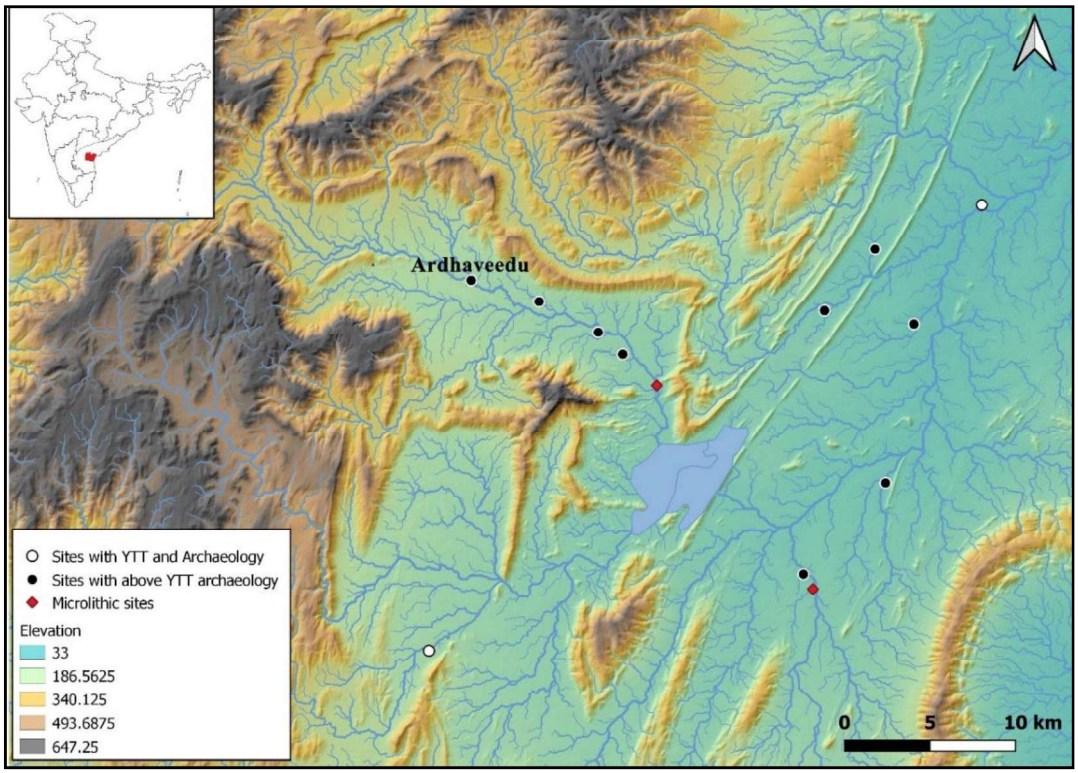

Map. 4.9.1: Map Showing the Location of The Site Ardhaveedu and other Palaeolithic sites in the upper reaches of The Gundlakamma River basin, Andhra Pradesh, India.

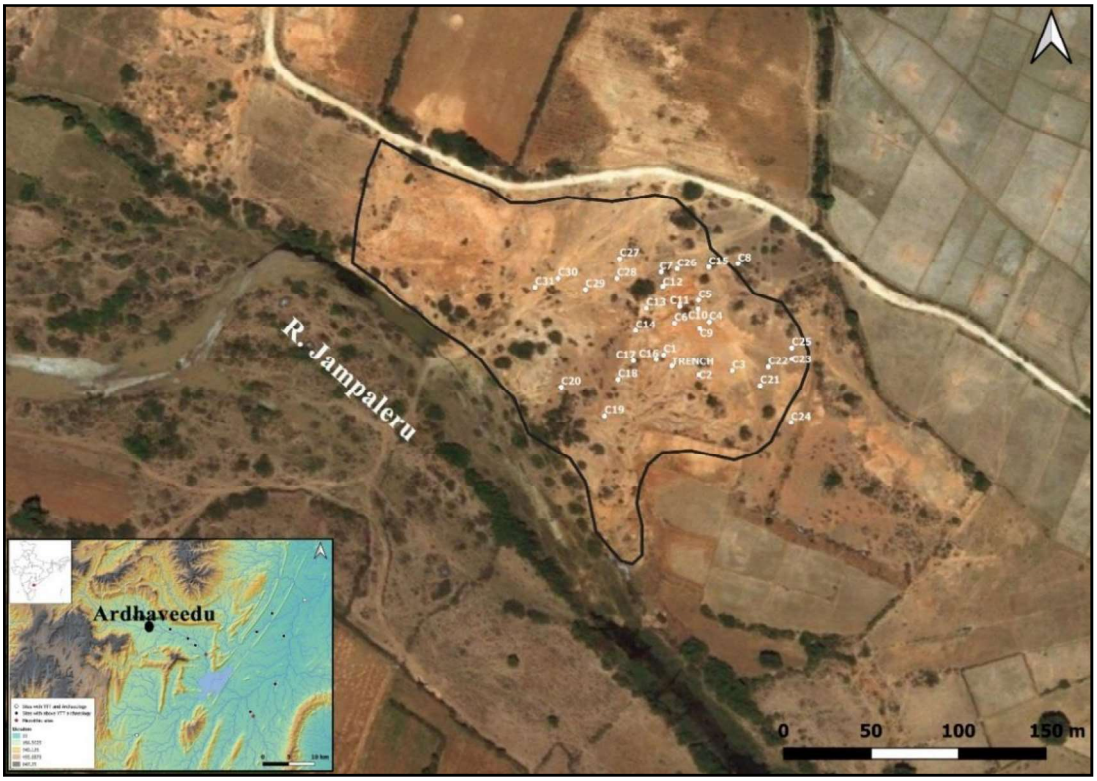

Map. 4.9.2: Distribution of artefact clusters at Ardhaveedu.

4.9.1 Stratigraphy

Excavations are conducted at artefact clusters exposed by rill erosion and at one of the sedimentary sections exposed by channel erosion to better understand the stratigraphic context of the artefacts. A 2x2 m trench was laid out and excavated to the depth of 70 cm, where the artefact concentration was decreased and became absent (Fig. 4.9.1). At a depth of 45 cm from the surface, artefact presence was observed and continued till the depth of 70 cm. Below the depth of 70 cm, the excavations were limited to a 1 m wide area on the eastern side of the trench, and there it continued to a depth of 165 cm. No artefacts were found below 70cm from the top and up to 165 cm.

Figure 4.9.1: Excavated trench at the site of Ardhaveedu.

Excavations have identified five distinct sedimentary Units of fluvial nature (Fig 4.9.2). Unit 1 consists of fluvially deposited sand with root casts and insect burrows. Unit 2 is of 10 cm thick palaeosol containing small-sized river pebbles. This palaeosol is underlain by ~ 40 to 30 cm thick silty-clay Unit and contains Palaeolithic artefacts (Fig. 4.9.3). Unit 3 contains calcrete deposits which were also observed on the artefact exposed on surfaces, suggesting that the artefacts are in situ within the Unit. Units 4 and 5 are brown-coloured clay-rich deposits devoid of any cultural material.

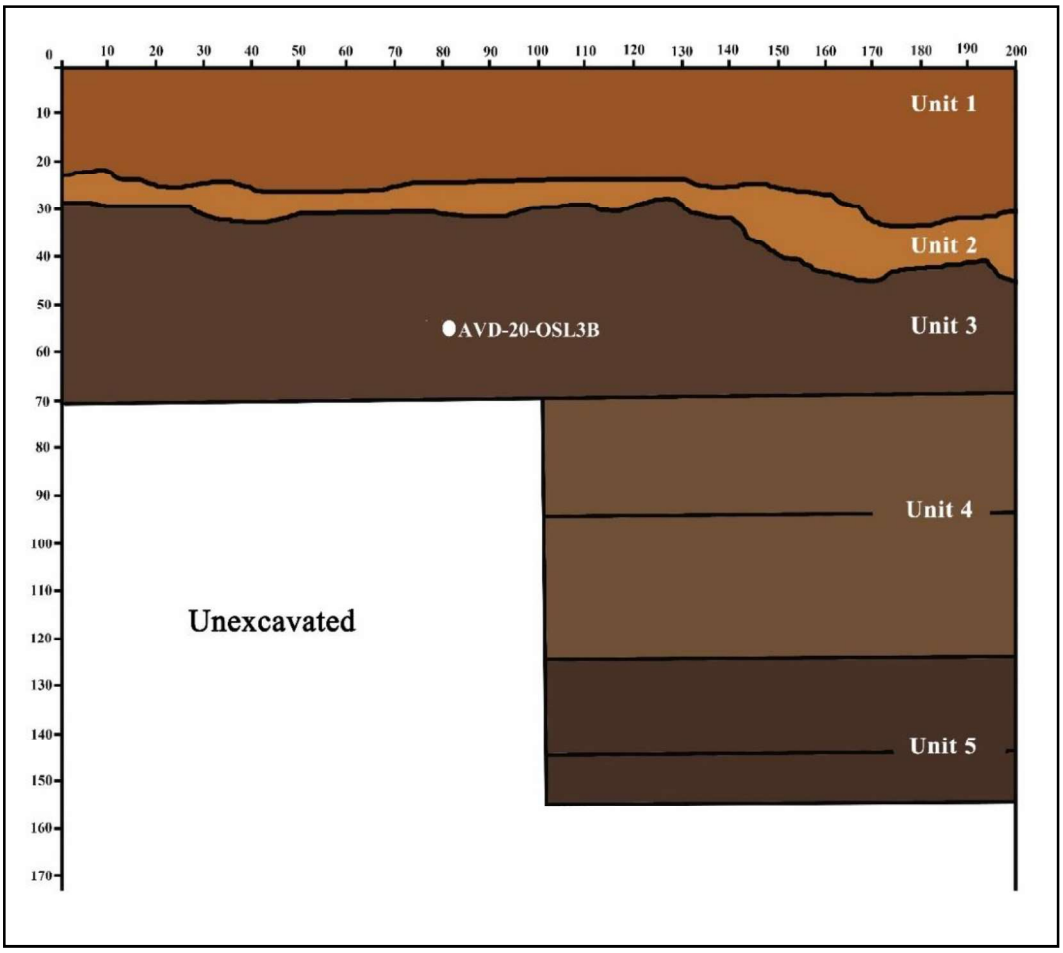

Figure. 4.9.2: Schematic sketch of the trench at Ardhaveedu.

Figure. 4.9.3: Artefact exposures within Unit 3. Black circles indicate the location of artefacts.

4.9.2 Luminescence Chronology

One sample, AVD-20-OSL 3B, from the Unit 3 at a depth of 55 cm was dated using the p-IR-IRSL method, which yielded an age of 41.2±3.1ka (Table 4.9.1). The sample from the Unit 3 showed less overdispersion value, suggesting well bleaching of the sample before burial (Fig. 4.9.4). Fading measurements do not show any significant fading of the p-IR-IRSL signal.

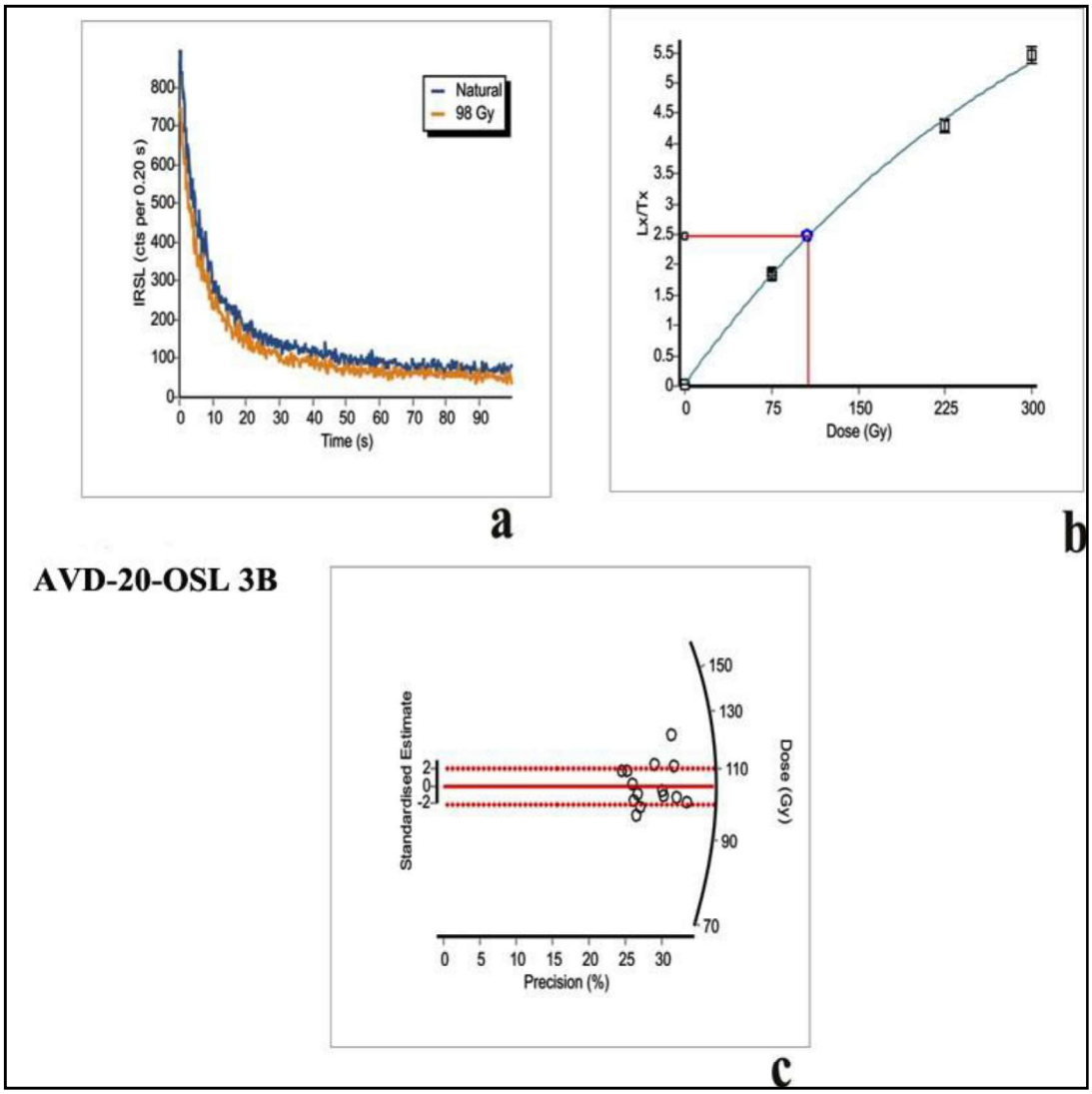

Figure. 4.9.4: Results of p-IR-IRSL analyses for sediment sample from Unit 3. a: typical feldspar shine down curve; b: typical growth curve; c: radial plot representing the estimated palaeodoses

Table 4.9.1: Dose rate data, D_e values and OSL ages for the sediment sample from the Site Ardhaveedu.

Sample Code	Depth (cm)	Radionuclide activity[a]				Equivalent doses				OSL age (ka)
		U (ppm)	Th (ppm)	K (%)	Total Dose rate[b,c] (Gy/ka)	No. of aliquots / grains	Water content (%)	OD (%)	D_e (Gy)[d]	
AVD-20-OSL 3B	55	2.6±0.3	6.5±1.2	0.9±0.06	2.4±0.2	14/ ~100	17	7.5	98.2±0.9	**41.2±3.1**

[a] Radioactivity measurement made on a dried, homogenized and powered sample by gamma-ray spectrometry and alpha counting.

[b] Includes cosmic-ray dose rate of 0.142 Gy ka^{-1}

[c] 12.5±0.5% and 200±20 ppm Rubidium (^{87}Rb) concentrations were used to estimate the internal dose rate

[d] after subtracting a residual dose of 20 Gy

4.9.3 Lithic Assemblage

The trench has yielded 95 artefacts that are not diagnostic enough to understand the lithic technology at the site. A grid measuring 7 x 6 m (42 m^2 area) was laid out at about 25 m northwest of the trench to increase the lithic sample size. Excavations at the site revealed the presence of a single artefact-bearing horizon, which was confined to a small area within the Unit 3. It is, therefore, reasonable to assume that the surface-exposed artefacts at Ardhaveedu are eroding from the Unit 3 sediments. Hence, the artefact assemblages from the trench and the grid were treated as a single assemblage. A total of 418 artefacts were collected from the trench and grid. All the artefacts were made of medium to fine grain quartzites that are readily available in the gravel bed of the Jampaleru stream. The quartzite gravels originated from the surrounding Bairenkonda quartzite formation and belong to the Cuddapah supergroup of rocks. Among the 418 artefacts recovered, 131 are debitage, 15 manuports, and eight are hammerstones (Table. 4.9.2). The three categories mentioned above, which form 36.84% of the total assemblage, play a crucial part in the lithic reduction sequence.

The lithic analyses and technological descriptions below are based on the rest of the 264 artefacts. A large portion of the assemblage was of debitage (< 2 cm in length) with 29% (n=131). Unretouched flakes, both complete and broken, are represented by 14.11% (n=59), followed by blades (10.53%, n=44). Cores, including all the diverse varieties, also comprise a considerable percentage of the assemblage (16.51%, n=61). Five hammerstones of sandstone, the most common type used, and 15 manuports or unworked pebbles were also identified in the assemblage (Fig. 4.9.5). Some of these unused rocks likely to have been transported to the site for use as cores; others may have been unused hammerstones. 47% of the assemblage contains cortex, where cores and flakes categories are dominant with 17.54% and 19.43%, respectively (Table. 4.9.3).

Table. 4.9.2: Composition of the lithic Assemblage from Ardhaveedu.

Type	Trench	%	Grid	%	Total	%
Core Types						
Unidirectional core	3	3.16	10	3.1	13	3.11
Bidirectional core	0	0	1	0.31	1	0.24
Blade Core	0	0	6	1.86	6	1.44
Preferential Levallois Core	0	0	2	0.62	2	0.48
Unidirectional Levallois core	0	0	1	0.31	1	0.24
Discoidal Core	1	1.05	2	0.62	3	0.72
Radial Core	4	4.21	6	1.86	10	2.39
Core-on-flake (Radial)	2	2.11	5	1.55	7	1.67

Core-on-flake (Unidirectional)	0	0	5	1.55	5	1.2
Amorphous Core	1	1.05	2	0.62	3	0.72
Core fragment	6	6.32	2	0.62	8	1.91
Chopper	0	0	2	0.62	2	0.48
Hammer stone	3	3.16	5	1.55	8	1.91
Manuports	2	2.11	13	4.02	15	3.59
Total Core	**22**	23.16	**62**	19.2	**84**	20.1
Flake Types						
Flakes	13	13.68	46	14.24	59	14.11
Blades	1	1.05	43	13.31	44	10.53
Convergent flake	0	0	4	1.24	4	0.96
Cortical flake	15	15.79	6	1.86	21	5.02
Laminar flake	0	0	12	3.72	12	2.87
Levallois flake	0	0	1	0.31	1	0.24
Prepared core flake	2	2.11	6	1.86	8	1.91
Redirecting flake	0	0	7	2.17	7	1.67
Debitage (<2 cm in length)	37	38.95	94	29.1	131	31.34
Total Flake	**68**	71.58	**219**	67.8	**287**	68.66
Retouched Flakes						
Side Scraper	0	0	1	0.31	1	0.24
End Scraper	0	0	3	0.93	3	0.72
Round Scraper	0	0	4	1.24	4	0.96
Scraper on Blade	0	0	1	0.31	1	0.24
Side Notch	0	0	2	0.62	2	0.48
End Notch	0	0	2	0.62	2	0.48
Backed Tabular Piece	0	0	1	0.31	1	0.24
Backed Blade	0	0	1	0.31	1	0.24
Levallois Point	0	0	4	1.24	4	0.96
Tanged Point	0	0	2	0.62	2	0.48
Retouched Point	0	0	1	0.31	1	0.24
Retouched Flake	5	5.26	15	4.64	20	4.78
Retouched Blade	0	0	2	0.62	2	0.48
Retouched Laminar Flake	0	0	3	0.93	3	0.72
Total Retouched	**5**	5.26	**42**	13	47	11.24
Total	**95**	100	**323**	100	**418**	100

Table. 4.9.3: Distribution of cortex on the artefacts

Type	with cortex	%	without Cortex	%	0-30 %	%	30-60%	%	60-90%	%
Cores	37	17.54	7	3.32	19	9.00	8	3.79	10	4.74
Flakes	41	19.43	84	39.81	34	16.11	7	3.32	0	0.00
Retouched Flakes	21	9.95	21	9.95	18	8.53	3	1.42	0	0.00
Total	**99**	**46.92**	**112**	**53.08**	**71**	**33.65**	**18**	**8.53**	**10**	**4.74**

The percentage of the cortex was estimated and grouped into three categories, i.e., 0-30%, 30-60%, and 60-90% (Table. 4.9.3). Two third of the artefacts that have cortex fall into the 0-30% category. It is notable that half of the artefacts (n=21) from the retouched flake category have cortex because, generally, little or no cortex is expected on this group of artefacts. All these raw materials appear to have been derived from the Jampaleru river, situated 50 m south of the site. The cortex on artefacts is of cobble cortex type indicating the riverine source; even though there are raw material outcrops nearby the site, no blocks were used to make artefacts.

Discarded flakes indicate the presence of an early-stage reduction of cores and the subsequent use of centripetal, unidirectional, and prepared core technology (Fig. 4.9.6). Initial stages of reduction sequence are revealed by the 21% of the flakes with cortical platforms. Intact flakes with two or more dorsal flake scars (n=86) are dominated by the flakes with unidirectional flake scars (from proximal) forming 72% (n=63). However, a few examples of one or two, or more rotations that are orthogonal to the percussive axis, classified as centripetal or radial reduction systems, are also present. Faceting and overhang removal accounts for 46% and 29%, respectively, of total platform preparations observed on complete flakes and are corroborated by the presence of a similar percentage of multi-conchoidal platform surfaces. Blades are defined as having a length more than twice the width with parallel lateral margins forming 13.5% (n=43) of the assemblage (Fig. 4.9.7). The metrical values such as mean length, width, and thickness for complete blades presented in Table 4.9.4 suggest the intentional production of blades. Only one Levallois and four prepared core flakes were identified in the assemblage. Retouched flakes were few in the assemblage, limited to only 13% (n=42), dominated by the

informal retouched flakes (n=20) category. However, retouched artefacts include scrapers, notched flakes, backed artefacts, and points (Fig. 4.9.8). Statistical data for the flake attributes are presented in Table 4.9.5.

Table. 4.9.4: Metrical attributes of the complete cores, flakes, and blades.

Artefacts	Length (mm)	Width (mm)	Thickness (mm)
Debitage			
Flakes (n=86)	54.39	40.79	13.34
Blades (n=24)	66.14	31.72	8.80
Cores			
Blade cores (n=6)	69.80	45.41	33.11
Unidirectional Cores (n=16)	91.23	82.39	41.34
Radial Cores (n=11)	64.69	73.26	26.10

Table. 4.9.5: Statistical data for flake attributes.

Attribute	N	Mean	SD	Min.	Max.
Length	179	54.85	18.02	17.20	138.50
Proximal Width	179	34.38	13.07	8.00	70.00
Medial Width	179	38.78	13.37	12.07	85.90
Distal Width	179	29.93	13.39	6.50	64.33
Medial Thickness	179	12.98	5.09	2.94	33.17
Elongation	179	1.53	0.56	0.51	3.51
Flatness	179	3.17	0.98	1.48	5.99
Proximal Shape	179	0.89	0.18	0.27	1.32
Distal Shape	179	1.44	0.69	0.84	8.05
Platform width	179	28.67	13.37	0.00	67.70
Platform Thickness	179	10.84	4.82	0.00	28.49
Platform area	179	354.73	293.21	0.00	1621.65
Platform Angle	179	76.15	12.88	0.00	110.00
Dorsal scar count	179	2.34	1.34	0.00	6.00
No. Unidirectional arrises	179	0.71	0.82	0.00	3.00
No. Radial arrises	179	0.39	0.89	0.00	4.00

As observed from the flakes, the core reduction strategies at Ardhaveedu exhibit various schemes suggesting an early-stage exploitation of quartzite pebbles. Pebbles of different size and shape were used in the preparation of cores by applying various techniques exploiting the natural flat surfaces (Fig. 4.9.9). Firstly, cores were classified based on scar patterns followed by attributing each core to a technological type where diagnostic reduction strategies could be identified (ex. Preferential Levallois and Blade cores). The cores (n=61) in the assemblage are classified into 12 categories based on the flake scar patterning and core preparation. The most

predominant type in the core assemblage is unidirectional cores (n=16), followed by radial cores (n=10), blade cores (n=6) and prepared cores (n=15) (Fig. 4.9.10 and Fig. 4.9.11).

Figure. 4.9.5: Hammerstones.

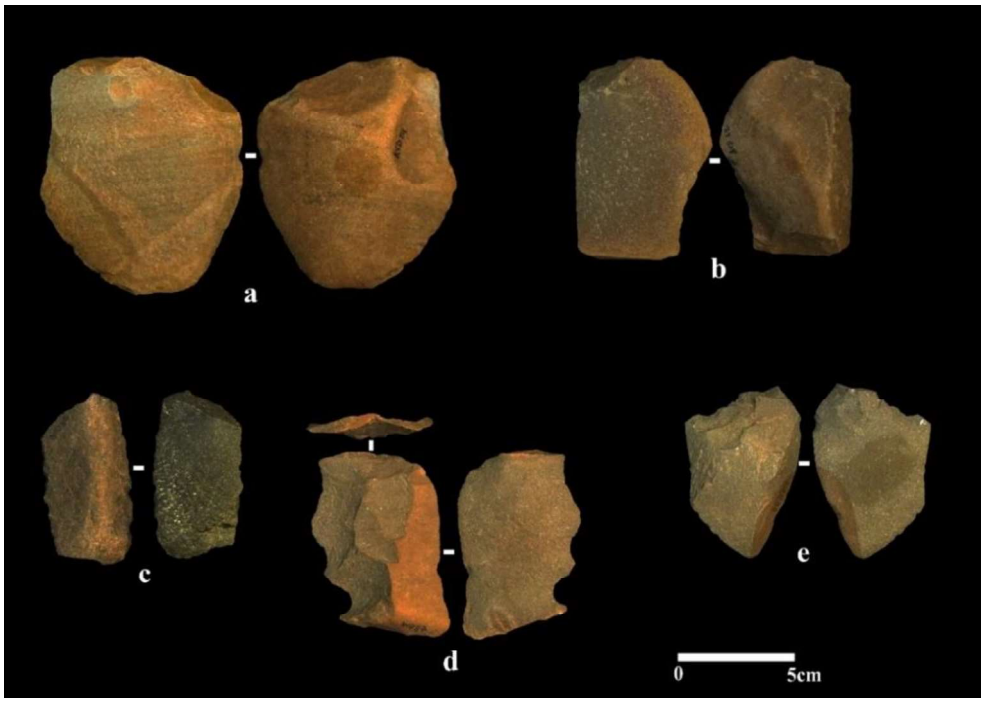

Figure. 4.9.6: Early stage flakes of core reduction sequence. a and b: Cortical flakes with cortical platforms; c to e: Cortical flakes with prepared platform

Figure. 4.9.7: Representative blade artefacts from the assemblage.

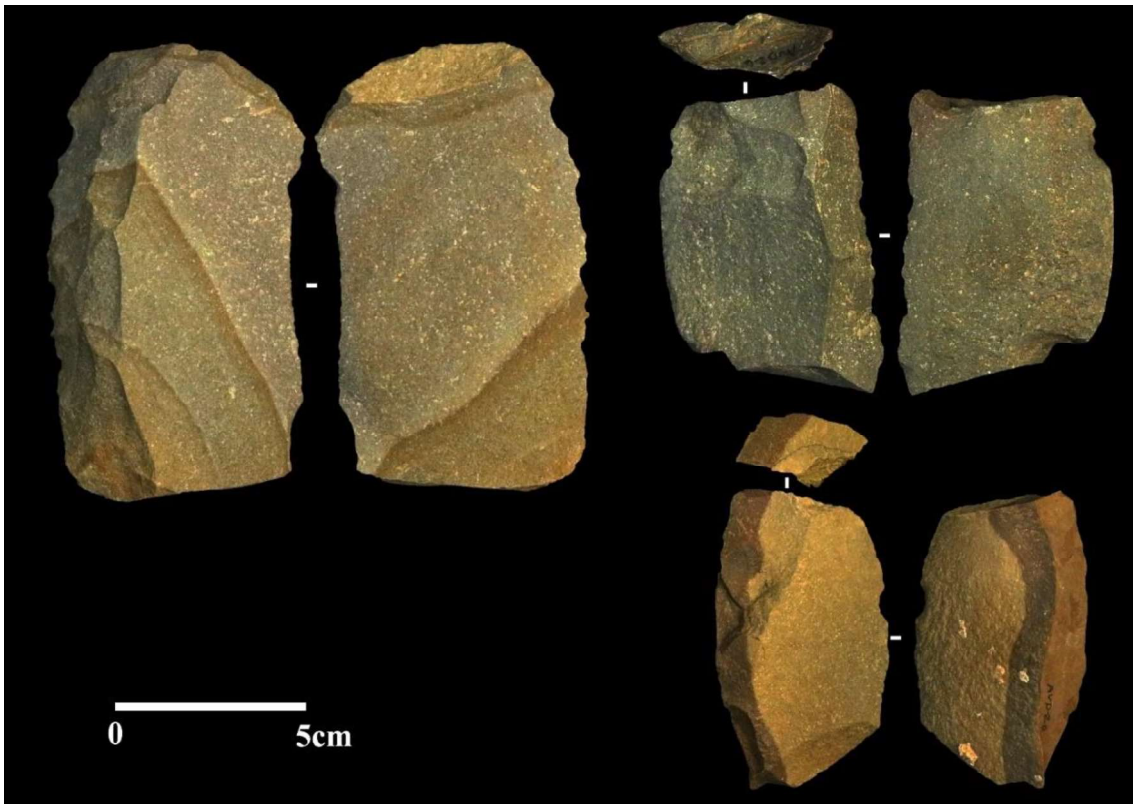

Figure. 4.9.8: Backed tabular piece (top left) and Backed blades.

Table. 4.9.6: Statistical data for core attributes.

Attribute	N	Mean	SD	Min.	Max.
Length	48	73.25	32.06	25.60	170.00
Proximal Width	48	58.12	21.61	16.40	116.40
Medial Width	48	68.01	25.83	17.50	126.30
Distal Width	48	52.81	22.11	12.80	110.20
Proximal Thickness	48	25.36	13.43	7.30	62.40
Medial Thickness	48	33.25	14.49	13.60	70.70
Distal Thickness	48	24.95	12.95	9.90	69.00
Proximal Shape	48	0.86	0.16	0.57	1.32
Distal Shape	48	1.33	0.24	0.97	1.93
Elongation	48	1.11	0.42	0.61	2.59
Flatness	48	2.31	0.72	0.97	3.98
No. of Core Rotations	48	1.37	1.53	0.00	6.00
Last Platform Angle	48	74.30	12.28	50.00	100.00
No. of Major Flake Scars	48	3.14	1.13	1.00	5.00
No. of Flake Scars	48	5.16	2.26	1.00	13.00
No. of Feather terminations	48	1.44	1.44	0.00	6.00
No. of non-feather Terminations	48	3.72	2.64	0.00	12.00
Last Scar Length	48	48.08	20.98	24.40	150.00
Last Scar Width	48	31.06	14.23	4.50	64.50
Last Scar Elongation	48	1.72	0.89	0.62	3.91

Levallois cores consist of one unidirectional and two preferential Levallois cores, indicating the intentional application of the Levallois core reduction technique (Fig. 4.9.12). Other core categories, such as discoidal and bidirectional cores, are also present in the assemblage in smaller quantities. Statistical data for the core attributes are presented in Table 4.9.6. The unidirectional and blade cores are dominant (n=19) among the core category indicating that the core technology at Ardhaveedu was predominantly aimed at producing elongated flakes and blades.

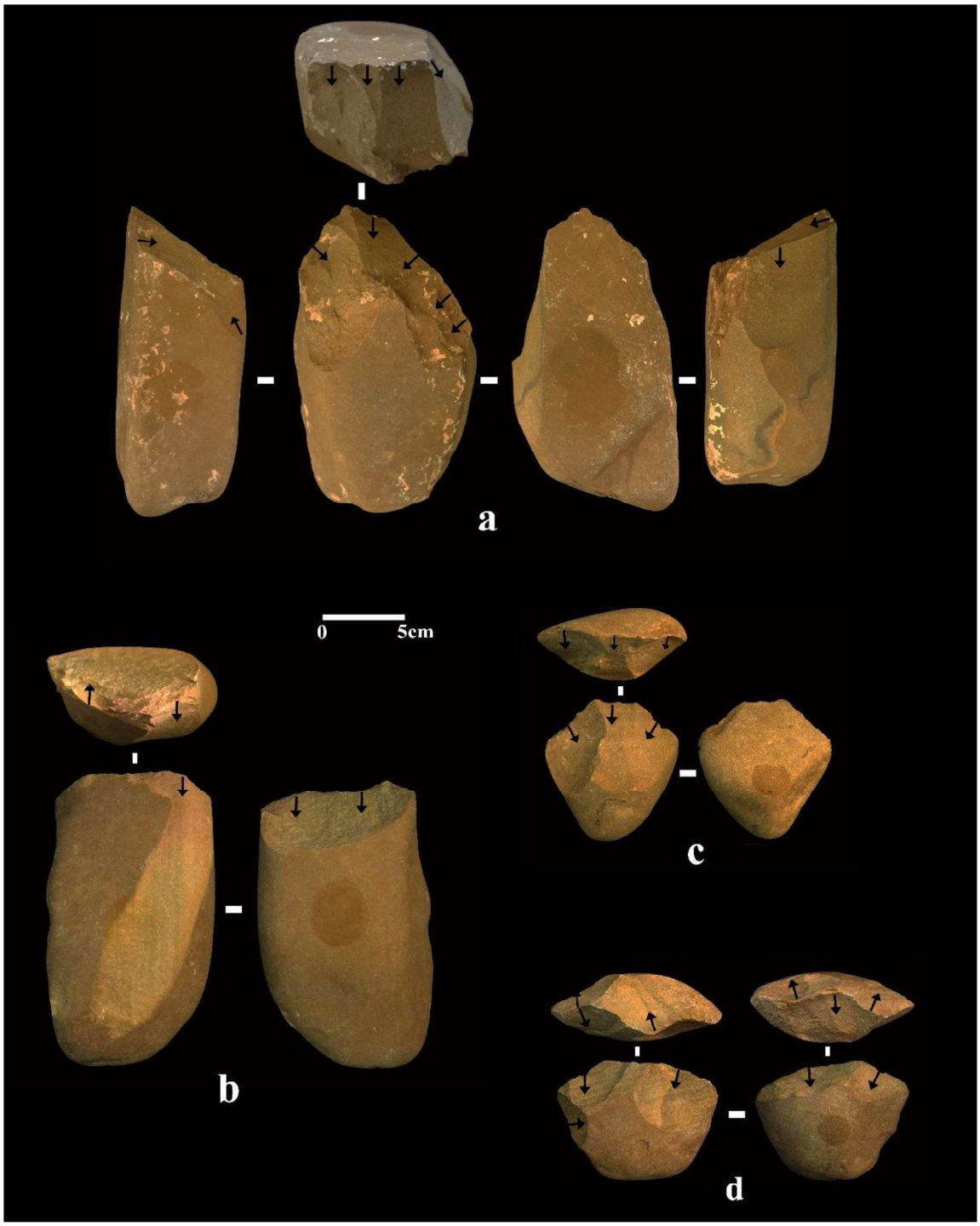

Figure. 4.9.9: Core showing the early-stage reduction from Ardhaveedu.

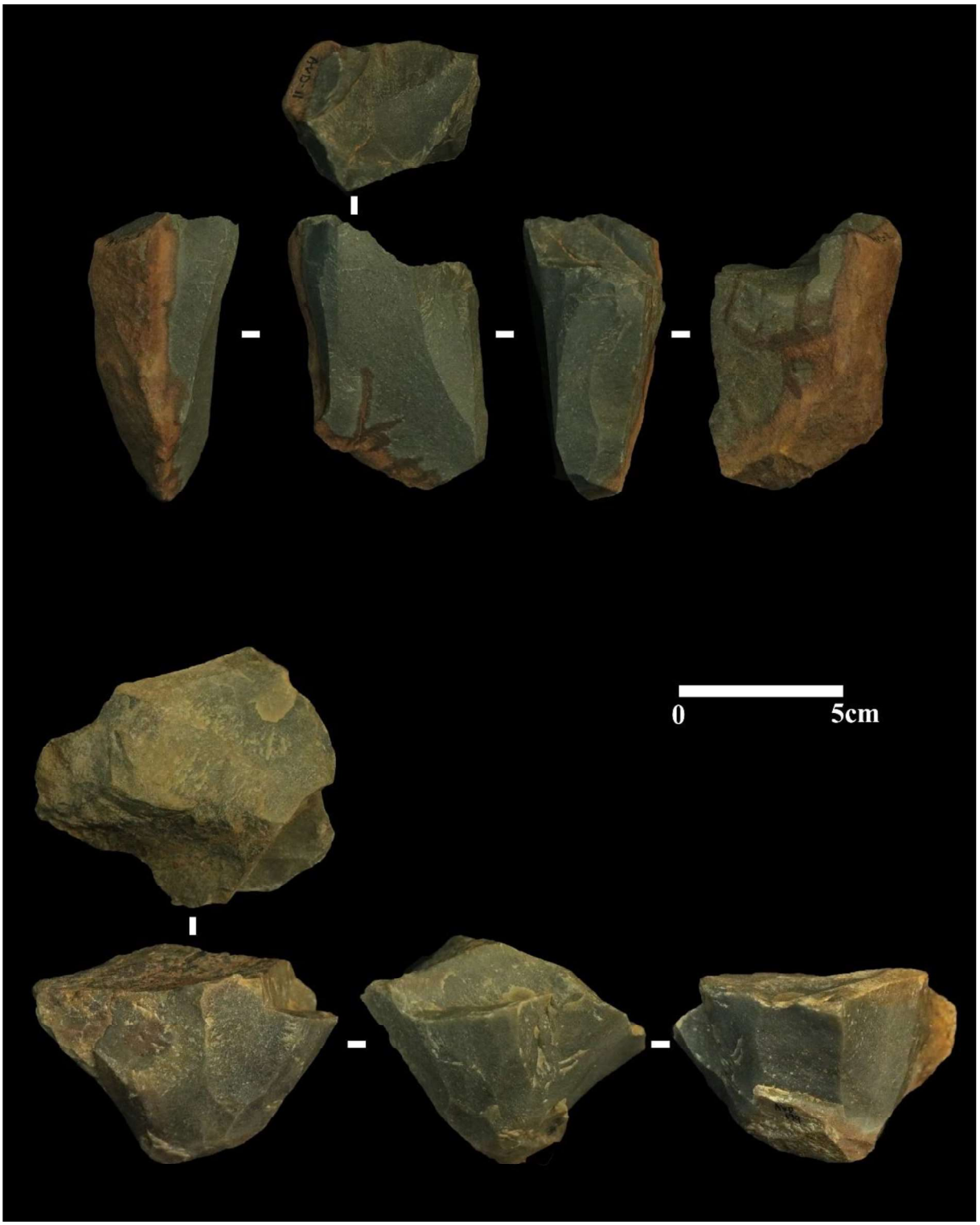

Figure. 4.9.10: Blade cores.

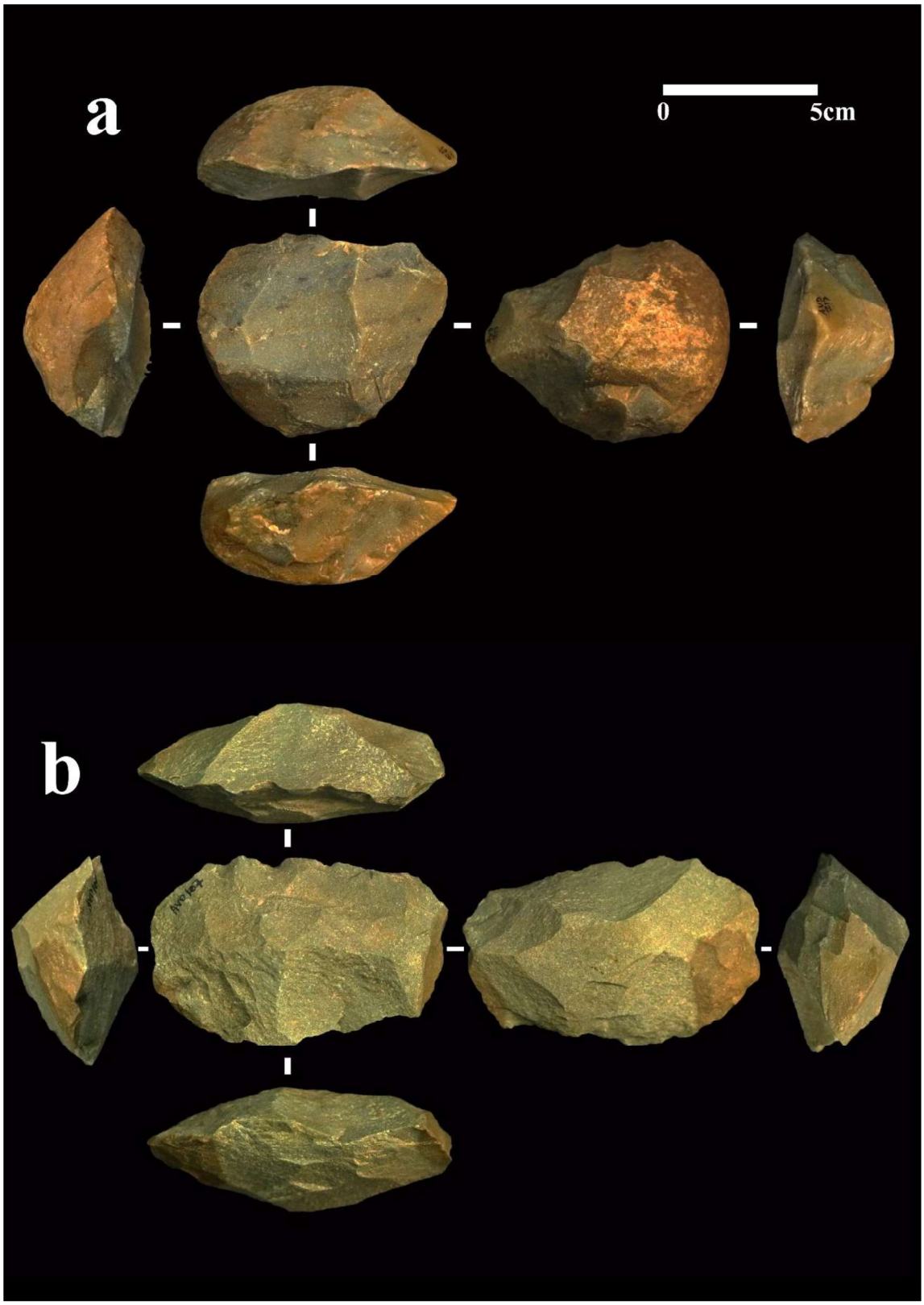

Figure. 4.9.11: Levallois cores.

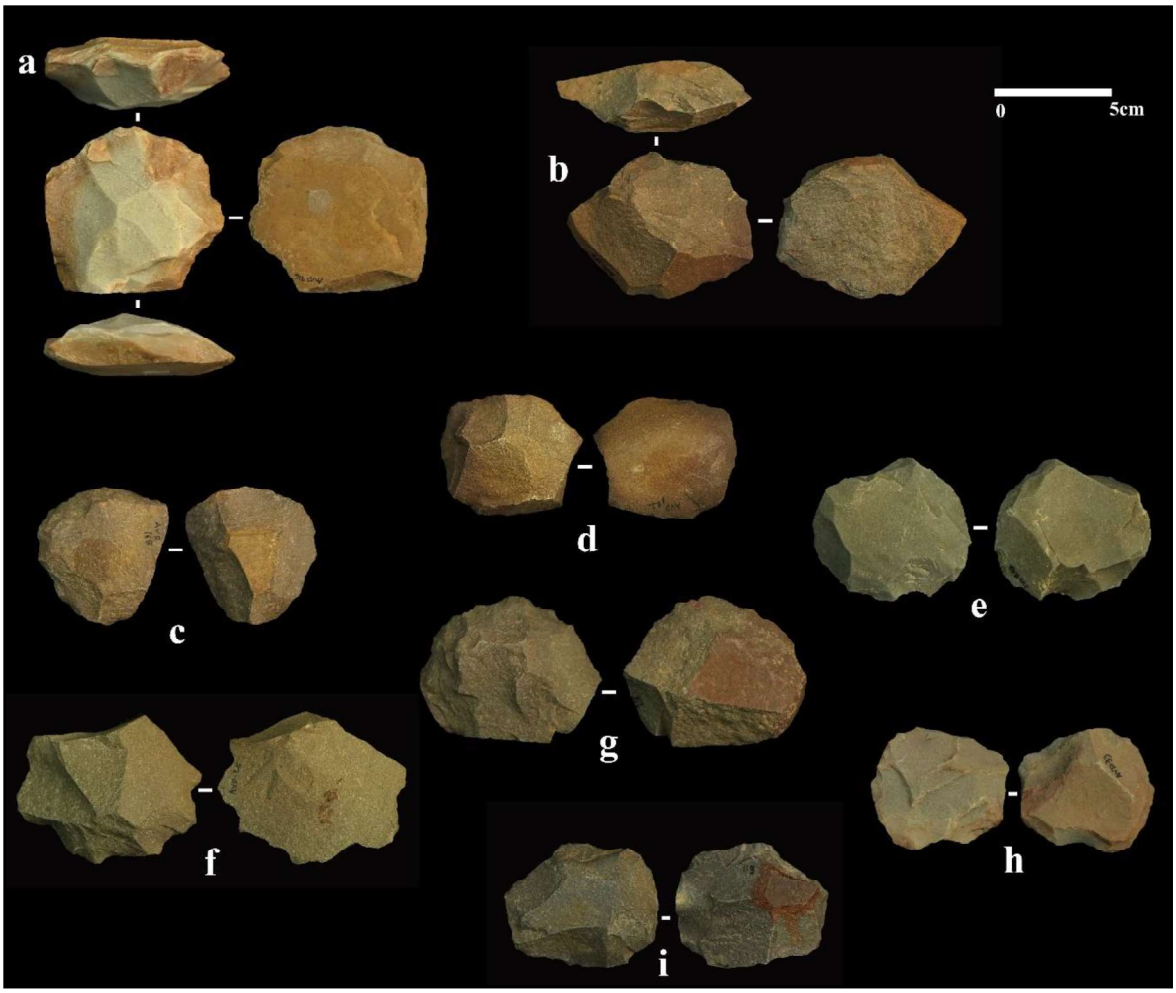

Figure. 4.9.12: Radial cores.

4.9.4 Summary

Ardhaveedu revealed a predominantly blade-based assemblage, with prepared core technologies dated to 41 ka. Typo-technological aspects of the Ardhaveedu assemblage suggest that the site functioned as a production site mainly focused on the reduction of quartzite nodules/cobbles recovered from the Jampaleru stream bed. The presence of flakes and cores that are part of different stages of lithic reduction sequence and high proportions of cortex on flakes and cores indicate the characteristics of a lithic production site. In addition, hammerstones and manuports in the assemblage corroborate the aforesaid observation. Excavations at the site indicate the surface exposed artefacts are eroding out from silt-dominated, brown-coloured sediment overlain by a palaeosol. No other artefact horizons were observed at the site associated with both overlying and underlying horizons of artefact bearing horizon suggesting the surface collection analyzed along with trench aretfacts are part of a single sediment horizon. Further, none of the artefacts shows any signs of abrasion, and major

edge damage patterns were observed. All these aforesaid observations indicate that the lithic assemblage analysed in the current study is an *in-situ* assemblage that belongs to a single artefact bearing horizon exposed in the recent past due to erosional activities. Therefore, the observations and interpretations made on the nature and technology of the assemblage are not hindered by issues of mixed surface collection or palimpsests.

Based on the characteristic features of the assemblage, the main objective of lithic reduction at Ardhaveedu was to produce elongated flakes and blades. The use of prepared core and Levallois technology seems minimal. The dorsal flake scar patterns on complete flakes and the dominant presence of unidirectional cores, suggest that the unidirectional reduction strategy was most preferred at the site. In addition, the presence of blade-cores and blades indicates a clear preference for elongated flakes and blades at the site. Similar blade-based assemblages have also been reported from other ten sites in the upper reaches of the Gundlakamma river basin that are associated with a similar geological context as of Ardhaveedu (Anil et al., 2022), indicating that it is a temporally distinct behaviour. Notably, only a small portion of the Ardhaveedu assemblage is made up of retouched artefacts that are dominated by informally retouched tools, thereby limiting our understanding of the nature of the retouched tool kit at the site. However, surface collections made from ten other sites in the region associated with similar geological contexts show the presence of Levallois points, scrapers, retouched flake-blades, blades, and points (Anil et al., 2022).